University of Leicester

Functional Consequences of Nociceptin Receptor Activation

John McDonald

University Department of Cardiovascular Sciences
(Pharmacology and Therapeutics Group)
University of Leicester

Thesis Submitted for the Degree of Doctor of Philosophy

June 2007

ProQuest LLC
789 East Eisenhower Parkway
P.O. Box 1346
Ann Arbor, MI 48106-1346

Abstract

Nociceptin orphanin FQ (N/OFQ) is the 17 amino acid endogenous ligand for the G_i-coupled N/OFQ-receptor (NOP). *In vivo* administration produces a wide range of physiological responses including; analgesia, hyperalgesia and anti-opioid actions.

In a series of *in vitro* assays including [*leucyl*-^{3}H]N/OFQ binding, GTPγ[^{35}S] binding and inhibition of cAMP formation the following linked studies were performed; (1)N/OFQ structure-activity relationships (SAR) in cells (CHO) stably expressing human NOP (2)evaluation of receptor density on efficacy using the ecdysone inducible expression system and native tissues, (3)an investigation of NOP/G-protein coupling efficiency.

SAR studies can be summarized as combining arginine^{14},lysine^{15} repeat in N/OFQ (increase affinity/potency) with C-terminal [F/G]N/OFQ(1-13)NH_2([F/G]) and [Nphe^1]N/OFQ(1-13)NH_2([Nphe^1]) modifications (reduce/eliminate efficacy). Arg^{14}/Lys^{15} increased the affinity (pK_i:10.31-11.16) and potency (pEC_{50}:8.98-9.85) of N/OFQ. [F/G] and [Nphe^1] reduced the efficacy of N/OFQ from 1.0 to 0.44 and 0. Combination of Arg^{14}/Lys^{15} and [Nphe^1] to UFP-101 produced the highest affinity peptide antagonist available (pA_2:9.13, [Nphe^1] alone:7.54). Using the ecdysone inducible expression system it was possible to vary the efficacy of [F/G], between antagonist (α:0 upstream/low density), partial agonist (α:0.3-0.75) and full agonist (α:1). In the mouse *vas deferens* and colon [F/G] displayed varying degrees of partial agonism possibly indicating differences in NOP receptor density. The binding of GDP and GTP in CHO_{hNOP} was to high and low affinity sites. The fraction of GDP binding to the high affinity site was reduced by N/OFQ (77% under basal to 32%). The reduction in high affinity binding of GDP appeared dependent on the efficacy of the ligand.

This thesis has identified several new peptides of varying efficacy/potency for use in defining the pathophysiological role(s) of N/OFQ-NOP. Efficacy is not just a property of the ligand but of the assay system and its input receptor density. A cautious approach to new ligands characterized at a single endpoint is advocated.

Acknowledgements

While this work carries only my name it truly is a team effort.

To my friend Dave (Professor Lambert), the greatest thanks are extended. Professionally and academically the assistance, support, guidance, wealth of knowledge and encouragement offered has been invaluable. On a personal level the support you and your family have extended to me has been colossal. I have so much gratitude for what you have given and continue to give me.

For all my friends who I have worked with, Tim (you take an extra one), John Williams (a great landlord and even better friend), Jim, Chris, Anton, Emma, Trish (you made it interesting!!), Dr Carra, Massimo, Masato, Eddy, Paul, Kathleen, Wei, I thank you all for help, encouragement and love. Thanks to my Italian buddies, Giro, Remo and all the lovely ladies!!! I am sure there is many, many more and I thank you all.

My gratitude list would not be complete without thanks to, Janet Harris, Bob Chamberlain and Margaret Crawford. I am indebted to you all for giving me yet another chance.

To the Living Room, specifically Danny, Alex, Alfie, Rochelle, Nancy, Janis and all the other counsellors and clients, who have loved me back to life! I am so, so grateful for all the empathy, altruism and love you have extended and continue to extend to me. You have made an atheist into an agnostic and given me a new way of living, all I had to bring was HOW.
To everybody in the "Fellowship" and all my peeps in recovery, I love you all!!

"For, to these people, I am truly related. First, through mutual pain and despair, and later through mutual objectives and new-found faith and hope. And, as the years go by, working together, sharing our experiences with one another, and also sharing a mutual trust, understanding and love-without strings, without obligation-we acquire relationships that are unique and priceless." -- *Alcoholics Anonymous,* p. 312"

To Dr Bob, I am truly blessed to have you in my life and privileged to call you a friend. So much thanks for all that you give me, you are a very special person in my world. May we continue to trudge the road of happy destiny!!

Last and by no means list I thank my family, Mum, Dad, Sis, Dave, Liam and Kieran. To Bev and Jenifer (not forgetting Si) – I love you all.

Not forgetting the Boyz, Stu (AKA "The Big Fella"), Arun, Dave, Pete and Keith, let there be many more years of drink and debauchery.

"Now there is a sense of belonging, of being wanted and needed and loved. In return for a bottle and a hangover, we have been given the Keys of the Kingdom."

--Alcoholics Anonymous, p. 276

Contents

List of Abbreviations

5-HT – 5-Hydroxy Tryptamine (serotonin)
AC – Adenylyl Cyclase
ADP – Adenosine Diphosphate
Bq – Becquerel = 1 disintegration/second
BSA – Bovine Serum Albumin
cAMP – Cyclic Adenosine Monophosphate
Ci – Curie = 3.7×10^{10} Bq
CNS – Central Nervous System
CTOP – D-Phe-Cys-Tyr-D-Trp-Orn-Thr-Pen-Thr-NH_2
CTx – Cholera Toxin (from *Vibrio cholerae*)
DAMGO - Tyr-D-Ala-Gly-N-methyl-Phe-Gly-ol
[$DPen^{2,5}$]enkephalin
EDTA – Ethylenediaminetetraacetic acid
FBS – Foetal Bovine Serum
GDP – Guanosine Diphosphate
GPCR – G-protein Coupled Receptor
GTP – Guanosine Triphosphate
HEPES – N-(2-Hydroxyethyl)piperazine-N'-(2-ethanesulphonic acid)
IBMX – 3-Isobutyl-1-methylxanthine
J113397 (CompB) – 1-[(3R,4R)-1-cyclooctylmethyl-3-hydroxymethyl-4-piperidyl]-3-ethyl-1,3-dihydro-2H-benzimidazol-2-one
JTC-801 – [N-(4-amino-2-methylquinolin-6-yl)-2-(4-ethylphenoxymethyl) benzamide monohydrochloride]
MEM – Minimal Essential Medium
N/OFQ – Nociceptin/OrphaninFQ
NOP – Nociceptin Receptor
NRM – Nucleus Raphe Magnus
NRPG – Nucleus Reticularis Paragigantocellularis
NSB – Non-Specific Binding
PAG – Periaqueductal Grey (matter)
PEI – Polyethylenimine
ppN/OFQ – preproNociceptin/OrphaninFQ
PTX – Pertussis Toxin (from *Bordetella pertussis*)
Ro64-6198 – Roche compound – (1*S*,3a*S*)-8-(2,3,3a,4,5,6-hexahydro-1*H*-phenalen-1yl)-1-phenyl-1,3,8-triaza-spiro[4.5]decan-4-one.
SA – Specific Activity
SG – Substantia Gelatinosa
U69593 – (+)-(5α,7α,8β)-N-Methyl-N-[7-(1-pyrrolidinyl)-1-oxaspiro[4.5]dec-8-yl]-benzeneacetamide

1 Introduction

Opium and its derivatives have been used for centuries both in a medicinal and "recreational" manner. Findings of fossilised opium poppy seeds dating as far back as 30,000 years suggest the use of opium by Neanderthal man. In 1799 Friedrich Serturner discovered the major active ingredient of opium, which he named morphine and opioid pharmacology was born (Hogshire, 1994). Morphine and its derivatives are used today for the treatment of acute and chronic pain. It is now understood that morphine and other opioid drugs act on endogenous opioidergic systems which are not only involved in setting pain (nociceptive) threshold and controlling nociceptive processing but also participate in modulation of gastrointestinal function, endocrine and autonomic function as well as a possible role in cognition (Feldman, 1997).

Given that the major use of opioid drugs historically and to date has been for the treatment of pain an initial description of human nociceptive physiology is essential. Sensation of pain has both an affective and cognitive element and a sensory element, whereby noxious stimuli are perceived by nociceptors, which are free nerve endings located at the terminals of nociceptive primary afferents (C and Aδ fibres). Nociceptors respond to all stimuli both physical or chemical which are noxious i.e. likely to cause tissue damage or harm. C-fibres are non-myelinated and therefore have slower transmission rates ($<2.5 m.s^{-1}$) and are associated with throbbing, aching or chronic pain. Aδ-fibres, in contrast are myelinated giving increased rates of transmission ($2.5\text{-}20 m.s^{-1}$) and represent fast, sharp or acute pain (Tortora *et al.*, 1990).

The cell bodies of nociceptive afferents lie within the dorsal root ganglia, situated just outside the spinal cord. The axon of these primary or first order nociceptive afferents (C and Aδ-fibres) synapses with the cell bodies of second order (spinothalamic) neurons, or interneurons, located in the I, II and V laminae of the spinal cord dorsal horn, see Figure 1-1. Cells of the dorsal horn lamina II, the substantia gelatinosa (SG), have short axons running to either laminae I or V and represent interneurons between first order neurons terminating in lamina II and the second order neurons of laminae I and V, see Figure 1-1. These interneurons are inhibitory and can be stimulated by non-nociceptive input, e.g.

mechanoreceptors, activation of which inhibits nociceptive afferents It is this region that represents the 'gate' in Melzack and Wall's original theory of spinal nociceptive transmission (Melzack *et al.*, 1996). Projections from laminae I and V are second order and travel to the thalamus via the lateral spinothalamic tract. Axons of cells in the thalamus further relay painful sensations to the samatosensory cortex-precentral gyrus (Rang *et al.*, 1995).

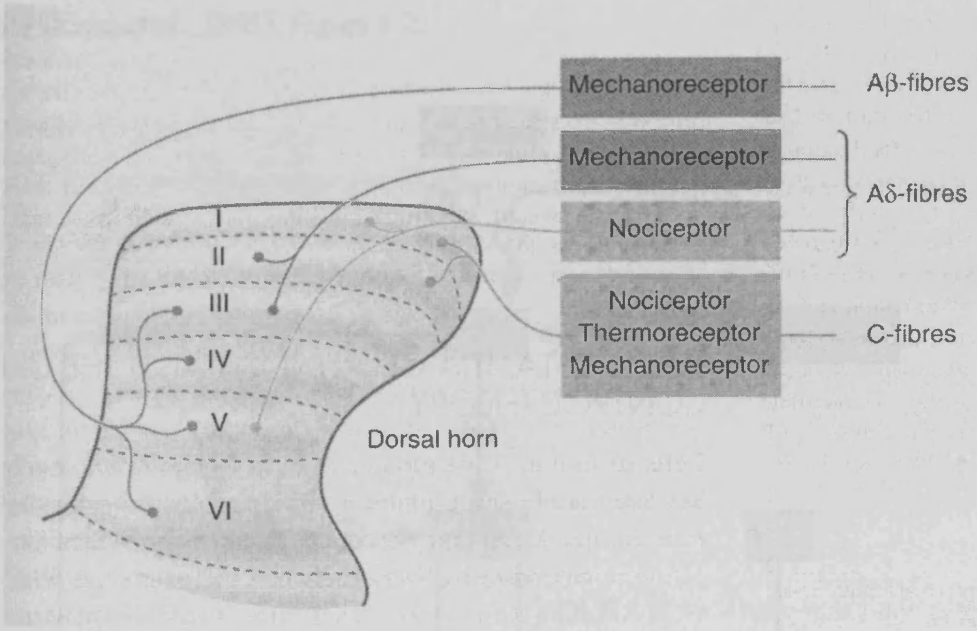

Figure 1-1. Structure of the different laminae in the dorsal horn of the spinal cord. Sensory nerves and the point of termination within the spinal cord are depicted (Rang *et al.*, 1995).

1.1 Regulation of painful stimuli by the CNS

CNS control of painful stimuli is via descending inhibitory control pathways, see Figure 1-2. Descending inhibitory pathways act to inhibit neurons within the dorsal horn. The periaqueductal grey (PAG) plays an important role in this, receiving inputs from various parts of the brain including the hypothalamus, cortex and thalamus. Stimulation of the neuronal pathway of the PAG descends to the rostral medulla of the midbrain, more specifically the nucleus raphe magnus (NRM). From here descending fibres running in the dorsolateral funiculus of the spinal cord form synaptic connections with SG interneurons of the dorsal horn, activation of which inhibits nociceptive transmission.

Spinothalamic neurons have pathways running to the NRM via nucleus reticularis paragigantocellularis (NRPG) and represent further input and control of the inhibitory descending pathways. Descending inhibitory control is mediated by the neurotransmitters enkephalins and 5-HT. Noradrenergic transmission from the *locus coeruleus* (LC) acts more directly to inhibit the dorsal horn. Opioids cause analgesia through stimulation of descending inhibitory pathways and by inhibiting the dorsal horn directly (Rang *et al.*, 1995), Figure 1-2.

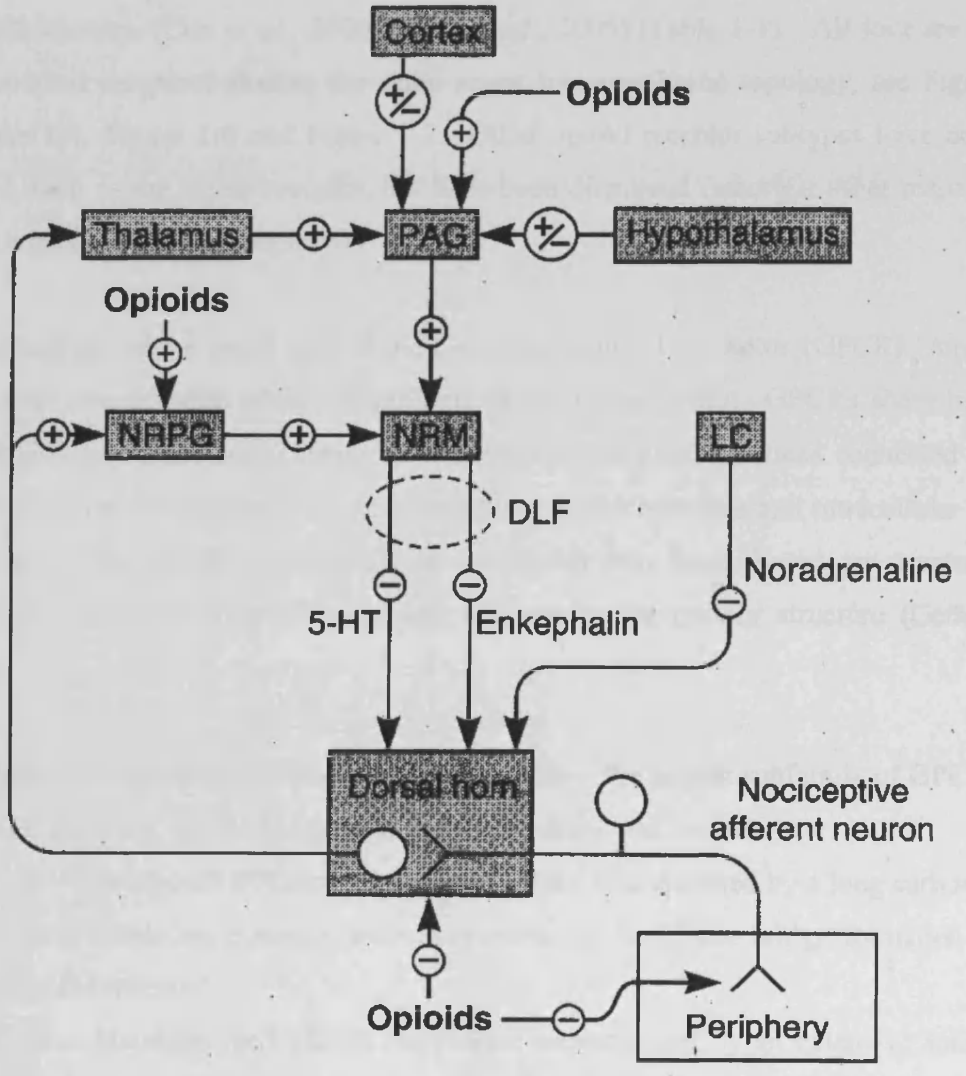

Figure 1-2. Schematic of descending inhibitory control of the dorsal horn, opioid sites of action are shown (Rang *et al.*, 1995).

1.2 Opioid Receptors

Evidence for the existence of multiple opioid receptor sub-types was reported based on the different anatomical locations and pharmacological profiles of compounds that were eventually used to name them i.e. *m*orphine (*m*u), *k*etocyclazocine (*k*appa) and vas *d*eferens (*d*elta). Recently a fourth opioid-like receptor has been included in this family and is termed the nociceptin orphanin FQ peptide receptor. Receptor nomenclature has changed numerous times but current IUPHAR (International Union of Pharmacology) opinion is MOP (mu), KOP (kappa), DOP (delta) and NOP for the nociceptin orphanin FQ peptide receptor (Cox *et al.*, 2000; Foord *et al.*, 2005) (Table 1-1). All four are G-protein coupled receptors sharing the same seven transmembrane topology, see Figure 1-3, Figure 1-4, Figure 1-6 and Figure 1-7. Other opioid receptor subtypes have been suggested, such as the sigma receptor, but have been dismissed (amongst other reasons) based on a lack of naloxone sensitivity.

Opioid receptors form a small part of the G-protein coupled receptor (GPCR) 'super-family' – the largest super-family of proteins in the human body. GPCRs share high structural similarities including seven transmembrane spanning α-helices connected by intracellular and extracellular loops, an extracellular amino terminus and intracellular C-terminal tail. The GPCR super-family is subdivided into three, based on structural identity and sequence conservation of key residues in the protein structure (Gether, 2000);

Subfamily A - Rhodospin/β2 adrenergic receptor-like – the largest subfamily of GPCRs and contains receptors for the biogenic amines, bradykinin and opioids.
Subfamily B – Glucagon/VIP/Calcitonin receptor-like – characterised by a long carboxyl tail comprising numerous cysteine residues involved in disulphide bridge formation to this region of the receptor.
Subfamily C - Metabotropic/Calcium receptors – characterised by an extensive amino terminus (~600 amino acids) believed to contain the binding region of the receptor. A very short third intracellular loop is conserved among type C GPCRs.

G-proteins consist three subunits designated alpha, beta and gamma and are discussed in greater detail later.

1.3 Endogenous and Exogenous Opiates

The endogenous opioid peptides are cleaved from four pro-hormone precursors; (i) proenkephalin, (ii) proopiomelanocortin, (iii) prodynorphin, (iv) pre-pro N/OFQ (pp-noc). The endogenous DOP receptor peptides are met-enkephalin and leu-enkephalin, cleaved from proenkephalin. Prodynorphin gives rise to the KOP receptor agonists dynorphin A and B whilst N/OFQ is from the polypeptide precursor pp-noc. Proopiomelanocortin encodes the peptide β-endorphin which has agonist activity at all three classical opioid receptors. The precursor protein(s) for the endogenous MOP receptor peptides endomorphin 1 and 2 is to date unknown (Akil *et al.*, 1998; Dhawan *et al.*, 1996).

The prototypical MOP agonist is the alkaloid morphine, purified from opium and chemically modified to produce the more potent diamorphine (Heroin). Of the synthetic opiate agonists, whose structures bear no resemblance to morphine, fentanyl and remifentanil are the more potent compounds used extensively in a clinical setting.
Pentazocine and buprenorphine are two commonly used partial agonists for the treatment of less severe pain (Rang *et al.*, 1995). Many of the opioid ligands lack specificity for a particular subtype of opioid receptor, for example the endogenous peptide β-endorphin has agonist activity at all three classical opioid receptors. Buprenorphine has partial agonist activity at MOP and NOP receptors and as a result has a bell shaped response curve for its analgesic activity *in vivo* i.e. at low and intermediate doses an analgesic response results, at higher doses the analgesic response is decreased back to baseline. The complex pharmacology of buprenorphine is explained by its agonist activity at both MOP, resulting in analgesia at low and intermediate doses, and NOP, resulting in an anti-opioid / anti-analgesic action at higher doses. (Lutfy *et al.*, 2003)
Some other opioid drugs have mixed actions at the different opioid receptors, for example pentazocine behaves as an antagonist at MOP receptors but a partial agonist at DOP and KOP receptors. Induction of analgesia via partial agonism at KOP and DOP, coupled

with subsequent antagonism of the MOP receptor is desirable due to the reduced risk of respiratory depression. There are currently no clinically selective drugs available that work via DOP, KOP or NOP receptors, see Table 1-1 (Dhawan *et al.*, 1996).

1.3.1 MOP

The MOP receptor was the last of the classical opioid receptors to be cloned and is located throughout the central nervous system in areas involved in sensory and motor function including regions concerned with the integration and perception of these senses, for example the cerebral cortex and amygdala (of the limbic system) (Dhawan *et al.*, 1996). The MOP receptor displays the classical GPCR Family A structure, see Figure 1-3. The highest density of MOP receptors are situated in the caudate putamen (of the basal ganglia). MOP receptors are located presynaptically on primary afferent neurons within the dorsal horn of the spinal cord where they inhibit glutamate release and hence transmission of nociceptive stimuli from C- and Aδ- fibres.

High densities of MOP receptors are found in the PAG and analgesia elicited by some opioids is proposed to come about from removal of an inhibitory γ-amino butyric acid (GABA)-ergic tone in this region of the brain. GABA is the main inhibitory transmitter in the brain and acts to reduce or prevent antinociceptive outflow from the PAG (Vaughan *et al.*, 1997b).

The major side effect that comes about from the use of classical MOP agonist is respiratory depression, through a reduction in the sensitivity of chemoreceptors (CNS/PNS) to hypercapnia. MOP agoinsts further inhibit gastrointestinal (GI) tract secretions and peristalsis, causing constipation. MOP opioids have further effects on the cardiovascular system, thermoregulation, hormone secretion and immune function (Dhawan *et al.*, 1996).

MOP receptor knockout mice show increased sensitivity to thermal pain, implicating the receptor in this mode of nociception. However, no change in threshold from pain elicited via mechanical stimuli was seen. None of the predicted effects or side effects of morphine were seen in mice lacking the MOP receptor. MOP receptor knockout mice showed no change in respiratory function demonstrating no tonic control of this system, also analgesia and reward were absent (Kieffer, 1999; Mogil *et al.*, 1998).

Current Receptor Nomenclature	**DOP**	**KOP**	**MOP**	**NOP**
Previous Nomenclature	OP_1, δ	OP_2, κ	OP_3, μ	OP_4, LC132, ORL_1
G-protein Coupling	$G_{i/o}$	$G_{i/o}$	$G_{i/o}$	$G_{i/o}$
Endogenous Ligand	Leu-enkephalin, Met-enkephalin	Dynorphin A	β-endorphins, endomorphins	Nociceptin
Synthetic Agonists	DPDPE	U69593	DAMGO	Ro64-6198
Selective antagonists	Naltrindole	Nor-BNI	CTOP	J-113397 (synthetic) UFP-101 (peptide)
Clinical Drugs	None	*Spiradoline *Enadoline	Morphine Remifentanil	None
Mixed Action	Pentazocine (partial agonist) Buprenorphine (inactive)	Pentazocine (partial agonist) Buprenorphine (inactive)	Pentazocine (antagonist) Buprenorphine (partial agonist)	Pentazocine (inactive) Buprenorphine (partial agonist)
Naloxone Sensitivity	Antagonist	Antagonist	Antagonist	Inactive

Table 1-1. Nomenclature for opioid receptor family (Cox *et al.*, 2000). Table information on the different drugs available for the specific opioid receptor subtypes, *Spiradoline (U-62,066E) and *Enadoline (CI-977) are KOP selective ligands that have undergone clinical trials but are not currently in use, information from various sources (Calo *et al.*, 2000c; Dhawan *et al.*, 1996; Wadenberg, 2003; Walsh *et al.*, 2001).

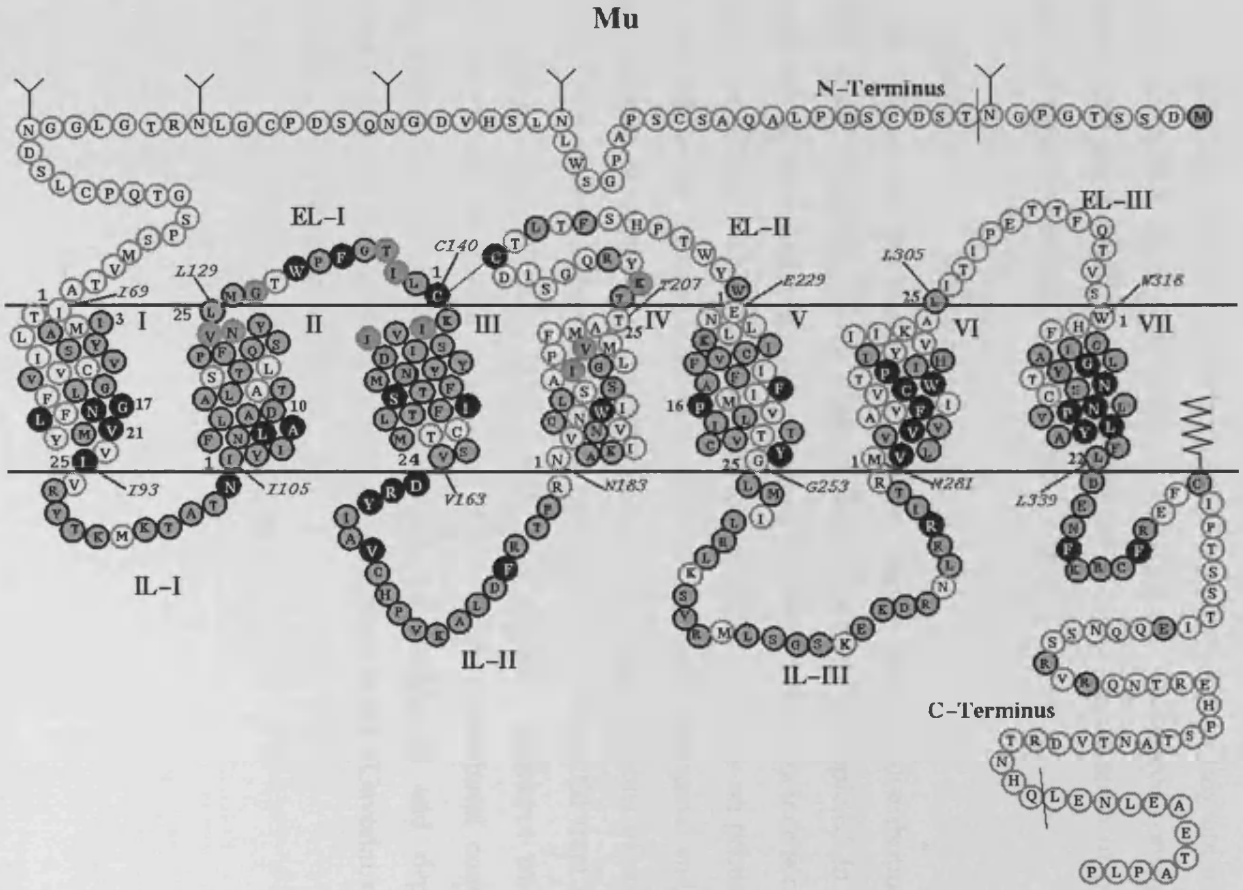

Figure 1-3. Seven domain spanning structure of Mu (MOP) opioid receptor. Original source **www.opioid.umn.edu/ ptmut.html**

Whilst the main analgesic effects of opioids are elicited by central activation of opioid receptors a number of the common side effects including reduced gastrointestinal motility, urinary retention and pruritus are regulated by activation of peripherally located opioid receptors. The use of peripherally acting opioid receptor antagonists may reduce a number of these side effects. Methylnaltrexone, a peripherally acting opioid antagonist, was shown in clinical trials to be effective at treating opioid induced constipation while alvimopan (peripheral MOP receptor antagonist) reduced the duration of postoperative ileus and postoperative nausea and vomiting (Yuan *et al.*, 2006).

1.3.2 DOP

The DOP receptor was the first to be cloned and shows restricted distribution relative to the other opioid receptors, seven transmembrane topology is depicted in Figure 1-4. Highest densities are found in the olfactory bulb, cerebral cortex, nucleus accumbens and the caudate putamen. DOP receptors are located presynaptically on primary afferents where they inhibit the release of neurotransmitters. Through both spinal and supraspinal sites the receptor is involved in the antinociceptive/analgesic actions of some opioids. However, DOP receptor agonists have also been shown to reduce GI tract motility and cause respiratory depression. Studies with DOP receptor knockout mice revealed hyperlocomotor activity and it is assumed the receptor, under basal conditions may dampen locomotion. These mice also displayed anxiogenic and depressive-like responses, suggesting that the receptor may act to regulate mood. (Gaveriaux-Ruff *et al.*, 2002; Kieffer, 1999; Mogil *et al.*, 1998)

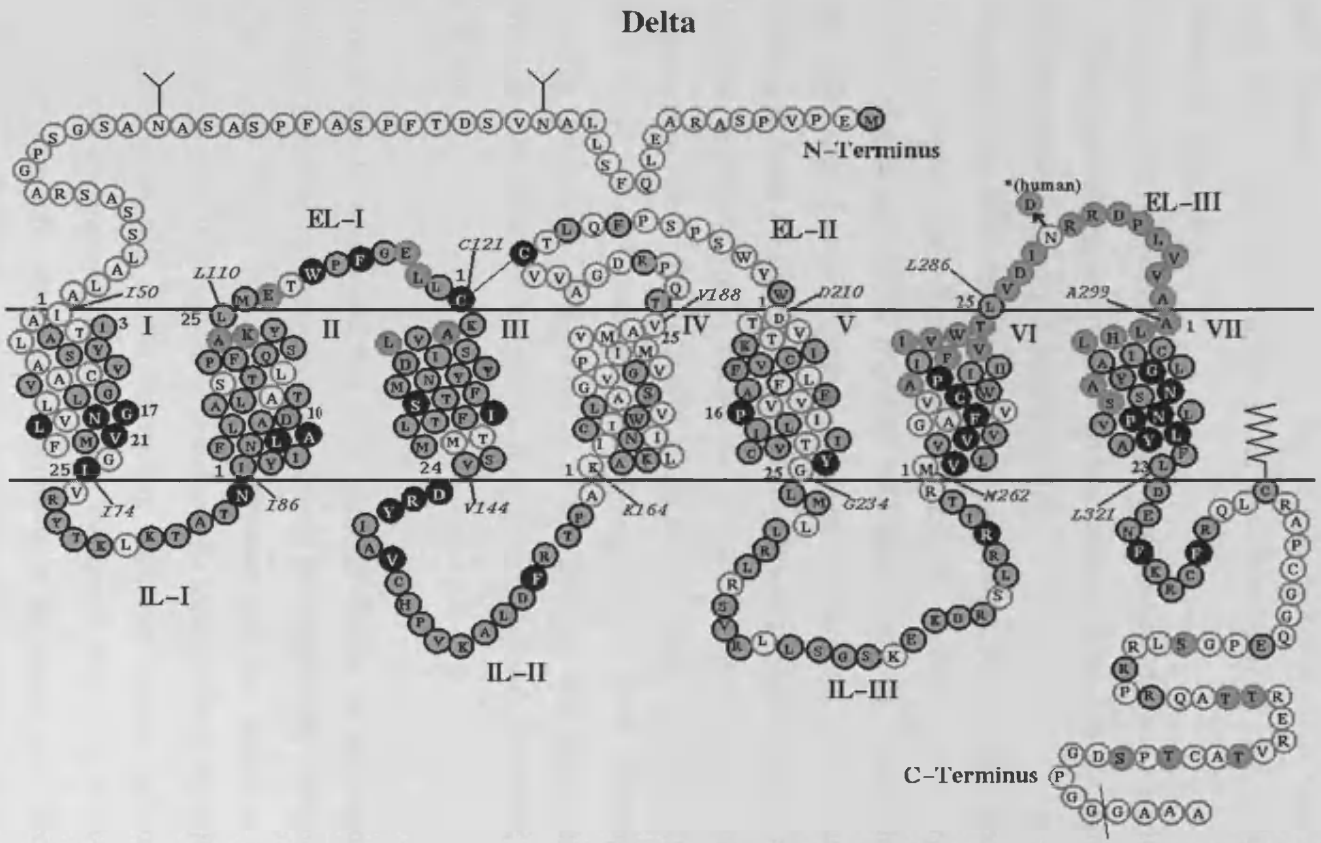

Figure 1-4. Seven domain spanning structure of *delta* (DOP) opioid receptor. Original source **www.opioid.umn.edu/ ptmut.html**

1.3.3 KOP

The kappa or KOP receptor was the second of the opioid receptor family to be cloned, see Figure 1-6. The prototypical agonist for the KOP receptor is the non-peptide benzomorphan, ketocyclazocine, the actions of which have been shown to be distinct from those elicited by stimulation of the MOP receptor, e.g. sedation without marked effects on heart rate.

In animals it is not possible to determine analgesia, which is a subjective state, therefore in animal paradigms antinociception is measured. However the term analgesia is used to describe antinociception in animal studies.

Two synthetic KOP receptor agonists, spiradoline (U-62,066E) and enadoline (CI-977) have undergone clinical trials for their analgesic actions (Wadenberg, 2003; Walsh *et al.*, 2001). Whilst spiradoline produced promising analgesia in animals, clinical data shows that spiradoline produces adverse effects such as diuresis, sedation and dysphoria at doses lower than those needed for analgesia. Enadoline produced similar side effects including sedation, confusion and dizziness along with increased urinary output and feelings of depersonalisation. The side effects elicited by these and other KOP receptor agonists have as yet limited their effective clinical usage. The advantage of KOP receptor agonists over other opioid ligands is that they do not cause respiratory depression, although their effective use may be limited by dysphoria. However, this is not seen in all subjects.

It must also be mentioned that KOP agonists display an anti-opioid action attenuating analgesia elicited by endogenously released or exogenously administered MOP agonists (Pan *et al.*, 2000). It has been hypothesised that this action is caused by a distinct distribution of KOP receptors on primary cells located within the NRM. The output from the NRM forms part of the descending inhibitory control pathway acting to dampen nociceptive transmission at the level of the spinal cord. The NRM consists of primary and secondary cells whose axons terminate in the spinal cord. Secondary cell firing is suggested to facilitate nociceptive transmission (important during opioid withdrawal) whilst primary cells are suggested to inhibit spinal pain transmission. Analgesia elicited by exogenously applied opioids is mainly via agonist activity at the MOP receptor. It has

been shown that MOP receptors are situated only on secondary cells of the NRM. Inhibition of secondary cells via MOP receptor activation removes the presynaptic GABA-ergic input to primary cells and dis-inhibition of them, see Figure 1-5. This dis-inhibition, which equates to primary cell stimulation, results in analgesia elicited at the level of the spinal cord. KOP receptors are localised only on the primary cells of the NRM and the anti-analgesic effect of KOP receptor agonists is caused by inhibition of the primary cells thus preventing indirect stimulation mediated through the MOP receptor pathway.

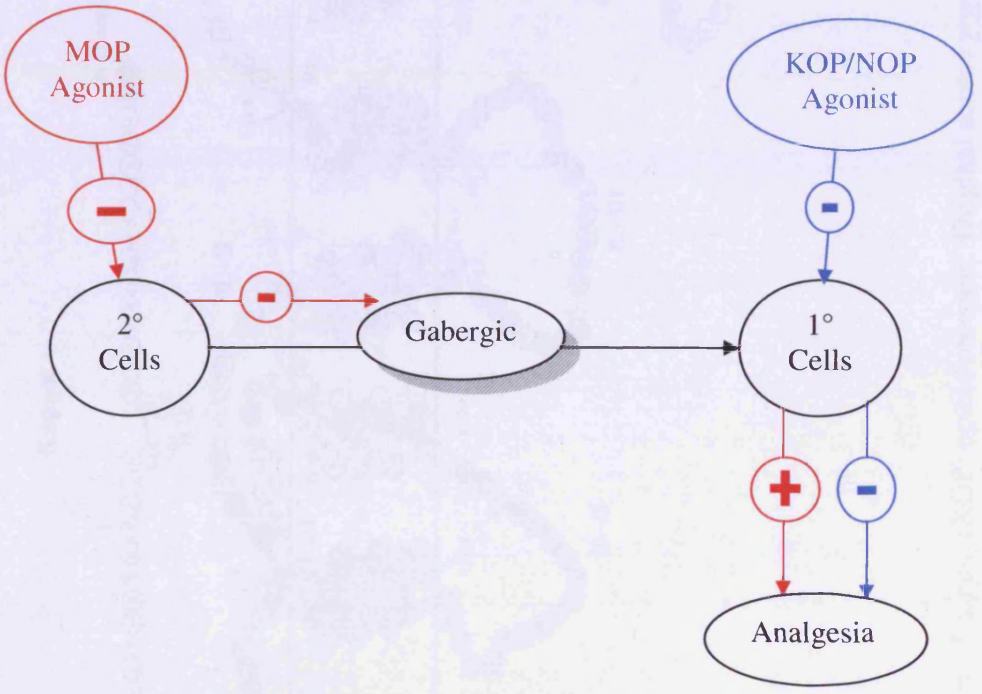

Figure 1-5. In the NRM stimulation of primary cells is suggested to induce analgesia via activation of descending inhibitory control pathways and release of endogenous opioids. MOP agonists cause analgesia through inhibition of secondary cells which removes a GABA-ergic tone and leads to disinhibiton of primary cells and analgesia (pathway highlighted in red). KOP and NOP receptors are situated on primary cells and their anti-opioid action is from a direct inhibition of these cells and prevention of the MOP mediated disinhibition (pathway highlighted in blue) (Modified from (Pan *et al.*, 2000))

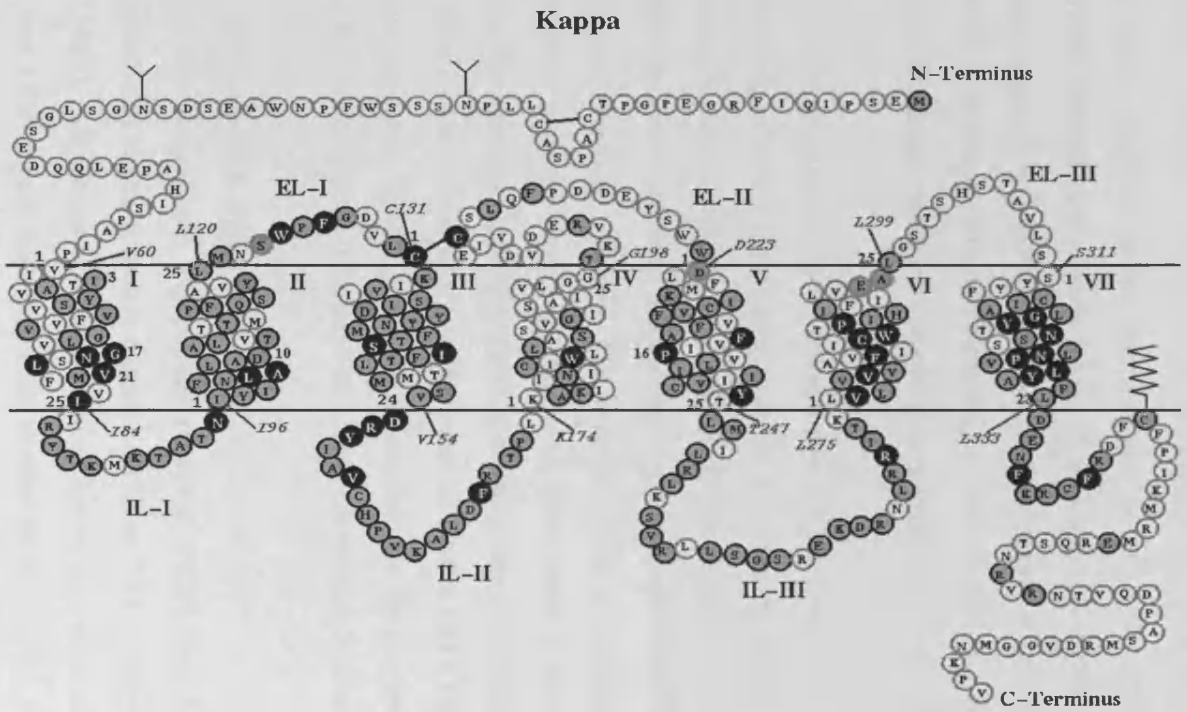

Figure 1-6. Seven domain spanning structure of *kappa* (KOP) opioid receptor. Original source **www.opioid.umn.edu/ ptmut.html**

Introduction

In KOP receptor KO mice no alteration in mechanical or thermal pain was measured although this species did show increased sensitivity to peritoneal acetic acid injections. This finding is in agreement with other studies that have demonstrated a role for KOP receptors in visceral pain. Neuropathic pain studies have been carried out in mice genetically modified to be devoid of prodynorphin. Persistent neuropathic pain through spinal nerve ligation caused hyperalgesia in both prodynorphin KO and wildtype littermates. Whilst hyperalgesia persisted in wildtypes, in prodynorphin KO animals pain response returned to base line values in a few days. Elevated dynorphin levels where measured in wildtype mice and believed to be responsible for the pronociceptive response caused in this neuropathic pain model (Gaveriaux-Ruff *et al.*, 2002; Kieffer, 1999).

1.3.4 Multiple classical opioid receptor knockout species

Interbreeding of individual opioid receptor KO species lead to the development of triple KO mice devoid of MOP, DOP and KOP receptors. The triple mutants developed normally and were healthy suggesting opioid receptors are not important for normal growth and viability. Triple KO animals have been used to study 'abnormal' or controversial pharmacology that surrounds some areas of the opioid receptor field. For example the immunosuppressor actions of delta-selective ligand naltrindole were shown to be independent of the DOP receptor and an absence of [^{3}H]naloxone binding in triple KO mice shows no further genes are responsible for the production of opioid receptors or opioid-like binding sites (Clarke *et al.*, 2002; Gaveriaux-Ruff *et al.*, 2002).

1.3.5 Nociceptin & NOP

The nociceptin orphanin FQ peptide receptor (NOP) was first reported as an opioid receptor-related clone, formerly named LC132 or ORL-1 (Mogil *et al.*, 2001; Reinscheid *et al.*, 1995). Alignment of cDNA-deduced amino acid sequences for human NOP, MOP, KOP and DOP reveal high sequence conservation (>70%) is restricted to the second, third and seventh transmembrane (TM) helices, see Figure 1-7 (Reinscheid *et al.*, 1996). Other TM regions show conservation to varying degrees, 50% in the TM 1, 5 and 6 sequences and 24% at TM 4. Sequence identity of NOP receptor intracellular loops are also closely conserved (56-86%) with classical opioid receptors. The majority of other

sites bear few similarities. Location of NOP-like receptor sequences in ancient species, such as teleost fish, propose close evolutionary ties to the opioid receptor family (Darlison *et al.*, 1997). The receptor remained orphan until its endogenous ligand, nociceptin/orphanin FQ (N/OFQ) was isolated simultaneously from brain extracts by Meunier (Meunier *et al.*, 1995) and Reinscheid (Reinscheid *et al.*, 1995).

Identification of GPCRs through homology screening has created a large pool of ligandless 'orphan' receptors. A process dubbed "orphan receptor strategy" has been applied in order that ligands for these receptors may be identified. The strategy works through recombinant expression of the orphan receptor in a host cell. Extracts from tissues that are believed to express the cognate ligand are screened against the orphan receptor. A second messenger pathway is studied to monitor receptor activity. Subsequent fractionation and purification is used to discover the specific ligand from the intial mixture of naturally occurring ligands, see Figure 1-8. Controls with non-transfected cells are made so activity at receptors natively expressed by the host cell is not mistaken. As well as N/OFQ other bioactive peptides identified using this methodology include hypocretins/orexins and Urotensin II (Ames *et al.*, 1999; Civelli *et al.*, 2001) Figure 1-8. This mode of receptor – ligand identification has been dubbed 'reverse pharmacology' i.e. receptor first and ligand second and identification of N/OFQ is the first published example of its use.

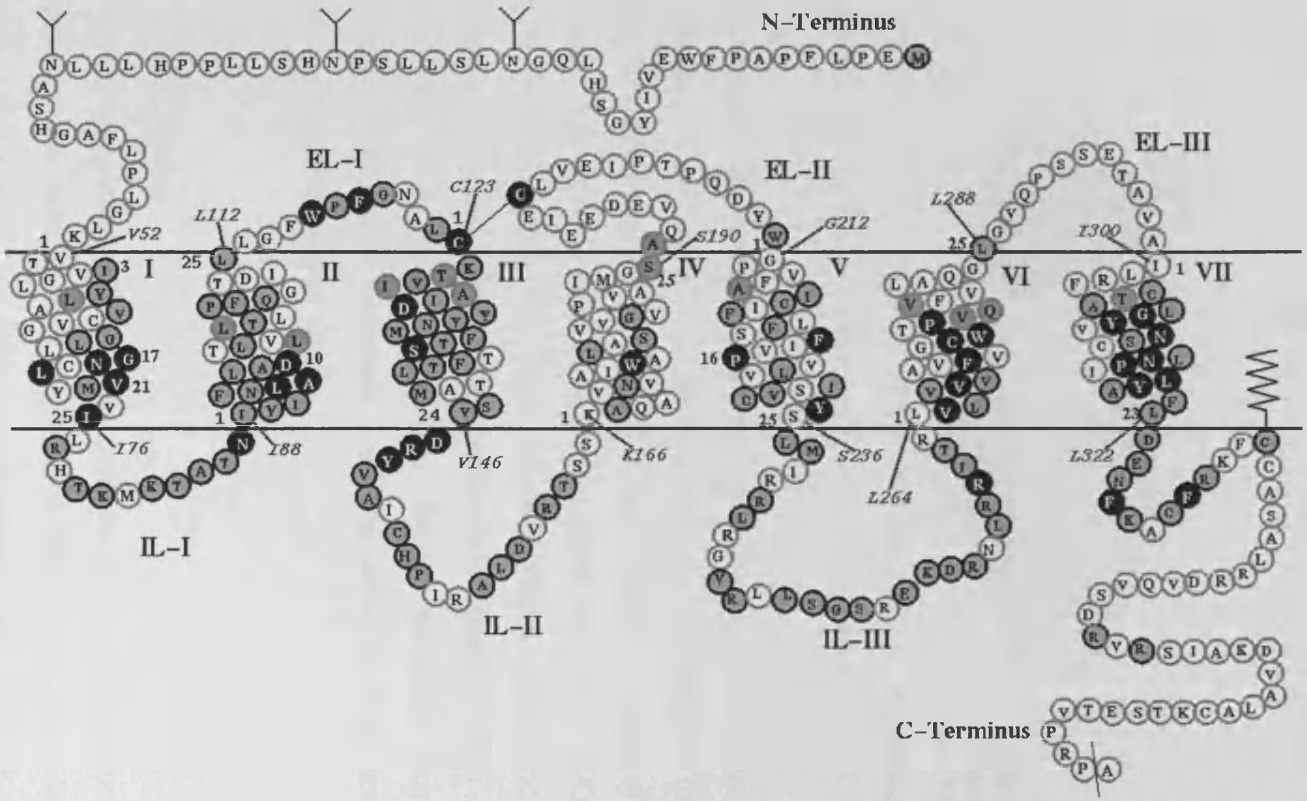

Figure 1-7. Seven domain spanning structure of *ORL1* (NOP) opioid receptor. Original source **www.opioid.umn.edu/ ptmut.html**

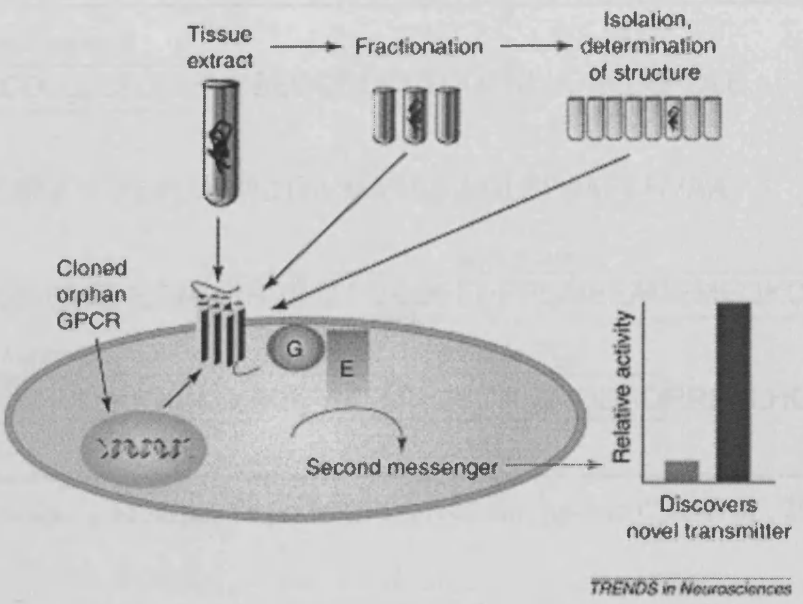

Figure 1-8 Depiction of the "orphan receptor strategy", taken from (Civelli *et al.*, 2001).

The observation that NOP regulates similar transduction mechanisms to those of opioids (see Cellular Actions of N/OFQ), the high sequence homology of the endogenous KOP receptor peptide dynorphin A to N/OFQ and abundant overlap of the NOP receptor distribution with classical opioid receptors suggest that NOP / N/OFQ are historically related to the opioid family. For these reasons IUPHAR recommendation is that NOP is considered a non-opioid branch of the opioid receptor family (Cox *et al.*, 2000).
However, the NOP receptor does not display naloxone sensitivity, a defining characteristic of all opioid rececptors – creating debate as to the taxonomy of the NOP receptor in the opioid receptor family.

1.4 N/OFQ Peptide

N/OFQ is a heptadecapeptide cleaved from the polypeptide precursor pre-pro N/OFQ (pp-noc). Several pairs of basic amino acids flank either side of the neuropeptide and represent excision motifs for proteolytic cleavage. Other peptides are also synthesised from the pp-noc precursor, the molecules orphanin FQ_2 and nocistatin (Figure 1-9) (Calo *et al.*, 2000c; Meunier, 2000).

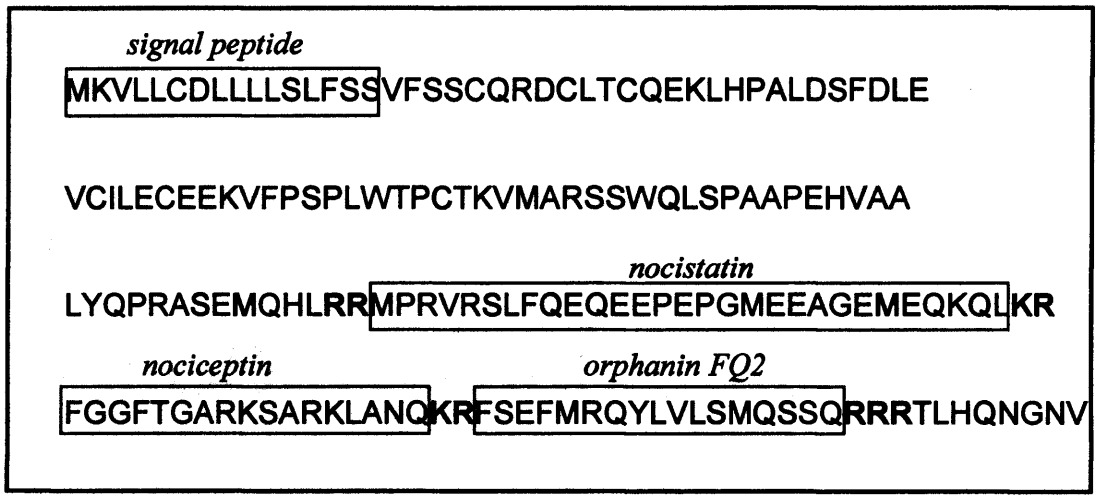

Figure 1-9. Amino acid sequence for N/OFQ precursor, pp-noc(Calo *et al.*, 2000c).

N/OFQ shows greatest sequence homology to the endogenous KOP opioid agonist dynorphin A. However, N/OFQ lacks the key to opioid receptor occupancy / activation, a N-terminal tyrosine and hence displays no selectivity for KOP (Meunier, 2000). Degradation of the N/OFQ peptide is principally via aminopeptidase N, which releases the inactive N/OFQ(2-17) and endopeptidase 24.15, which cleaves a variety of bonds to release inactive fragments, Figure 1-10 (Terenius *et al.*, 2000). It has been shown that some N-terminal cleavage fragments of N/OFQ, whilst lacking activity at NOP, can cause primary afferent C-fibres to release substance-P. The mechanism of action for this release has yet to be determined (Terenius *et al.*, 2000).

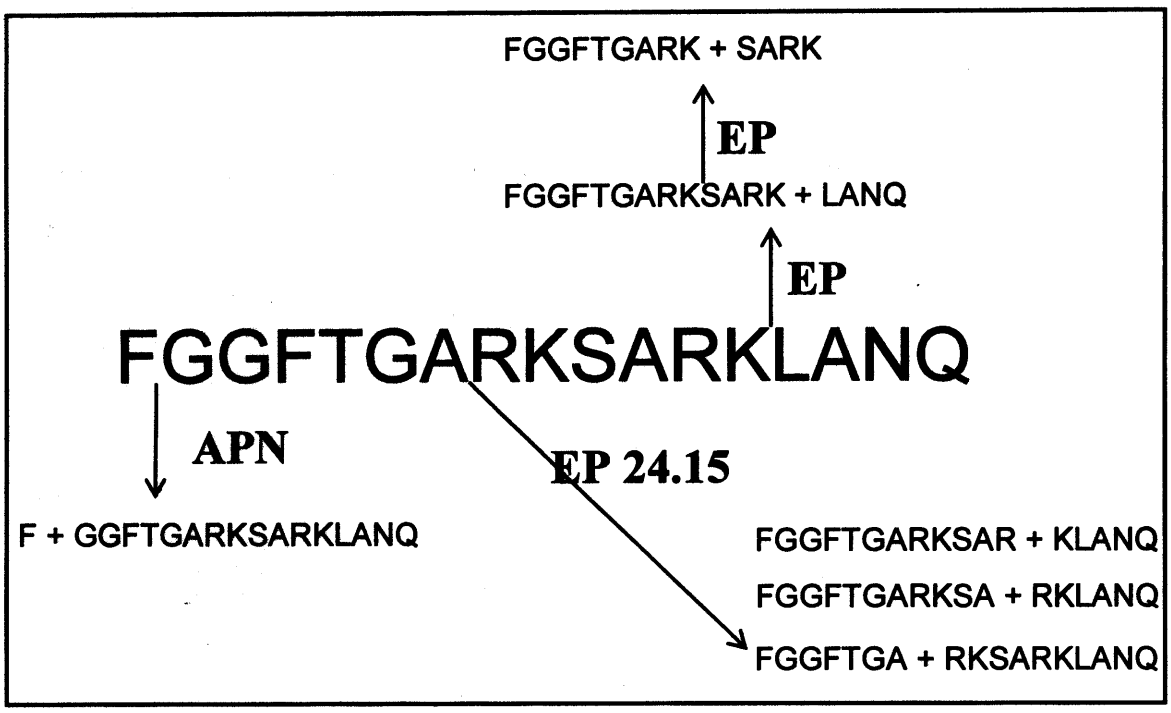

Figure 1-10. N/OFQ metabolism by aminopeptidase N (APN) and endopeptidases, from(Calo *et al.*, 2000c) .

Removal of the first amino acid (Phe^1) of N/OFQ results in decreased affinity by ≥2000-fold at the NOP receptor. C-terminal degradation also leads to a reduction in binding affinity of N/OFQ for NOP, loss of the 4 amino acids from the C-terminal tail as in N/OFQ(1-13) results in a 30-fold reduction in potency (Butour *et al.*, 1997). However amidation of the C-terminus of N/OFQ(1-13) restores ligand affinity and potency, consequently N/OFQ(1-13)NH_2 is the shortest sequence retaining the full biological activity of the endogenous ligand (Guerrini *et al.*, 1997). There is a stepwise reduction in affinity with the subsequent removal of C-terminal amino acids from N/OFQ(1-13).

1.5 Cellular effects of N/OFQ

The cellular actions of the classical opioid receptors (MOP/KOP/DOP) and the NOP opioid receptor have been shown to be pertussis toxin (PTX) sensitive and therefore couple to inhibitory G-proteins i.e. G-proteins with $G_{i/o}$ alpha subunits (Reinscheid *et al.*, 1996). Activation of all opioid receptors leads to; (i) closing of voltage sensitive calcium channels (VSCCs), (ii) stimulation of potassium efflux leading to hyperpolarisation, and (iii) reduced cyclic adenosine monophosphate (cAMP) production via inhibition of adenylyl cyclase. Overall this results in reduced neuronal cell excitability leading to a reduction in transmission of nerve impulses along with inhibition of neurotransmitter release (see Figure 1-11) (Hawes *et al.*, 2000).

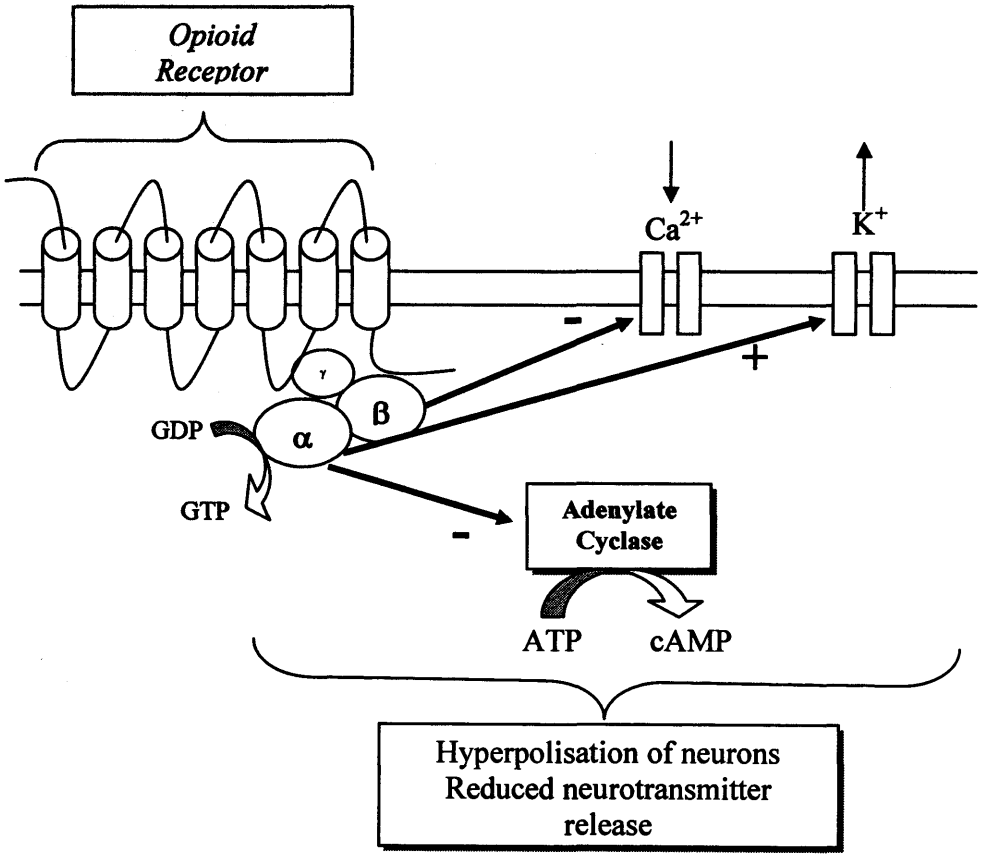

Figure 1-11. Cartoon depiction of intracellular responses to NOP opioid receptor activation.

Introduction

Opioid receptors regulate the G-protein activated inwardly rectifying K^+ channel (GIRK) (Ikeda *et al.*, 1997). Through a direct interaction with GIRK, βγ subunits released from activated G-proteins activate the channel leading to potassium efflux and a more negatively charged (hyperpolarised), less excitable membrane. The current / voltage relationship of the N/OFQ induced potassium current has a reversal potential of ~-100mV and produces an outward current at a holding potential of ~-70mV (Luo *et al.*, 2001). N/OFQ mediated activation of GIRK has been demonstated in a variety of central sites including spinal cord (Faber *et al.*, 1996), locus coeruleus (Connor *et al.*, 1996), periaqueductal grey (Vaughan *et al.*, 1997a) and hypothalamus (Lee *et al.*, 1997).

High voltage activated calcium channels such as N- and P/Q-type channels are crucial for neurotransmitter release. VSCCs are inhibited by some GPCRs through voltage-independent (VI) and voltage-dependent (VD) processes. The VI inhibition can occur via multiple second messenger pathways and can be mediated by different subtypes of Gα and Gβγ. The VD inhibition is fast, can be removed through membrane depolarisation and is mediated through a direct interaction of the channel with Gβγ. Typically VD inhibition is from Gβγ released from PTX-sensitive G-proteins, G_o is believed to be the preferred donor (Dascal, 2001; Hille, 2001). N/OFQ inhibits VSCCs in a manner characteristic of βγ subunit mediated voltage-dependent block. N-type and P/Q-type calcium currents were the most sensitive. VSCCs inhibition has been demonstrated in a variety of preparations including the locus coeruleus (Connor *et al.*, 1999b), PAG neurons (Connor *et al.*, 1998) and trigeminal ganglion neurons (Borgland *et al.*, 2001). Overal the effect of N/OFQ on VSCCs leads to reduced transmitter release.

Activation of NOP inhibits forskolin stimulated cAMP production (Hawes *et al.*, 2000; Okawa *et al.*, 1998a). A role for cAMP in pain transmission, although not fully understood, has been suggested via regulation of a membrane K^+ current I_h. I_h is involved in the repolarisation of the membrane following action potential firing. Cyclic AMP enhances I_h causing a reduction in the refractory period. Hence elevated cAMP levels, as caused by some mediators of pain such as prostaglandins, will increase the frequency of action potential discharge and heighten pain sensation. By

reducing cAMP levels, as caused by N/OFQ and opiates, the converse is true and nociceptive transmission is reduced. Whilst this has been shown for the opioid drugs, N/OFQ has not been shown to interact with I_h (Ingram *et al.*, 1994).

Importantly, cAMP levels have been shown to play a role in the expression of the N/OFQ precursor. Elevated cAMP results in increased expression of N/OFQ. Since N/OFQ inhibits cAMP formation the system appears to show negative feedback regulation and may be important in the development of tolerance (Hawes *et al.*, 2000). Through cAMP dependent protein kinases the phosphorylation state of ion channels and receptors can be affected. In this way cAMP/adenylyl cyclase can influence neuronal synaptic transmission. For full review see (Mons *et al.*, 1995).

1.6 Spinal NOP Pre & Post-synaptic Effects of N/OFQ

N/OFQ has been shown to have both pre- and post- synaptic sites of action, consistent with an inhibitory mode of action. The superficial dorsal horn expresses high levels of NOP receptor and N/OFQ peptide mRNA (Anton *et al.*, 1996). The substantia gelatinosa of the superficial dorsal horn is an important point of regulation for signalling through Aδ and C-fibre primary afferent neurones. The evoked excitatory post-synaptic potentials (eEPSP) generated by Aδ and C-fibre primary afferents terminating on interneurons of the SG neurones are inhibited by N/OFQ, C-fibres were more sensitive to this action (Luo *et al.*, 2002). Luo *et al* hypothesise a pre-synaptic site of action for N/OFQ given; (i) a reduction in the frequency or inter-event interval of mEPSP is seen but their amplitude is unaltered (ii) no effect on exogenously applied AMPA. Significantly N/OFQ had no effect on evoked inhibitory post-synaptic current (eISPC), measured after the blockade of glutamatergic signalling by CNQX addition, gylcinergic and GABAergic pathways measured in the presence of strychnine and bicuculline respectively. Those currents measured were monosynaptic hence NOP receptors are inferred to be located on primary afferents but not SG neurons, this pattern of receptor distribution mirrors that of the MOP receptor (Luo *et al.*, 2002). In contrast to this study N/OFQ stimulated an outward potassium current at neurons in the SG of the trigeminal nucleus caudalis (Jennings, 2001). Hence a pre and post-synaptic site of action can be inferred for N/OFQ dependent on the site of administration/measurement. Neurons of the amygdala have additionally been shown to be sensitive to N/OFQ through a postsynaptic site of action (Meis *et*

al., 1998). In both the lateral and central amygdala projection neurons, the latter being more responsive, N/OFQ brought about a reduction in cell excitability through activation of inwardly rectifying potassium currents (Meis *et al.*, 1998). Amygdala is a central site for integration of fear and anxiety hence reduction in its activity is synonymous with the anxiolytic profile of N/OFQ in behavioural paradigms.

Additional studies of N/OFQ using spinal electrophysiology have shown a bidirectional effect on Aδ-fibre evoked monosynaptic electrical field potential responses in superficial spinal dorsal neurons but a unidirectional response when measuring polysynaptic field potentials. For monosynaptic Aδ-fibre evoked potentials low doses of N/OFQ potentiated the response whilst higher doses were inhibitory, N/OFQ depressed polysynaptic Aδ-fibre evoked potentials (Ruscheweyh *et al.*, 2001). Certainly this highlights a knowledge that N/OFQ acts at primary junctions between Aδ-fibres and spinal neurons but also impinges on synapses further down stream.

The bidirecional activity of N/OFQ seen in spinal electrophysiology is mirrored in numerous analgesiometric studies of N/OFQ which have shown bell shaped response curves. N/OFQ administered i.t. at low doses (attomolar to picomolar) has been shown to drive spontaneous nociceptive behaviours, thermal hyperalgesia in both the hot plate and tail flick tests, hyperalgesia in formalin test and allodynia by innocuous tactile stimuli (Minami *et al.*, 1997). At higher doses N/OFQ produces analgesia in the tail flick test (King *et al.*, 1997) and formalin test (Wang *et al.*, 1999) and has further been shown to have anti-allodynic actions (Hao *et al.*, 1998).

In the tail flick test N/OFQ at pictogram doses induced hyperalgesia, mediated through the Neurokinin 1 (NK1) receptor - given the absence of an N/OFQ effect in the presence of NK1 receptor antagonists and NK1 receptor knockout mice. Therefore through substance-P mediated release and concomitant stimulation of primary afferent nerve fibres N/OFQ elicits hyperalgesia (Inoue *et al.*, 1998). In the spinal cord prostaglandin D_2 (PGD_2) causes hyperalgesia when administered alone but can block prostaglandin E_2 (PGE_2)-induced allodynia through activation of prostanoid receptors. PGD_2 blocked N/OFQ-induced allodynia but had no effect on hyperalgesic responses (Minami *et al.*, 1997). The prostanoid receptor agonist BW 245C also blocked N/OFQ-induced allodynia however N/OFQ was not implicated in release of

PGE_2 since pre-treatment with indomethacin was ineffective against N/OFQ induced allodynia (Minami *et al.*, 1997).

1.7 NOP Receptor Binding

Monovalent and divalent cations have been shown to play an important role in the binding of N/OFQ to NOP. Ardati *et al* (Ardati *et al.*, 1997) found that reducing the concentration of $MgCl_2$ to 0.125mM yielded non-analysable binding profiles. A minimum concentration of magnesium in the region of 1mM is required for saturation binding of [^{125}I]-Tyr-N/OFQ or [^{3}H]N/OFQ to HEK_{293} and CHO cells expressing the NOP receptor. Sodium is known to play an important role in ligand binding to classical opioid receptors hence its effect at the NOP receptor has come under scrutiny. NaCl at 5mM had little or no effect on the binding of [^{3}H]N/OFQ or [^{125}I]-Tyr-N/OFQ only reducing binding of the former by ~10%. Conversely at 120mM NaCl a 68% reduction in the binding capacity of [^{3}H]N/OFQ occurs whilst ≈80% reduction of [^{125}I]-Tyr-N/OFQ binding capacity is achieved at 100mM NaCl (Ardati *et al.*, 1997). Overall it was found that N/OFQ binding to NOP is sensitive Na^{+}, Ca^{2+}, Mn^{2+} and Zn^{2+} and optimal binding requires 5mM $MgCl_2$ (Ardati *et al.*, 1997). Worthy of a mention is the knowledge that physiological sodium concentrations are >100mM.

As mentioned the sequential shortening of N/OFQ(1-13) results in further and further loss of ligand affinity and potency, the 2 pairs of positively charged residues Arg and Lys at positions 8 ,9 and 12, 13 have been shown as an essential requirement for binding to the NOP receptor, for this reason it has been suggested that the C-terminal region after the 5th residue of N/OFQ is important for binding to the NOP receptor, the so-called address region (Guerrini *et al.*, 1997; Guerrini *et al.*, 2000b), see Figure 1-12.

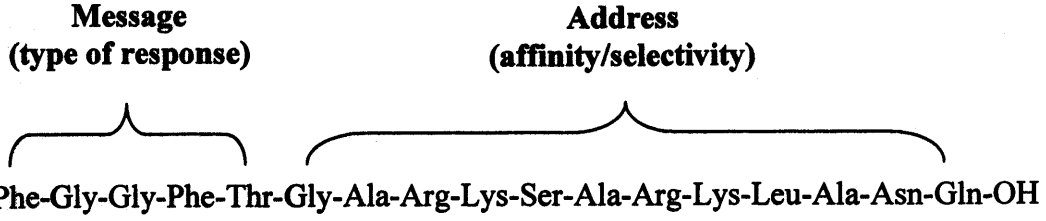

Figure 1-12. Peptide sequence of N/OFQ and hypothesised message and address domains (Guerrini *et al.*, 2000b).

Loss of the first amino acid, Phe^1, results in a complete loss of activity at NOP, although substitution of this residue for others with different chemical groups i.e. aromatic or aliphatic, is well tolerated. Indeed susbstitution of Phe^1 for Tyr^1 gives an analog of N/OFQ that has activity at classical opioid receptors and NOP, Tyr^1 is an essential requirement for classical opioid receptor binding. Phenylalanine in position four represents a determinant pharmacophore of N/OFQ since substitution with residues containing similar or different chemical groups is not tolerated, i.e. inactivity at the NOP receptor results. The spatial orientation of the N-terminal tetrapeptide is also essential for NOP receptor activity, substitution of Gly^2 and Gly^3 results in inactivity / reduced activity at the NOP receptor. For these reasons the N-terminal portion of N/OFQ is assumed the 'message' region of the peptide conferring information regarding receptor activation (Guerrini *et al.*, 1997; Guerrini *et al.*, 2000b).

In the absence of a high resolution 3D structure for the NOP receptor Topham *et al* utilized computational techniques in conjunction with data from mutation studies in order to develop an image of the functional architecture of the NOP receptor (Paterlini *et al.*, 1997; Pogozheva *et al.*, 1998). The Herzyk & Hubbard C^{α} template (Herzyk *et al.*, 1995) was used as a starting point for modelling the NOP receptor. Subsequent refinement of this model predicted that the first four amino acids of N/OFQ (FGGF) bind a transmembrane domain comprising elements of TM helices 3, 5, 6 and 7, analogous to the alkaloid binding pocket of the classical opioid receptors (Topham *et al.*, 1998). Two distinct hydrophobic pockets were shown to house the side chains of phenylalanine in positions 1 and 4. Chimeric studies of NOP-KOP receptors

highlight contact with the EL2 loop essential for N/OFQ activation of NOP. The highly basic core of N/OFQ (i.e. residues 8-13) is also necessary for receptor activation appearing to make contact with the acidic EL2. The first residues may aid the positioning of a ligand within the receptor binding pocket, consistent with the lack of activity of opioid ligands at NOP.

Overall a 3D image of the N/OFQ-NOP complex shows the binding of aromatic moieties of Phe 1 and 4 to a pocket located in a cavity formed by TM helices 3, 5, 6 and 7. Residues 5-7 of N/OFQ develop important associations with EL2, the connection of which is important for selectivity at NOP over KOP receptor.

1.8 N/OFQ metabolites

The major N/OFQ metabolic fragments produced in the brain of both rat and mouse, for example N/OFQ(1-13) and N/OFQ(1-7), lack substantial affinity for NOP, see Table 1-2. N/OFQ metabolites from human plasma N/OFQ(2-17) and N/OFQ(3-17) also lack activity at the NOP receptor, (Sandin *et al.*, 1999; Suder *et al.*, 2000).

Species	*Tissue*	*Bioactive Procedure*	*Main Fragemnts*
Rat	Brain	Microinjection into hippocampus	N(1-13), N(1-9)
Mouse	Brain	Incubation with cortical slices	N(1-7), N(1-11)
Rat	Brain cells in culture	Incubation with cell extract	N(1-13), N(1-9)
Rat	Spinal cord	Incubation with spinal cord tissue	N(1-11), N(1-6)
Human	Tumour cells in culture	Incubation with cell extract	N(1-13), N(1-9)
Human	Plasma	Incubation with plasma	N(2-17), N(3-17)

Table 1-2. Fragment determination of N/OFQ exposed to different *in vivo* samples/environments, from (Terenius *et al.*, 2000).

Despite several reports showing a lack of affinity of C-terminal N/OFQ fragments, some groups have demonstrated nociceptive responses from their application. Nociceptive flexor responses were measured in response to intraplantar injection of N/OFQ, N/OFQ fragments and other known nociceptive agents. C-terminal

fragments (8-17), (12-17), (13-17) and (14-17) all elicited nociceptive responses whilst N-terminal fragments (1-7) and (2-7) were devoid of this action. The hypothesised mode of action of the nociceptive flexor response is via the release of substance-P since the NK1 antagonist CP-99994 blocked the response to N/OFQ(13-17) (the most potent of the fragments under investigation). Interestingly the action of N/OFQ(13-17) was still present in NOP receptor knockout species whereas the nociceptive flexor response to N/OFQ was abolished. N/OFQ(13-17) has also been shown to have a pronociceptive action when applied to the spinal cord. The mechanism of N/OFQ(13-17) pronociception is not known (Inoue *et al.*, 2001; Rossi *et al.*, 1998). The N/OFQ fragment (1-11) whilst lacking appreciable affinity at the NOP receptor has been found to have antinociceptive actions *in vivo*. Curiously the action of N/OFQ(1-11) in the mouse tail withdrawal assay (a measure of nociceptive threshold) was seen to be sensitive to the opioid antagonist naloxone. Since naloxone lacks affinity at the NOP receptor either N/OFQ(1-11) antinociceptive action is mediated through a complex pathway leading to opioid release or N/OFQ(1-11) recognises a subtype of receptor *in vivo* sensitive to the opioid antagonist (Mathis *et al.*, 1998).

1.9 NOP localisation

Studies mapping the binding of N/OFQ and measuring mRNA for NOP indicate approximately the same distribution (Mollereau *et al.*, 2000). N/OFQ and its receptor are widely expressed throughout both CNS and PNS and show broad overlap with classical endogenous opioids and receptors. The rat cerebral cortex shows the greatest density of NOP receptors, B_{max} 179.7±15.3 fmol[^{125}I]Tyr^{14}-N/OFQ/mg protein, gross components of the brain stem show substantially lower expression B_{max} 52.3±0.8 fmol[^{125}I]Tyr^{14}-N/OFQ/mg protein, as does the cerebellum B_{max} 12.4±1.8 fmol[^{125}I]Tyr^{14}-nociceptin/mg protein (Okawa *et al.*, 1998b). In peripheral tissue NOP is located on the endings of sensory, parasympathetic and sympathetic nerves, where N/OFQ controls presynaptic release of signal mediators (Mollereau *et al.*, 2000). For example, in mouse and rat *vas deferens* N/OFQ inhibits twitches evoked by electrical field stimulation but not by exogenously applied noradrenaline, suggesting presynaptic NOP localisation on sympathetic nerve terminals (Calo *et al.*, 1996).

1.10 Spinal & Supraspinal Responses to N/OFQ

Application of N/OFQ has been shown to cause hyperalgesia, allodynia and analgesia. These conflicting findings are confounded by species and or strain differences in test animals, known to be fundamental in the supraspinal effects of nociception (Mogil *et al.*, 1999). However, the route of administration and nociceptive paradigm under investigation are of paramount importance.

There is much controversy over the supraspinal effects of N/OFQ. Original studies reported intracerebroventricular (i.c.v.) administration caused hyperalgesia compared to vehicle-treated groups (Meunier *et al.*, 1995; Reinscheid *et al.*, 1995). It has since been shown that there is no difference in the pain threshold of i.c.v. N/OFQ administered-groups and vehicle administered groups. Therefore it is assumed that N/OFQ does not cause hyperalgesia but reverses the opioid mediated stress induced analgesia caused by the experimental procedure (Calo *et al.*, 1998). The anti-opioid role of N/OFQ has subsequently been validated and N/OFQ is known to counteract analgesia elicited through the endogenous opioid system and analgesia from exogenously applied morphine. Chronic use of MOP receptor analgesics, such as morphine, results in tolerance and a reduction in analgesia from a fixed dose. The anti-analgesic action of the NOP – N/OFQ system may play a key role in development of this type of tolerance. Indeed it has been shown that NOP knockout mice show a partial loss of tolerance to morphine and that there is up regulation of N/OFQ production in chronic morphine tolerant mice (Kest *et al.*, 2001). Ueda *et al* demonstrated that the analgesic tolerance developed from repeated exposure to morphine was markedly attenuated in NOP knock out mice. Acute morphine analgesia was unaffected in NOP KO species. This action has also been confirmed through the actions of potent selective NOP antagonists, which additionally attenuate morphine tolerance (Ueda *et al.*, 2000). These findings suggest the NOP / N/OFQ system contributes to the neuro-plasticity that accompanies tolerance from chronic morphine exposure (Ueda *et al.*, 2000). NOP blockade may prove useful in reducing tolerance to opioids and/or reducing the dose required to provide analgesia (Kest *et al.*, 2001).

Tolerance to the analgesia elicited by spinal application of N/OFQ develops after repeated administration although cross-tolerance to classical opioid drugs is not apparent. This suggests a unique distribution of classical opioid and NOP receptors in

the spinal cord. The spinal dose response curve for N/OFQ has been shown by some to be bell shaped, with low femto-molar doses causing hyperalgesia and higher nano-molar doses generating anti-nociception (Inoue *et al.*, 1998; Sakurada *et al.*, 1999).

1.11 Physiology of N/OFQ anti-opiate action

Early studies of the NOP / N/OFQ system concentrated on a role in pain, elucidating the anti-opioid action of N/OFQ. Immunostaining of the PAG reveals high levels of NOP distinct from those of the opioid receptor MOP (Meunier *et al.*, 1995). The anti-opioid effect of N/OFQ is caused by NOP receptor localisation on primary cells of the NRM giving rise to their inhibition, analogous to the KOP receptor pathway mentioned previously, Figure 1-5. It is believed that endogenous levels of N/OFQ may act to set threshold to pain, since NOP receptor antagonists have been shown to give rise to a long lasting analgesia. NOP receptor antagonists may have a possible future as novel analgesics or may be used as an adjuvant to reduce the amount of classical opioid drug required to produce analgesia. Consequently this may reduce the side effects encountered when using classical opioids (Calo *et al.*, 2005; Heinricher *et al.*, 2001; Pan *et al.*, 2000).

1.12 NOP and Anxiolytic-like Action

N/OFQ has been studied in a number of different paradigms that probe anxiety elicited through different stimuli, for example light-dark preference, elevated plus maze test and operant conflict. Low i.c.v. doses (0.1-3mmol) of N/OFQ provide anxiolysis to these acute anxiogenic environments. Further, low doses of N/OFQ stimulate exploratory behaviour that is believed to be through an anxiolytic action, since exploration is a manifestation of reduced anxiety in animals and classical anxiolytic drugs display a similar action profile (Jenck *et al.*, 1997). Higher doses of N/OFQ cause impairment of and reductions in locomotor activity.

1.13 Modulation of Spontaneous Locomotor Activity

At higher doses (1-10nmol) N/OFQ inhibits locomotion, an action which is insensitive to naloxone, reversed by naloxone benzoylhydrazone (NalBzOH) – (a NOP receptor antagonist, and agonist of classical opioid receptors), and absent in NOP receptor deficient mice (Noda *et al.*, 1998). The locomotor inhibitory effect of N/OFQ is potentiated by addition of peptidase inhibitors although the inhibitors have

no activity alone, suggesting that N/OFQ is not tonically involved in locomotor activity. Conversley other groups have reported hyperlocomotor actions of N/OFQ (Florin *et al.*, 1996), however these actions were reported at lower doses than those demonstrating hypolocomotor activity. The hypolocomotor effect seen in wild-type animals is not seen in NOP receptor KO species validating the role of NOP receptors in this action. NOP receptor KO mice displayed no change in basal locomotor activity suggesting that endogenous NOP tone does not play a role in the regulation of locomotion (Nishi *et al.*, 1997b).

1.14 G-protein Structure

Heterotrimeric G-proteins, as the name suggests, are made from three distinct subunits; alpha (α), beta (β) and gamma (γ). There are numerous gene products encoding for the different subunits; 20 for α, 6 for β and 12 for γ are currently known (Pierce *et al.*, 2002). The NOP receptor activates G-proteins possessing inhibitory α-subunits i.e. G-$\alpha_{i/o}$ subunits.

1.14.1 Alpha Subunit Structure

The alpha subunit has two distinct domains one involved with the binding of GTP and responsible for GTP hydrolysis i.e. its GTPase activity, the other, a coiled region responsible for directing the GTP nucleotide into the core of the subunit. Alpha subunits contain flexible regions designated "Switches", three are apparent designated Switcth; I, II and III. Switch regions are characterised by the more rigid structure they adopt on binding GTP. The core of Gα consists of a guanine nucleotide binding site (made from ~200 residues), which forms a centrally located six-strand β sheet surrounded by 5 α-helices. Polypeptide loops, designated G1-G5 form the guanine nucleotide binding site and are responsible for linking the α-helices and β strands, for example the G-1 loop (a diphosphate-binding loop) links α1 and β1 and makes contact with guanine nucleotides at α and β phosphates. G-3 is situated at the N-terminus of α2 links subsites that are important for the binding of GTP and Mg^{2+}, see Figure 1-13.

A conserved sequence on G-4, the link between the β5 strand and α4 helix, recognises the guanine ring whilst G-2 between α1 and β2 takes part in the coordination of Mg^{2+} adherence through a conserved threonine residue.

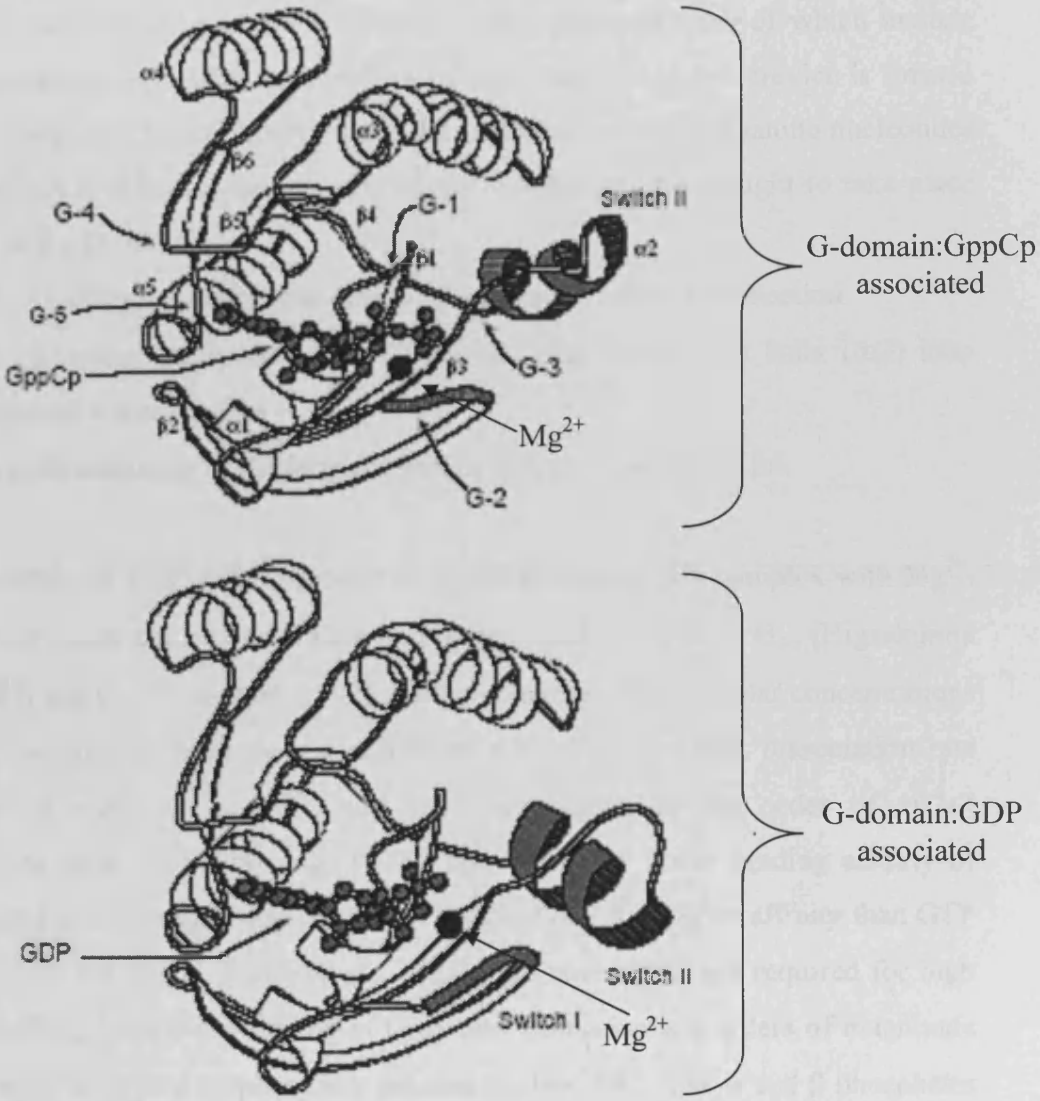

Figure 1-13. Schematic of Ras, representative of the G-domain of heterotrimeric G-proteins. Top is the G-domain in complex with GppCp (stable analog of GTP) and Mg^{2+}, bottom is the same G-domain in complex with GDP and Mg^{2+} (Sprang, 1997).

It is relevant at this point to establish a basic nomenclature to aid future description; G-box will be used to denote elements of the guanine nucleotide binding site or residues located within them whilst G-domain denotes the entire Ras-like or GTPase domain that is the conserved core in all G-proteins, see Figure 1-13.

G-protein alpha subunits are characterised by the G-domain with an additional four insertions (see Figure 1-14);

1. The largest insertion is between the α1 helix and β2 strand of the G domain. An independently folded 6-helical domain, proposed roles of which include increasing GTP affinity as well as effector recognition. A crevice is formed between this helical insertion and the G-domain in which guanine nucleotides associate, although the majority of the connections are thought to take place with the G-domain
2. An Asp/Glu-rich loop extending the β4 strand – helix α3 connection
3. A 20 residue extension of the β5 strand that folds into a helix (αG) loop segment following G-4
4. A short extension of the loop connecting helix α4 and strand β6.

The association of GTP with G-protein α-subunits happens as a complex with Mg^{2+}. Off rates for guanine nucleotides have been determined, for GTP at $G_{o\alpha}$ (Higashijima *et al.*, 1987) and $G_{i\alpha1}$ (Lee *et al.*, 1992), (in the presence of micromolar concentrations of Mg^{2+}) dissociation rates were found to be $<10^{-3}s^{-1}$. For GDP, dissociation rate constants (at subtypes $G_{i\alpha}$, $G_{o\alpha}$ and $G_{s\alpha}$), are greater in the order of $10^{-2}s^{-1}$ (Higashijima *et al.*, 1987; Sprang, 1997). This relatively lower binding affinity of GDP is not a conserved phenomenon, for example GDP has higher affinity than GTP at $G_{z\alpha}$. Both the α and β phosphates of guanine nucleotides are required for high affinity binding, indeed the binding of GMP and guanosine is 6-orders of magnitude lower relative to di- and tri-phosphate guanine nucleotides . The α and β phosphates of guanosine diphosphate are enveloped by the G-1 arm of the G-alpha subunit, amide groups of which offer hydrogen bond donors to phosphate oxygen acceptors on guanine nucleotide molecules. This process being central for binding. The binding of GTPγ-phosphate and magnesium converge at G-2 (switch I) and G-3 (switch 2) of the G-domain. The binding of Mg^{2+}, in the presence of GTP, is coordinated through association with six different regions, two of which are located on GTP. Upon hydrolysis of GTP the γ-phosphate magnesium scaffold diminishes, reducing the affinity of magnesium for the G-domain (Sprang, 1997).

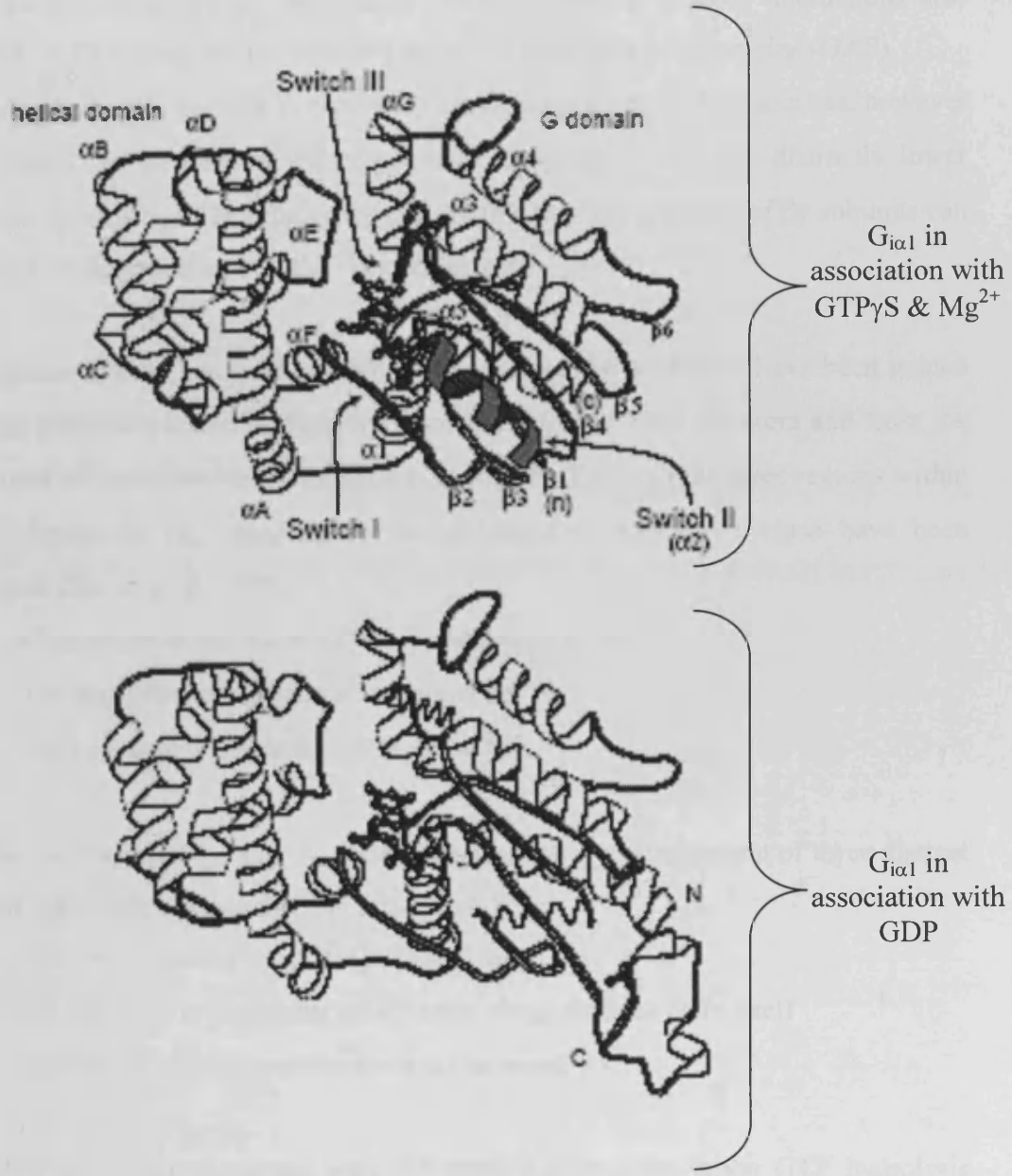

Figure 1-14. Heterotrimeric G-protein alpha subunit in association with GTPγS (Top) and GDP (Bottom). Switch regions are marked as darkened regions (Sprang, 1997).

While magnesium is important for the binding of GTP it has no effect on binding affinity of GDP for Gα-subunits. Mg^{2+} and GTP binding sites are closely associated with one another such that in the absence of Mg^{2+} the dissociation rate of GTP is increased ten-fold. Through acquisition of energy on the binding of GTP, Gα-subunits go through a structural re-conformation, by means of stabilisation of the switch regions. These changes in the tertiary structure of Gα expose regions of the

subunit involved with effector association and activation. Energy from effector-Gα-GTP association stabilises the binding of GTP, however effector interactions also facilitate GTP hydrolysis, i.e. effectors act as GTPase activating proteins (GAP).
The affinity of GDP for free Gα-subunits is moderate and slowly dissociates, however when Gα is in association with βγ-subunit dissociation rates are distinctly lower therefore increasing GDP affinity for Gα. In this way the presence of βγ subunits can preclude the dissociation of GDP (Higashijima *et al.*, 1987).

Elucidation of sites involved in effector recognition and activation have been gained through chimeric protein studies on Gα-subunits for different effectors and from the structures of Gα-GTPγS-Mg^{2+} relative to Gα-GDP. For example three regions within the G-domain of $G_{\alpha s}$ involved in the activation of adenylyl cyclase have been identified (Berlot *et al.*, 1992);

1. C-terminus of the α2-helix, encompassed by switch II
2. the loop connecting helix α3 to strand β5
3. the loop connecting helix α4 to strand β6

In a similar manner $G_{i\alpha 1}$ and $G_{t\alpha}$ show conformational rearrangement of three distinct regions upon GTP hydrolysis (Itoh *et al.*, 1991);

1. Switch I, also known as the 'effector' loop
2. Switch II, loop preceding the α2 helix along with the helix itself
3. Switch III, loop connecting helix α3 to strand β5.

Switch I and II are important sites for effector interaction, upon GTP hydrolysis rearrangement or distortion of these flexible regions leads to the opening of a cleft between the G-domain structure and the helical domain. This conformational change facilitates the accessibility of GDP for the guanine nucleotide binding site. The different affinities of Gα-GDP and Gα-GTP for effectors further highlights distinctions in their tertiary structures.

It has been shown from crystal structure that the point of contact between GPCR and Gα is 20°A($20*10^{-10}$metres or 2nm) away from the GDP binding site of Gα, thus receptor mediated GDP disociation is not caused by local contact with the

corresponding guanine nucleotide binding site but acts at a distance. This produces a conformational change in protein structure and subsequent release of GDP.

The putative point of contact between G-protein alpha subunits and their concomitant GPCR is believed to be located in the Gα C-terminus. Studies using receptor binding peptides (either acting to mimic the G-protein or to prevent receptor association with the G-protein) suggest that the last 7 C-terminal amino acid residues are important for selectivity/affinity of G-protein and receptor association. (Martin *et al.*, 1996). The importance of the extreme C-terminus of the Gα subunit in receptor interaction can be highlighted through the use of pertussis toxin, which causes ADP-ribosylation of the last four residues of Gα of $G_{i/o}$ G-proteins, in this way preventing their activation (Milligan, 1988).

1.14.2 Beta, Gamma Subunit Structure

The structure of the Gβ subunit consists of two structurally distinct regions: (a) an amino terminal segment 20 amino acids in length and (b) a propeller like structure formed from 7 WD40 repeats (aspartic acid / tryptophan repeats) see Figure 1-15. WD repeats form part of a family of proteins with diverse roles, hence no distinct functional role is afforded to these proteins -although one common theme is a position within larger protein structures suggestive of a role as an assembly protein (Smith *et al.*, 1999). This would correspond with the role of Gβ within the heterotrimeric structure. Gγ is a helical protein and makes numerous connections to the base of Gβ, the N-termini of both subunits form a coiled coil structure with the two proteins only separable under protein denaturing conditions. The connection of Gα and Gβγ subunits is through association of the βγ dimmer with a hydrophobic pore present on α-GDP, the presence of this pore is compromised by GTP binding to α-subunits leading to reduced affinity for βγ and subsequent dissociation of the heterotrimer (Cabrera-Vera *et al.*, 2003).

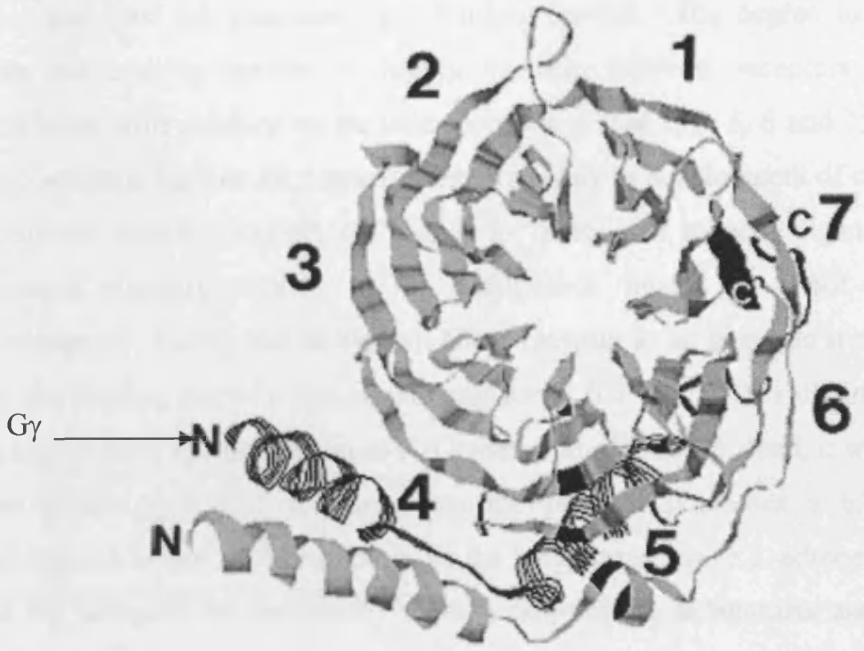

Figure 1-15. Gβ and Gγ dimer. Gβ forms a 7-bladed propeller and Gγ is an alpha helical structure situated toward the base of Gβ. A coiled coil structure can be seen formed by the N-termini of Gβ and Gγ.

Current consensus is that the Gβγ subunit is either essential or greatly enhances receptor Gα association (Sprang, 1997). The Gβγ has further been implicated in Gα guanine nucleotide exchange and hence G-protein activation and dissociation. Studies have revealed a distinct cavity between the Gα and Gβγ subunits into which Gβγ is orientated upon receptor activation and a subsequent conformational change is believed to facilitate the dissociation of GDP from Gα, hence Gβγ is hypothesised to be acting like a gate for the exchange of GDP for GTP.

1.14.3 Peptide-Receptor Interactions

Small molecule transmitters such as the biogenic amines (epinephrine, norepinephrine, dopamine, histamine etc) tend to bind to discrete sites within the binding pocket of the recptor whereas the binding of peptide ligands also involves interactions with the extracellular loops. With regard to family A peptide receptors which include angiotensin, bradykinins and opioids, there is evidence for important interactions of ligands with the amino terminus and extracellular loops of these receptors. Ligand interactions with this group of receptors often requires critical

involvement of the transmembrane binding crevice. The degree to which ligands enter the binding crevice is highly variable between receptors and comprise association with residues on the outer portions of TM 2, 3, 5, 6 and 7. Identification of non-peptide ligands for peptide receptors is key to development of clinically useful therapeutic agents. Indeed, the search for functional mimetic ligands, given their structural disparity relative to the endogenous ligand, is a hot topic in drug development. Taking the tachykinin NK-1 receptor as an example it has been shown that the binding site of a non-pepide antagonist (CP-96, 345) is distinct from that of the endogenous agonist substance P (Gether *et al.*, 1993). Indeed, it was summarized from studies of NK-1 receptors that the receptor possesses a binding crevice, synonymous to that of the receptors for the biogenic amine (e.g. adrenergic receptors), that are occupied by structurally distinct non-peptide antagonists and interact with distinct receptor sites. Importantly those regions of the receptor occupied by these non-peptide ligands appear not to be involved in the binding of the endogenous agonist substance P (Gether *et al.*, 1993). Consequently competitive antagonism need not always require overlapping of the binding site with that of the agonist.

These differences in ligand-receptor interactions of peptide and non-peptide ligands has been demonstrated for many family A GPCRs including opioids, showing that non-peptidic ligands are interacting with a binding crevice formed by the TM domains whilst peptidic ligands will interact to varying degress with the binding crevice, they preferentially have major interactions with the extracellular loops of GPCRs (Kong *et al.*, 1994).

1.15 G-protein coupled receptor architecture

Knowledge of 'general' GPCR architecture has been gained from studies with rhodopsin, bovine rhodopsin providing the first atomically resolved (9°A) structures from electron cryomicroscopy of 2-D crystals (Schertler *et al.*, 1993).

Projection maps of the crystallographies and alignment of different receptor sequences has been used to detail the position and orientation of the transmembrane helixes. These studies have revealed sequential ordering of the helices in an anticlockwise manner (as viewed from the extracellular side) Figure 1-16. The

helices do not typically appear perpendicular to the membrane plane, indeed helices 1, 2 and 3 are tilted 27-30 degrees, helix 5 a 23 degree angle, 4, 7 and 6 are close to perpendicular although the extracellular portion of 6 is tilted (Unger *et al.*, 1997). The arrangement of the helices is such that they are more open on the extracellular surface, forming a hypothesized binding crevice lined by helices 3, 4, 5, 6 and 7, whilst at the cytoplasmic face the arrangement is such that the helices are closer to one another (Unger *et al.*, 1997).

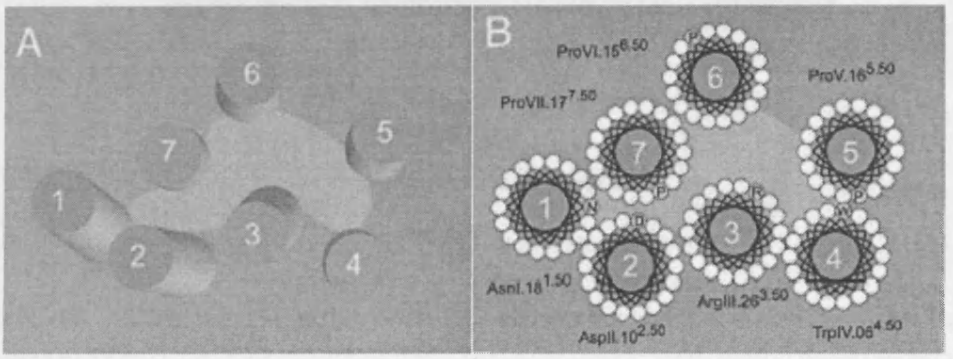

Figure 1-16. (A) presumed structure of rhodopsin-like GPCR as viewed from the extracellular side, transmembranes subunits run in a counter clockwise fashion (# 1-7) (Unger *et al.*, 1997; Unger *et al.*, 1995). (B) "helicial wheel" diagram position according to frog rhodopsin, conserved "finger-print" residues are numbered to facilitate comparisons of residues between receptors (Gether, 2000).

The cytosolic end of the 3rd transmembrane membrane segment in family A GPCRs contains the so called "DRY" (Asp-Arg-Tyr) motif (Wess, 1998). In rhodopsin-like GPCRs Tyr is least conserved ~67% (Mirzadegan *et al.*, 2003), Asp as an acidic residue or Glu shows ~86% conservation (Mirzadegan *et al.*, 2003) and Arg is the most conserved with only 3% of family A receptors not carrying the residue in this position (Rosenkilde *et al.*, 2005). The Arg (R) residue of the DRY motif is believed important for GPCR coupling to G-proteins either through a direct interaction with or through the stabilising of the receptor in its active conformation (Capra *et al.*, 2004). The Tyr (Y) residue is not believed to be important in receptor activation/G-protein coupling whilst Asp (D) through its acidic side chain is important for receptor activation and G-protein coupling (Wess, 1998), see Figure 1-7.

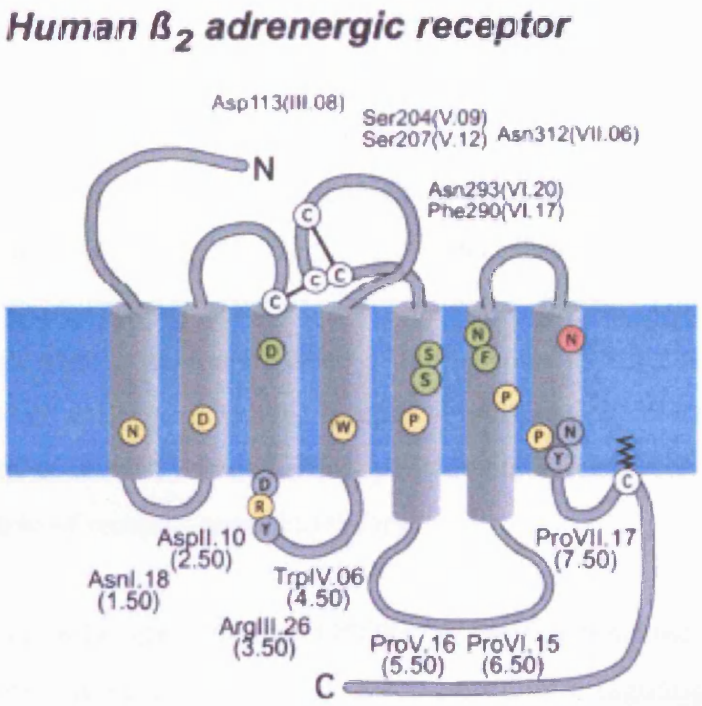

Figure 1-17. Structural topology of β_2 adrenergic receptor. The most highly conserved residues (in yellow) in each TM domain are named and numbered, the conserved DRY motif is also highlighted as are points of contact (green) with agonists (Gether, 2000).

1.16 GPCR Activation

Where used the number of amino acids within the GPCR structure take one of 2 formats (Gether, 2000; Gether *et al.*, 1998);

1. residues denoted by their 'real' number e.g. Ala 293
2. Schwartz numbering scheme whereby residues are numbered according to their position in the helix e.g. ProV.16 indicates residue number 16 in TM5.

Numerous studies have revealed that activation of GPCRs does not follow strict pattern(s) even for distinct subtypes of receptor. Antibodies directed against adrenergic α_1 and β_1 extracellular loops are capable of causing receptor activation contrary to the docking of their endogenous ligands in the transmembrane binding crevice.

GPCRs remain in a quiescent state, believed to be maintained through intramolecular interactions. However, the dormant state represents a more unique conformation of the receptor given that mutations typically result in constitutive activity (Gether, 2000; Scheer *et al.*, 1997). This was eloquently demonstrated for the α1b receptor where multiple substitutions of Ala293 on the third intracellular loop resulted in constitutive activity of varying degrees (Kjelsberg *et al.*, 1992). This suggests that this residue is important in the maintenance of the receptor in a non-activated form, mutations of which make the active receptor conformation more permissible. Strangely the mutants showed reduced efficacy relative to agonist activated wild type receptors, suggestive of receptor ensemble theory.

However, it is currently assumed that GPCRs in their unliganded state are not completely inactive but have a degree of basal constitutive (agonist independent) activity. Constitutively active mutants can be formed by modifications to most receptor regions including the extracellular structures. In fact hereditary thyroid adenomas are associated with mutations of the thyroid stimulating hormone (TSH) receptor leading to constitutive activity (Persani *et al.*, 2000).

It is therefore becoming clear that receptor activation requires the disruption of stabilizing intramolecular forces either through ligand binding or mutation. Research with rhodopsin and adrenergic receptors suggest one of the key processes to receptor activation is protonation of aspartic acid in the conserved D/E RY (Glu/Asp-Agr-Tyr) sequence of the third intracellular loop. Data from rhodopsin imply protonation of Glu134 accompanies its transition to metarhodopsin II, whilst in the α1b and β2 adrenergic receptors substitution of charge neutralizing residues, synonymous to Asp/Glu protonation, result in high rates of receptor activation.

From these and additional studies two hypotheses have been developed to accommodate the consequences of receptor activation on Asp/Glu residues of the third intracellular loop. The first model proposes that the conserved ArgIII.26 is located within a polar pocket formed by polar residues on TM helixes 1, 2 and 7. Receptor activation results in protonation of AspIII.25 and possible disruption of an ionic interaction between AspII.10, and ArgIII.26 resulting in the movement of the

latter residue out of the polar pocket and changes in receptor conformation. The arginine cage hypothesis suggests the ArgIII.26 forms an ionic interaction with AspII.10 as opposed to AspIII.25 upon receptor activation and protonation of AspIII.25. The latter hypothesis is given substance by mutation of AspII.10 which was shown to disturb functional receptor coupling, see (Gether, 2000) for review.
Labelling of cystine residues with the sulphydryl reactive fluorophore IANBD coupled with fluorescence spectroscopic techniques has allowed the study of receptor conformational changes through study of changes in the emission spectra of labeled receptors. For example addition of β-adrenergic receptor agonist (isoproterenol) to IANBD labelled receptors resulted in a dose dependent decrease in emissions suggestive of movement of labelled residues to a more hydrophilic environment. Site directed IANBD labelling of cystines has shown that on β-adrenergic receptor activation there is a counter-clockwise movement of both TM 3 and 6 (Gether *et al.*, 1995). A common proline rich region situated on TM6 provides a hinge, the flexibility of which is believed important for the rotational movement seen with labeled Cys-285, situated in close proximity (Gether *et al.*, 1995).

Regions implicated in GPCR coupling to their respective G-protein have been assumed from mutational/chimeric approaches of both muscarinic and adrenergic receptors and emphasize the third intracellular loop as key. Other studies encompassing further receptor types suggest that IL3 is important for specificity of G-protein coupling whilst IL2 is important for coupling efficiency.

1.16.1 Multistate model of receptor activation

As mentioned previously receptors do not reside in a quiescent state but appear to flux between multiple states or conformations, which can be both active and inactive. The ability of a ligand to cause a perturbation, to be more specific - the type of perturbation a ligand will produce, depends on the ligands selective affinity for the different states of a receptor. The model accommodates the idea that ligand binding sites at a receptor can be specific and need not overlap. Preferential ligand binding and stabilization of specific receptor states will increase the proportion of receptor residing in that form. The model suggests the rate limiting step in receptor activation would be the binding of ligand to its preferred conformation, the transitional rate of

the receptor would thus govern the tempo of activation. However studies comparing rates of receptor ligand association with those of ligand induced conformational changes indicate the former to be faster. Therefore a sequential model has been proposed for GPCR activation, see Figure 1-18 (Gether *et al.*, 1998). This model accommodates the knowledge that ligand binding to GPCR occurs at a greater rate than its conformational change and subsequent effector pathway activation.

The model predicts that transition of a receptor from an inactive conformation (R_o) to an active conformation (R*) occurs through sequential transition to a number of structurally unique receptor conformations (R, R^I and R^{II}) (Gether *et al.*, 1998). Spontaneous receptor activation can occur and accounts for the basal activity of GPCR. Inverse agonists show high affinity for and stabilise receptors in a non-activate state, in this way preventing or reducing basal activity. On binding of agonist to the inactive form of the receptor and through GPCR movements and subsequent interaction with different regions of the agonist the receptor will be structurally modified via a number of intermediaries leading finally to the active form. In this way the receptor can interact with functionally distinct regions of a ligand. It is hypothesized that G-protein association will have a positive influence on receptor transition through states to R*. This idea is suggested by the substantially reduced kinetics of receptor re-conformation seen in the absence of G-protein (Gether *et al.*, 1995).

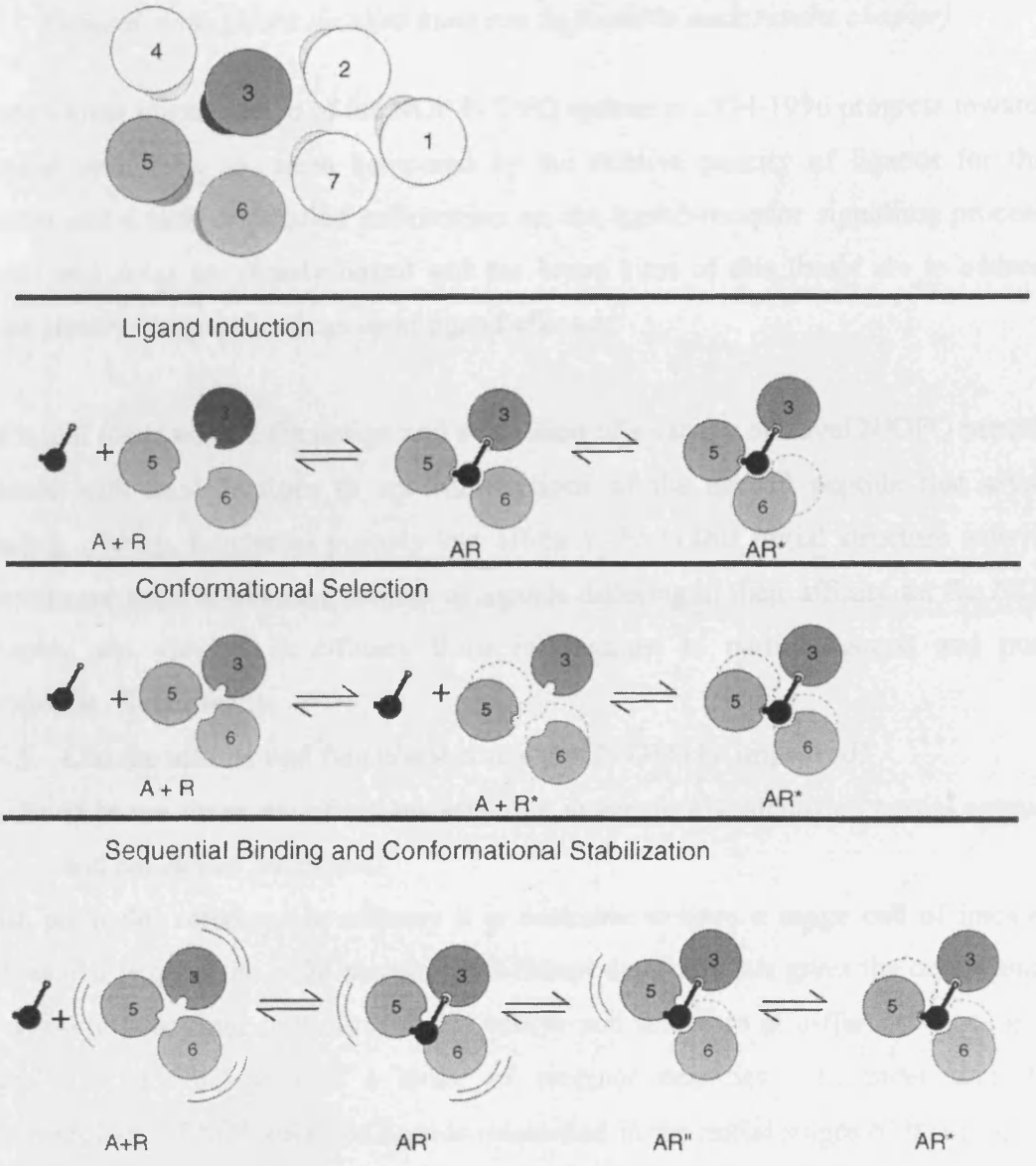

Figure 1-18. Schwartz multistate model of receptor activation (Gether *et al.*, 1998; Schwartz *et al.*, 1995). Ligand induction – transition from inactive receptor to active is nominal in the absence of an agonist. Agonist application facilitates transition to R*. Conformational selection – through the selective affinity of ligands for unique conformations of receptor a ligand can enrich specific conformations. As to the conformations selected, this will depend on the efficacy of the receptor.

Sequential Binding – the unliganded inactive form of receptor is denoted as R, whilst its active form is R*, R^{I} and R^{II} are intermediate receptor states or conformations between the two. This model adheres to findings showing rapid ligand association with receptor i.e. formation of R^{I} but a slower conformational change to R*(Gether *et al.*, 1998).

1.17 General Aims (More detailed aims can be found in each results chapter)

Since formal identification of the NOP-N/OFQ system in 1994-1996 progress towards clinical evaluation has been hampered by the relative paucity of ligands for this system and a lack of detailed information on the ligand-receptor signalling process. These two areas are clearly linked and the broad aims of this thesis are to address these areas with specific focus upon ligand efficacy.

An initial focus will be the design and evaluation of a variety of novel N/OFQ peptide ligands with modifications to specific sections of the natural peptide that affect binding affinity, functional potency and efficacy. From this initial structure activity exercise we hope to obtain a number of ligands differing in their affinity for the NOP receptor and varying in efficacy from full agonist to partial agonist and pure antagonist. Specifically;

1. Can the affinity and functional potency of N/OFQ be improved?
2. If so are these modifications effective in previously identified partial agonist and antagonist templates.

With particular reference to efficacy it is desirable to have a range cell of lines or tissues that express the NOP receptor at different densities, this gives the opportunity to assess efficacy not only in different assays and therefore at different stages in a signal cascade, but also at a range of receptor densities. In order that the pharmacology of NOP receptor ligands (identified in the initial stages of this project) can be assessed over a range of receptor densities whilst maintaining a consistant cellular background, the NOP receptor is used in an inducible expression system ($CHO_{INDhNOP}$). A particular problem in the N/OFQ field has been the variable efficacy described for [F/G]N/OFQ(1-13)NH_2 with antagonist, partial agonist and full agonist activity observed and hypothesised to result from expression differences in the tissues used to investigate this ligand. The inducible system will provide a novel yet simple way to address this question.

One of the gaps in the literature relating to NOP-N/OFQ transduction, and again in relation to efficacy, is G-protein activation. Specifically:

1. Do ligands of differing efficacy (identified in the initial stages of this project) produce differences in guanine nucleotide requirements ?
2. Is there an interplay with receptor density ?

2 Materials & Methods

2.1 Sources of Materials

Amersham Biosciences (Buckinghamshire, UK): [*leucyl*-^{3}H]N/OFQ

Fisher Scientific (Leicestershire, UK): Sodium chloride, Magnesium chloride, Magnesium sulphate, Tris-HCL, Sodium hydroxide, Potassium hydroxide, Hydrogen chloride, Folin's reagent, HEPES, EGTA, Whatman G/F B filters.

Invitrogen (Scotland): Hams-F12, Dulbecco's modified minimum essential media (DMEM), HAMS-F12/DMEM (1:1 mix v:v), Penicillin/streptomycin, Fungizone, Bovine foetal calf serum, Trypsin / EDTA, Geneticin (G418), Hygromycin B, Zeocin, Ponasterone A.

Perkin Elmer Life Sciences (Boston, Mass., USA): GTPγ[^{35}S] (1250Ci/mmol), [^{3}H]Diprenorphine (56Ci/mmol), [^{3}H]cAMP (30-50Ci/mmol).

Neosystems (Strasbourg, France): III-BTD.

Sigma Aldrich (Poole, Dorset, UK): Bacitracin, Amastatin, Bestatin, Captopril, Phosphoramidon, GDP, GTPγS, Pertussis toxin, BSA, Ipegal, Triton X-100, EDTA, Naloxone Benzoylhydrazone, Forskolin, Trypan blue.

Peptides: All peptides where synthesied at the University of Ferrara (Italy)

Hoffman La-Roche Laboratories: Ro64-6198.

Roche pharmaceuticals (Indianapolis, USA): mini-complete EDTA-free protease inhibitor tablets.

Autogen Bioclear, Santa-Cruz, (Wiltshire, UK): Anti-$G_{\alpha i1\text{-}3}$ antibody (C-10), protein-A agarose.

2.2 Buffer compositions

2.2.1 Tissue culture buffers

- Harvest: HEPES(10mM), EDTA(1.1mM), NaCl(154mM), pH7.4 NaOH.

2.2.2 GTPγ[^{35}S] Buffers

- GTPγ[^{35}S] Reconstitution: Tris-HCl(50mM), DTT(10mM), pH7.4 NaOH.
- GTPγ[^{35}S] Homogenising: Tris-HCl(50mM), EGTA(0.2mM), pH7.4 NaOH.
- GTPγ[^{35}S] Assay: Tris-HCl(50mM), EGTA(0.2mM), NaCl(100mM), $MgCl_2$(1mM), pH7.4 NaOH.

2.2.3 Immunoprecipitation Buffers

- Assay Buffer: Tris-HCl (50mM), NaCl (100mM), EGTA (0.2mM), $MgCl_2$ (5mM), pH7.4 with NaOH.
- Solubilisation Buffer: Tris-HCl (50mM), NaCl (150mM), EDTA (5mM), Igepal (1.25% v/v), pH7.4 with NaOH.

2.2.4 [leucyl-^{3}H]-nociceptin saturation/competition buffers

- Wash/Homogenising: Tris-HCl(50mM), $MgSO_4$(5mM), pH7.4 KOH.
- Assay: Tris-HCl(50mM), $MgSO_4$(5mM), pH7.4 KOH, 0.5% BSA.

2.2.5 Bioassays buffer compositions

- *Mouse Vas Deferens (Krebs buffer)*
  - (mM): NaCl (118.5), KCl (4.7), $MgSO_4$ (1.2), KH_2PO_4 (1.2), $NaHCO_3$ (25), $CaCl_2$ (1.8), glucose (10)
- *Mouse colon (modified Krebs buffer)*
  - (mM): NaCl (118.5), KCl (4.7), $MgSO_4$ (1.2), KH_2PO_4 (1.2), $NaHCO_3$ (25), $CaCl_2$ (2.5), glucose (10)

2.3 Cell culture

In general, cells were cultured at 37°C in 5% carbon dioxide humidified air, sub-cultured as required using trypsin EDTA and used experimentally when confluent.

CHO_{hNOP} cells were cultured in Dulbecco's MEM / HAMS F12 (50/50) supplemented with 5% foetal bovine serum (FBS), penicillin (100 IU/ml), streptomycin (100μg/ml) and fungizone (2.5μg/ml). Stock cultures were further supplemented with geneticin (G418) (200μg/ml) and hygromycin B (200μg/ml) - used to maintain expression of the plasmids encoding for the human NOP receptor and a reporter gene (not used in this work) respectively .

$CHO_{INDhNOP}$ cells were cultured in HAMS-F12 supplemented with 10% FBS, penicillin (100 IU/ml), streptomycin (100μg/ml) and fungizone (2.5μg/ml). Stock cultures were further supplemented with geneticin (G418) (1mg/ml), zeocin (250μg/ml) - to maintain expression of plasmids for the ecdysone inducible system and that of the inducible gene respectively. Cells were induced to express the human NOP receptor by replacement of medium for fresh supplemented with the required concentration of induction agent, ponasterone A. This was carried out 20hr prior to experimentation.

Both CHOhNOP and CHOINDhNOP cell lines were kindly provided by Dr. F. Marshall and Mrs. N. Beavan of GSK (Stevenage, Herts, UK).

2.3.1 PTX pre-treatment

Pertussis toxin (PTX) is isolated from the supernatant of cultures of *Bordetella pertussis* and causes ADP-ribosylation of $G_{i/o}$ G-proteins in non-retinal tissue, PTX was obtained from Sigma. The toxin was resuspended in sterile dH_20 and added to nearly confluent cultures at a concentration of 100ng/ml, 20-24hr prior to experimentation (Smart *et al.*, 1997).

2.3.2 Cell counting and trypan blue staining

Cells were harvested using trypsin EDTA and resuspended in a known volume of media or buffer to give a high density of cells typically ~$1\text{-}2*10^6$ cells/ml. Trypan blue (0.4% in 0.85% saline) was diluted 1:1 with cell suspension and using a haemocytometer with a glass cover slip attached a small volume of the cell suspension/trypan blue solution was pipetted onto the haemocytometer, the capillary action under the cover slip will draw the suspension into the counting chamber. The

space between the cover slip and the haemocytometer counting chamber ensures a specific volume of cell suspension is present. Under a microscope the number of viable and non-viable (stained blue) cells in diagonally opposite counting areas were counted, Figure 2-1. Cells in contact with two of the counting area boundaries (triple etched lines in figure) are included in the count while those in contact with the opposite sides are not counted. The grid surface is 0.1mm below the coverslip, therefore the volume of fluid above one of the $1.0mm^2$ counting areas is 0.0001ml. The viable cells from 2 chambers are determined and then divided by two determining cells/mm^2. This value is then doubled (taking the trypan blue dilution into account) and increased by a factor of 10^4, to give the number of cells/ml. The total number of viable cells can then be determined by multiplying the number of cells/ml by the volume (in ml) of cell suspension prepared at the start (Phillips, 1973; Tennant, 1964).

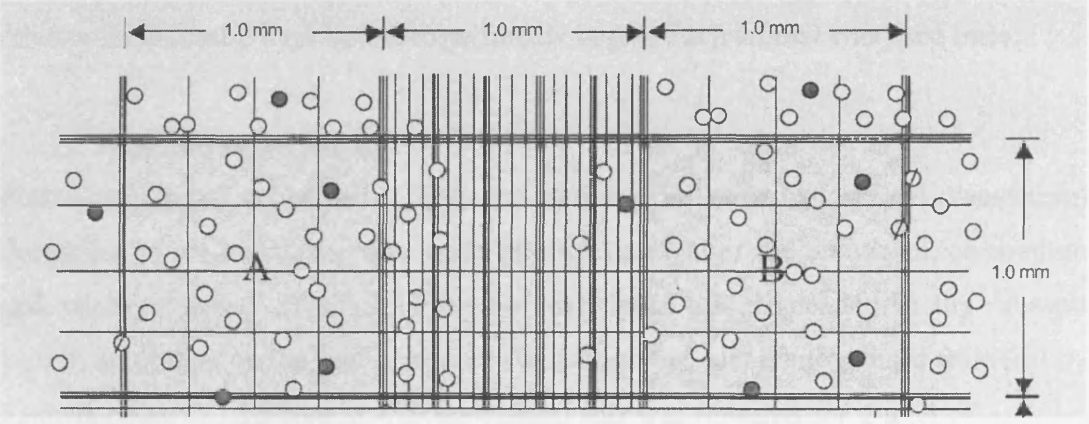

Figure 2-1. Haemocytometer counting chamber (2 counting chambers, A and B, of four are shown). The grid surface is 0.1mm below the coverslip therefore the volume of fluid over one of $1.0mm^2$ counting areas is 0.0001ml.

2.4 Membrane preparation

2.4.1 Recombinant cell lines

Cells were harvested from sterile tissue culture flasks using harvest buffer and gentle agitation. Cells were suspended in either wash buffer (saturation, displacement assays) or homogenising buffer (GTPγ[^{35}S] assay), homogenised using an Ultra Turrax, for 10 seconds followed by 6 consecutive 1-second bursts. The homogenate was then centrifuged at 13,500rpm for 10min at 4°C, this was carried out a total of

three times. The membrane fraction was resuspended in an appropriate volume of assay buffer and the total protein content determined as set out below.

2.5 Animal care/ethics and tissue preparation

2.5.1 Ethics and Housing

Female Wistar rats were housed at the University of Leicester in accordance with the Animal Act 1996. Male Swiss (Morini, Reggio Emilia, Italy) and male CD1/C57-BL6J/129 WT ($NOP^{+/+}$) and KO ($NOP^{-/-}$) mice weighing 20-25 g were housed at the University of Ferrara Italy. All transgenic animals were genotyped by PCR. Detail of the generation and breeding of mutant mice have been published previously (Nishi *et al.*, 1997a). The animals were handled according with guidelines published in the European Communities Council directives (86/609/EEC). Animals were housed under standard conditions (22°C, 12-h light-dark cycle) with food and water *ad libitum* for at least 2 days before experiments began. Each animal was used once.

2.5.2 Preparation of rat tissue

Following Class I scheduled killing (pre-stunning followed by cervical dislocation) dissection of cortical tissue was made through removal of the brainstem, cerebellum and midbrain areas. The remaining cortical tissue was suspended in the relevant buffer, dependent on the post-analysis to be carried out, and homogenised followed by centrifugation (13,500rpm at 4°C for 10min) this was repeated for a total of 3 times. Membrane fractions were finally resuspended in a volume of buffer dependent on the starting mass of tissue. Membrane suspensions were aliquoted and stored at -70°C.

2.5.3 Preparation of dog tissue

Male and female Beagle dogs were housed at Pfizer Ltd. and animal work was carried out in compliance with UK law and was approved by local animal ethical review as appropriate. Dog brain preparation, dogs (9-14kg) were humanely killed by pentobarbital overdose. Brain was prepared at Pfizer Ltd and shipped to Leicester on dry ice.

2.5.4 Preparation of mouse tissue

Following Class I scheduled killing (pre-stunning followed by cervical dislocation),

tissues were isolated from male Swiss Morini mice (25-30g). The prostatic portion (section running from the testicles to the prostate) of the *vas deferens* (mVD) were isolated and prepared according to (Hughes *et al.*, 1975b) and segments of transverse and descending colon (1 cm in length) (Figure 2-2) were removed (Hughes *et al.*, 1975a; Yazdani *et al.*, 1999). Both tissues were suspended into tissue chambers (described later) containing 5ml of heated Krebs (33°C mVD, 37°C mC). A resting tension of 0.3g was applied to mVD and 1g used for mC preparations. Tissues were left for ~1hr to obtain a stable baseline and both tissues were washed every twenty minutes during this period.

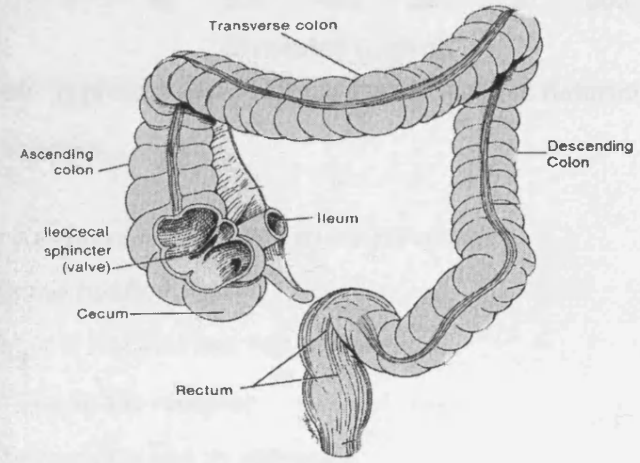

Figure 2-2. Diagram of colon, transverse and descending sections were used in bioassays (Tortora *et al.*, 1990).

2.6 Protein assay (Lowry)

The protein concentration was determined for membrane fractions using the method of Lowry (Lowry *et al.*, 1951):

BSA protein standards at set concentrations of 0, 50, 100, 150, 200, 250µg protein/ml were made up in 0.1M NaOH. Samples of unknown protein concentration were diluted in 0.1M NaOH. 0.5ml volumes of standards and samples were incubated for 10min in 2.5ml of solution consisting of, A ($NaHCO_3$ in 0.1M NaOH) B (1% $CuSO_4$) and C (2% Na^+ K^+ tartrate) mixed to the ratio 100:1:1. Folin's reagent (diluted 1:4 in dH_2O) was then added and incubated at room temperature for a further 30min. The absorbance at 750nm for standards and samples was then determined using a spectrophotometer. Linear regression of the known BSA protein concentrations was

used to produce a standard curve (Figure 2-3) from which sample protein concentrations were determined.

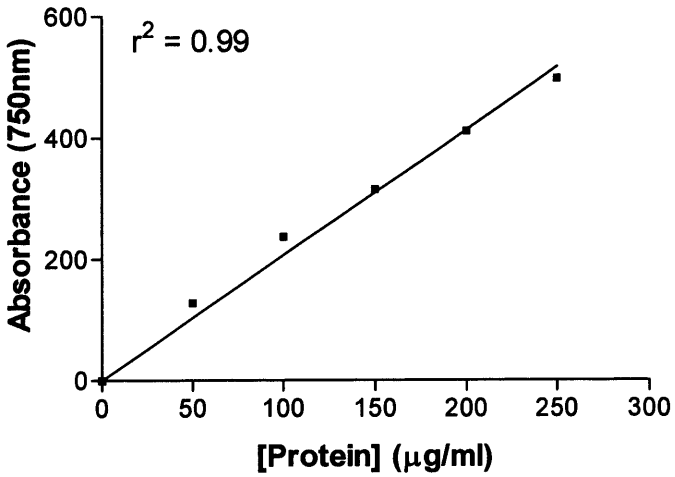

Figure 2-3. Example of protein assay standard curve used to determine the protein mass of unknown samples.

2.7 Theories of radiolabel binding and assay parameters

2.7.1 Receptor ligand binding

The action of a drug at a receptor has two elements:

- Binding of the drug to the receptor
- Activation of the receptor and its response.

Binding (saturation and displacement) assays use radiolabelled ligands to measure the first element whilst functional assays, for example GTPγ[^{35}S] and cAMP, are used to measure the second element.

The binding process can be represented as follows:

$$[D] + [R] \underset{K_{-1}}{\overset{K_{+1}}{\rightleftharpoons}} [DR]$$

Where [D] concentration of drug

[R] concentration of free receptors

[DR] concentration of drug/receptor complex

K_{-1} dissociation rate constant

K_{+1} association rate constant

The forward rate of the reaction is $K_{+1}[D]$ [R] and the backward rate is K_{-1} [DR]. At equilibrium these two rates are equal i.e. there is no net movement of the drug onto or off the receptor. The total amount of drug bound, the B_{max}, is determined by the drug/receptor interaction and tissue preparation under investigation. The equilibrium dissociation rate constant for the drug/receptor interaction (K_d) is numerically equal to the concentration of drug required to occupy 50% of the receptor population and is a universally quoted value for the affinity of a drug at a specific receptor.

$$K_d = \frac{K_{-1}}{K_{+1}} = \frac{[D][R]}{[DR]}$$

When occupancy is at 50% $[R] = [DR]$ so that: $K_d = [D]$.

Above is a case of the Langmuir absorption isotherm, which describes the absorbance of substances onto surfaces and can be represented graphically for drug receptor occupancy using a one site binding hyperbola or Langmuir isotherm, this is typically converted to sigmoid concentration response curve using a semi-log plot Figure 2-4 (Kenakin, 1997).

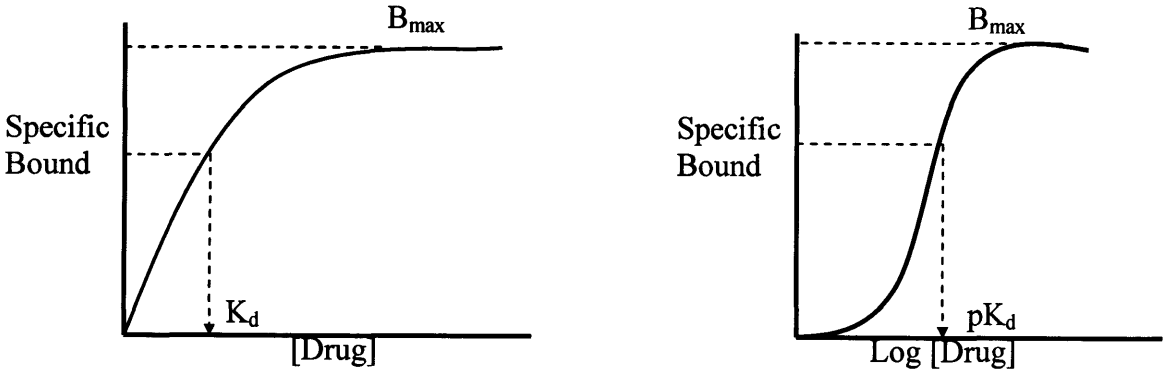

Figure 2-4. Langmuir Isotherm for drug/receptor binding (left) and semi-log form of same curve (right) (Kenakin, 1997).

Saturation binding assays measure the affinity of a radiolabelled drug for a receptor (K_d) and also give a measure of the receptor density (B_{max}) (Kenakin, 1997).

Typically data are presented as a pK_d, which is the negative log_{10} of the concentration required to occupy 50% of the receptors.

Whilst the use of radiolabelled ligands allows measures of ligand affinity, radiolabelling drugs is a costly and timely procedure. Competition binding studies allow determination of binding affinities for non-labelled ligands. These binding studies utilise a fixed concentration of radiolabel and the affinity of the non-labelled ligand is determined by its ability to compete for the same binding site.

Increasing concentrations of a non-labelled ligand will displace or out-compete the fixed concentration of a radiolabel, generating an IC_{50} for the competing ligand. The value of the IC_{50} is determined by three factors:

- The affinity of the competing ligand for the receptor
- The concentration of the radiolabel
- The affinity of the radiolabel for the receptor, its K_d.

The Cheng and Prusoff equation takes these factors into account allowing the affinity of the non-labelled competing ligand to be determined (Cheng *et al.*, 1973). This value is designated pK_i and is the log concentration of the competing ligand required to displace 50% of the radiolabel through 50% occupancy of the total receptor population. This value is therefore equivalent to a pK_d.

Cheng and Prusoff equation:

$$K_i = \frac{IC_{50}}{1 + \left[\frac{[Ligand]}{K_d}\right]}$$

Where;

IC_{50} = IC_{50} of competing ligand

[ligand] = concentration of radiolabel

K_d = equilibrium dissociation constant for radiolabel

2.7.2 Saturation binding methodology

Membranes were prepared as per section 2.4 and the mass of membrane protein used was varied in a manner dependent on the receptor expression of the tissue source. This was done to gain optimal signal to noise ratios for the binding of radiolabel in

tissues expressing the NOP receptor at different densities, typically high expressing tissues a low mass (20μg) was included and for low expressing tissue a high mass (>100μg) was include. Membrane protein was added to 0.5ml of saturation/competition binding buffer (see section 2.2.4) containing amastatin, bestatin, captopril, phosphramidon (10μM) and varying concentrations of [*leucyl*-^{3}H]N/OFQ (~2nM – 0.002pM). Reactions were incubated at room temperature for 1h and terminated via vacuum filtration through polyethyleneimine (PEI) soaked Whatman GF/B filters using a Brandel-harvester. The percentage of radiolabel bound was always <<10% of the total included. Non specific binding (NSB) was determined in the presence of 1μM N/OFQ.

2.7.3 Competition binding methodology

A 0.5ml volume of saturation/competition binding buffer (see section 2.2.4) containing amastatin, bestatin, captopril, phosphramidon (10μM), and a fixed concentration of [*leucyl*-^{3}H]N/OFQ (200pM) was incubated with varying concentrations of non-labelled competing ligands and 20-40μg of membrane fraction. Non-specific binding was determined in the presence of 1μM unlabelled N/OFQ. Assays were incubated at room temperature for 1h and reactions terminated via filtration through PEI soaked Whatman GF/B filters using a Brandel-harvester.

2.7.4 System bias

It is worthy of a mention that use of different tissue preparations, i.e. whole-cell systems relative to membranes may bias measures of affinity. In membranes the propensity of receptors coupled to G-protein will be high given a lack of guanine nucleotides that prevent this association or promote G-protein-GPCR dissociation. Hence the active conformation of the receptor is likely to be the only form present, so long as G-protein density is not a limiting factor. In this way membrane preparations will be biased to detect binding of ligands with positive efficacy, which have higher affinity for this form of the receptor. A factor highlighting this is the knowledge that the affinity, certainly for agonists, is affected by the presence of GTP i.e. the so called 'GTP-shift'. The presence of GTP means that receptors will spend less time coupled to G-protein, as GTP will promote dissociation of ternary complex or receptor G-protein complexation, hence the tendency of the active form of the receptor will

decrease. In this way the binding affinity of agonist will decrease and the nature of its saturation curve is likely to be complex given the multiple affinity states present. Therefore it can be suggested that membrane preparations overestimate affinity, certainly for positive agonists. Nevertheless care must be taken with the use of whole living cells for radiolabelled binding studies due the effects of receptor desensitisation and down regulation. This phenomenon is unlikely to occur in membrane fractions because the intracellular "machinery", such protein kinases and arrestins, are absent. Indeed in whole rat cerebella cells it can be seen that there is a rapid decrease in the binding of carbachol to muscarinic receptors attributable to receptor desensitisation (Maloteaux *et al.*, 1983). Conversely in membrane fragments from the same cerebella cells no such decrease is seen highlighting a lack of receptor desensitisation in these fragments. See Figure 2-5.

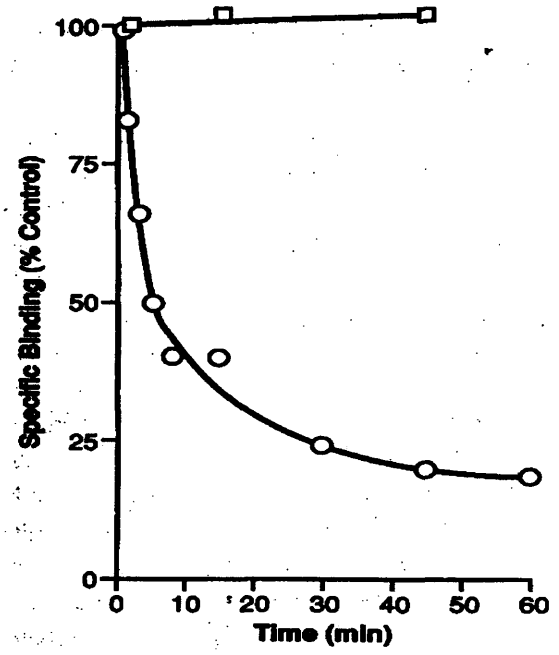

Figure 2-5. Time course depicting the loss of carbachol displacement of [^{3}H]quinuclidinylbenzylate and [^{3}H]QNB, in intact cerebella cells (circle symbol) and membranes of the same cells (square symbol) (Maloteaux *et al.*, 1983).

Despite the knowledge that membrane fractions may bias for recognition of positive efficacy ligands their use is favourable in the sensitivity they offer coupled with ease of use. Further the presence of one high affinity binding site allows the use of lower

concentrations of both tracer and competitor, which make experiments more cost effective. These discussions underscore the need for multiple system testing so that a potential 'hit' is not missed from testing in the wrong system e.g. the possibility of missing an inverse agonist through testing in a non constitutively active system.

2.7.5 Guanine nucleotide binding

Functional assays measure the activation and response elements of a drug/receptor interaction. The GTPγ[^{35}S] assay measures the coupling of the receptor to a G-protein. Ligand binding at a G-protein coupled receptor alters the conformation of the receptor in a way that allows interaction with G-protein(s). This interaction leads to the exchange of GDP for GTP. A radiolabelled, stable analog of GTP, GTPγ[^{35}S] is used to measure the exchange of GDP for GTPγ[^{35}S] elicited by different ligands. Since the conformation of a receptor is not fixed but in a state of flux there will be some tonic activation of G-proteins via non-ligand bound receptors. This basal level of G-protein activation (GTPγ[^{35}S] binding) is measured in the absence of ligand and the final results expressed as either the ratio increase over basal binding (stimulation factor) or as net dpm (minus basal dpm).

2.7.6 GTPγ[^{35}S] binding assay

CHO_{hNOP} membranes were prepared as described in 2.4.1. 20μg of CHO_{hNOP} and 40μg of $CHO_{INDhNOP}$ were incubated in 0.5ml volumes of GTPγ[^{35}S] buffer (section 2.2.2) containing bacitracin (0.15mM), amastatin, bestatin, captopril and phosphramidon (10μM), BSA 1mg/ml and ~150pM GTPγ[^{35}S]. Agonist and antagonist assays were performed with GDP concentrations of either 100μM or 5μM. NSB was determined in the presence of 10μM GTPγS in all experiments. Reactions were incubated at 30°C with gentle shaking for 1h.

2.7.7 GTPγ[^{35}S] Association Kinetics

The observed association rate of GTPγ[^{35}S] was assessed using CHO_{hNOP} homogenate. The effect of ligands of different efficacy and different GDP concentrations (0.1 and 5μM) on the observed association rate of GTPγ[^{35}S] was assessed over a 4hr time course. Buffers were GTPγ[^{35}S] assay buffer (section 2.2.2) containing bacitracin (0.15mM), amastatin, bestatin, captopril and phosphramidon

(10μM), BSA 1mg/ml and ~70pM GTPγ[^{35}S] and assays were incubated over 4hr using 20μg of membrane homogenate, added at set time points.

2.7.8 GTPγ[^{35}S] competition/isotope dilution binding

To determine the affinity of GTPγS and GDP for G-proteins, competition binding studies were performed on CHO_{hNOP}, $CHO_{INDhNOP}$ and rat brain homogenate using GTPγ[^{35}S]. All assays were performed on 20μg of membrane fraction and incubated in 0.5ml volumes of assay buffer supplemented with bovine serum albumin (0.1%), bacitracin (150μM), peptidase inhibitors (amastatin, bestatin, phosphoramidon and captopril, all at 10μM), GDP (1mM – 10pM) or GTPγS (1μM-10pM) and GTPγ[^{35}S] ~70pM. The binding profile of competitors (GDP and GTP) are less effected by this reduced concentration of GTPγ[^{35}S]. GDP was omitted from studies examining total saturation of GTPγS binding sites but was included at 5μM when measuring the effects of ligands on GTPγS binding parameters. NSB was defined in the presence of 10μM GTPγS. All reactions were incubated for 1hr at 30°C with gentle shaking except for total saturation and time course assays which were performed over a 4hr period.

2.7.9 Extraction and counting

For [^{3}H]N/OFQ and GTPγ[^{35}S] binding protocols experiments were terminated via vacuum filtration through Whatman GF/B filters using a Brandel-harvester. For [^{3}H]N/OFQ filters were pre-soaked in 0.5% PEI, for GTPγ[^{35}S] filters were not treated with PEI and were loaded onto the harvester dry. Radioactivity was determined after an eight hour extraction period in scintillation cocktail and samples were counted using scintillation spectrophotometry.

2.7.10 Immunoprecipitation of specific G-α subunits

Methodology is based on that described by (Cordeaux *et al.*, 2000). 40μg of CHO_{hNOP} and 150μg of dog (used as a low density, natively expressing NOP tissue) membranes were incubated in 0.5ml immunoprecipitation buffer supplemented with 1mg/ml BSA, 150μM bacitracin, 10μM peptidase inhibitors (as previously), 5μM GDP, ~150pM GTPγ[^{35}S] and 1μM N/OFQ for 1h at 30°C with gentle shaking. NSB

was defined in the presence of 10μM GTPγS. Reactions were terminated by the addition of 1ml ice-cold immunoprecipitation buffer (see section 2.2.3), followed by centrifugation for 5min at 16,000g. Pellets were resuspended in 100μl solubilisation buffer supplemented with 0.2% (w/v) sodium dodecyl sulphate (SDS) and protease inhibitors (1 Roche mini-complete EDTA-free/10ml) and incubated for 5min. A further 100μl solubilisation buffer (SDS-free) was added and the mixture incubated for a further 5min. Samples were pre-cleared with the addition of 15μl protein-A agarose for 30min at 4°C. Anti-$G_{\alpha i1-3}$ antibody (4μg) was added and incubated for 13hr at 4°C. Antibody was precipitated by the addition of 30μl of protein-A agarose for 2hr at 4°C, followed by 5min centrifugation at 16,000g. Samples were resuspended in 750μl solubilisation buffer (protease inhibitor free), centrifuged for 5min at 16,000g and finally resuspended in scintillation cocktail and counted after 8hr extraction.

2.7.11 Inhibition of adenylate cyclase

cAMP measurements are achieved through a competitive binding assay. The binding protein, extracted from bovine adrenal glands, has a finite number of binding sites for which labelled ([^{3}H]cAMP) and unlabelled cAMP (either forskolin stimulated samples or standard controls) compete. The concentration of binding protein and [^{3}H]cAMP are kept constant and hence the concentration of unlabelled cAMP present in a given sample can be determined from the relative displacement of [^{3}H]cAMP from the binding protein The concentration of cAMP in a given sample can be determined through the construction of a standard curve (0.25-10pmol/tube). Whole cell suspensions were incubated in the presence of 1mM isobutylmethylxanthine (IBMX) and forskolin (1μM) for 15 minutes. NOP ligands were included in various combinations and at different concentrations. Reactions were terminated using 10M HCl and neutralised with 10M NaOH/1mM Tris, pH7.4. The concentration of cAMP was measured using the protein binding method set out by (Brown *et al.*, 1971).

2.8 Non-specific Binding

Non-specific binding represents binding of a radiolabel to sites other than the receptor or protein under investigation. The nature and percentage of the non-specific binding will vary with different radiolabels, factors such as hydrophobicity and the lipophilic

nature of the ligand being important. The degree of NSB may also be affected by the system under study, where transporters and pumps may or may not be active or where access to the receptor binding site is restricted through compartmentalisation. Where used the filtration process can also play a role in the amount of NSB since radiolabel binding to filters will form an element of the NSB, for this reason (in binding experiments) filters are treated with PEI – a detergent shown to reduce NSB (Dooley *et al.*, 2000). However, for GTPγS experiments PEI is used not because it causes dissociation of GTPγ[^{35}S]. NSB is defined in the presence of a saturating concentration of 'cold' or non-labelled ligand. In this way all specific binding sites are occupied and any radiolabel left bound is to non-specific sites and is subsequently removed from all data, rendering specific values.

2.8.1 Ex Vivo Bioassays, Mouse Vas Deferens And Mouse Colon

Two chambered glass baths were used for isolated tissue bioassays. The outer chamber is perfused with water heated at 33°C whilst the inner chamber holds 5ml of Krebs buffer oxygenated with 95% O_2 and 5% CO_2 at pH 7.4. The isolated tissue is suspended in the inner chamber anchored at the bottom end and the top end attached via surgical string, to a force transducer, see Figure 2-6. The transducer acts to convert the mechanical movement of the tissue into an electrical signal, which is amplified and recorded by a chart recorder (Calo *et al.*, 1996).

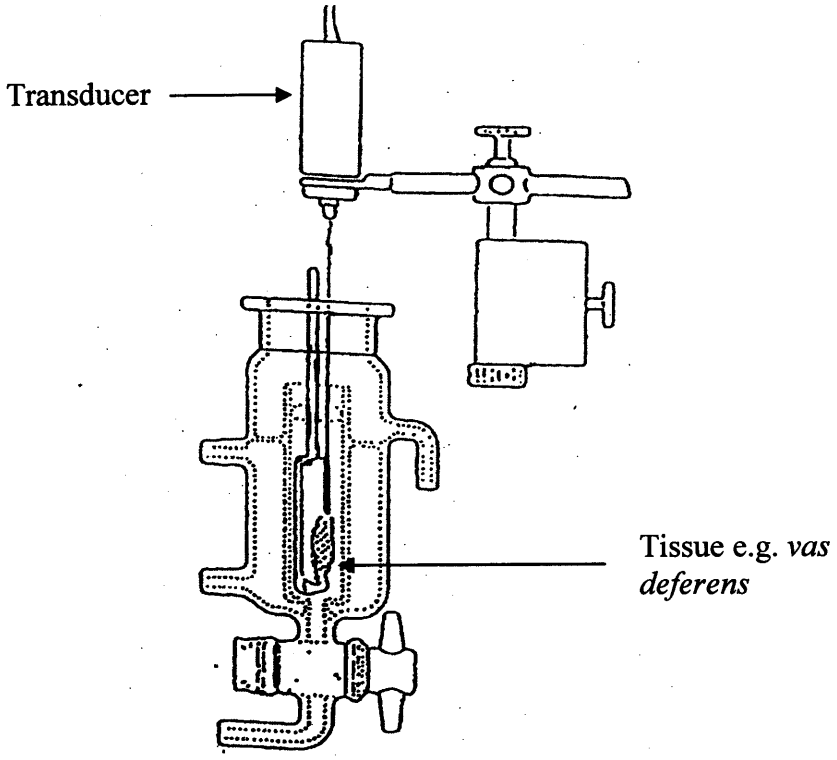

Figure 2-6. Diagram of the tissue chamber used for mouse colon and vas deferens assays.

2.8.2 Vas deferens

Mouse *vasa deferens* (mVD) were continuously stimulated via two platinum ring electrodes with 30V rectangular pulses of 1msec duration at a frequency of 0.05Hz. Electric field stimulation (EFS) was used to induce isotonic contractions, the degree of which was determined using a strain gauge transducer (Basile 7006) and recorded on a Linseis multichannel chart recorder. Concentration response curves to peptides were performed cumulatively without replacing the Krebs solution in the chamber between concentrations. Tissues responses were required to plateau before the addition of the next concentration. A period of one hour is left between concentration response curves (CRC) to allow tissue recovery. For experiments using antagonists a pre-incubation of 15min is required before the CRC of the agonist is performed.

2.8.3 Mouse Colon

For mouse colon (mC) experiments tissues were not electrically contracted and recording was through longitudinal isometric smooth muscle contractions (Osinski *et*

al., 1999). For mC tissues CRC were performed non-cumulatively, adding drugs every 20min with two washes between additions. Carbachol (10μM) was used to determine tissue responsiveness and responses to NOP peptides are expressed as either grams or percentage response relative to that of carbachol.

2.8.4 Statistical Analysis

All data are expressed as mean±SEM. N numbers refer to the number of individual experiments, data plots are determined individually in each separate experiment. All curve fitting was performed using GraphPad Prism V3, except for the 2-site Scatchard analysis of GTPγ[^{35}S] total saturation data which was analysed with Kell VI (Biosoft). pK_i values were calculated using the Cheng and Prusoff equation ($\log\{IC_{50}/(1+[\text{Radiolabel}]/K_D)\}$) (Cheng *et al.*, 1973). Antagonist affinity was calclulated either as (i) pK_B values using the formula $pK_B = -\log\{(CR-1)/[\text{antagonist}]\}$, where CR is the ratio of the EC_{50} of the agonist in the presence and absence of antagonist, assuming a slope value of unity or (ii) via full Schild analysis. In GTPγ[^{35}S] binding studies data are either presented as DPM [^{35}S] bound (in studies where the GDP concentration is varied, as "stimulation factor" is GDP dependent) or stimulation factor (i.e. the ratio between specific agonist-stimulated GTPγ^{35}S binding and basal specific binding.). cAMP data are presented as percentage inhibition of the forskolin stimulated response. Statistical analyses (paired/unpaired Students' t-test and ANOVA with Bonferoni correction for multiple comparison where appropriate) were performed using PRISM V3.0 (GraphPad, San Diego, USA), $p \leq 0.05$ considered significant.

3 Structure Activity Relationship Studies of N/OFQ

3.1 Introduction

Structure activity relationship studies and high throughput screening techniques have benefited from the use of immortalised recombinant cell lines that typically express high receptor densities (1-3pmol/mg protein) (Hashiba *et al.*, 2002a). These high receptor densities are desirable as they increase the chance of measuring a response or seeing a 'hit' from a drug, as they provide good signal to noise ratios. However, high receptor densities can produce pseudo-physiological responses such as promiscuity with regard to G-protein coupling and intracellular mediators.

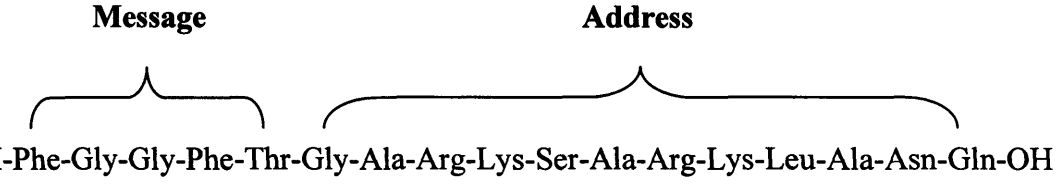

Figure 3-1. Peptide sequence of N/OFQ and hypothesised message and address domains (Guerrini *et al.*, 2000b).

In N/OFQ (Figure 3-1) the loss of the first amino acid, Phe^1, results in a complete loss of activity at NOP, although substitution of this residue for others with different chemical groups is well tolerated. The spatial orientation of the N-terminal tetrapeptide is also essential, substitution of Gly^2 and Gly^3 results in inactivity / reduced activity at the NOP receptor. For these reasons the N-terminal portion of N/OFQ is assumed to be the 'message' domain of the peptide and confers information regarding receptor activation (efficacy) (Guerrini *et al.*, 1997; Guerrini *et al.*, 2000b). The C-terminal region after the 5^{th} residue of N/OFQ is important for binding to the NOP receptor, the so-called 'address' region (Guerrini *et al.*, 1997; Guerrini *et al.*, 2000b)

The first ligand to show increased affinity and potency over N/OFQ was an analog containing an additional arginine and lysine repeat in positions fourteen and fifteen (Okada *et al.*, 2000). This so called Arg, Lys triple repeat analog emphasizes the importance of the C-terminal portion of the peptide with regard to ligand affinity at

the NOP receptor. Whilst N-terminal modifications typically affect ligand efficacy (Guerrini *et al.*, 1997), substitution of a fluorine or nitrogen atom to the phenyl ring of phenylalanine in position four gives analogs of N/OFQ with increased affinity and potency (Bigoni *et al.*, 2002b; Guerrini *et al.*, 2001).

Given the knowledge that removal of phenylalanine from position 1 results in a complete loss of activity at the NOP receptor, modifications to this region of the peptide were developed in an attempt to increase the stability of N/OFQ. Reduction of the peptide bond between phenylalanine in position 1 and glycine in position 2 produced a ligand [$Phe^1\Psi(CH_2\text{-}NH)Gly^2$]N/OFQ(1-13)-$NH_2$ ([F/G]N/OFQ(1-13)-NH_2) that showed greater stability, as seen through increased potency *in vivo* (where peptidase activity is greater) but not *in vitro* (where ligand degradation is limited) (Calo *et al.*, 2000c). The rationale for Phe-Gly modification was for the identification of a ligand with greater metabolic stability, issues of peptide stability are more relevant *in vivo* where enzymatic degradation is likely to be greater than *in vitro.* Indeed *in vitro* binding studies here utilise a low mass (20μg) of membrane, the homogemate of which has been washed multiple times, thus removing enzymes present in the cytosol. Further the addition of a cocktail of peptidase inhibitors are included which have been shown effective in prevention of the breakdown of N/OFQ (Bigoni *et al.*, 2001).

Indeed the pseudo-peptide [F/G]N/OFQ(1-13)NH_2, displays a profile of agonism, antagonism or partial agonism dependent upon the system in which it is screened (this will be discussed in more detail later) (Guerrini *et al.*, 1998).

The first peptide NOP receptor antagonist was produced by shifting the phenyl ring of phenylalanine in position 1 by a single atom, from its native carbon to the nitrogen, generating the analog [$Nphe^1$]N/OFQ(1-13)NH_2 (Guerrini *et al.*, 2000a). This ligand has been shown to produce competitive antagonism of the NOP receptor in numerous systems, importantly in recombinant overexpressed systems, albeit with low potency (Calo *et al.*, 2000b; Calo *et al.*, 2005).

3.2 Aims

The aim of this chapter is to examine the effects of the [Arg^{14},Lys^{15}] and [(pF)Phe^4] substitutions to determine what effects they would have when they are combined in the different modified templates discussed (see Figure 3-2, Table 3-1);

(i)N/OFQ(1-17)NH_2 (**a series**, full sequence agonist)

(ii)[F/G]N/OFQ(1-17)NH_2 (**b series**, full sequence partial agonist)

(iii)[Nphe^1]N/OFQ(1-17)NH_2 (**c series**, full sequence antagonist)

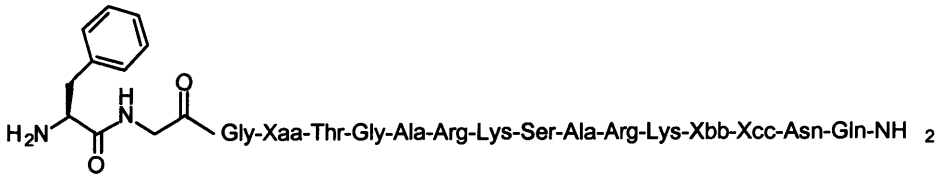

Phe^1-Gly^2 (**a series**)

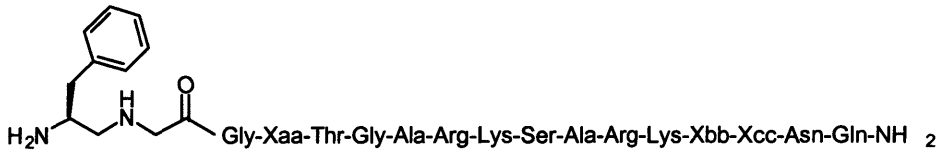

Phe$^1\Psi$(CH_2-NH)Gly^2 (**b series**)

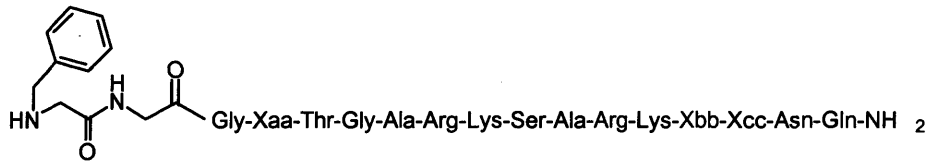

Nphe^1-Gly^2 (**c series**)

Xaa = Phe; Xbb = Leu; Xcc = Ala; Compounds **1a-c**
Xaa = (pF)Phe; Xbb = Leu; Xcc = Ala; Compounds **2a-c**
Xaa = Phe; Xbb = Arg; Xcc = Lys; Compounds **3a-c**
Xaa = (pF)Phe; Xbb = Arg; Xcc = Lys; Compounds **4a-c**

Figure 3-2. Structures of the three template ligands along with a key to the sites where the various substitutions are made.

Compound n°	Abbreviated names
1a	N/OFQ(1-17)-NH_2
2a	[(pF)Phe^4]N/OFQ(1-17)-NH_2
3a	[$Arg^{14}Lys^{15}$]N/OFQ(1-17)-NH_2
4a (UFP-102)	[(pF)$Phe^4Arg^{14}Lys^{15}$]N/OFQ(1-17)-NH_2
1b	[$Phe^1\Psi(CH_2\text{-}NH)Gly^2$]N/OFQ(1-17)-$NH_2$
2b	[$Phe^1\Psi(CH_2\text{-}NH)Gly^2(pF)Phe^4$]N/OFQ(1-17)-$NH_2$
3b	[$Phe^1\Psi(CH_2\text{-}NH)Gly^2Arg^{14}Lys^{15}$]N/OFQ(1-17)-$NH_2$
4b (UFP-103)	[$Phe^1\Psi(CH_2\text{-}NH)Gly^2(pF)Phe^4Arg^{14}Lys^{15}$]N/OFQ(1-17)-$NH_2$
1c	[$Nphe^1$]N/OFQ(1-17)-NH_2
2c	[$Nphe^1$(pF)Phe^4]N/OFQ-NH_2
3c (UFP-101)	[$Nphe^1Arg^{14}Lys^{15}$]N/OFQ-NH_2
4c	[$Nphe^1$(pF)$Phe^4Arg^{14}Lys^{15}$]N/OFQ-NH_2

Table 3-1. List of the full names of those ligands used in this SAR study.

In order to characterise the pharmacology of these 12 compounds a number of different assays were employed;

(i)[*leucyl*-^{3}H]N/OFQ competition binding assays (measures of affinity)

(ii)GTPγ[^{35}S] binding assays, post receptor (functional potency, efficacy)

(iii)cAMP inhibition assays, downstream effector (functional potency, efficacy)

Additional data with truncated analogs of N/OFQ will also be included along with data on several synthetic ligands Ro64-6198 (Jenck *et al.*, 2000) (agonist) and J-113397 (Kawamoto *et al.*, 1999), III-BTD (Becker *et al.*, 1999) (peptoid antagonists), see Figure 3-3.

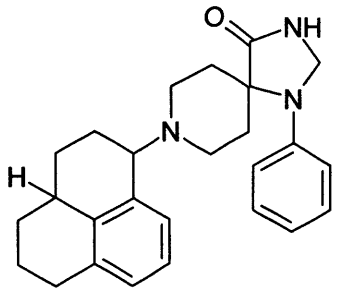

Ro-64-6198

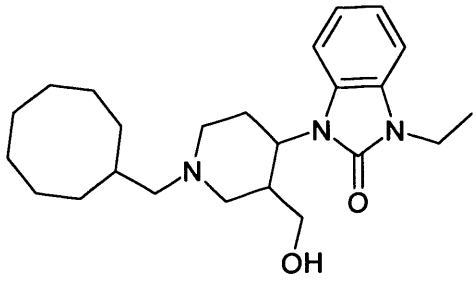

J-113397

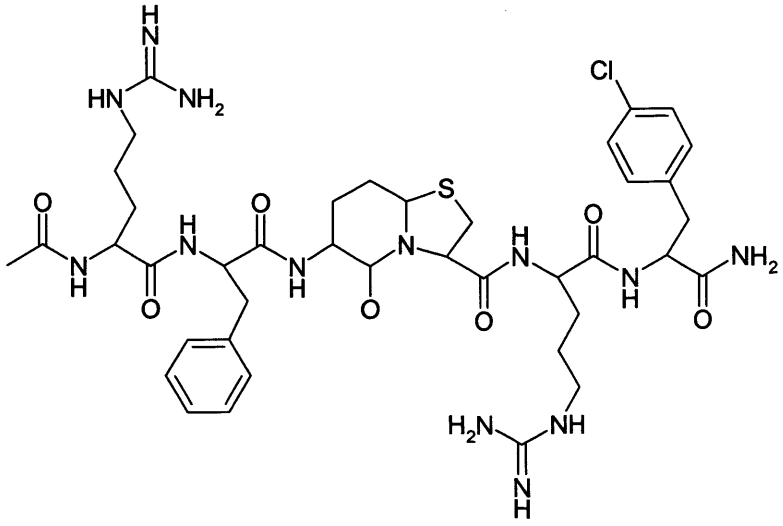

III-BTD

Figure 3-3. Structures of synthetic NOP ligands, Ro64-6198 (agonist), J-113397 and III-BTD (antagonists).

3.3 Results

3.3.1 [leucyl-^{3}H]N/OFQ competition binding

All ligands tested produced a concentration dependent and saturable (100%) displacement of [*leucyl*-^{3}H]N/OFQ. The pK_i values were determined for these ligands using Cheng and Prusoff correction assuming a pK_D of 70.9pM for [*leucyl*-^{3}H]N/OFQ derived from previous saturation experiments on the CHO cells expressing the human recombinant NOP receptor (CHO_{hNOP}), B_{max} 1913fmol/mg protein (Hashiba *et al.*, 2001) and in use in this laboratory. In the three different templates (series a, b & c) the individual modifications of [Arg^{14},Lys^{15}] and [(pF)Phe^4] gave an increase in ligand binding affinity at the human recombinant NOP receptor, see Table 3-2 and Figure 3-4. Further, when the two modifications are combined in the same template there is an additive increase in affinity. Worthy of a mention is the finding that both the pseudo-peptide [Phe$^1\Psi$(CH_2-NH)Gly^2]N/OFQ(1-17)-NH_2 ([F/G]N/OFQ(1-17)-NH_2 series (b-series) and [Nphe^1] N/OFQ(1-17)-NH_2 (c-series) had reduced binding affinity relative to N/OFQ(1-17)NH_2 (a-series).

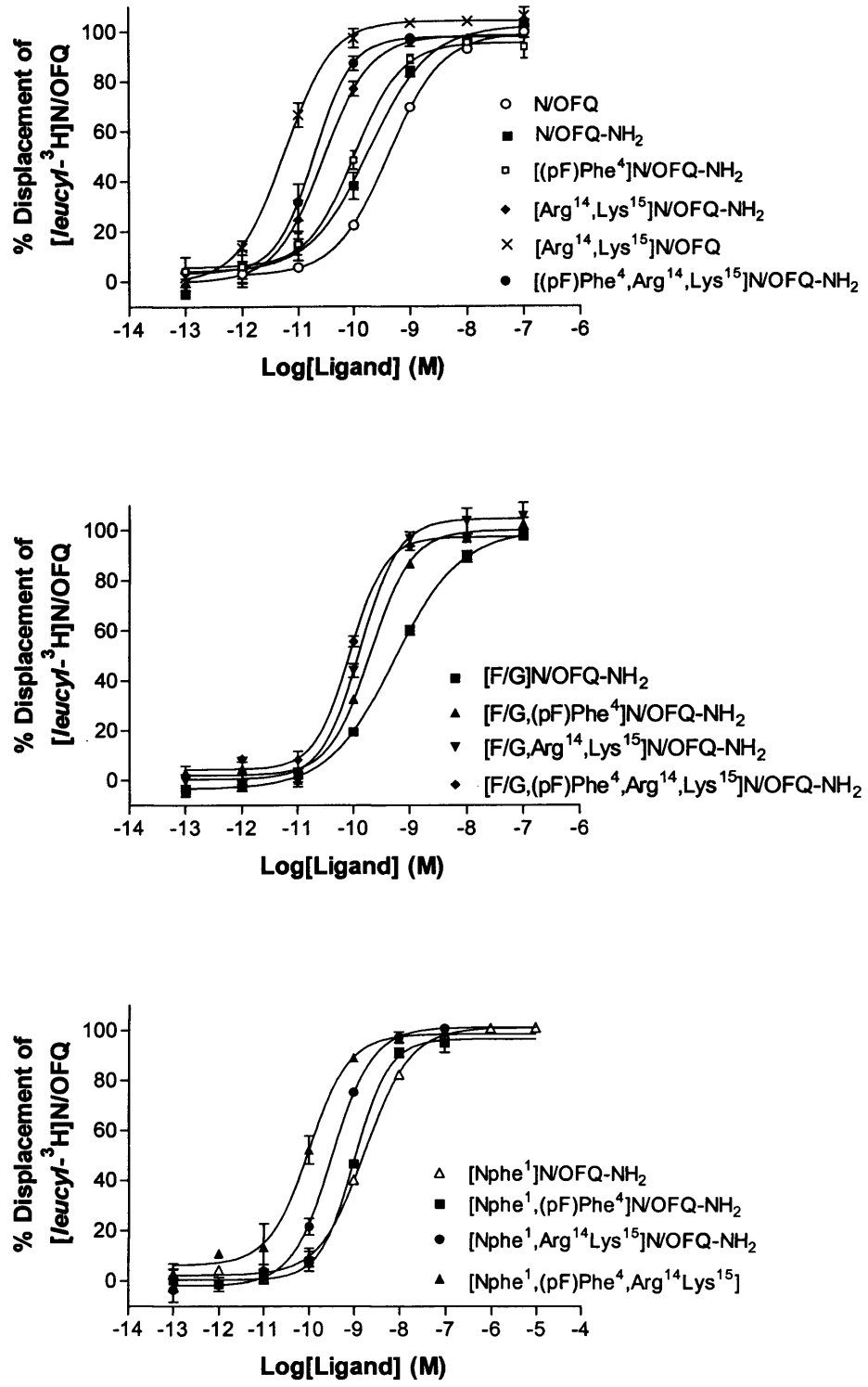

Figure 3-4. Binding displacement curves for compounds N/OFQ(1-17)NH_2 (a-series) Top, [F/G]N/OFQ(1-17)-NH_2 series (b-series) Middle and [$Nphe^1$]N/OFQ(1-17)-NH_2 (c-series) Bottom. Experiments were performed on CHO_{hNOP} cell homogenates. Data are mean±SEM (n≥3 indiviual experiment, data points are measured individually in each separate experiment).

Compound n° **[Xaa^{4}Xbb^{14}Xcc^{15}]**	**Phe^1-Gly^2 (a series)** pK_i	**Phe$^1\psi$(CH_2-NH)-Gly^2 (b series)** pK_i	**Nphe^1-Gly^2 (c series)** pK_i
1 [Phe^{4}Leu^{14}Ala^{15}]	10.31±0.04	9.89±0.08	9.38±0.01
2 [(pF)Phe^{4}Leu^{14}Ala^{15}]	10.66±0.09*	10.32±0.04*	9.62±0.02*
3 [Phe^{4}Arg^{14}Lys^{15}]	11.16±0.10*	10.50±0.03*	9.89±0.01*
4 [(pF)Phe^{4}Arg^{14}Lys^{15}]	11.32±0.08*	10.70±0.03*	10.60±0.10*

Table 3-2. Receptor Binding affinities of compounds 1-4a, 1-4b, and 1-4c (see table 3-1 for full peptide titles) at recombinant human NOP expressed in CHO cells. Data are mean±SEM of n≥3 experiments. Data analysed by ANOVA with Bonferroni correction, * $p<0.05$ significant difference to compound 1 of the respective series.

3.3.2 GTPγ[^{35}S] Functional binding assay

Membrane preparations of CHO_{hNOP} were used to study the ability of these ligands to promote guanine nucleotide exchange. Initially a comparison between the natural free acid form of the peptide N/OFQ(1-17)-OH (N/OFQ) was characterised against the amide form N/OFQ(1-17)NH_2 (compound 1a) and the truncated N/OFQ(1-13)-NH_2 peptide, see Figure 3-5, Table 3-3. The full sequence amidated N/OFQ(1-17)NH_2 (1a) was statistically more potent than the natural N/OFQ peptide. No statistical difference in potency was measured between the truncated (N/OFQ(1-13)-NH_2) and full sequence amidated peptide (N/OFQ(1-17)NH_2) . Hence overall it can be seen that amidation of N/OFQ affords an increase in ligand potency and truncation of the C-terminus, by four amino acids, has no detriment on potency at the human NOP receptor. Of note, E_{max} values showed no difference from one another. It must be mentioned at this point that the measure of E_{max} is affected by a number of factors including GDP concentration, variation in GTPγ[^{35}S] batches – as radiolabels show decomposition with age. E_{max} values are very sensitive to GDP concentration, decreasing the GDP concentration results in increased raw dpm bound, such that the increase above basal, i.e. the stimulation factor, is decreased (Berger *et al.*, 2000a; Berger *et al.*, 2000b). For the NOP receptor in the CHO cell line here 100μM GDP was the optimal concentration to measure increases in GTPγ[^{35}S] binding over basal. This GDP concentration is nevertheless not optimal for other receptor types, including classical opioid receptor subtypes (Albrecht *et al.*, 1998; Traynor *et al.*, 1995).

GTPγ[^{35}S] binding stimulated by [(pF)Phe^4]N/OFQ-NH_2 (compound 2a) [Arg^{14},Lys^{15}]N/OFQ-NH_2 (compound 3a), and [(pF)Phe^4,Arg^{14},Lys^{15}]N/OFQ-NH_2 (compound 4a) were all compared to the template peptide N/OFQ(1-17)-NH_2, see Table 3-4, Figure 3-6. All ligands showed increases in potency relative to N/OFQ(1-17)NH_2, the greatest seen was a pEC_{50} of 10.12±0.04 for [(pF)Phe^4,Arg^{14},Lys^{15}]N/OFQ-NH_2 (4a).

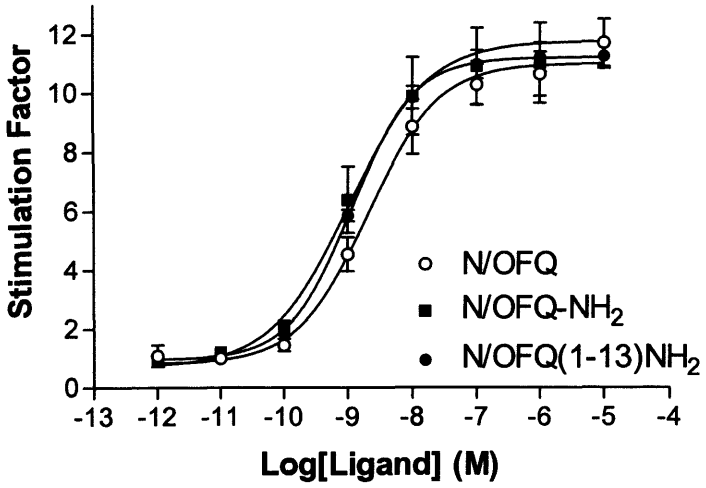

Figure 3-5. Comparison of different agonist templates of N/OFQ, for ability to stimulate GTPγ[^{35}S] binding. Amidation of the C-terminus affords a slight increase in ligand potency and C-terminal truncation by four amino acids had no effect in this template. N/OFQ-NH_2 = N/OFQ(1-17)-NH_2 (1a). Data are mean±SEM (n≥3 experiments).

Ligand	*pEC_{50}*	*E_{max} (stimulation factor)*
N/OFQ	8.70±0.07	10.71±0.73
N/OFQ(1-17)-NH_2	8.98±0.08*	10.98±1.30
N/OFQ(1-13)-NH_2	8.94±0.01	11.19±0.48

Table 3-3. Potency (pEC_{50}) and efficacy values for comparison of the natural form of N/OFQ with the amidated full sequence and truncated analogs of the peptide. Data are n≥3 experiments ±SEM, * pEC_{50} value significantly different from N/OFQ ($p<0.05$) ANOVA with Bonferroni's correction.

Compound n° [Xaa^{4}Xbb^{14}Xcc^{15}]	Phe^1-Gly^2 (a series) agonist		Phe$^1\psi$(CH$_2$-NH)-Gly^2 (b series) agonist		antagonist	Nphe^1-Gly^2 (c series) agonist		antagonist
	pEC_{50}	E_{max}	pEC_{50}	E_{max}	pK_b	pEC_{50}	E_{max}	$pA_2/(^apK_b)$
1 [Phe^{4}Leu^{14}Ala^{15}]	8.98±0.08	10.98±1.30	8.28±0.57	4.85±0.52	ND	Inactive	Inactive	7.54±0.16
2 [(pF)Phe^{4}Leu^{14}Ala^{15}]	9.51±0.16*	11.42±0.72	9.09±0.29	4.30±0.28	ND	8.23±0.30	1.36±0.11	^{a}8.32±0.02*
3 [Phe^{4}Arg^{14}Lys^{15}]	9.85±0.12*	9.70±0.69	9.03±0.09	5.29±0.27	ND	Inactive	Inactive	9.13±0.23*
4 [(pF)Phe^{4}Arg^{14}Lys^{15}]	10.12±0.04*	12.26±0.39	9.68±0.10	4.19±0.07	ND	9.39±0.20	2.03±0.01	9.71±0.05*

Table 3-4. Potencies of compounds 1-4a, 1-4b, and 1-4c (see table 3-1 for full peptide titles) at recombinant human NOP expressed in CHO cells: GTPγ[^{35}S] binding assay

Data are the mean±SEM from n≥3 experiments. Antagonist activity was measured with N/OFQ as the agonist. ND: not determined, compounds behaved as partial agonists. *$p<0.05$ significant difference relative to compound 1 from the respective series.

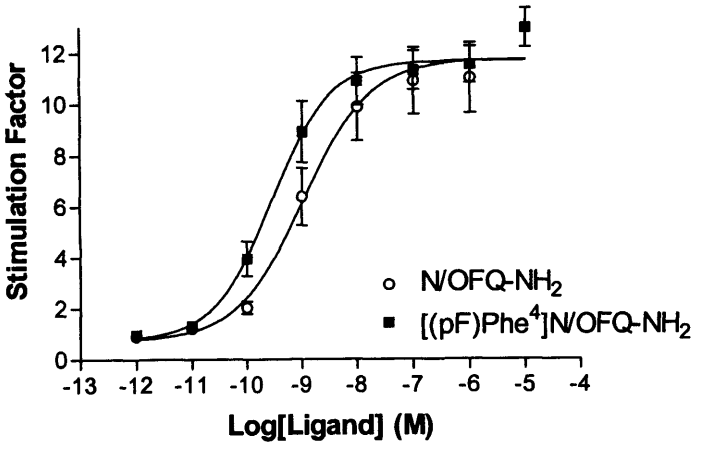

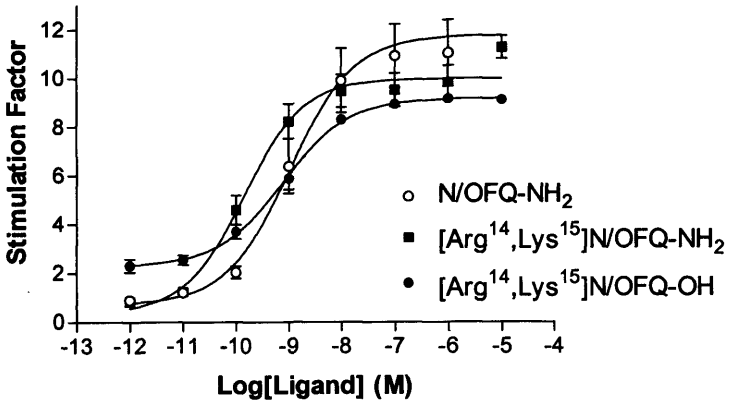

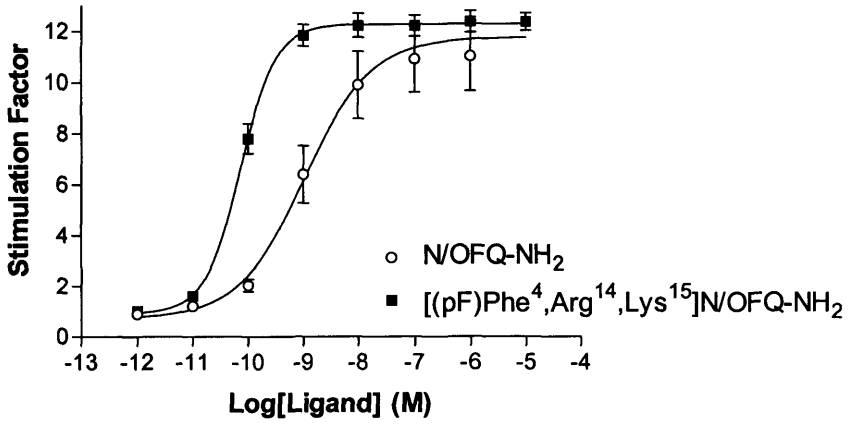

Figure 3-6. Comparison of compounds [(pF)Phe^4]N/OFQ(1-17)-NH_2 (2a), [Arg^{14}Lys^{15}]N/OFQ(1-17)-NH_2 (3a) and [(pF)Phe^{4}Arg^{14}Lys^{15}]N/OFQ(1-17)-NH_2 (4a)with N/OFQ(1-17)NH_2 (1a). [Arg^{14},Lys^{15}]N/OFQ-OH is also included as a reference ligand, pEC_{50} 9.12±0.11 and E_{max} 9.09±0.04. Data are mean±SEM for n≥4 experiments.

The truncated analog of [(pF)Phe^4]N/OFQ-NH_2 (2a), [(pF)Phe^4]N/OFQ(1-13)-NH_2 was also measured for ability to stimulate GTPγ[^{35}S] binding and compared to its parent molecule, N/OFQ(1-13)NH_2, see Figure 3-7. [(pF)Phe^4]N/OFQ-NH_2 (2a) had increased potency relative to N/OFQ(1-17)-NH_2 (1a) ($p<0.05$), see Table 3-4. Importantly [(pF)Phe^4]N/OFQ(1-13)NH_2 showed increased ($p<0.05$) potency pEC_{50} of 9.55±0.01 relative to N/OFQ(1-13)NH_2 pEC_{50} of 8.94±0.5, however there was no difference in potency for [(pF)Phe^4]N/OFQNH_2 (2a) and [(pF)Phe^4]N/OFQ(1-13)NH_2 ($p>0.05$). To further characterise the pharmacology of [(pF)Phe^4]N/OFQ(1-13)NH_2 the effect of two synthetic NOP antagonists, III-BTD and J113397 were studied. Both III-BTD and J113397 caused a rightward shift in the [(pF)Phe^4]N/OFQ(1-13)NH_2 concentration response curve (for GTPγ[^{35}S] stimulated binding), with pA_2 values of 8.53±0.06, and 7.96±0.05 respectively, see Figure 3-8 and Table 3-5. III-BTD and J-113397 were both inactive as agonists.

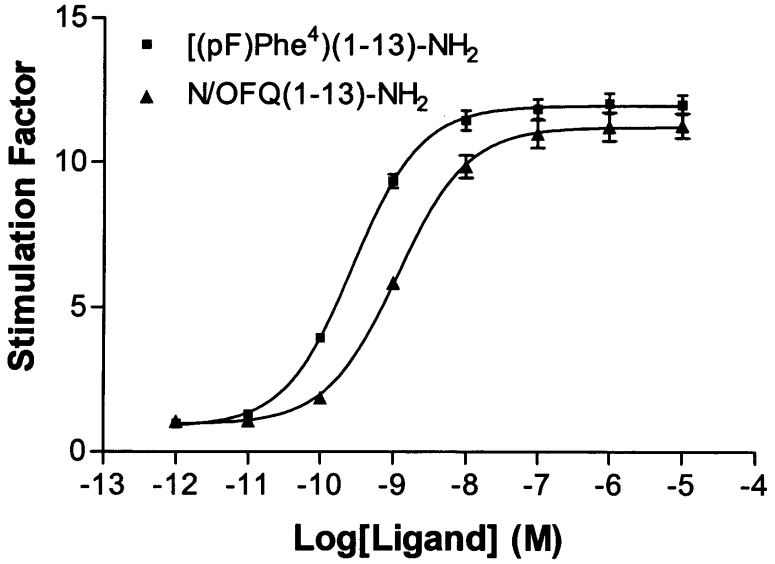

Figure 3-7. Comparison of functional potency and efficacy of [(pF)Phe^4]N/OFQ(1-13)NH_2 and N/OFQ(1-13)NH_2, for stimulation of GTPγ[^{35}S] binding. Data are mean±SEM for n≥4 experiments.

Antagonist Concentration	Potency (pEC_{50}/pA_2)
[(pF)Phe^4]N/OFQ(1-13)NH_2 (control)	9.56±0.01
+100nM J113397	7.86±0.01
+10nM J113397	8.82±0.03
+1nM J113397	9.45±0.02
pA_2 (slope)	8.53±0.06 (1.13±0.05)
[(pF)Phe^4]N/OFQ(1-13)NH_2 (control)	9.53±0.01
+100nM III-BTD	8.48±0.01
+10nM III-BTD	9.23±0.01
+1nM III-BTD	9.50±0.01
pA_2 (slope)	7.96±0.05 (1.07±0.07)

Table 3-5. Effect of different concentrations of both J113397 and III-BTD on the potency of [(pF)Phe^4]N/OFQ(1-13)NH_2 for GTPγ[^{35}S] binding. Data are mean±SEM (n≥3 experiments).

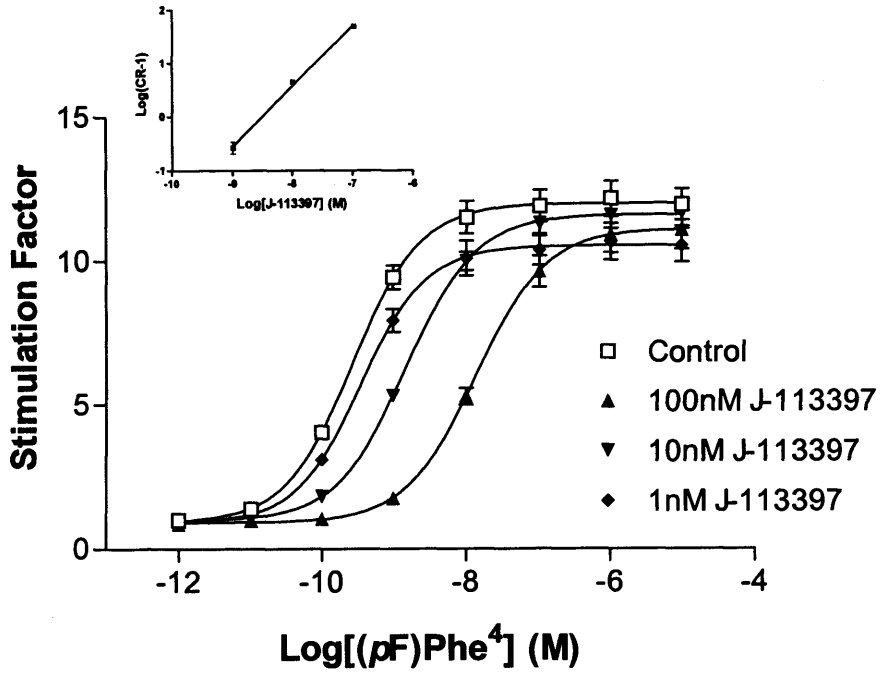

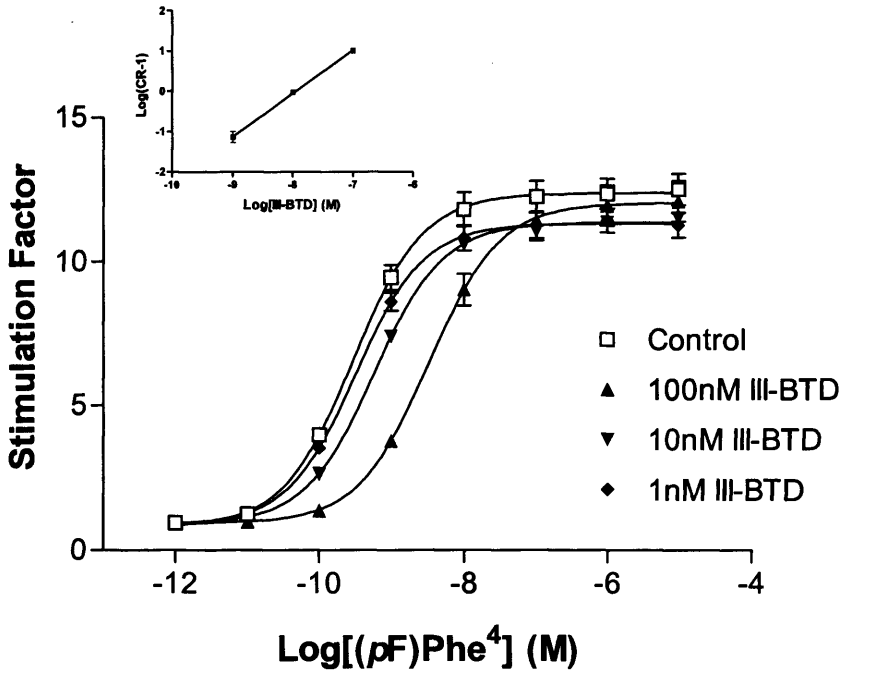

Figure 3-8. Antagonism of [(pF)Phe^4]N/OFQ(1-13)NH_2 stimulated GTPγ[^{35}S] binding by J113397 and III-BTD. Data are mean±SEM for n≥3 experiments. Inserts show respective Schild plots.

[F/G]N/OFQ(1-17)NH_2 (compound 1b) was a partial agonist for stimulated GTPγ[^{35}S] binding, relative intrinsic activity was in the order of α=0.5 (50%) see Table 3-4 and Figure 3-9. [F/G,(pF)Phe^4]N/OFQ(1-17)-NH_2 (2b), [F/G,Arg^{14},Lys^{15}]N/OFQ(1-17)-NH_2 (3b) and [F/G,(pF)Phe^4,Arg^{14},Lys^{15}]N/OFQ(1-17)-NH_2 (4b) all displayed increased functional potency with pEC_{50} values of 9.09±0.29, 9.03±0.09 and 9.68±0.10 respectively, relative to the parent ligand [F/G]N/OFQ(1-17)-NH_2 (1b) pEC_{50} of 8.28±0.57. However, it can be seen that while these substitutions augment functional potency they have no effect on the efficacy of the [F/G]N/OFQ(1-17)-NH_2 series. Relative intrinsic activities were consistent, at between α=0.5-0.6, for all these ligands.

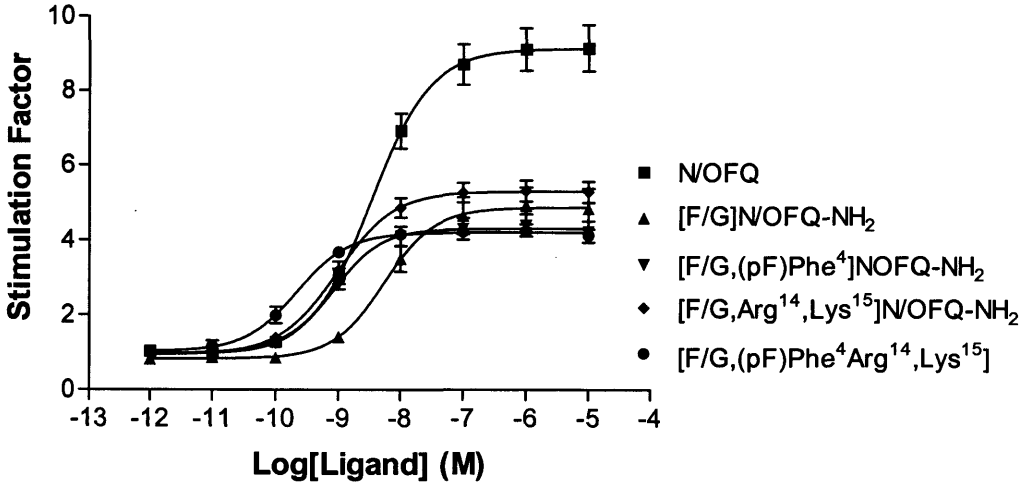

Figure 3-9. Comparison of [F/G]N/OFQ(1-17)-NH_2 (1b), [F/G,(pF)Phe^4]N/OFQ(1-17)-NH_2 (2b), [F/G,Arg^{14},Lys^{15}]N/OFQ(1-17)-NH_2 (3b) and [F/G,(pF)Phe^4,Arg^{14},Lys^{15}]N/OFQ(1-17)-NH_2 (4b) for stimulation of GTPγ[^{35}S] binding. N/OFQ(1-17)NH_2 (1a) is shown as a full agonist reference ligand. Data are mean±SEM for n≥4 experiments.

Finally the [Nphe^1]N/OFQ(1-17)NH_2 (1c) series (c-series) were examined for their ability to stimulate the binding of GTPγ[^{35}S], see Table 3-4 and Figure 3-10. [Nphe^1]N/OFQ(1-13)NH_2, the first NOP peptide antagonist, antagonised the response to N/OFQ with a pA_2 value and slope of 7.33±0.08 and 1.02±0.06 respectively, see Figure 3-11. The full sequence template compound [Nphe^1]N/OFQ(1-17)NH_2 (1c) used in this study had a similar pA_2 to the truncated analog and both ligands were devoid of agonist activity (Table 3-4). The only other c-series analog to show no residual agonist activity was [Nphe^1,Arg^{14},Lys^{15}]N/OFQ(1-17)NH_2 (3c). With [Nphe^1,(pF)Phe^4]N/OFQ(1-17)NH_2 (2c) there was a small increase in efficacy which was further increased when combined with [Arg^{14},Lys^{15}] substitution - [Nphe^1,(pF)Phe^4,Arg^{14},Lys^{15}]N/OFQ(1-17)NH_2 (4c), E_{max} values were 1.36±0.11 and 2.03±0.01 (α=0.12 and 0.18) respectively.

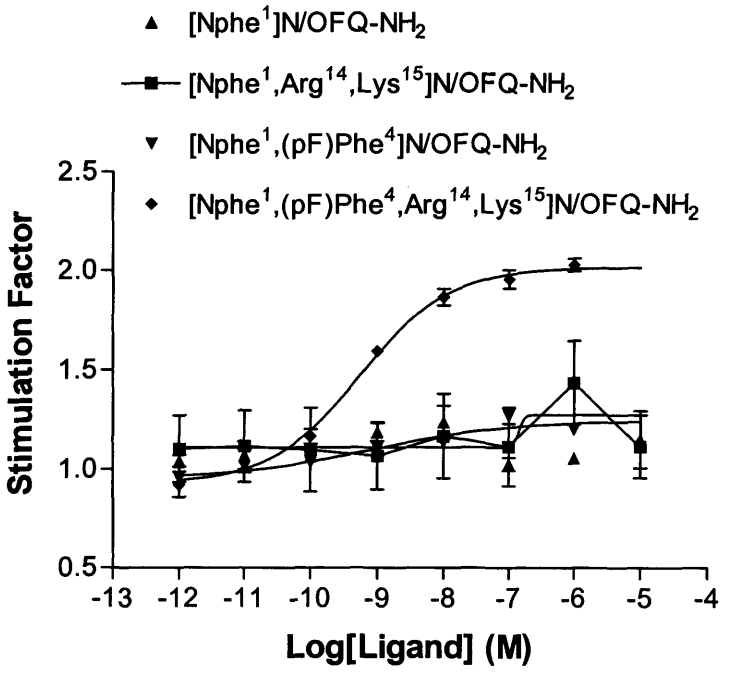

Figure 3-10. [Nphe^1]N/OFQ(1-17)NH_2 (1c), [Nphe^1,(pF)Phe^4]N/OFQ(1-17)NH_2 (2c), [Nphe^1,Arg^{14},Lys^{15}]N/OFQ(1-17)NH_2 (3c) and [Nphe^1,(pF)Phe^4,Arg^{14},Lys^{15}]N/OFQ(1-17)NH_2 (4c), c-series lignads stimulation of GTPγ[^{35}S] binding in CHO_{hNOP} membranes. Values are mean±SEM for n≥3 experiments. Note the Y-axis scale has been reduced to emphasize the low agonist activity of these compounds.

SAR Studies

All [Nphe^1] ligands (c-series) were subsequently screened for their ability to antagonise the activity of N/OFQ. All behaved as competitive antagonists producing a rightward shift in the concentration response curve for N/OFQ. The competitive nature of [Nphe^1]N/OFQ(1-17)NH_2 (1c), [Nphe^1,Arg^{14},Lys^{15}]N/OFQ(1-17)NH_2 (3c) and [Nphe^1(pF)Phe^4,Arg^{14},Lys^{15}]N/OFQ(1-17)NH_2 (4c) was confirmed from Schild regression with slope factors close to 1. The uniformity of Schild plots demonstrated antagonists reached equilibrium during the 1hr incubation. The antagonist potency of the full sequence template ligand [Nphe^1]N/OFQNH_2 was defined in GTPγ[^{35}S] binding studies with N/OFQ as the agonist, yielding pA_2 and slope values of 7.54±0.16 and 1.13±0.07 respectively, see Figure 3-11.

[Nphe^1,(pF)Phe^4]N/OFQ(1-17)NH_2 (2c) despite residual agonist activity anatagonised the N/OFQ response yielding a pK_B value of 8.32, see Table 3-4 and Figure 3-12.

Since [Nphe^1,Arg^{14},Lys15]N/OFQ(1-17)NH_2 (3c) represented the most potent 'pure' antagonist identified here further analysis of its pharmacology was performed. Its ability to antagonise the actions of a series of NOP receptor ligands, both peptide and synthetic in nature was assessed. N/OFQ, N/OFQ(1-13)NH_2, [(pF)Phe^4]N/OFQ(1-13)NH_2, [Arg^{14},Lys^{15}]N/OFQ-OH and Ro64-6198 (synthetic NOP receptor agonist) all produced a concentration-dependent and saturable stimulation of GTPγ[^{35}S] binding. There was no statistical difference in the maximum stimulation (E_{max}) measured for N/OFQ(1-13)NH_2, [(pF)Phe^4]N/OFQ(1-13)NH_2, [Arg^{14},Lys^{15}]N/OFQ and Ro64-6198, when compared to the reference full agonist N/OFQ ANOVA ($p>0.05$). Moreover, these data (i.e., full agonist activity of these molecules) are consistent with previous reports (Guerrini *et al.*, 2001; Hashiba *et al.*, 2002b). Concentration response curves to all agonists were shifted parallel to the right in a concentration dependent manner by [Nphe^1,Arg^{14},Lys^{15}]N/OFQ-NH_2, see Figure 3-13 ([Arg^{14},Lys^{15}]N/OFQ not shown). Schild regression analysis of these data yielded pA_2 values for [Nphe^1,Arg^{14},Lys^{15}]N/OFQ-NH_2 in the range of 8.37-9.06 with Schild slope factors of unity, see Table 3-6.

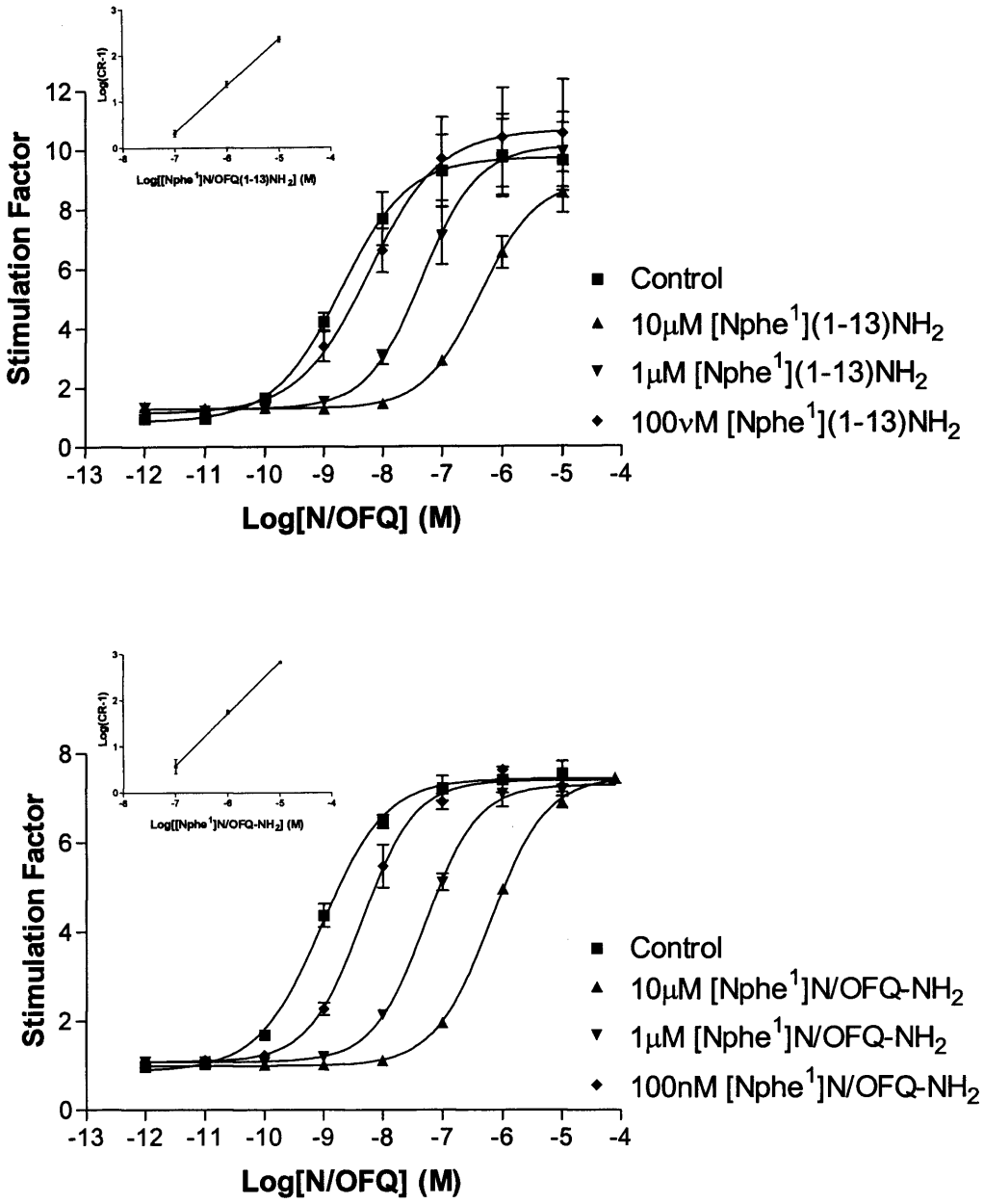

Figure 3-11. Schild regression for antagonist [Nphe^1]N/OFQ(1-13)NH_2 (top) and [Nphe^1]N/OFQ(1-17)NH_2 (1c) (bottom), with N/OFQ as the agonist in CHO_{hNOP} cell membranes, data are mean±SEM from n≥3 experiments. Inserts are the respective Schild plots.

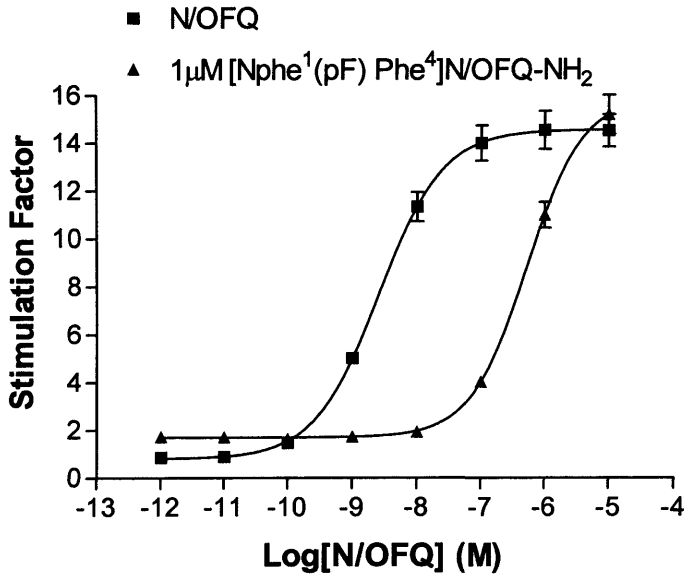

Figure 3-12. pK_B analysis for 1μM [Nphe^1,(pF)Phe^4]N/OFQ (2c) in CHO_{hNOP} membranes, N/OFQ agonist. Data are from mean±SEM (n≥3 experiments).

Agonist	Competing Antagonist			
	[Nphe^1,Arg^{14},Lys^{15}] (3c)		[Nphe^1,(pF)Phe^4,Arg^{14},Lys^{15}] (4c)	
	pA_2	Slope	pA_2	Slope
N/OFQ	9.13±0.23	1.05±0.03	9.71±0.05	1.08±0.03
N/OFQ-NH_2	Not tested	Not tested	9.54±0.17	1.11±0.07
N/OFQ(1-13)-NH_2	9.06±0.08	1.09±0.01	Not tested	Not tested
[(pF)Phe^4]-N/OFQ(1-13)-NH_2	8.98±0.04	1.02±0.01	Not tested	Not tested
Ro64-6198	9.31±0.08*	1.13±0.01	Not tested	Not tested

Table 3-6. pA_2 and slope factors for [Nphe^1,Arg^{14},Lys^{15}]N/OFQ(1-17)NH_2 (3c) and [Nphe^1,(pF)Phe^4,Arg^{14},Lys^{15}]N/OFQ(1-17)NH_2 (4c) determined with a range of different agonists. Values are mean±SEM from n≥3 experiments. *pA_2 value significantly ($p<0.05$) different to that derived with N/OFQ as the agonist (Bonferroni). [Nphe^1,(pF)Phe^4,Arg^{14},Lys^{15}]N/OFQ(1-17)NH_2 pA_2 values were not significantly different from one another.

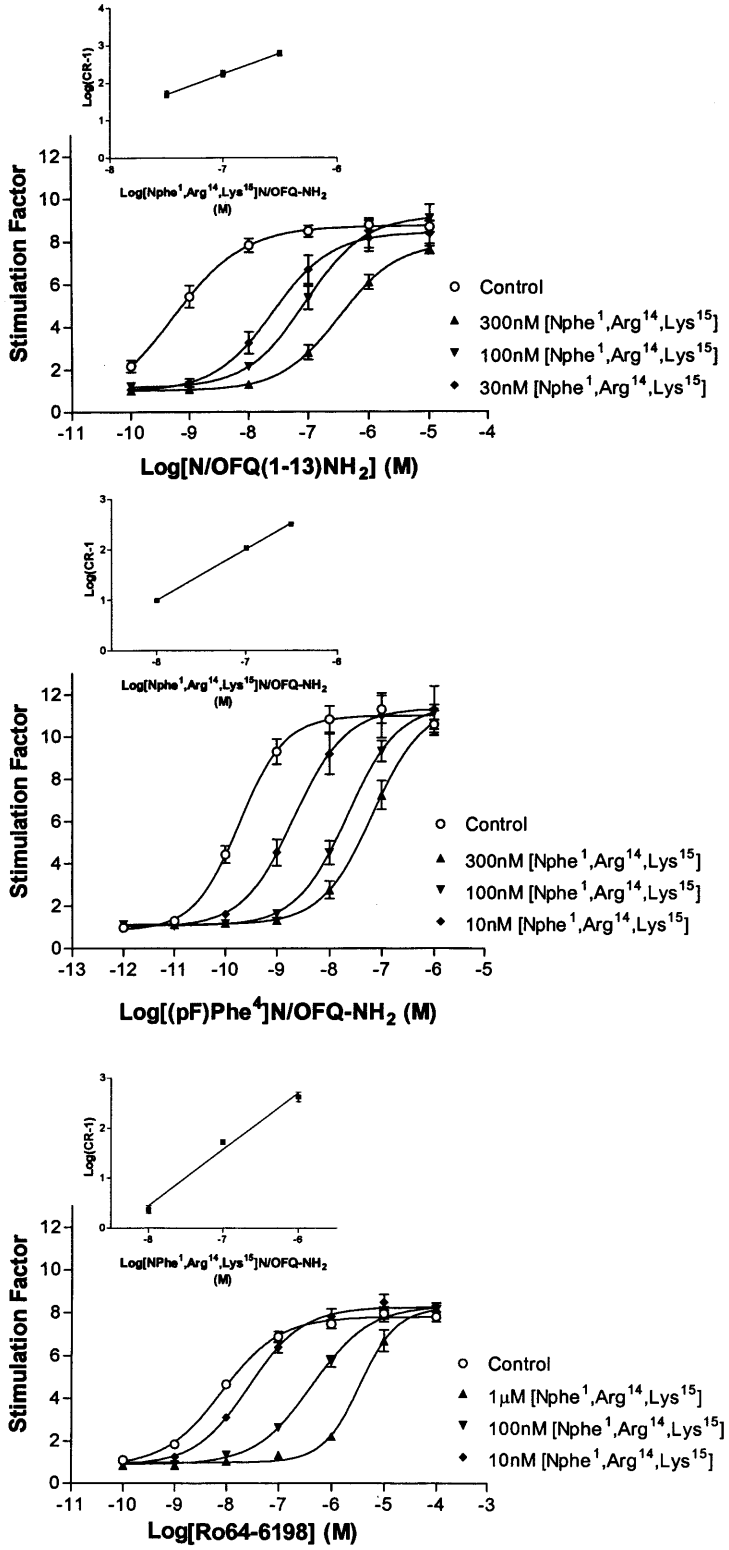

Figure 3-13. Competitive antagonism for [Nphe^1,Arg^{14},Lys^{15}]N/OFQ(1-17)NH_2 (3c) with N/OFQ(1-13)NH_2 (top) [(pF)Phe4]N/OFQ-NH_2 (middle) and Ro64-6198 (bottom) as agonists. Inserts represent relevant Schild plots. Values are mean±SEM from n≥3 experiments.

The pA_2 value for [Nphe^1,(pF)Phe^4,Arg^{14},Lys^{15}]N/OFQ(1-17)NH_2 (4c) of 9.54±0.17 obtained with N/OFQ(1-17)NH_2 as the agonist was additionally confirmed using the endogenous NOP receptor agonist N/OFQ, generating a pA_2 value of 9.71±0.05 and slope factor of 1.08±0.03, see Figure 3-14 and Table 3-6. Regardless of the residual agonist activity of compound 4c, it still antagonised the response of the agonists under investigation. Although the baseline response, i.e. binding of GTPγ[^{35}S] will be elevated relative to basal, the degree of which will be dependent on the concentration of [Nphe^1,(pF)Phe^4,Arg^{14},Lys^{15}]N/OFQ(1-17)NH_2 (4c). This can be clearly seen on the bottom graph of Figure 3-14. In essence compound 4c should be considered a low efficacy partial agonist whose maximal relative intrinsic activity, for the binding of GTPγ[^{35}S] to recombinant human NOP receptors, is α=0.2.

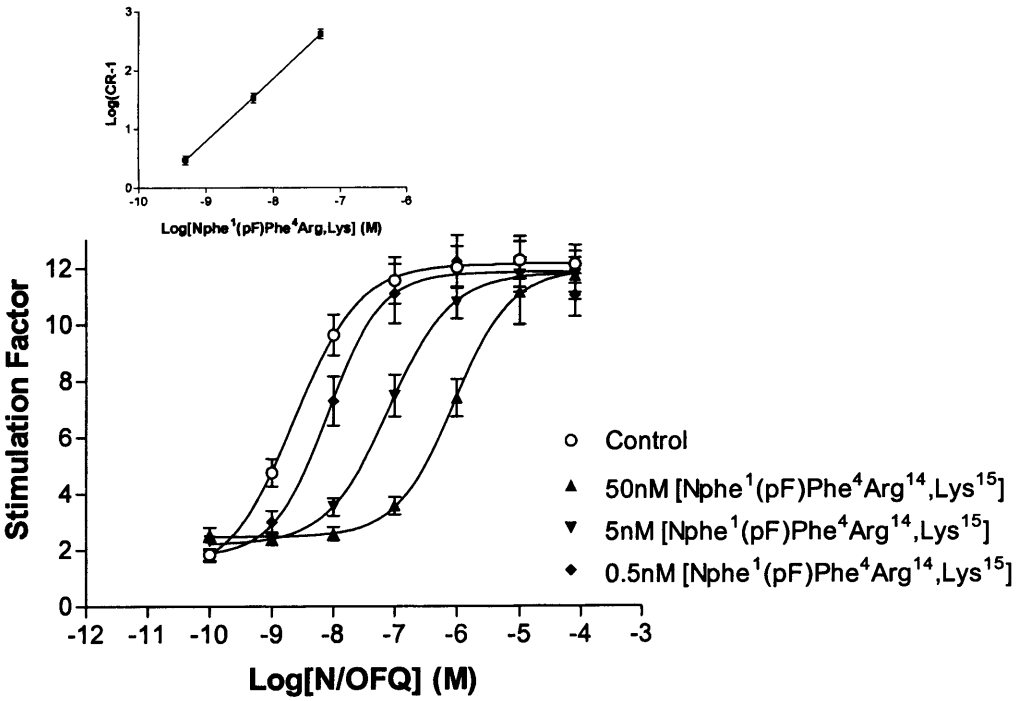

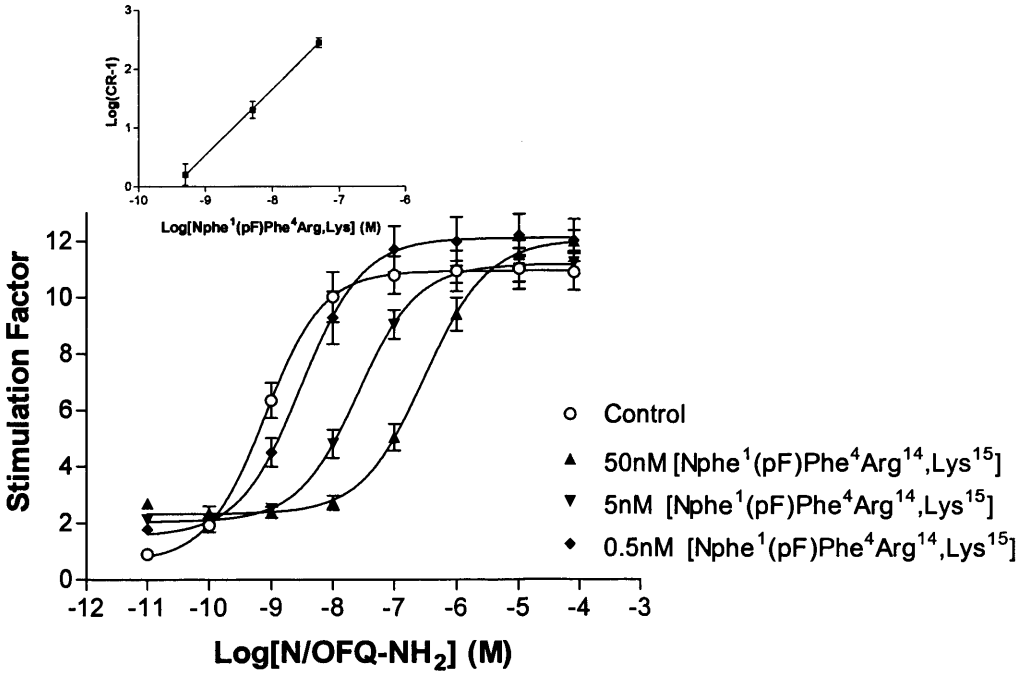

Figure 3-14. Antagonism by [Nphe^1,(pF)Phe^4,Arg^{14},Lys^{15}]N/OFQ(1-17)NH_2 (4c) of the natural N/OFQ ligand and the amidated analog. Inserts represent relevant Schild plots. Values are mean±SEM from n≥3 experiments.

3.3.3 Inhibition of forskolin stimulated cAMP

(This SAR study was performed in collaboration with Dr. T.A. Barnes as part of his Ph.D. who carried out the cAMP studies. In both theses there is data exchange, cAMP data are tabulated only, (Guerrini *et al.*, 2005).

Experiments were performed on whole CHO_{hNOP} cells and represent a functional measure of a downstream bioactive response. Therefore the assay is a useful screen in the detection of residual agonist activity.

In the N/OFQ(1-17)NH_2 template all ligands acted as full agoinsts for inhibition of forskolin stimulated cAMP formation. All substitutions produced increases in ligand potency with a rank order of [(pF)Phe^4,Arg^{14},Lys^{15}]= [Arg^{14},Lys^{15}]> [(pF)Phe^4], see Table 3-7. In the [F/G] series (b-series) of ligands it was seen that all pseudo-peptide analogs behaved as full agonists, i.e. E_{max} values ~100% for inhibition of forskolin stimulated cAMP. The potency of the template ligand [F/G]N/OFQ(1-17)NH_2 (1b) rose from a pEC_{50} of 9.12 to 9.32 and 9.62 with the [(pF)Phe^4] (2b) and [Arg^{14},Lys^{15}] (3b) substitutions respectively. However, in the [F/G] template combined substitutions as in [F/G(pF)Phe^4,Arg^{14},Lys^{15}]N/OFQ(1-17)NH_2 did not produce an additive increase in potency, pEC_{50} of 9.42.

The [Nphe^1] series (c-series) of ligands displayed varying degrees of residual agonist activity with the exception of [Nphe^1,Arg^{14},Lys^{15}]N/OFQ(1-17)NH_2 (3c). [Nphe^1]N/OFQ(1-17)NH_2 (1c) template ligand and [Nphe^1(pF)Phe^4]N/OFQ(1-17)NH_2 (2c) displayed only low efficacy residual agonist activity with an E_{max} of 26.28±2.95 and 28.12±9.86 respectively. Despite residual agonist activity [Nphe^1]N/OFQ(1-17)NH_2 (1c) antagonised the activity of N/OFQ with a pK_B of 6.81 which predicted the pEC_{50} of 6.78 - measured for its agonist activity. [Nphe^1,(pF)Phe^4]N/OFQ(1-17)NH_2 was not tested as an antagonist although it can be suggested, from its increased affinity and agonist potency that this ligand would have greater antagonist potency over the non-substituted version of the ligand. [Nphe^1,(pF)Phe^4,Arg^{14},Lys^{15}] displayed full agonist activity E_{max} value of 91.35±9.55 (% inhibition), this is consistent with the degree of agonist activity seen with the GTPγ[^{35}S] and the degree of amplification when measuring the cAMP effector. Due to its high efficacy [Nphe^1,(pF)Phe^4,Arg^{14},Lys^{15}] could not be tested as an antagonist in this assay.

Compound n° [Xaa^{4}Xbb^{14}Xcc^{15}]	Phe^1-Gly^2 (a series) agonist		Phe$^1\psi$(CH$_2$-NH)-Gly^2 (b series) agonist		antagonist	Nphe^1-Gly^2 (c series) agonist		antagonist
	pEC_{50}	E_{max}	pEC_{50}	E_{max}	pK_b	pEC_{50}	E_{max}	pK_b
1 [Phe^{4}Leu^{14}Ala^{15}]	9.94±0.04	102.7±1.38	9.12±0.09	97.37±8.60	ND	6.78±0.47	26.28±2.95	6.81±0.13
2 [(pF)Phe^{4}Leu^{14}Ala^{15}]	10.18±0.09	101.4±1.35	9.26±0.07	104.3±4.15	ND	7.26±0.61	28.12±9.86	ND
3 [Phe^{4}Arg^{14}Lys^{15}]	10.00±0.09	102.3±0.97	9.62±0.08	88.53±9.37	ND	Inactive	Inactive	7.11±0.16
4 [(pF)Phe^{4}Arg^{14}Lys^{15}]	10.17±0.07	103.8±1.07	9.42±0.06	91.62±2.34	ND	8.31±0.15	91.35±9.55	ND

Table 3-7. Potencies of compounds 1-4a, 1-4b, and 1-4c (see table 3-1 for full peptide titles) at recombinant human NOP expressed in CHO cells in the cAMP assay. Data are the mean of n≥3 ±SEM. Antagonist activity was measured with N/OFQ as the agonist. ND: not determined because the compounds behave as partial or full agonists. Data for ligand 3c ([Nphe^{1}Arg^{14},Lys^{15}]N/OFQ-NH$_2$ is from original paper (Calo *et al.*, 2002). There is no significant ($p>0.05$) difference in the pEC_{50} values of the a- and b-series of compounds, relative to the respective parent compound in the series i.e. compound 1.

3.4 Discussion

In the N/OFQ(1-17)NH_2 (a-series) agonist template all three substitutions gave increases in affinity and functional potency. For [*leucyl*-^{3}H]N/OFQ competition binding and stimulation of GTPγ[^{35}S] binding the rank order of affinity/potency was [(pF)Phe^4] > [Arg^{14},Lys^{15}] > [(pF)Phe^4,Arg^{14},Lys^{15}]. All ligands behaved as full agonists in GTPγ[^{35}S] and cAMP assays, these data are further confirmed in native tissue bioassays using the mouse *vas deferens*, see Table 3-8. The introduction of a pseudo-peptide bond between Phe^1 and Gly^2 in the [F/G] series (b-series) resulted in a small loss of ligand affinity. The C-terminal substitutions [(pF)Phe^4] (2b), [Arg^{14},Lys^{15}] (3b) and [(pF)Phe^4,Arg^{14},Lys^{15}] (4b) made to [F/G]N/OFQ(1-17)NH_2 (1b) resulted in both an increase in affinity and functional potency. Regarding efficacy, the [F/G] modification results in loss of intrinsic activity for GTPγ[^{35}S] binding although, in cAMP assays, this series displayed relative intrinsic activities of α=1. The [(pF)Phe^4], [Arg^{14},Lys^{15}] and [(pF)Phe^4,Arg^{14},Lys^{15}] substitutions had no bearing on ligand efficacy in the [F/G] template (b-series) for binding of GTPγ[^{35}S].

In the antagonist [Nphe^1]N/OFQ(1-17)NH_2 template (c-series) the transposition of the phenyl ring of phenylalanine in position one resulted in a decrease of affinity at the human recombinant NOP receptor. However, affinity was markedly increased through the substitutions outlined previously. [Nphe^1,Arg^{14},Lys^{15}] (3c) was devoid of residual agonist activity in functional studies and displayed potent antagonism with a pA_2 (GTPγ[^{35}S]) of 9.13 and pK_B (cAMP) of 7.11. [Nphe^1]N/OFQ(1-17)NH_2 (1c) was devoid of agonist activity for GTPγ[^{35}S], however [Nphe^1(pF)Phe^4]N/OFQ(1-17)NH_2 (2c) displayed agonism, which was further increased when combined with [Arg^{14},Lys^{15}].

For measures of cAMP both [Nphe^1]N/OFQ-NH_2 (1c) and [Nphe^1,(pF)Phe^4]N/OFQ-NH_2 (2c) showed agonist activity, albeit with low efficacy, of 26% and 28% respectively. [Nphe^1,(pF)Phe^4,Arg^{14},Lys^{15}] (4c) behaved as a full agonist. In this SAR study three ligands of particular importance are identified, [(pF)Phe^4,Arg^{14},Lys^{15}]N/OFQ-NH_2 (2a) a highly potent full agonist, [F/G,(pF)Phe^4,Arg^{14},Lys^{15}]N/OFQ-NH_2 (4b), a highly potent partial agonist and finally [Nphe^1,Arg^{14},Lys^{15}]N/OFQ-NH_2 (3c) a high potency competitive antagonist. These ligands are currently manufactured and sold for laboratory research by our

collaborators in Italy under the names UFP-101 ([Nphe^1,Arg^{14},Lys^{15}]N/OFQ-NH_2), UFP-102 ([(pF)Phe^4,Arg^{14},Lys^{15}]N/OFQ-NH_2) and UFP-103 ([F/G,(pF)Phe^4,Arg^{14},Lys^{15}]N/OFQ-NH_2). In the subsequent chapters ligands will be named using the UFP number abbreviation.

A pEC_{50} of 9.0±0.30 was originally reported for [Arg^{14},Lys^{15}]N/OFQ-OH regarding stimulated GTPγ[^{35}S] binding (Okada *et al.*, 2000) and this value was further confirmed here, pEC_{50} for [Arg^{14},Lys^{15}]N/OFQ-OH of 9.12±0.11, see Figure 3-6. This is different to the pEC_{50} 9.85±0.12 measured in this study as the C-terminus of [Arg^{14},Lys^{15}]N/OFQ is amidated (-NH_2), compound (3a). *In vivo* [Arg^{14},Lys^{15}]N/OFQ-NH_2 (3a) is ~30 fold more potent with greater longevity relative to N/OFQ. The potency ratio of [Arg^{14},Lys^{15}]N/OFQ-NH_2 (3a) and N/OFQ is greater *in vivo* than *in vitro*, revealing increased metabolic stability *in vivo* (Rizzi *et al.*, 2002b).

[Arg^{14},Lys^{15}]N/OFQ-OH was the first peptide to have greater affinity over the natural N/OFQ ligand, until the identification of [(pF)Phe^4]N/OFQ(1-13)-NH_2 (Guerrini *et al.*, 2001). [(pF)Phe^4]N/OFQ(1-13)-NH_2 showed increased affinity over N/OFQ in mouse forebrain and increased potency relative N/OFQ for cAMP inhibition in CHO_{hNOP} cells (Guerrini *et al.*, 2001). The full sequence analog [(pF)Phe^4]N/OFQ-NH_2 (2a) also had increased affinity (pK_i of 10.66±0.09) and potency (pEC_{50} of 9.51±0.16 GTPγ[^{35}S]) in CHO_{hNOP} cell membranes. To further assess the pharmacology of the [(pF)Phe^4] substitution the ability of the NOP selective and non-selective antagonists J-113397 and III-BTD to competitively inhibit [(pF)Phe^4]N/OFQ(1-13)-NH_2 was measured. The pA_2 values for J-113397 and III-BTD, being comparable to other groups, confirms [(pF)Phe^4]N/OFQ(1-13)-NH_2 acts solely through the NOP receptor.

Combining [Arg^{14},Lys^{15}] and [(pF)Phe^4] gave [(pF)Phe^4,Arg^{14},Lys^{15}]N/OFQ-NH_2 (4a). The affinity of [(pF)Phe^4,Arg^{14},Lys^{15}]N/OFQ-NH_2 (4a), (pK_i of 11.32±0.08), demonstrates the additive effect of these two substitutions, this was also true for potency in GTPγ[^{35}S], see Table 3-2. The actions of these agonist peptides were shown to be pertussis toxin (PTX) sensitive, resulting in a complete loss of stimulated GTPγ[^{35}S] binding (data not shown).

Compound n° [Xaa^{4}Xbb^{14}Xcc^{15}]	Phe^1-Gly^2 (a series)			Phe$^1\psi$(CH$_2$-NH)-Gly^2 (b series)			Nphe^1-Gly^2 (c series)		
	agonist		antagonist	agonist		antagonist	agonist		antagonist
	pEC_{50}	E_{max}	pK_b	pEC_{50}	E_{max}	pK_b	pEC_{50}	E_{max}	pK_b
1 [Phe^{4}Leu^{14}Ala^{15}]	8.27 (8.11-8.43)	95 ± 2%	ND	Variable effects		7.17 (6.87-7.47)	Inactive		6.07 (5.92-6.22)
2 [(pF)Phe^{4}Leu^{14}Ala^{15}]	8.59 (8.30-8.88)	92 ± 1%	ND	Variable effects		7.90 (7.65-8.15)	-20% at 10μM		6.61 (6.37-6.86)
3 [Phe^{4}Arg^{14}Lys^{15}]	9.12 (8.93-9.31)	95 ± 1%	ND	Variable effects		8.04 (7.75-8.33)	Inactive		7.24 (7.06-7.45)
4 [(pF)Phe^{4}Arg^{14}Lys^{15}]	9.36 (9.14-9.58)	94 ± 1%	ND	8.99 (8.73-9.25)	53±3	9.20 (9.00-9.40)	-30% at 10μM		*7.97 (7.79-8.15)

Table 3-8 Potencies of compounds 1-4a, 1-4b, and 1-4c (see table 3-1 for full peptide titles) at NOP receptors expressed in the electrically stimulated mouse *vas deferens*. See table 3-1 for For pEC_{50} and pK_B values 95% confidence limits are given. E_{max} values are mean ±SEM. Antagonist activity was measured with N/OFQ as the agonist. ND: not determined because the compounds behave as full agonists. Variable effects indicate a clear reduction of electrically induced contractions (not exceeding 50%) was evident only in some tissues (~50%). Data are from Anna Rizzi, University of Ferrara (unpublished observations 2002).

SAR Studies

The reduced efficacy of the [F/G] (b-series) analogs is beleived to be through greater spacing of determinant pharmacophores (Phe^1 and Phe^4) at the N-terminus affecting location of the Phe^4 pharamacophore in the NOP receptor binding pocket (Guerrini *et al.*, 2000b). *In vivo,* the pseudopeptide is assumed to have greater metabolic stability based on a decreased potency ratio with N/OFQ relative to that *in vitro*. The increase in stability of [F/G] is further confirmed from a longer duration of action *in vivo* compared to N/OFQ and by peptidase inhibitors increasing N/OFQ potency but not that of [F/G]N/OFQ-NH_2 in the rat *vas deferens* (Okawa *et al.*, 1999).

The reduced efficacy of [F/G] (b-series), caused by N-terminal modification, led to further exploration of this site. Shifting the benzyl side chain of Phe^1 by one atom from chiral carbon to nitrogen resulted in a complete loss in efficacy and the identification of the pure antagonist [$Nphe^1$]N/OFQ(1-13)NH_2 (Guerrini *et al.*, 2000a). However the utility of [$Nphe^1$]N/OFQ(1-13)NH_2 was limited by the ligand's low antagonist potency, pK_B 7.33±0.08, in GTPγ[^{35}S]. In order to increase the potency/affinity of [$Nphe^1$]N/OFQ(1-13)NH_2 both the Arg^{14},Lys^{15} and (pF)Phe^4 substitutions alone and in combination were made. The pK_i 10.14±0.10 for [$Nphe^1$,Arg^{14},Lys^{15}]N/OFQ-NH_2 (3c) shows a 60-fold increase in affinity compared with the pK_i of 8.39 reported by Calo *et al* for [$Nphe^1$]N/OFQ(1-13)-NH_2 in CHO_{hNOP} membranes (Calo *et al.*, 2000b). [$Nphe^1$,Arg^{14},Lys^{15}]N/OFQ-NH_2 (3c) was devoid of residual agonist activity and its pA_2 of ~9 shows more than a 10-fold increase in potency over the original [$Nphe^1$]N/OFQ(1-13)-NH_2.

At this point it is worth mentioning that the pA_2 and pK_i for an antagonist should be the same or very similar. There are minor discrepancies in pA_2 and pK_i values reported here. However, pA_2 values were obtained from functional assays in the presence of sodium ions (100mM) which reduce binding to opioid receptors. Sodium ions are essential for measuring G-protein coupling. The presence of guanine nucleotides will reduce the affinity of N/OFQ for NOP (Ardati *et al.*, 1997). pK_i measurements were performed in buffers where all physiological regulators of ligand binding have been removed (Calo *et al.*, 2000c). Therefore direct comparison may not be wise and should explain the small differences seen here.

[Nphe^1,(pF)Phe^4]N/OFQ-NH_2 (2c) also showed an increase in binding affinity over the parent peptide, but to a lesser extent. [Nphe^1(pF)Phe^4,Arg^{14},Lys^{15}]N/OFQ-NH_2 (4c) had increased potency pA_2 9.5-9.7. This is reflected in the pK_i 10.60±0.10 for [Nphe^1,[(pF)Phe^4,Arg^{14},Lys^{15}]N/OFQ-NH_2 (4c) which is an increase of >160-fold relative to [Nphe^1]N/OFQ(1-13)NH_2 (Calo *et al.*, 2000b).

However, [Nphe^1,(pF)Phe^4]N/OFQ-NH_2 (2c) and [Nphe^1,(pF)Phe^4,Arg^{14},Lys^{15}]N/OFQ-NH_2 (4c) did show agonist activity in GTPγ[^{35}S] binding and inhibition of forskolin stimulated cAMP assays. Therefore it should be argued that these compounds are low and high efficacy partial agonists, respectively. [Nphe^1,Arg^{14},Lys^{15}]N/OFQ-NH_2 (3c) had no such residual agonist activity.

Inducible Expression

4 *Partial Agonist Behaviour Depends Upon The Level of NOP Receptor Expression, Studies Using The Ecdysone Inducible Mammalian Expression System.*

4.1 Introduction

A range of currently available molecules has greatly enhanced our understanding of the physiological role(s) of the N/OFQ-NOP system. These molecules include peptides; [(pF)Phe^4]N/OFQ(1-13)-NH_2 (full agonist), [F/G]N/OFQ(1-13)-NH_2 (partial agonist) , [Nphe^1]N/OFQ(1-13)-NH_2 / UFP-101 (antagonists) and non peptides; Ro65-6570 / Ro64-6198 (agonists) and J-113397 / JTC-801 (antagonists) (Bigoni *et al.*, 2002b; Guerrini *et al.*, 2000a; Guerrini *et al.*, 1998; Jenck *et al.*, 2000; Ozaki *et al.*, 2000; Yamada *et al.*, 2002). From a combinatorial library of 52 million hexapeptides, Dooley and colleagues identified 5 with high affinity for the NOP receptor, two of which, Ac-RYYRWK-NH_2 and Ac-RYYRIK-NH_2 are reported here (Berger *et al.*, 2000a; Dooley *et al.*, 1997). Functionally these hexapeptides are all partial agonists with varying degrees of efficacy. The opioid antagonist naloxone benzoylhydrazone (NalBzOH) has been further shown to possess low partial agonist activity at the NOP receptor (Bigoni *et al.*, 2002a; Nicholson *et al.*, 1998).

Initial studies with [F/G]N/OFQ(1-13)NH_2 in the mouse *vas deferens* and guinea pig ileum indicated that the peptide behaved as a NOP selective antagonist (Guerrini *et al.*, 1998). This finding is further confirmed with the full sequence equivalent of this ligand tested in the mouse *vas deferens* (see Section 3). However, in GTPγ[^{35}S] and cAMP assays, [F/G]N/OFQ(1-17)-NH_2 showed partial and full agonism. Therefore the true nature of the efficacy of [F/G]N/OFQ was unclear from these initial studies.

A paper by (Mason *et al.*, 2001) addresses the question(s) of partial agonism and the effect that NOP receptor density plays in ligand relative intrinsic activity. However in order to acquire tissue with different NOP receptor density a variety of different tissues from different species and both central and peripheral sites were used as well as native and recombinantly expressed NOP.

To date the NOP receptor has been expressed in a variety of mammalian cell lines including CHO and HEK-293 cells (Dautzenberg *et al.*, 2001; Guerrini *et al.*, 2000a), which either utilize a transient expression strategy (hence relatively uncontrolled

expression) or are used to generate stable clones (usually with high levels of expression). With particular reference to the evaluation of agonist intrinsic activity, it would be desirable to have a cell line available with a range of differing levels of receptor expression.

In this chapter the ecdysone inducible expression system is utilised and offers a simple method for allowing the production of cultures with differing expression of the NOP receptor. The system is based on that of the insect *Drosophila* which utilities the steroid hormone 20-OH ecdysone to activate gene expression through the ecdysone receptor and cause both metamorphosis and moulting. This system has been modified for use in mammalian cell lines so that a chosen gene can be expressed by the application of a steroid promoter. The ecdysone inducible mammalian expression system makes use of a heterodimer of the ecdysone receptor (VgEcR) and the retinoid X receptor (RXR, modified from mammalian cells) that binds a hybrid response element (E/GRE) in the presence of the plant derived analog of ecdysone, Ponasterone A. The hybrid response element lies upstream of the gene of interest (human NOP here) activation of which leads to transcription and expression of the chosen gene (No *et al.*, 1996). Since mammalian cells are un-responsive to ecdysone and do not contain the ecdysone receptor, basal levels of transcription are very low or absent, see Figure 4-1.

More recently it has been shown that the ecdysone system can induce and/or repress gene transcription in human colon carcinoma cell lines (RKO cells), ecdysone analogs and mimics protect RKO cells from hFasL- and TRAIL-induced cell death (Oehme *et al.*, 2006).

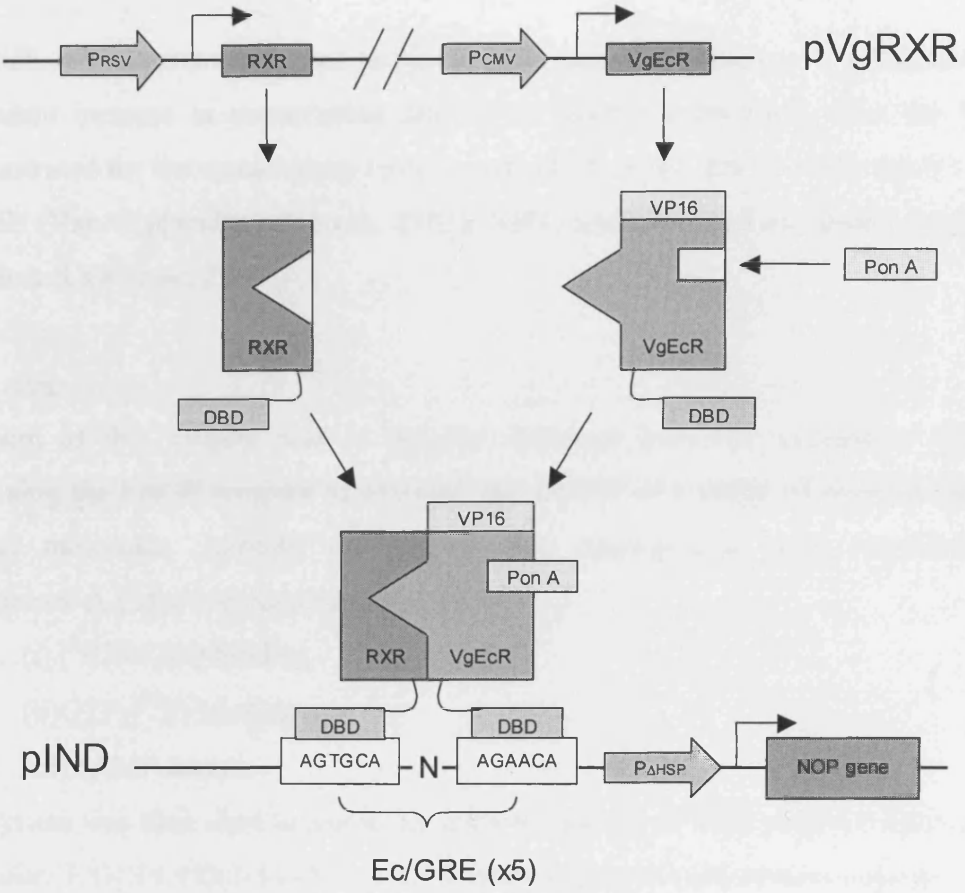

Figure 4-1. Illustration of components of the inducible system, DBD = DNA binding domain, RXR = mammalian retinoid X receptor, Vg = VgECR, the ecdysone receptor.

Briefly, CHO cells were transfected with two plasmids;

1. The inducible expression plasmid containing the hybrid response element to which the gene of interest is added, human NOP receptor here. This plasmid also confers Geneticin (G418) resistance.
2. A plasmid (pVgRXR) encoding the receptor subunits, which respond to ponasterone A, VgEcR and RXR. This plasmid also contains a gene for resistance to the toxin Zeocin.

Inducible Expression

Once cells stably expressing the ecdysone inducible mammalian expression system have been established, selection is maintained by the addition of both Geneticin (G418) and Zeocin to culture media.

Addition of ponasterone A (an ecdysone analogue) will produce a concentration dependent increase in transcription and hence receptor expression. This has been demonstrated for the somatostatin receptor sst2 (Cole *et al.*, 2001), 5-HT (h5-HT 1B, 1F, 4B) (Van Craenenbroeck *et al.*, 2001), 5-HT_7 (Andressen *et al.*, 2006) and DOP receptors (Law *et al.*, 2000).

4.2 Aims

The aim of this chapter was to use the ecdysone inducible expression system containing the hNOP receptor to examine the activity of a range of possible partial agonist molecules. Initially the system was characterised with reference to ponasterone A induction concentrations using;

(i) [^{3}H]N/OFQ binding

(ii)GTPγ[^{35}S] binding

(iii) cAMP assays.

The system was then used to assess the intrinsic activity of NOP receptor ligands, in particular [F/G]N/OFQ(1-13)-NH_2 was of interest given the controversy regarding the efficacy of this ligand. The true nature of the intrinsic activity of [F/G]N/OFQ(1-13)-NH_2 is arguable given some studies have shown antagonist activity whilst others partial and full agonism. The efficacy of a range of proposed partial agonists including [F/G]N/OFQ(1-13)-NH_2, Ac-RYYRIK-NH_2 / Ac-RYYRWK-NH_2 (the hexapeptides of Dooley) and NalBzOH will be assessed at different levels of NOP receptor expression and characterised functionally with respect to GTPγ[^{35}S] and cAMP measurements.

Inducible Expression

4.3 Results

(cAMP assays were performed in collaboration with Dr. T.A. Barnes. In both theses there is data exchange, cAMP data are tabulated only.)

4.3.1 Saturation binding assays

Incubation of $CHO_{INDhNOP}$ cells with ponasterone A for 20hr induced expression of the NOP receptor as measured by the binding of [*leucyl*-^{3}H]N/OFQ. Total specific binding of [*leucyl*-^{3}H]N/OFQ increased from 24 to 1101 fmol/mg protein as the concentration of ponsterone A was increased (1-10μM) (Table 4-1, Figure 4-3). In non-induced cultures there was no significant specific binding despite using a large mass of membrane protein. The induction-expression relationship appeared to be bell-shaped, such that an apparent maximum was obtained at 10μM ponasterone A, above which (i.e. 20μM ponasterone A) binding decreased. The reduced expression at the higher 20μM ponasterone A concentration may have been due to cytotoxicity. However, trypan blue exclusion experiments (n=6) revealed that this concentration of ponasterone A did not cause any reduction in cell viability when present for a 20hr period, 83.53± 1.5% viability for control samples and 89.27±2.7% in th 20μM ponasterone A treated group (n=6 experiments).

Inducible Expression

Induction [Ponasterone A]	*pK_D*	*K_D (pM)*	*B_{max} (fmol/mg protein)*
0μM (non-induced)	----	----	----
1μM	9.91±0.04	123	23.5±4.4
2μM	9.83±0.09	148	68.3±9.7
5μM	10.22±0.15	60	190.6±25.5
10μM	9.89±0.14	129	1101.0±145.3
20μM	9.89±0.13	129	191.2±33.9

Table 4-1. The binding of [*leucyl*-^{3}H]N/OFQ to $CHO_{INDhNOP}$ was ponasterone A dependent. Saturation analysis of log transformed data was used to estimate B_{max} and pK_D. Data are mean±SEM for n≥3 experiments. pK_d values are not significantly different from one another ($p>0.05$). The 1μM ponasterone A induction is significantly different to all other induction concentrations except for 2μM ponasterone A ($p<0.05$, ANOVA with Bonferoni Correction). 20μM ponasterone A expression was significantly less than that induced with 10μM ponasterone A ($p<0.05$, unpaired t-test).

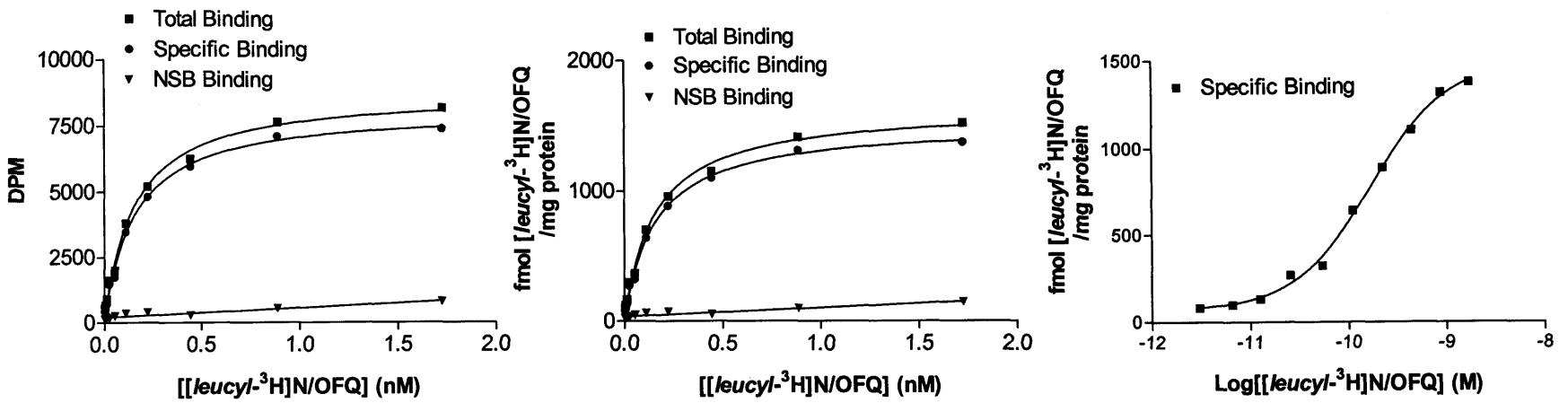

Figure 4-2 Example of a saturation binding experiment in $CHO_{INDhNOP}$ membranes 10μM Ponasterone induction. Right – plot of raw DPM data, Middle – hyperbola plot of same data converted to fmol[*leucyl*-^{3}H]N/OFQ/mg protein and Left – semi-logarithimic plot of specific fmol[*leucyl*-^{3}H]N/OFQ/mg protein data. The Left plot is from which measures of B_{max} and K_D are determined.

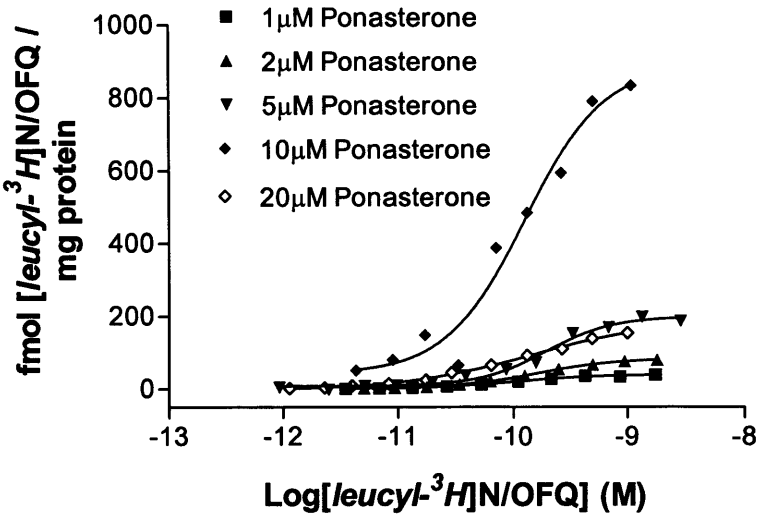

Figure 4-3. Representative [*leucyl*-^{3}H]N/OFQ saturation curves for $CHO_{INDhNOP}$ induced at 1, 2, 5, 10 and 20μM ponasterone A.

4.3.2 Displacement binding assays

In order to show that the protein expressed through the ecdysone inducible expression system is the same as that seen in recombinant CHO_{hNOP} cells a number of displacement binding studies were performed so that ligand affinities could be compared. The binding of a fixed concentration of [*leucyl*-^{3}H]N/OFQ was displaced in a concentration dependent and saturable manner by a range of NOP peptide and non-peptide ligands in membranes prepared from $CHO_{INDhNOP}$ cells induced with 5μM ponasterone A. Values (pK_i) for these data are summarised in Table 4-2. The rank order of affinity was N/OFQ-NH_2=N/OFQ(1-13)-NH_2>N/OFQ=Ac-RYYRWK-NH_2>[F/G]N/OFQ(1-13)-NH_2> Ac-RYYRIK-NH_2= J-113397> NalBzOH.

Inducible Expression

Ligand	pK_i $CHO_{INDhNOP}$
Agonist	
N/OFQ	9.93±0.08
N/OFQ-NH_2	10.37±0.04
N/OFQ(1-13)-NH_2	10.35±0.04
Partial Agonists	
[F/G](1-13)NH_2	7.10±0.02
Ac-RYYRIK-NH_2	9.60±0.10
Ac-RYYRWK-NH_2	9.12±0.02
NalBzOH	9.99±0.03
Antagonists	
J-113397	9.09±0.11

Table 4-2. pK_i values for a range of NOP ligands measured in $CHO_{INDhNOP}$ membranes induced with 5μM ponasterone A. pK_i values were calculated using the Cheng and Prusoff equation using a K_D of 60.3pM in $CHO_{INDhNOP}$ and 70.8pM in CHO_{hNOP} for [leucyl-^{3}H]N/OFQ (Hashiba *et al.*, 2001). Data are mean±SEM (n=4).

4.3.3 GTPγ^{35}S binding data

In membranes prepared from $CHO_{INDhNOP}$ cells incubated with 1, 2, 5 and 10μM ponasterone A, both N/OFQ(1-13)-NH_2 and [F/G]N/OFQ(1-13)-NH_2 stimulated the binding of GTPγ[^{35}S] in a concentration dependent and saturable manner, see Figure 4-4. As the induction concentration of ponasterone A was increased the E_{max} (stimulation factor) of N/OFQ(1-13)-NH_2 increased, from 1.28 (1μM) to 6.95 (10μM) see Table 4-3. The E_{max} of [F/G]N/OFQ(1-13)-NH_2 also increased as a function of the induction concentration, from 0.98 i.e. basal (1μM ponasterone A) to 3.21 (10μM ponasterone A). However, the intrinsic activity of [F/G]N/OFQ(1-13)-NH_2 relative to N/OFQ(1-13)-NH_2 remained similar at between 0.37 – 0.55 for all induction levels.

4.3.4 Inhibition of forskolin stimulated cAMP (McDonald et al., 2003)

In cAMP inhibition studies the E_{max} of both N/OFQ(1-13)-NH_2 and [F/G]N/OFQ(1-13)-NH_2 increased as a function of increasing induction concentration. E_{max} (% inhibition of forskolin stimulated cAMP) increased from 41% to 86% and 20% to

83% at low (1μM) and high (10μM) ponasterone A induction concentrations with N/OFQ(1-13)-NH_2 and [F/G]N/OFQ(1-13)-NH_2 respectively. The intrinsic activity of [F/G]N/OFQ(1-13)-NH_2 relative to N/OFQ(1-13)-NH_2 increased from 0.48 to 0.97 indicating that this molecule, in this assay, behaved as both a partial and full agonist, Table 4-3. At the lower 1μM ponasterone A induction, due to low expression of hNOP receptors and sensitivity of this assay, data for cAMP studies could not be reliably analysed.

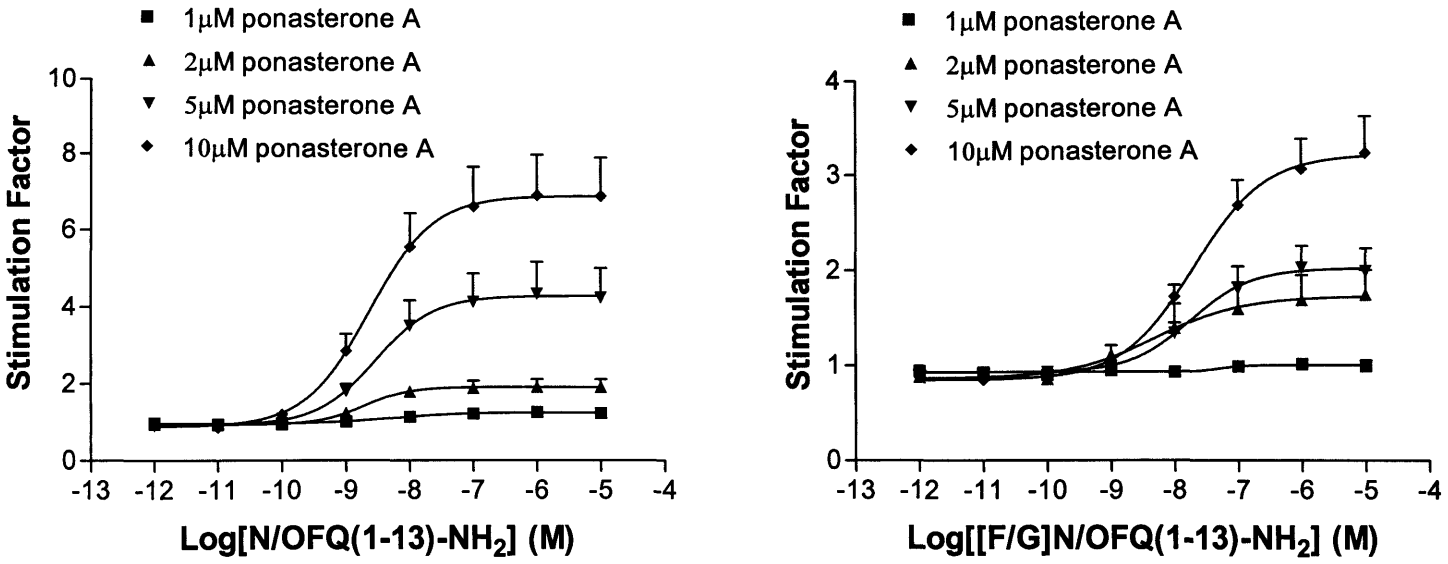

Figure 4-4. N/OFQ(1-13)-NH_2 (Left panel) and [F/G]N/OFQ(1-13)-NH_2 (Right panel) stimulated GTPγ[^{35}S] binding to membranes prepared from $CHO_{INDhNOP}$ cells induced with 1, 2, 5 and 10μM ponasterone A. Data are mean±SEM for n≥4 experiments.

Induction [Ponasterone A]	GTPγ[^{35}S] pEC_{50}/E_{max} N/OFQ(1-13)NH_2	GTPγ[^{35}S] pEC_{50}/E_{max} [F/G](1-13)NH_2	GTPγ[^{35}S] Relative Intrinsic Activity (α)	cAMP pEC_{50}/E_{max} N/OFQ(1-13)NH_2	cAMP pEC_{50}/E_{max} [F/G](1-13)NH_2	cAMP Relative Intrinsic Activity (α)
1μM	8.12±0.32 1.28±0.03	Non-analysable	----	Non-analysable	Non-analysable	----
2μM	8.68±0.11 1.93±0.20	7.23±0.38 1.51±0.15	0.55	9.42±0.49 40.9±2.2	8.26±0.87 19.6±4.8	0.48
5μM	8.52±0.06 4.33±0.80	7.68±0.10 2.01±0.23	0.30	9.72±0.40 79.5±4.1	8.99±0.18 59.37±5.8	0.75
10μM	8.60±0.07 6.95±1.05	7.72±0.06 3.21±0.38	0.37	10.35±0.22 86.0±3.7	8.32±0.13 83.23±4.0	0.97

Table 4-3. N/OFQ(1-13)-NH_2 and [F/G]N/OFQ(1-13)-NH_2 stimulate GTPγ[^{35}S] binding and inhibit cAMP formation in $CHO_{INDhNOP}$ membranes and cells respectively, induced for 20hr with 1, 2, 5, 10μM ponasterone A. cAMP data in (McDonald *et al.*, 2003). Data are mean±SEM for n≥3 experiments. pEC_{50} values for N/OFQ(1-13)-NH_2 and [F/G](1-13)-NH_2 did not differ as a function of Ponasterone A ($p>0.05$, ANOVA). There was a ponasterone concentration dependent increase in E_{max} for N/OFQ(1-13)-NH_2 and [F/G](1-13)-NH_2 ($p<0.05$, ANOVA).

Inducible Expression

4.3.5 Pertussis toxin (PTX) sensitivity

In order to further characterise the action of the NOP receptor expressed via the ecdysone inducible system the sensitivity of the GTPγ[^{35}S] and cAMP responses to PTX pre-treatment were studied. $CHO_{INDhNOP}$ cells were induced for 20hr at 5μM ponasterone A in the absence and presence of PTX (100ng/ml). PTX pre-treatment clearly prevented the agonist actions of N/OFQ, N/OFQ(1-13)-NH_2 and [F/G]N/OFQ(1-13)-NH_2 confirming NOP action through G_i and/or G_o in $CHO_{INDhNOP}$ cells, see
Table 4-4.

Ligand	GTPγ[^{35}S] (Stimulation Factor)		cAMP (% inhibition)	
	Control	+PTX	Control	+PTX
N/OFQ	2.45±0.34	1.01±0.16*	43.1±8.9	0.0±9.6*
N/OFQ(1-13)NH_2	2.49±0.38	1.17±0.13*	50.3±8.8	1.7±7.0*
[F/G](1-13)NH_2	1.48±0.13	0.74±0.20*	45.5±16.7	3.4±15.3*

Table 4-4. PTX sensitivity of agonist stimulated GTPγ[^{35}S] binding and cAMP inhibition for $CHO_{INDhNOP}$ membranes and cells (5μM ponasterone A) respectively, cAMP from (McDonald *et al.*, 2003). Agonists were included at 10μM for GTPγ[^{35}S] experiments and 100nM for cAMP measurements. Data are mean±SEM n≥3. *values are significantly reduced compared with control, $p<0.05$ (paired t-test).

4.3.6 The Influence of GDP concentration on partial agonist efficacy

It is suggested that low-efficacy agonists can activate G-proteins with vacant guanine nucleotide binding sites more effectively. Therefore reducing the GDP concentration should lead to fewer occupied guanine nucleotide binding sites and may lead to increases in relative intrinsic activity (Berger *et al.*, 2000b; Bigoni *et al.*, 2002a; Breivogel *et al.*, 1998). A comparison of GTPγ[^{35}S] binding stimulated by N/OFQ(1-13)-NH_2 and [F/G]N/OFQ(1-13)-NH_2 in CHO_{hNOP} and $CHO_{INDhNOP}$ cells (5μM ponasterone A induction) at high (100μM) and low (5μM) concentrations of GDP was therefore investigated to further determine differences in the activity of partial agonists at the NOP receptor.

Inducible Expression

The stable CHO_{hNOP} cell line used here expresses ~1.9pmol/mg protein NOP, at 100μM GDP both N/OFQ(1-13)-NH_2 and [F/G]N/OFQ(1-13)-NH_2 stimulated GTPγ[^{35}S] binding in a concentration dependent and saturable manner with pEC_{50} values of 9.11 and 8.28 respectively. N/OFQ(1-13)-NH_2 was a full agonist, E_{max} 10117 net DPM, whilst [F/G]N/OFQ(1-13)-NH_2 displayed partial agonist activity in this preparation with an E_{max} of 6221 net DPM, (Figure 4-5 and Table 4-5). At 5μM GDP the potency of both [F/G]N/OFQ(1-13)-NH_2 (pEC_{50} 8.68) and N/OFQ(1-13)-NH_2 (pEC_{50} 9.57) increased as did the net stimulated binding of GTPγ[^{35}S], 24255 and 16999 DPM respectively. More importantly the relative intrinsic activity of [F/G]N/OFQ(1-13)-NH_2 compared to N/OFQ(1-13)-NH_2 increased from 0.61 at 100μM GDP to 0.70 at 5μM GDP. In the stable CHO_{hNOP} clones, using the natural full agonist N/OFQ and the putative partial agonist Ac-RYYRWK-NH_2, the relative intrinsic activity of Ac-RYYRWK-NH_2 increased from 0.55 at 100μM GDP to 0.79 at 5μM GDP. These studies for N/OFQ(1-13)-NH_2 and [F/G]N/OFQ(1-13)-NH_2 were replicated using membranes from 5μM ponasterone A induced cells (Table 4-5) where the rise in relative intrinsic activity was from 0.38 at 100μM GDP to 0.81 at 5μM GDP for [F/G]N/OFQ(1-13)-NH_2.

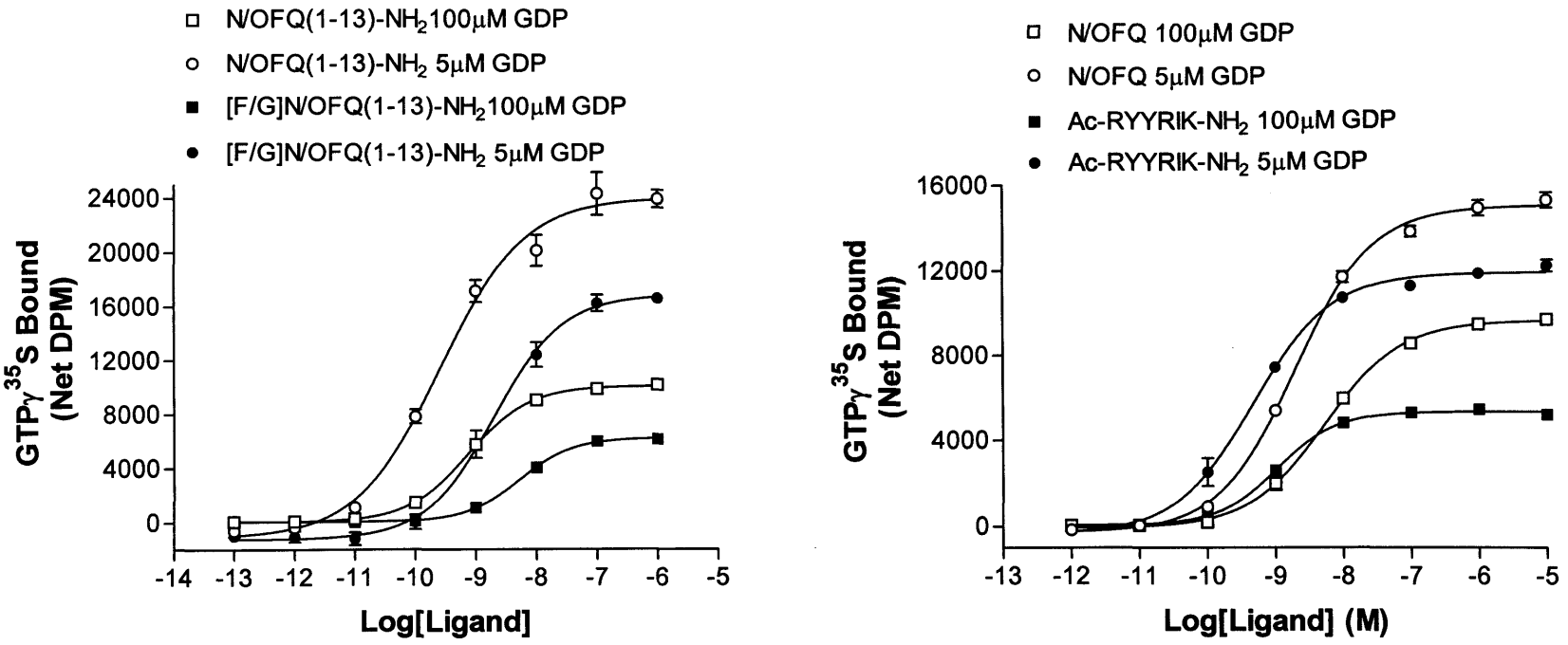

Figure 4-5. Comparison of the effect of 100 and 5μM GDP concentrations on the relative intrinsic activity of [F/G]N/OFQ(1-13)-NH_2 (Left) and Ac-RYYRIK-NH_2 (Right), relative to N/OFQ(1-13)-NH_2 and N/OFQ respectively. Data are for the stimulated binding of GTPγ[^{35}S] in CHO_{hNOP} membranes and are presented as net DPM bound i.e. minus basal DPM. Data mean±SEM for n=3 experiments.

	CHO_{hNOP}		$CHO_{INDhNOP}$		CHO_{hNOP}	
	100μM GDP					
	N/OFQ(1-13)	[F/G](1-13)	N/OFQ(1-13)	[F/G](1-13)	N/OFQ	Ac-RYYRWK
pEC_{50}	9.11±0.03	8.28±0.01	8.65±0.07	7.72±0.05	8.30±0.04	8.97±0.03
E_{max} (dpm)	10117±134	6221±374	2368±301	908±104	9548±86	5291±78
α	1.00	0.61	1.00	0.38	1.00	0.55
	5μM GDP					
	N/OFQ(1-13)	[F/G](1-13)	N/OFQ(1-13)	[F/G](1-13)	N/OFQ	Ac-RYYRWK
pEC_{50}	9.57±0.02*	8.68±0.12*	9.27±0.12*	8.02±0.03*	8.70±0.01*	9.34±0.09*
E_{max} (dpm)	24255±964*	16999±242*	6635±1080*	5388±834*	14894±317*	11775±130*
α	1.00	0.70	1.00	0.81	1.00	0.79

Table 4-5. Ability of [F/G]N/OFQ(1-13)-NH_2 and Ac-RYYRWK-NH_2 to stimulate GTPγ[^{35}S] binding in CHO_{hNOP} and $CHO_{INDhNOP}$ (5μM ponasterone A) membranes in the presence of 100 or 5μM GDP. N/OFQ(1-13)-NH_2 and N/OFQ were used as reference full agonists. Data are mean±SEM (n≥3). *$p<0.05$ (paired t-test) pEC_{50} / E_{max} different to that at 100μM GDP.

Inducible Expression

In $CHO_{INDhNOP}$ induced at 1, 5 and 10μM ponasterone A those ligands shown to behave as partial agonists i.e. Ac-RYYRIK-NH_2, Ac-RYYRWK-NH_2 and NalBzOH were tested for their ability to stimulate the binding of GTPγ[^{35}S], see Table 4-6 and Figure 4-6. At 5μM ponasterone A both N/OFQ and N/OFQ-NH_2 produced concentration dependent and saturable increases in the binding of GTPγ[^{35}S] with E_{max} values of 3.72±1.01 and 4.13±0.62 respectively. At the same induction concentration Ac-RYYRIK-NH_2 and Ac-RYYWK-NH_2 were clear partial agonists (E_{max} 1.66±0.02 and 2.16±0.08 respectively) with intrinsic activity values of 0.40 and 0.52 relative to N/OFQ-NH_2. At the reduced induction concentration of 1μM ponasterone A Ac-RYYRIK-NH_2 and Ac-RYYWK-NH_2 showed low agonist activity. NalBzOH produced no measurable stimulation of GTPγ[^{35}S] binding up to 100μM even in membranes from cells induced at the highest ponasterone A concentration (10μM).

Ligand	*Induction [Ponasterone A]*	*pEC_{50}*	*E_{max}*
N/OFQ	5μM	8.26±0.01	3.72±1.01
N/OFQ-NH_2	5μM	8.92±0.05	4.13±0.62
NalBzOH	1μM	No response at 100μM	
	5μM	No response at 100μM	
	10μM	No response at 100μM	
Ac-RYYRIK-NH_2	1μM	7.76±0.26	1.10±0.04
	5μM	8.27±0.27	1.66±0.02*
Ac-RYYRWK-NH_2	1μM	8.39±0.27	1.22±0.07
	5μM	8.69±0.11	2.16±0.08*

Table 4-6. Effects of NalBzOH, Ac-RYYRIK-NH_2 and Ac-RYYRWK-NH_2 at different induction concentrations on GTPγ[^{35}S] binding, comparison with N/OFQ and N/OFQ-NH_2. Data are mean±SEM for n≥3 experiments. *$p<0.05$ (unpaired t-test) significantly different compared with 1μM ponasterone A induced cells. pEC_{50} values for Ac-RYYRIK-NH_2 and Ac-RYYRWK-NH_2 were not significantly different at their respective 1μM and 5μM Ponasterone A inductions.

Inducible Expression

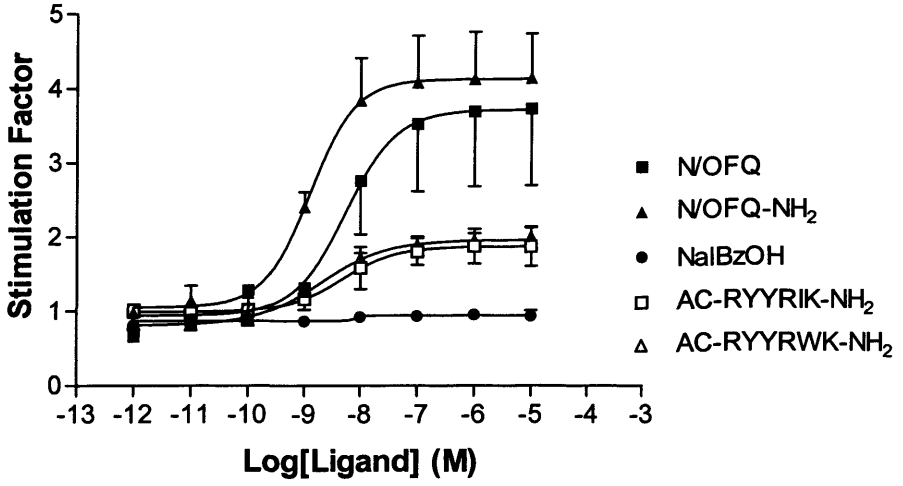

Figure 4-6. GTPγ[^{35}S] binding in $CHO_{INDhNOP}$ induced with 5μM ponasterone A, stimulated by N/OFQ, N/OFQ-NH_2, NalBzOH, Ac-RYYRWK-NH_2, Ac-RYYRWK-NH_2. Data are mean±SEM for n ≥3 experiments.

4.3.7 Antagonism Experiments

In $CHO_{INDhNOP}$ cells induced at 5μM ponasterone A 100nM of J113397 antagonised the N/OFQ(1-13)NH_2 stimulated binding of GTPγ[^{35}S] with a pK_B of 8.45 Figure 4-7. This value is essentially identical to the pA_2 for J113397 of 8.53 measured in CHO_{hNOP} membranes, see section 3.

Since [F/G]N/OFQ(1-13)-NH_2 displayed no measurable stimulation of GTPγ[^{35}S] at the 1μM ponasterone A induction concentration this level of expression of the NOP receptor was used to determine the antagonist activity of this ligand. The binding of GTPγ[^{35}S] stimulated by N/OFQ(1-13)-NH_2 was competitively antagonised by 1μM [F/G]N/OFQ(1-13)-NH_2 with a pK_B of 7.62±0.08 (pEC_{50} 7.68±0.10 at 5μM ponasterone A). At the same induction concentration 10μM NalBzOH also competitively antagonised the actions of N/OFQ(1-13)-NH_2 with a pK_B of 7.02±0.13, Figure 4-7.

Inducible Expression

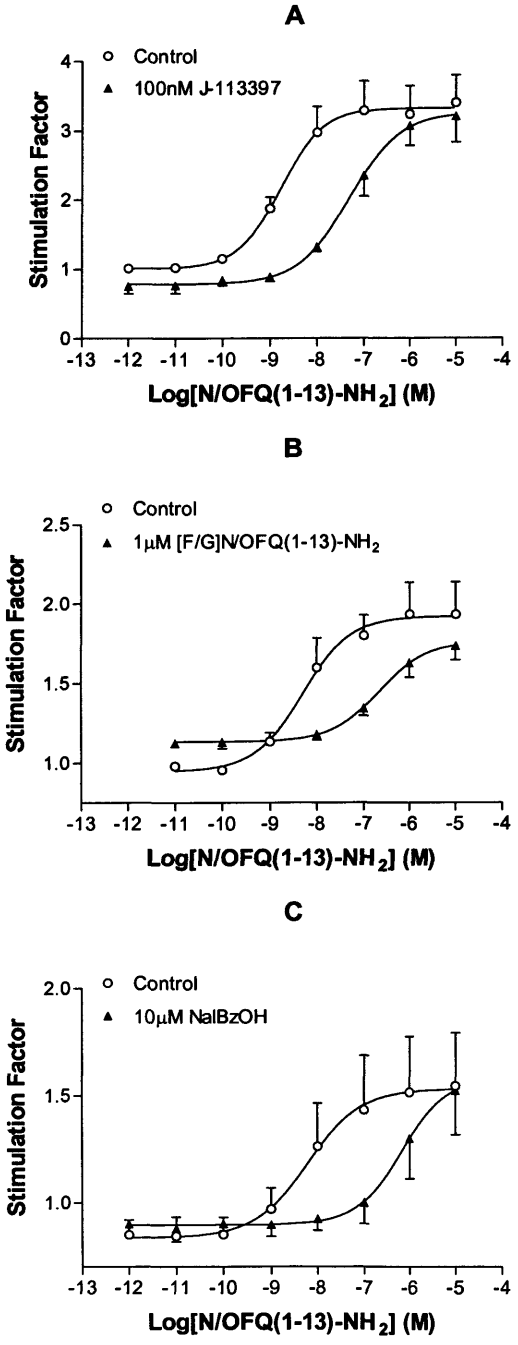

Figure 4-7. N/OFQ(1-13)-NH_2 stimulated GTPγ^{35}S binding is antagonised by 100nM J-113397 at 5μM ponasterone A induction (A), 1μM [F/G]N/OFQ(1-13)-NH_2 at 1μM ponasterone A induction (B) and 10μM NalBzOH at 1μM ponasterone A induction (C). Data are mean±SEM, n=3 experiments.

4.4 Discussions

Earlier studies have reported variable intrinsic activity for [F/G]N/OFQ(1-13)-NH_2 from zero (pure antagonism) to one (full agonism) (Calo *et al.*, 2000a; Calo *et al.*, 1998; Grisel *et al.*, 1998; Mason *et al.*, 2001; Meis *et al.*, 1998; Menzies *et al.*, 1999; Okawa *et al.*, 1999). Consensus is that [F/G]N/OFQ(1-13)-NH_2 is in fact a low efficacy partial agonist (Calo *et al.*, 2000c).

In this chapter it is shown that estimates of relative intrinsic activity for a range of NOP receptor partial agonists are dependent upon receptor density and assay system. The NOP receptor expressed through the ecdysone inducible expression system, not only displays the same pharmacology observed in different cell lines and tissues, but also gives a reliable method for titration of receptor density.

Conflicting data from different groups using similar and differing preparations reported agonism, partial agonism and antagonism for [F/G]N/OFQ(1-13)-NH_2 and also for Ac-RYYRIK-NH_2, Ac-RYYRWK-NH_2 and NalBzOH (Berger *et al.*, 2000a; Calo *et al.*, 2000a; Mason *et al.*, 2001; Okawa *et al.*, 1999). *In vitro* [F/G]N/OFQ(1-13)-NH_2 was a full agonist for inhibition of cAMP formation in CHO_{hNOP} cells and inhibition of glutamate release from synaptosomes (Okawa *et al.*, 1999). Following i.c.v. injection in rats, [F/G]N/OFQ(1-13)-NH_2 caused a decrease in heart rate, mean arterial pressure, urinary sodium excretion and a marked increase in urine flow, similar to N/OFQ but of longer duration (Kapusta *et al.*, 1999). Partial agonism was reported for the stimulation of GTPγ[^{35}S] binding in mouse N1E-115 cells (Olianas *et al.*, 1999). For a detailed review of the actions of [F/G]N/OFQ(1-13)-NH_2 see (Calo *et al.*, 2000a). This difference in signalling between central and peripheral NOP was explained by [F/G]N/OFQ(1-13)-NH_2 being a partial agonist with strong coupling at central receptors and high expressing transfected systems and weak coupling in peripheral tissue and low expression systems (Okawa *et al.*, 1999). To date the variable pharmacology of these partial agonists has not been carefully examined in the same expression system.

The problem has been addressed by only a few groups, using either cells transfected with different levels of NOP or using peripheral and central tissue (Mason *et al.*, 2001). A study by Mason and colleagues showed differences in the relative intrinsic activities of

Inducible Expression

[F/G]N/OFQ(1-13)-NH_2, Ac-RYYRIK-NH_2, and Ac-RYYRWK-NH_2 using transfected cells, central tissue preparations and peripheral tissue (Mason *et al.*, 2001). Differences in coupling efficiency are just one variable seen between different tissue preparations and native and recombinant NOP, which can affect values of relative intrinsic activity. Hence, differences in relative intrinsic activity may not be the result of changes in receptor number but due to changes in coupling efficiency or other local cellular factors such GDP concentration. Recent suggestions and data have shown that agonists can differ in their efficacy for different cellular responses or subtypes of downstream effectors (Berg *et al.*, 1998; Cordeaux *et al.*, 2000). Indeed N/OFQ can stimulate phospholipase C (PLC) activity, with differential potency via a $G_{\alpha 14}$ mediated PTX insensitive pathway (in $G_{\alpha 14}$ transfected cells, EC_{50} 5nM (Yung *et al.*, 1999)) and via a $G_{\alpha i}$ PTX sensitive pathway (EC_{50} 0.4nM (Reinscheid *et al.*, 1995)). Therefore different subtypes of effector or cellular pathways leading to a given response, between different cell types or tissue preparations, could give rise to differential efficacy/potency and hence make conclusions about intrinsic activities of a ligand awkward, i.e. differences in relative efficacy of a ligand between tissues may not be due to receptor density alone.

The ecdysone expression system has been used previously for the variable expression of other GPCRs (Van Craenenbroeck *et al.*, 2001), here it is used for the human isoform of the NOP receptor. A higher induction concentration (10μM ponasterone A) produced receptor densities (~1pmol/mg) similar to many of the commonly used transfected cell systems e.g. CHO_{hNOP} used here (1.9pmol/mg) (Hashiba *et al.*, 2002b), HEK 293 (1.2pmol/mg) (Dautzenberg *et al.*, 2001), CHO_{hNOP} (0.9pmol/mg) (Mason *et al.*, 2001). Receptor density induced at 5μM ponasterone A (~200fmol/mg) was similar to that reported in rat central tissue, e.g. rat cortex (236fmol/mg) (Berger *et al.*, 2000a), rat frontal cortex (246fmol/mg) (Mason *et al.*, 2001) and rat cerebral cortex (180fmol/mg) (Okawa *et al.*, 1998b) and represents a 'pseudo-physiological' level of receptor expression. [*leucyl*-^{3}H]N/OFQ competition binding assays at this expression indicated a pharmacology consistent with that reported in the literature for the human NOP receptor. In GTPγ[^{35}S] and cAMP assays at 5μM induction, N/OFQ and N/OFQ-NH_2 were both full agonists with pEC_{50} values of 8.26 and 8.92 - GTPγ[^{35}S], 9.38 and 9.66 – cAMP,

respectively. In all assays agonist functional responses were PTX sensitive confirming the expected G_i/G_o coupling in this system.

As noted, it has been suggested that the variable activity reported for the actions of [F/G]N/OFQ(1-13)-NH_2 i.e. agonist, partial agonist and antagonist, were the result of different expression of the NOP receptor at those sites assayed. Since the ecdysone system allows control of the expression of hNOP, by changing the induction concentration of ponasterone A, the effect this had on the intrinsic activity of both N/OFQ(1-13)-NH_2 and [F/G]N/OFQ(1-13)-NH_2 in two functional assays could be measured. The efficacy of N/OFQ(1-13)-NH_2 with respect to its ability to stimulate GTPγ[^{35}S] binding and inhibit adenylyl cyclase was assumed to be full agonist in nature for all expression levels.

The relative intrinsic activity of [F/G]N/OFQ(1-13)-NH_2 varied at different expression levels and between assays. For cAMP measurements [F/G]N/OFQ(1-13)-NH_2 was a full agonist at 10μM ponasterone A and partial agonist at all other induction concentrations. The suspected presence of a receptor reserve at the 10μM ponasterone A induction along with amplification steps in the pathway leading to the inhibition of adenylyl cyclase are the likely explanation of this finding. However, it could be more fitting to suggest a coupling reserve (i.e. only a small proportion of the activated G-proteins are required to generate a full response) since no change in relative intrinsic activity is seen in GTPγ[^{35}S] binding, suggesting no receptor reserve. At 1μM ponasterone A [F/G]N/OFQ(1-13)-NH_2 produced no response. At expression greater than that induced by 1μM ponasterone A i.e. ~30fmol/mg, [F/G]N/OFQ(1-13)-NH_2 was a partial agonist in GTPγ[^{35}S] measurements. Indeed it is tempting to suggest that in previous studies where [F/G]N/OFQ(1-13)-NH_2 behaved as an antagonist that tissue receptor densities would be in the region of 30fmol/mg, although as mentioned previously other factors also play a role in measures of ligand efficacy.

Inducible Expression

To discriminate between antagonists and partial agonists Berger (Berger *et al.*, 2000b) described a method based upon decreasing the GDP concentration in GTPγ[^{35}S] binding studies. High GDP (≥100μM) concentration can mask the low activity of partial agonists. Previous studies have shown that stimulation of GTPγ[^{35}S] binding by the partial agonist NalBzOH depended on the GDP concentration (Bigoni *et al.*, 2002a; Okawa *et al.*, 1999). In a similar manner the maximal response and the relative intrinsic activity of both [F/G]N/OFQ(1-13)-NH_2 and Ac-RYYWK-NH_2 could be altered through manipulating the GDP concentration. Decreasing the GDP concentration to 5μM not only increased net stimulated GTPγ[^{35}S] binding but also the intrinsic activity of [F/G]N/OFQ(1-13)-NH_2 and Ac-RYYRWK-NH_2, relative to N/OFQ and N/OFQ(1-13)-NH_2, in both CHO_{hNOP} and $CHO_{INDhNOP}$ (5μM ponasterone A) cells. This increase in intrinsic activity for [F/G]N/OFQ(1-13)-NH_2 and Ac-RYYRWK-NH_2 suggests that partial agonists and full agonists differ in their dependency for GDP, see section 7. Indeed it has been demonstrated that different ligands at native CB-1 receptors all differed in their dependence for GDP. It therefore seems apparent that individual ligands will have unique requirements in order to achieve maximal agonist responses, GDP requirement being one example. The specific needs of specific ligands is suggestive of agonist trafficking whereby ligands have a 'personal' profile of response pathways that they can elicit along with differing efficacies for these responses. It can be seen that intrinsic activity is a property of both the ligand and the tissue, hence relative values change with hNOP expression.

Finally, the issue that for a partial agonist the pEC_{50} should predict its pA_2 or pK_B has been addressed. Using the lowest induction concentration of 1μM ponasterone A, the ability of N/OFQ(1-13)-NH_2 to stimulate GTPγ[^{35}S] binding was competitively antagonised by [F/G]N/OFQ(1-13)-NH_2 with a pK_B of 7.62, which is essentially identical to its pEC_{50} of 7.68 (5μM ponasterone A). This was also true for NalBzOH which antagonised N/OFQ(1-13)-NH_2 stimulated GTPγ[^{35}S] binding with a pK_B of 7.02 (pEC_{50}7.00, GTPγ[^{35}S] binding (Bigoni *et al.*, 2002a)). NalBzOH was devoid of agonist activity and is therefore a very-low efficacy partial agonist. Ac-RYYRIK-NH_2 and Ac-

Inducible Expression

RYYRWK-NH_2 displayed similar efficacy to [F/G]N/OFQ(1-13)-NH_2 for GTPγ[^{35}S] binding. Overall, these partial agonists display a rank order intrinsic activity of Ac-RYYRWK-NH_2>[F/G]N/OFQ(1-13)-NH_2>Ac-RYYRIK-NH_2>NalBzOH.

5 *In vitro Bioassays using Mouse Colon and Vas Deferens (These experiments were performed whilst on an exchange visit to the University of Ferrara, Italy)*

5.1 Introduction

The nociceptin receptor was initially reported to be located not only in the central nervous system but also has been identified in a number of peripheral tissues (Wang *et al.*, 1994). Subsequently a number of peripheral tissue preparations have been shown to be sensitive to N/OFQ through inhibition of evoked transmitter release from cholinergic, noradrenergic and sensory nerves in;

(i) guinea pig ileum, left atrium, trachea, bronchus, renal pelvis and colon

(ii) mouse, colon and *vas deferens*

(iii) rat trachea, anococcygeus and *vas deferens,*

see (Berzetei-Gurske *et al.*, 1996; Bigoni *et al.*, 1999; Calo *et al.*, 1996; Fischer *et al.*, 1998; Giuliani *et al.*, 1996; Giuliani *et al.*, 1997; Helyes *et al.*, 1997; Patel *et al.*, 1997)

The *vas deferens* is a classical preparation used to measure the activity of DOP (Hughes *et al.*, 1975a) receptor ligands, indeed this preparations was first used to identify, name and characterise the DOP receptor. In the *vas deferens* DOP receptor activation inhibits electrically induced contractions. The mouse and rat *vas deferens* were shown to be sensitive to N/OFQ, where the ligand produced a dose dependent inhibition of electrically stimulated contractions (Calo *et al.*, 1996). In the mouse *vas deferens* the action of the DOP receptor agonist deltorphin I can be inhibited by naloxone whilst the agonist activity of N/OFQ is insensitive to this antagonist. It has further been demonstrated that the human *vas deferens* is also sensitive to the actions of N/OFQ although the use of high concentrations of peptidase inhibitors are required to prevent rapid degradation of the peptide (Bigoni *et al.*, 2001).

Murine proximal and distal colon, suspended along the axis of the longitudinal muscle, has been shown to be sensitive to N/OFQ where it causes dose dependent isometric smooth muscle contractions (Osinski *et al.*, 1999). The isolated mouse colon tissue preparation has also been used historically for the study of classical opioid receptor ligands, specifically the preparation is sensitive to MOP receptor ligands (Paton, 1957).

5.2 Aims

The aim of this chapter is to examine the effects of the partial agonist [F/G]N/OFQ(1-13)NH_2 in both the mouse isolated colon and *vas deferens*. Additionally genetically modified CD1/C57-BL6J/129 mice either homozygous for the NOP receptor gene ($NOP^{+/+}$) or homozygous for the absence of the gene encoding NOP receptor ($NOP^{-/-}$) were characterised for their responsiveness to N/OFQ in both those preparations discussed above. These data address the question of efficacy at native NOP receptors in a native cellular environment.

5.3 Results

5.3.1 Mouse vas deferens

In the mouse *vas deferens* (mVD) the truncated amidated analog N/OFQ(1-13)NH_2 inhibited the electrical field stimulation (EFS) induced twitches by 86.74% with a pEC_{50} of 7.80±0.25, see Figure 5-1. [F/G]N/OFQ(1-13)NH_2 inhibited tissue twitch but with reduced potency pEC_{50} 6.61±0.23 and efficacy, 63.5% inhibition of EFS induced twitch (intrinsic activity α=0.73) see Figure 5-1.

[F/G]N/OFQ(1-13)NH_2 was used to antagonize the response of N/OFQ(1-13)NH_2 following a 15min pre-incubation, see Figure 5-2. [F/G]N/OFQ(1-13)NH_2 caused a rightward shift in the concentration response curve of N/OFQ(1-13)NH_2 consistent with competitive antagonism, pK_B of 6.49±0.18 (n=5). However, [F/G]N/OFQ(1-13)NH_2 displayed a high degree of agonist activity and so the data were further analysed with the baseline reset to the residual agonist activity of [F/G]N/OFQ(1-13)NH_2. This would allow the rightward shift to be seen more clearly and to determine the accuracy of the pK_B derived using the raw data. With the data normalized a pK_B of 6.68±0.23 was determined, not significantly different from that calculated using the raw data pK_B of 6.49±0.18.

Figure 5-1. Percentage inhibition (contraction size) of EFS induced twitches in mouse vas deferens by N/OFQ(1-13)NH_2 and [F/G]N/OFQ(1-13)NH_2, data are mean±SEM n= 3 experiments.

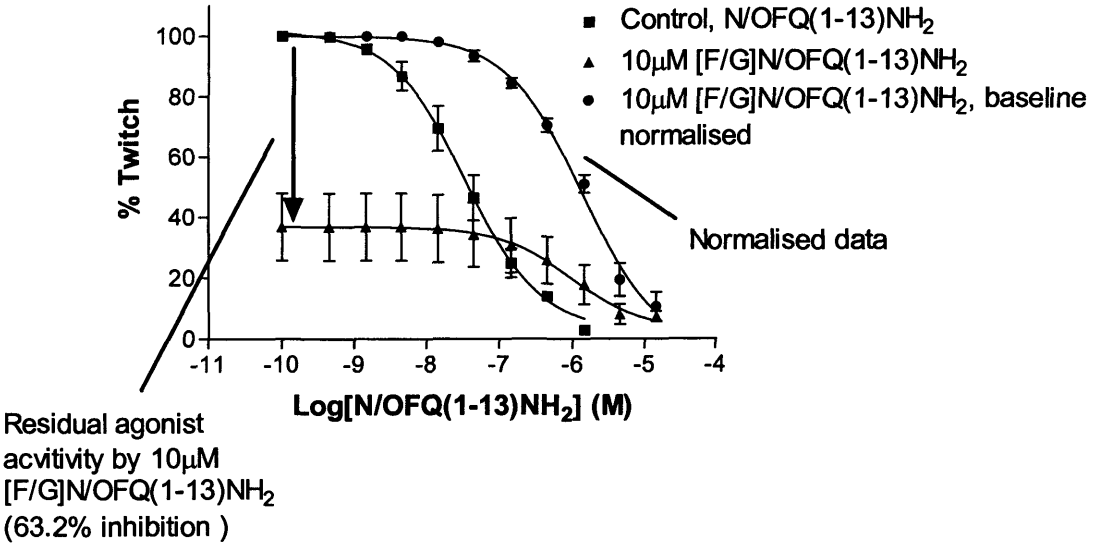

Figure 5-2. Antagonism of N/OFQ(1-13)NH_2 twitch inhibition in mouse *vas deferens* by 10μM [F/G]N/OFQ(1-13)NH_2 (15min pre-incubation.). Data are mean±SEM for n≥5 experiments and additionally presented normalized with the baseline set to that of [F/G]N/OFQ(1-13)NH_2 hence the residual agonist activity is absent.

5.3.2 Mouse Colon

In the mouse colon (mC) a range of NOP selective ligands induced potent contractions. The endogenous MOP selective ligand, endomorphin, also caused a potent contraction of this tissue, see Figure 5-3 and Table 5-1. The efficacy of the opioid induced contractions are ~50% less relative to those generated by carbachol. The intrinsic activities of the NOP ligands are compared to N/OFQ(1-13)NH_2, which behaved as a full agonist in this tissue preparation. The maximal response of the natural peptide N/OFQ was reduced in the mC, compared to the E_{max} of N/OFQ(1-13)NH_2, this may be due to higher enzymatic activity. The agonist activity of [F/G]N/OFQ(1-13)NH_2 was high in the mC suggesting either high NOP receptor density or efficient stimulus response mechanisms in this

preparation. The hexapeptide ligand Ac-RYYRWK-NH_2 was a full agonist and showed greater relative intrinsic activity than N/OFQ.

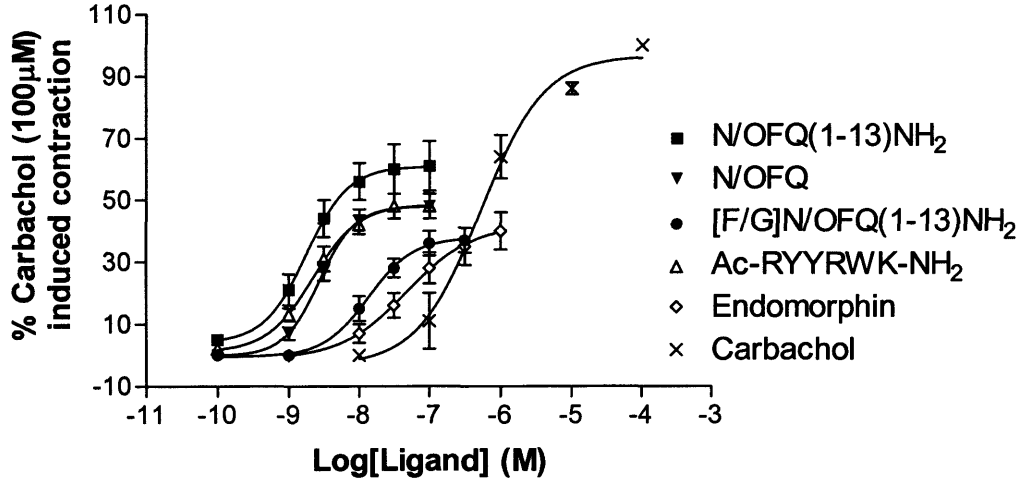

Figure 5-3. Contractions in isolated mouse colon induced by a range of NOP selective ligands, endomorphin (the putative endogenous MOP ligand) and carbachol (cholinergic agonist). Experiments are mean±SEM for n=4 experiments, normalised to carbachol response (100μM).

Agonist	*E_{max} (grams)*	*α*	*pEC_{50}*	*pK_B (10μM [Nphe^1])*	*E_{max} (% of carbachol)*	*α*	*pEC_{50}*	*pK_B (10μM [Nphe^1])*
N/OFQ	1.30±0.01	0.79	8.6±0.01	5.96	48±0.31	0.79	8.56±0.01	5.97
N/OFQ(1-13)NH_2	1.65±0.01	1.0	8.70±0.01	6.33	61±0.42	1.0	8.75±0.01	6.00
[F/G]N/OFQ(1-13)NH_2	1.13±0.04	0.68	7.89±0.04	5.73	38±0.90	0.62	7.86±0.03	5.91
Ac-RYYRWK-NH_2	1.65±0.04	1.0	8.68±0.04	6.31	49±0.88	0.80	8.66±0.03	6.28
Endomorphin	1.14±0.02	----	7.28±0.02	----	42±1.20	----	7.31±0.04	----
Carbachol	2.27±0.2*	----	6.25±0.2	----	97±6.90	----	6.28±0.19	----

Table 5-1. Mouse colon E_{max} and pEC_{50} values to a range of NOP ligands, endmorphin and carbachol. Data are expressed as both response as tension in grams and relative to the contraction induced by 100μM carbachol. NOP selective ligands were antagonized by the selective antagonist [Nphe^1]N/OFQ(1-13)NH_2. Data analysed by ANOVA with Bonferroni correction, *$p<0.05$ significant difference compared to the E_{max} of the other ligands. Data are the mean±SEM for $n\geq3$ experiments.

In vivo Studies

To confirm the activity of these ligands through the NOP receptor [Nphe^1]N/OFQ(1-13)NH_2 antagonism was studied. [Nphe^1]N/OFQ(1-13)NH_2 inhibited the contractions induced by those ligands dubbed here as 'NOP selective' pK_B values calculated for [Nphe^1]N/OFQ(1-13)NH_2 were comparable against the different agonists and no residual agonist activity was seen, see Figure 5-4 and Table 5-1. [Nphe^1]N/OFQ(1-13)NH_2 was ineffective against the endomorphin response, Figure 5-5.

5.4 NOP Receptor Knockout Studies, mouse vas deferens & colon

5.4.1 Mouse vas deferens studies

The DOP receptor agonist deltorphin-I and N/OFQ both inhibited the electrically induced contraction of the mouse *vas deferens* from $NOP^{+/+}$ mice in a concentration dependent manner (Figure 5-6). The values of potency and maximal effect of the two peptides were very similar to those obtained in tissues from wild-type swiss mice (Table 5-2). In tissues from $NOP^{-/-}$ mice, deltorphin-I inhibited the electrically induced contraction with pEC_{50} and E_{max} values comparable to those obtained in $NOP^{+/+}$. In contrast, in $NOP^{-/-}$ mice tissues N/OFQ was inactive (Figure 5-6).

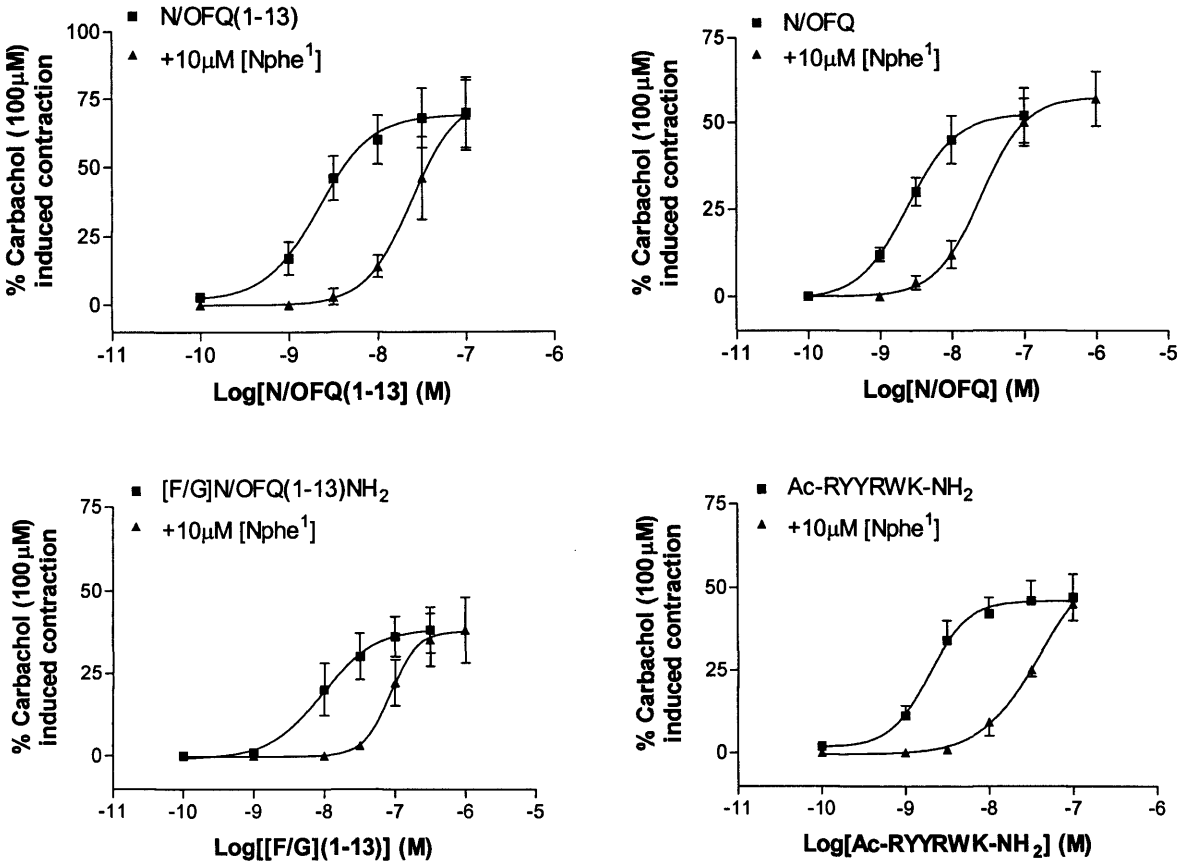

Figure 5-4. Antagonism of agonist contractile response in isolated mouse colon tissue using 10μM [Nphe^1]N/OFQ(1-13)NH_2 for N/OFQ (Top right), N/OFQ(1-13)NH_2 (Top left), [F/G]N/OFQ(1-13)NH_2 (Bottom left) and Ac-RYYRWK-NH_2 (Bottom right). Data are mean±SEM for n=4 experiments.

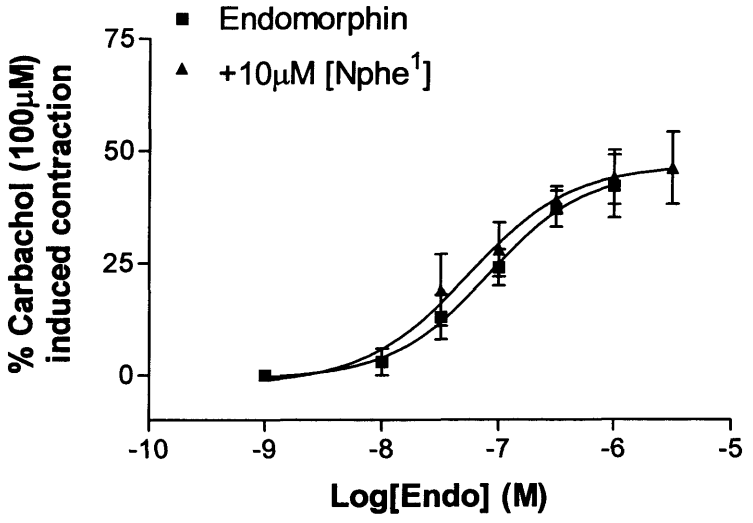

Figure 5-5. Inability of the NOP selective antagonist [Nphe^1]N/OFQ(1-13)NH_2 (10μM) to antagonise endomorphin induced contraction in mouse isolated colon. Experiments are mean±SEM for n=4.

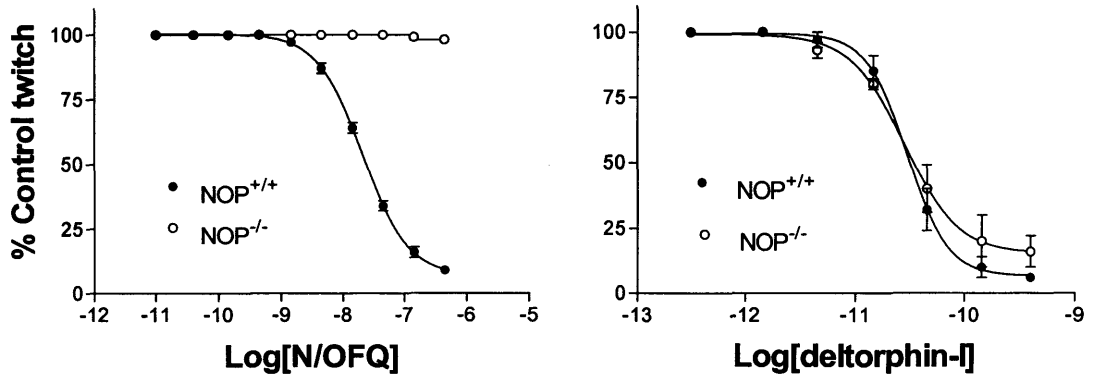

Figure 5-6. Effects of Deltorphin-I and N/OFQ in the electrically stimulated *vas deferens* from wild type ($NOP^{+/+}$) and NOP receptor knockout ($NOP^{-/-}$) mice. Data are mean±SEM (n≥3 experiments).

Ligand	*$NOP^{+/+}$ mice*		*$NOP^{-/-}$ mice*	
	pEC_{50}	E_{max} %	pEC_{50}	E_{max} %
Deltorphin-I	10.56±0.04	94±1	10.52±0.12	85±6
N/OFQ	7.62±0.05	91±1	< 6	ND

Table 5-2. pEC_{50} and E_{max} values of Deltorphin-I and N/OFQ in the electrically stimulated vas deferens from Swiss mice PCR confirmed as either $NOP^{+/+}$ (wildtype - WT) or $NOP^{-/-}$ (knockout - KO). Data are mean±SEM of n≥5 separate experiments.

5.4.2 Mouse colon studies

In the mouse colon experiments, N/OFQ(1-13)NH_2, [F/G]N/OFQ(1-13)NH_2, endomorphin-1 and carbachol produced a concentration-dependent contraction of mouse colon from $NOP^{+/+}$ mice. In tissues from $NOP^{-/-}$ mice N/OFQ(1-13)NH_2 and [F/G]N/OFQ(1-13)NH_2 were inactive while endomorphin-1 produced concentration-dependent contractions with similar potency and efficacy to those obtained from $NOP^{+/+}$ tissues, see Figure 5-7 and Table 5-3.

Ligands	*$NOP^{+/+}$ mice*		*$NOP^{-/-}$ mice*	
	pEC_{50}	E_{max}	pEC_{50}	E_{max}
N/OFQ(1-13)NH_2	9.34±0.14	53.7±22.5	----	NR
[F/G]N/OFQ(1-13)NH_2	8.22±0.11	69.7±12.9	----	NR
Endomorphin-1	8.15±0.22	52.5±9.0	7.90±0.07	49.8±4.72

Table 5-3. pEC_{50} and E_{max} values for N/OFQ(1-13)NH_2, [F/G]N/OFQ(1-13)NH_2 and endomorphin-1 in the isolated mouse colon from $NOP^{+/+}$ and $NOP^{-/-}$ mice. E_{max} expressed as % contraction relative to the response elcited by 100μM carbachol. The data are the mean±SEM of n≥4 separate experiments, NR = non-responsive.

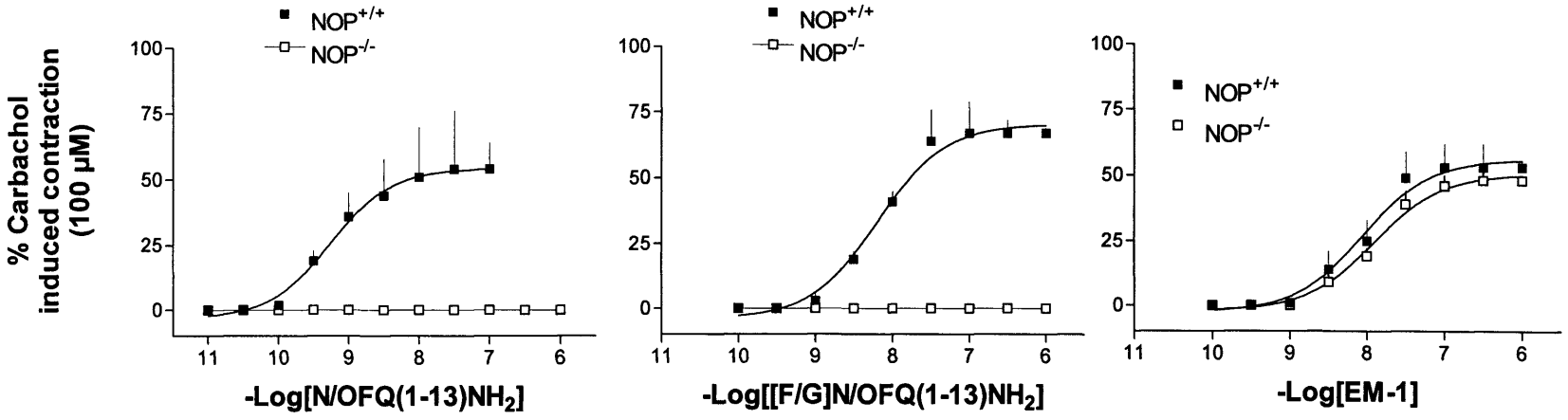

Figure 5-7. Effects of N/OFQ(1-13)NH_2, [F/G]N/OFQ(1-13)NH_2 and endomorphin-1 in the isolated mouse colon from $NOP^{+/+}$ and $NOP^{-/-}$ mice expressed as as % contraction relative to the response elcited by 100µM carbachol.

5.5 Discussions

In the mouse *vas deferens* N/OFQ(1-13)NH_2 inhibited EFS induced twitches by 86.74% with a pEC_{50} of 7.80±0.25. [F/G]N/OFQ(1-13)NH_2 also inhibited tissue twitch but with reduced potency pEC_{50} 6.61±0.23 and efficacy, 63.5%. Therefore in this isolated tissue preparation [F/G]N/OFQ(1-13)NH_2 had a relative intrinsic activity of 0.73. This is contrary to the original finding that showed [F/G]N/OFQ(1-13)NH_2 was an antagonist of N/OFQ in the mouse *vas deferens*.

In the mC the addition of N/OFQ caused a concentration dependent contractile response. The partial agonists [F/G]N/OFQ(1-13)NH_2 and Ac-RYYRWK-NH_2 also caused contractile responses similar to that reported previously (Mason *et al.*, 2001; Rizzi *et al.*, 1999). [F/G]N/OFQ(1-13)NH_2 behaved as a high efficacy partial agonist with a relative intrinsic activity of 0.68, while Ac-RYYRWK-NH_2 and N/OFQ(1-13)NH_2 were full agonists. Although Ac-RYYRWK-NH_2 and N/OFQ(1-13)NH_2 behaved as full agonists, the maximal response to N/OFQ appeared lower (although this failed to reach statistical significance), E_{max} 1.30g (N/OFQ) relative to E_{max} 1.65g (Ac-RYYRWK-NH_2 / N/OFQ(1-13)NH_2). The maximal response of the natural peptide N/OFQ being slightly reduced in the mC may be due to higher enzymatic activity in this tissue coupled with increased susceptibility to degradation of N/OFQ relative to N/OFQ(1-13)NH_2.

The full agonist nature of Ac-RYYRWK-NH_2, coupled with the high efficacy of [F/G]N/OFQ(1-13)NH_2 implies that the mouse colon displays a relatively high level of NOP receptor expression or that coupling efficiency in this tissue is high. To confirm the action of N/OFQ, N/OFQ(1-13)NH_2, [F/G]N/OFQ(1-13)NH_2 and Ac-RYYRWK-NH_2 was via the NOP receptor [Nphe^1]N/OFQ(1-13)NH_2 was shown to antagonise their action. The response of endomorphin-1 was unaffected by [Nphe^1]N/OFQ(1-13)NH_2.

The response expressed as tension in grams is susceptible to differences in tissue sensitivity, which is seen as the variation in the carbachol response during experimentation and between animals. Therefore data are expressed relative to carbachol which normalises any variaion in tissue response. For example the response as tension produced in grams varied for N/OFQ(1-13)NH_2 from an E_{max} of 1.65g in Swiss Morini mice to 0.57g in the $NOP^{+/+}$. Whilst species variability may

account for these differences, responses were comparable, at ~50% of the carbachol response.

Despite [F/G]N/OFQ(1-13)NH_2 displaying agonist activity in the mouse *vas deferens*, it still antagonised the activity of N/OFQ(1-13)NH_2. The parallel rightward shift in the concentration response curve (i.e. derivation of pK_B) caused by the inclusion of 10μM [F/G]N/OFQ(1-13)NH_2 was independent of data being normalised to the residual agonist activity of [F/G]N/OFQ(1-13)NH_2, pK_B values of 6.68±0.23 (normalised) and 6.49±0.18 (non-normalised).

Agonist activity has been reported in other peripheral tissue preparations for the partial agonists Ac-RYYRWK-NH_2 and Ac-RYYRIK-NH_2 for example, relative intrinsic activities of 0.76 and 0.56 respectively in the rat *vas deferens*, 0.67 and 0.30 respectively in rat anococcygeus smooth muscle (Mason *et al.*, 2001). This has also been shown in the mouse *vas deferens* where Ac-RYYRWK-NH_2 has an α of 0.70 (Rizzi *et al.*, 2002a). Collectively these data (both measured here and from other groups) reveals a rank order of efficacy of Ac-RYYRWK-NH_2>[F/G]N/OFQ(1-13)NH_2> Ac-RYYRIK-NH_2 in mouse *vas deferens*.

In the mouse colon the rank order of efficacy of [F/G]N/OFQ(1-13)NH_2 and Ac-RYYRWK-NH_2 were the same as in the *vas deferens* and at recombinant NOP. Ac-RYYRWK-NH_2 behaved as a full agonist in the mouse colon suggesting high NOP receptor density, although the relative intrinsic activity of [F/G]N/OFQ(1-13)NH_2 was very similar in the colon and *vas deferens,* 0.68 and 0.73 respectively.

For both mouse *vas deferens* and colon, genetically engineered populations homozygous for the absence of the receptor gene ($NOP^{-/-}$) were studied. In the *vas deferens* the response to the DOP receptor agonist deltorphin I was consistent in mice homozygous for the presence or absence of the NOP receptor gene. $NOP^{+/+}$ mice were responsive to N/OFQ however in $NOP^{-/-}$ no response was measurable. Colon taken from $NOP^{+/+}$ and $NOP^{-/-}$ mice was also studied for responsiveness to N/OFQ(1-13)NH_2 and [F/G]N/OFQ(1-13)NH_2. In tissues derived from $NOP^{-/-}$ mice both N/OFQ(1-13)NH_2 and [F/G]N/OFQ(1-13)NH_2 were devoid of agonist activity, the

integrity of these tissues was confirmed via endomorphin contraction. In $NOP^{+/+}$ mice endomorphin responses were the same as those in knockout species and responses to $N/OFQ(1\text{-}13)NH_2$ and $[F/G]N/OFQ(1\text{-}13)NH_2$ were present and equi- efficacious. This genetic approach further defines the function of these ligands through the NOP receptor.

6 *Extending the utility of the GTPγ[^{35}S] assay: Immunoprecipitation of Gi/o G-proteins.*

6.1 Introduction

Like the classical opioid receptors (MOP, DOP, KOP) the NOP receptor couples to G-proteins that are substrates for pertussis toxin (PTX), a toxin isolated from the supernatant of cultures of *Bordetella pertussis* (Milligan, 1988; Taylor, 1990). This toxin can be used broadly to define receptor G-protein coupling. However, in non-retinal tissue this toxin will interact with both G_i and G_o and subtypes thereof, hence it is of limited use in defining specific G-protein isoforms involved in receptor coupling. In addition, the use of PTX in non-immortalised cell lines is difficult given the relatively long incubation required for the toxin to be effective.

The use of antibodies raised to specific G-protein subtypes has revealed much about classical opioid receptor coupling, not only to specific subtypes but has also highlighted preferences in receptor coupling to specific subtypes of G-protein, see Figure 6-1 (Connor *et al.*, 1999a).

Antibodies raised to specific Gα subunits can be used to immunoprecipitate G-protein subtypes. Specific receptor G-protein coupling can be investigated when this approach is combined with a classical GTPγ[^{35}S] binding technique (Milligan, 2003). Due to variances in the density of G-protein subtypes and differences in their guanine nucleotide exchange rate it is not always possible to use the 'classical' GTPγ[^{35}S] binding technique for certain receptor G-protein associations. Immunoprecipitation is suitable to measure coupling to G-proteins that are not highly expressed in cell membranes and hence those that are not easily measurable by traditional GTPγ[^{35}S] radiolabled techniques. The relatively higher density and higher rates of guanine nucleotide exchange seen with $G_{i\alpha}$ subunits tend to mask or promote non-favourable signal to noise ratios when measuring coupling to other G-protein subtypes e.g. G_q or G_s (Milligan, 2003; Milligan, 1988).

6.2 Aim

Using Chinese hamster ovary cells expressing the human NOP the aim of this section was to measure receptor coupling to G_{i1-3} using specific antisera and GTPγ[^{35}S]

binding techniques. Data are compared with canine brain in which the expression of the NOP receptor is extremely low (Johnson *et al.*, 2003).

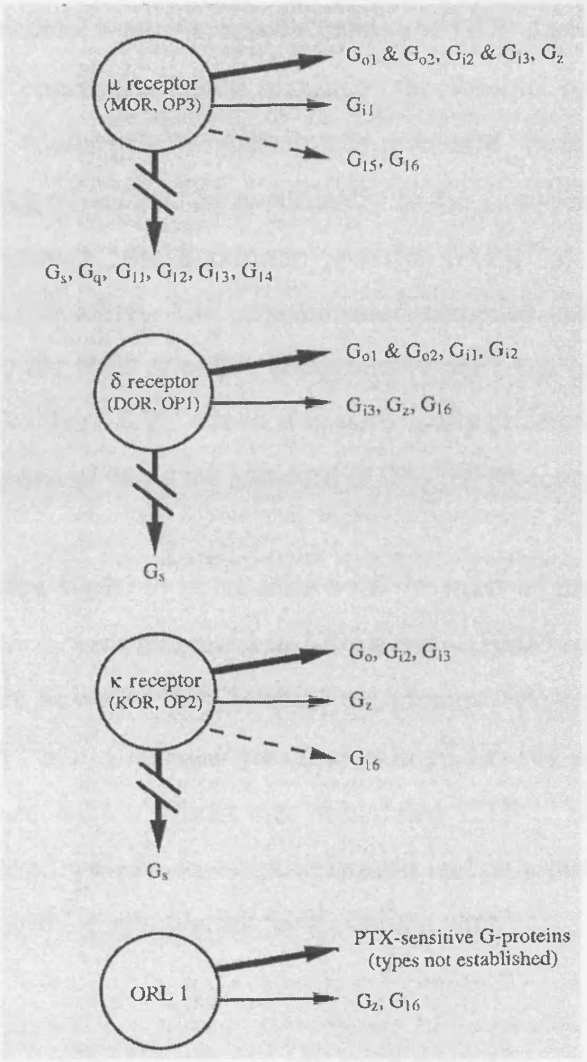

Figure 6-1. Summary of the different subtypes of G-protein to which opioid receptors couple. Heavy arrow represents subtypes of G-protein preferentially activated including those for which evidence for binding in native tissues has been demonstrated, light arrow indicates subtypes of G-protein activated by the respective receptor but where the functional significance is unclear. Dashed arrow represents cases where coupling is modest with recombinant G-protein and receptor. Broken indicates those G-protein subtypes to which the receptor does not couple (Connor *et al.*, 1999a).

6.3 Results

Analogous to the standard GTPγ[^{35}S] protocol used previously (Albrecht *et al.*, 1998; Hashiba *et al.*, 2002b) radiolabel was included at a concentration of 150pM, while magnesium concentrations were increased (5mM) and GDP decreased (5μM). It was believed these assay conditions would maximise the absolute binding of GTPγ[^{35}S]. Under these assay conditions in membranes prepared from CHO_{hNOP}, N/OFQ stimulated the binding of GTPγ[^{35}S] specifically to $G_{i1\text{-}3\alpha}$ subunits with a pEC_{50} of 9.36, Table 6-1. However, the maximum specific GTPγ[^{35}S] immunoprecipitated amounted to only 1176 DPM. The concentration response curve for N/OFQ was shifted to the right by the NOP selective antagonist [Nphe^{1},Arg^{14},Lys^{15}]N/OFQ (UFP-101) yielding a pK_B value of 8.09, which was statistically different to the pA_2 value of 9.13 for UFP-101 measured using the standard GTPγ[^{35}S] protocol.

In order to increase the signal to noise ratio both the mass of membrane protein and GTPγ[^{35}S] concentration were increased to 100μg and ~350pM respectively. All other assay conditions were as above for CHO_{hNOP} membranes. Again N/OFQ stimulated the binding of GTPγ[^{35}S] in CHO_{hNOP} membranes in a UFP-101 sensitive manner (see Table 6-1 and Figure 6-2). Whilst net stimulated GTPγ[^{35}S] binding increased relative to that measured with the lower protein mass and radiolabel concentration, the increase relative to basal i.e. stimulation factor did not alter.

Protein mass (μg)	G_{i1-3} mass (μg)	GDP	GTPγ[^{35}S] (pM)	pEC_{50} (N/OFQ)	E_{max} (net DPM)	E_{max} (stimulation factor)	pK_B (100nM UFP-101)
Immunoprecipitation							
20	2	5	150	9.36±0.38	1176±228	2.63±0.16	8.09±0.26[a]
100	2	5	350	9.12±0.36	5976±1426*	2.20±0.17	8.10±0.43
Standard GTPγ[^{35}S] procedure							
20	----	5	150	9.60±0.02	24255±964	3.67±0.26	----
20	----	100	150	8.75±0.11	3929±358	10.2±0.79	8.85

Table 6-1. Potency (pEC_{50}) and E_{max} (net DPM or stimulation factor) values for N/OFQ stimulated GTPγ[^{35}S] binding under low and high protein mass/radiolabel assay conditions derived from Figure 6-2. pK_B values for UFP-101 are also presented. Data are mean±SEM for n=3 experiments. *$p<0.05$ significantly different to the value with low protein mass and radiolabel concentration. Data for standard GTPγ[^{35}S] procedure taken from sections 3 and 4. [a] UFP-101 pK_B derived with 20μg membrane significantly ($p<0.05$) different to the pA_2 determined using standard GTPγ[^{35}S] procedure (pEC_{50} 8.85).

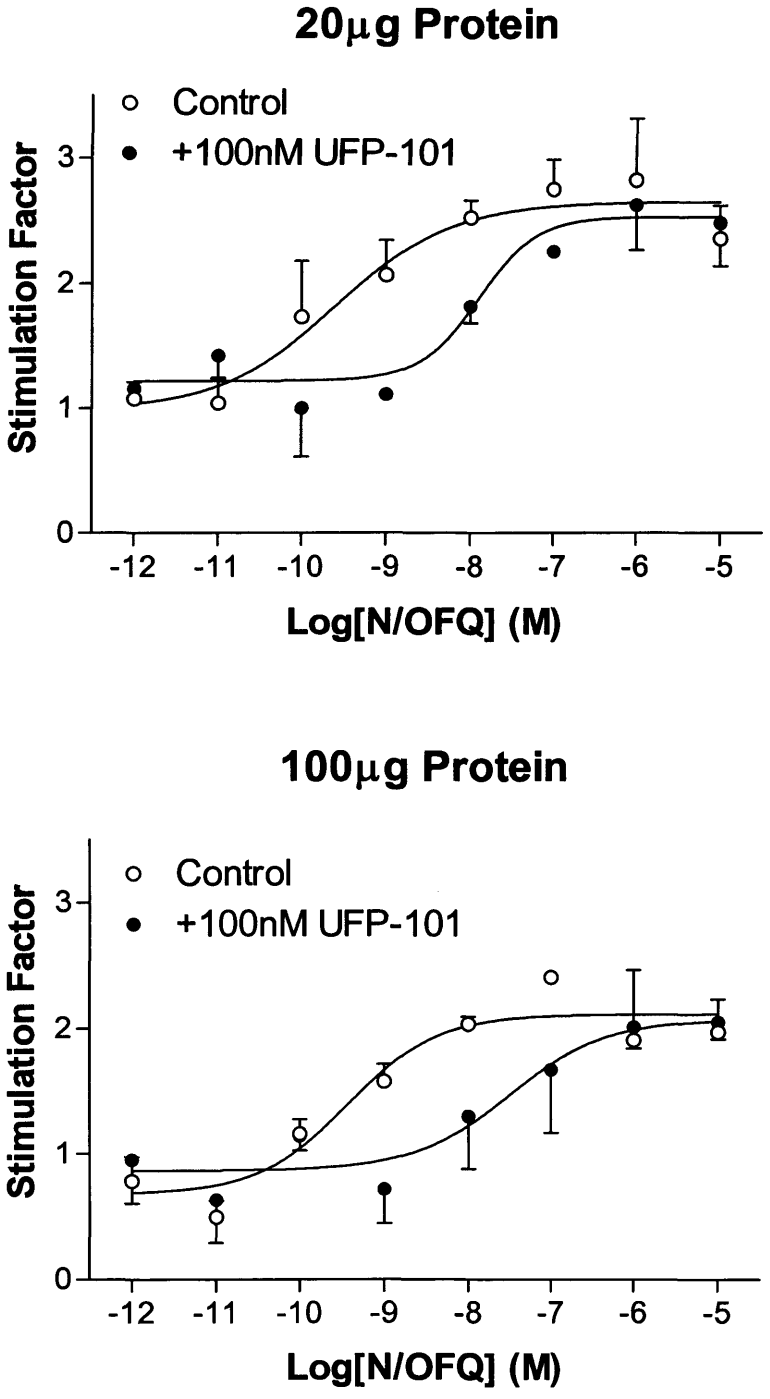

Figure 6-2. Antagonism by 100nM UFP-101 of N/OFQ stimulated GTPγ[^{35}S] binding to $G_{i1\text{-}3\alpha}$ subunits in membranes prepared from CHO_{hNOP} cells. (Top) was performed with a low concentration of GTPγ[^{35}S] (150pM) and protein (20μg), (Bottom) comprised high protein (100μg) and GTPγ[^{35}S] (350pM). Data are mean±SEM from n=3 experiments.

6.3.1 Comparison of Immunoprecipitation between highly expressing recombinant systems and low expressing native systems

Since the CHO_{hNOP} recombinant cell line used above displays high hNOP receptor densities the ability and suitability of the assay for use with natively expressed NOP was assessed. The B_{max} for the binding of [^{3}H]N/OFQ to dog membranes was 28.7±2.8 fmol/mg protein (Johnson *et al.*, 2003). This is in marked contrast to the high density seen with the recombinant cell line which expresses ~1.9pmol/mg protein (Hashiba *et al.*, 2001). N/OFQ (1μM) stimulated the binding of GTPγ[^{35}S] to $G_{\alpha i1-3}$ subunits in both dog and CHO_{hNOP} membranes with agonist stimulated specific binding of 2311 and 3140 DPM, respectively, see Table 6-2. Concentration response curves were not derived in these studies instead a single supra-maximal concentration of N/OFQ (1μM) was used.

The E_{max} values for N/OFQ, of 3140 (net DPM) and 3.90 (stimulation factor) are higher than those reported above for CHO_{hNOP} cells, see Table 6-1. This may be accounted for by the higher mass of protein (40μg) that was used in the later experiment.

	Tissue of Origin	
	Dog (150μg)	*CHO_{hNOP} (40μg)*
Total DPM	8321±±1021	1488±144
NSB DPM	375±37	280±21
1μM N/OFQ DPM	10632±1531	4629±786
Net Stimulated DPM	2311±605	3140±912
Stimulation Factor	1.28±0.06	3.90±1.18

Table 6-2. N/OFQ (1μM) stimulated GTPγ[^{35}S] binding to $G_{\alpha i1-3}$ subunits, 5μM GDP. Differences in total DPM bound represent the different mass of tissue used. Data are mean±SEM (n=3).

6.4 Discussions

In this chapter it can be seen that recombinant human NOP expressed in CHO cells couples to G_{i1-3} G-proteins. This was demonstrated by immunoprecipitation of N/OFQ stimulated GTPγ[^{35}S] binding with an antibody directed to G_{i1-3}. In these experiments the N/OFQ response was sensitive to the selective NOP antagonist UFP-101 confirming responses are mediated through NOP receptor activation. The assay was also used to determine the ability of N/OFQ to stimulate GTPγ[^{35}S] binding to G_{i1-3} at natively expressed NOP, using cerebral cortex prepared from dog. In dog NOP receptor expression is low (28.7±2.8 fmol/mg protein) (Johnson *et al.*, 2003).

Data were reported as stimulation factor, which represent a factorial increase over basal, and those values measured here were <3 which is lower than responses measured using the standard GTPγ[^{35}S] protocol, typically greater than 7.
Standard GTPγ[^{35}S] binding responses in CHO_{hNOP} cells are sensitive to PTX indicating coupling to G_i and/or G_o (and excluding $G_{q/11}$ and G_s (Taylor, 1990)). Antibody data here prove conclusively that NOP responses are mediated through G_{i1-3} G-protein subtypes but tell us nothing of coupling to other PTX sensitive G-proteins i.e. G_o. The reduced response measured solely at G_{i1-3}, relative to the standard assay that employs all G-protein subtypes involved in NOP activation, suggest that NOP receptor responses may be mediated through other PTX sensitive G-proteins i.e. G_o.

For the same assay conditions i.e. mass of protein, concentration of radiolabel and concentration of GDP the net DPM measured using the immunoprecipitation technique is only 5% of that measured using the standard protocol. The standard protocol will measure stimulated binding of GTPγ[^{35}S] to all subtypes of G-protein activated by NOP receptors and the IP assay only to G_{i1-3}. However, this difference in net stimulated DPM is believed to be due to low expression of G_{i1-3} relative to the other subtypes but from the low efficiency of the antibody purification step. Indeed the relative expression and guanine nucleotide exchange at G_i is high, typically masking GTPγ[^{35}S] binding to other G-protein subtypes and restricting the use of the standard to $G_{i/o}$ coupling receptors (Milligan, 2003).

Immunoprecipitation Studies

At natively expressed NOP from dog cerebral cortex stimulation factors for both assays have been determined. The immunoprecipitation procedure gave a greater (1.28±0.06) stimulation factor than the standard protocol (1.16±0.02). However it must be stated that these assays are not directly comparable given the higher protein mass (150μg compared to 20μg) and lower GDP concentration (5μM compared to 100μM) used for the immunoprecipitation procedure. Overall the reduced GTPγ[^{35}S] binding probably results from the low efficiency of the immunoprecipitation procedure, which should be considered a drawback of this technique.

7 The effect of ligand efficacy on guanine nucleotide binding parameters

7.1 Introduction

To date a variety of ligands varying in efficacy; full / partial agonists, antagonists and nature; peptide / synthetic have been identified for the NOP receptor (Calo *et al.*, 2000a; Calo *et al.*, 2000c). To define the true efficacy of these ligands testing in multiple systems and measurements at different endpoints in signal cascades are required. The response measured for a ligand will be influenced by numerous factors including cell surface receptor density (receptor reserve), G-protein density (coupling reserve), cell type (different isoforms of effector(s)) and the response measured. Indeed ligand efficacy can differ regarding ability to affect different intracellular responses in a single cell line (Cordeaux *et al.*, 2000). Further, it has been shown with the NOP receptor partial agonist [F/G]N/OFQ(1-13)NH_2 that relative intrinsic activity can vary between zero and one, in a manner dependent upon receptor density and the response measured in the signal transduction cascade.

The kinetics for binding of GTPγS to oligomeric G_i and G_o has been shown to be 3-4 orders of magnitude slower than that expected for a diffusion-controlled reaction and has been resolved as a complex biomolecular interaction, where an inhibitor guanine diphosphate (GDP) must first dissociate in order that GTPγS can bind (Ferguson *et al.*, 1986). Studies with cannabinoid receptors have shown that the affinity of GTPγS is unaffected by receptor activation, whereas the affinity of GDP is negatively regulated (decreased) (Breivogel *et al.*, 1998). Thus it is believed that receptor ligand complexation reduces GDP affinity, leading to increased association of GTP.

The activity of the NOP receptor, be it measured with the complexities of a whole organism or in a relatively more basic system such as tissue, cell or membrane preparation, is dependent upon receptor coupling to specific G-protein subtype(s). The use of non-hydrolysable, radiolabelled analogs of GTP, such as GTPγ[^{35}S], allows receptor activation to be measured at the earliest point in a signal transduction cascade i.e. GDP for GTP exchange. In order that ligand stimulated binding of GTPγ[^{35}S] can be measured, micro-molar concentrations of GDP are required, to reduce basal binding of GTPγ[^{35}S] (Albrecht *et al.*, 1998; Traynor *et al.*, 1995). Maximally stimulated GTPγ[^{35}S] binding can be used to determine relative differences in ligand efficacy. However, it has been shown for the NOP receptor, that

ligands of different efficacy can vary in their requirement for GDP (Berger *et al.*, 2000a; Bigoni *et al.*, 2002a). Specific agonist GDP requirement has also been shown for the $G_{\alpha i/0}$ coupled cannabinoid receptor (Breivogel *et al.*, 1998).

A further complexity that can confound measurements of ligand efficacy is the stoichiometry between activated receptor and G-protein. The MOP receptor, when highly expressed in CHO cells, activates ~20-fold less G-proteins per receptor compared to MOP receptors at relatively lower expression in SK-N-SH cells (Selley *et al.*, 1998). Whilst this may simply be an issue of coupling efficiency between the two cells tested it is important to determine if the same receptor in a given cell line could alter its ability to couple to G-protein(s) via changes in cell surface receptor numbers.

7.2 Aims

The aim of this chapter was to examine;

(i)how the binding parameters of GTPγS and GDP, to G-proteins activated by the NOP receptor, were affected by ligands of differing efficacy

(ii)the distinction in GDP requirements for different ligands

(iii)the effect of NOP receptor density on guanine nucleotide affinity and guanine nucleotide binding capacity

(iv)the effect of ligand efficacy and GDP concentration on GTPγS association kinetics.

7.3 A note on data analysis for this Chapter

A number of isotope dilution / displacement experiments are presented. Raw DPM data were plotted as sigmoid curves of variable slope and where slope factors were less than unity, data were further fitted to an equation that assumed competition for two binding sites. Where used, raw DPM binding affinity data are presented as pIC_{50} ($\log_{10}$ of the concentration required to inhibit 50% of the binding of GTPγ[^{35}S]), see Figure 7-1. The same data were also fitted with a 2-site Scatchard equation using KELL (from Biosoft) and data presented as GTPγS affinity K_D (nM) and B_{max} (pmol/mg protein), Figure 7-1.

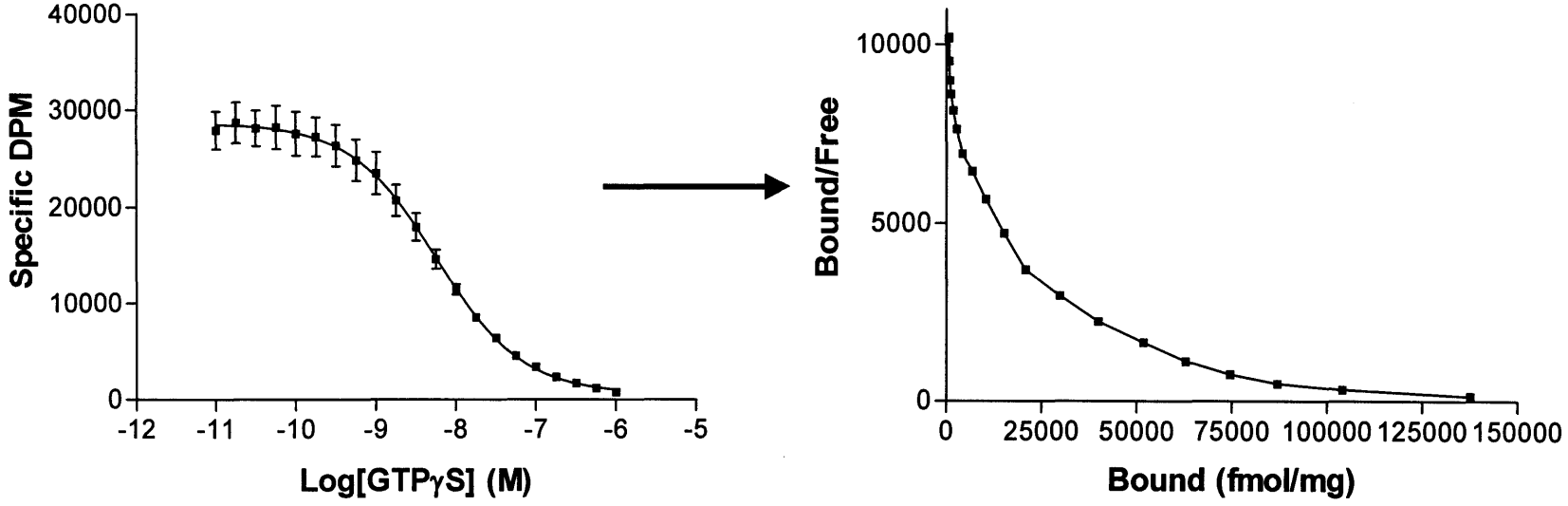

Figure 7-1. Example of GTPγ[^{35}S] isotope dilution presented as raw DPM plot (left), from which pIC_{50} data are taken and the formatting of the same data for plotting using 2-Scatchard analysis (right) from which pK_D and B_{max} values were derived.

7.4 Results

7.4.1 GTPγ[^{35}S] Total Saturation Binding

The displacement of a fixed concentration of GTPγ[^{35}S] by varying concentrations of non-labelled GTPγS were plotted as raw dpm (see Figure 7-1). Data were fitted to sigmoid curves of variable slope, giving measures of affinity (pIC_{50}) e.g. CHO_{hNOP} 8.24±0.01, see Table 7-1. Slope factors were <1, hence data was further modelled to a 2-site sigmoid curve giving high and low affinity for the binding of GTPγS e.g. CHO_{hNOP} pIC_{50} values of 8.58±0.13 (high) and 7.42±0.3 (low). Proportions of high and low affinity binding sites were determined to be close to 50:50, see Table 7-1.

2-site analysis of dpm data revealed consistent high (8.58-9.05) and low (7.42-7.70) GTPγS affinity binding between cell types and tissue preparations regardless of receptor density or PTX treatment. Relative proportions of the high and low affinity sites were close to 50:50 in the CHO cell lines however, the high affinity site was in greater abundance for rat cerebral cortex (77%) and decreased by PTX pre-treatment of CHO_{hNOP} cells. These results suggest differences in guanine nucleotide populations for different tissue types.

Data are presented as pIC_{50} values, which in essence should be corrected for the competing mass of GTPγ[^{35}S] in combination with its K_D, see section 2.7.1. However, given the low concentration of GTPγ[^{35}S] (70pM) and the low affinity of GTPγS, it is not unreasonable to report the data as pIC_{50} values. Further it may be assumed that there are more than 2-affinity sites for GTPγ[^{35}S] given the number of different G-α subunits and the sub-types thereof. It is unlikely that these different alpha subunits will have identical affinities for GTPγ[^{35}S] and therefore Cheng and Prusoff (Cheng *et al.*, 1973) correction of IC_{50} values may be inappropriate.

Scatchard transformation of dpm data was used to determine K_D and B_{max} values. Scatchard analysis of data gave curvilinear plots that had to be fit with a 2-site equation, see Figure 7-1. The binding of GTPγS was to both a high affinity site (pK_D between 8.44 and 8.84) and low affinity site (pK_D between 6.60 and 7.03). The capacity of the high affinity site was lower at between 6.43-13.10pmol/mg protein relative to the low affinity site which had a B_{max} ~10-fold greater at between 61.4-81.4pmol/mg protein, see Figure 7-1. Scatchard plots were used in an attempt to

define site density, an example of the curvelinear Scatchard plot and DPM sigmoid plot for the same set of GTPγ[^{35}S] saturation data are shown in Figure 7-2.

Effects of Receptor Density on GTPγ[^{35}S] Binding Parameters

The N/OFQ binding affinity and capacity for GTPγS was measured in $CHO_{INDhNOP}$ cells differentially induced with ponasterone A, see Figure 7-3. Under basal conditions, i.e. no ligand present, the binding affinity of GTPγS was lower than that measured in GTPγS saturation binding assays and did not vary over the range of receptor expression tested here, pIC_{50} 7.18±0.05 (1μM ponasterone A) and 6.87±0.17 (10μM ponasterone A). This lower GTPγS affinity, relative to the saturation binding pIC_{50} value of 8.20±0.04 measured in $CHO_{INDhNOP}$ (10μM ponasterone A) is attributed to the presence of 5μM GDP. As the expression of the human NOP receptor increased, maximal stimulated (1μM N/OFQ) binding of GTPγS increased from 476fmol GTPγS/mg protein at 23.5fmol [^{3}H]N/OFQ/mg protein to 1090fmol GTPγS/mg protein at 1101 fmol [^{3}H]N/OFQ/mg protein, see Figure 7-3 and Table 7-2. Values of GTPγS/mg protein and pK_D were determined from Scatchard analysis of net (minus basal GTPγS binding) N/OFQ stimulated dpm.

Sigmoid plots of net N/OFQ stimulated raw dpm were used further to derive affinity of GTPγS at the different hNOP receptor densities. The only difference in the binding affinity of the stimulated GTPγS fraction was seen at the lowest hNOP receptor expression, pIC_{50} of 8.51±0.05 (1μM ponasterone A). At all other receptor densities the GTPγS binding affinity was conserved, pIC_{50} of between 8.86±0.08 and 9.07±0.07. The reduced affinity for the binding of GTPγS at the 1μM ponasterone A induction is ascribed to the lower expression of hNOP receptor at this induction concentration and consequent reduction in the signal to noise ratio. The slope factors for net stimulated DPM are less than unity (1) at induction concentrations 1-5μM ponasterone A but a slope of 1 is measured for the 10μM induction. It is assumed the low stimulation factors are the result of a less favourable signal to noise ratio seen with lower receptor expression given the knowledge that at >1000fmol/mg protein slope factors were of unity, Table 7-2 and Table 7-3 – N/OFQ data. Therefore a single binding site for GTPγ[^{35}S] in the presence of N/OFQ is assumed.

Membrane	DPM Sigmoid Plot					Scatchard Data			
	1-site analysis		2-site analysis						
	pIC_{50} (nM)	Slope	High pIC_{50} (nM)	Fraction (high)	Low pIC_{50} (nM)	pK_d (High)	B_{max} (High) pmolGTPγS/mg protein	pK_d (Low)	B_{max} (Low) pmolGTPγS/mg protein
CHO_{hNOP}	8.24±0.01 (5.75)	0.81±0.07	8.58±0.13 (2.63)	63.31	7.42±0.3 (38)	8.54±0.04	11.7±2.60	6.67±0.14	77.3±4.6
$CHO_{INDhNOP}$ (Non-induced)	8.26±0.05 (5.50)	0.79±0.01	8.80±0.14 (1.58)	47.47*	7.74±0.16 (18.2)	8.52±0.03	10.6±0.46	6.60±0.21	62.2±11.1
$CHO_{INDhNOP}$ (10μM induced)	8.20±0.04 (6.31)	0.73±0.07	8.67±0.11 (2.14)	58*	7.48±0.06 (33.1)	8.51±0.02	9.41±0.98	6.79±0.07	78.3±17.1
$CHO_{INDhNOP}$ (PTx-treated)	8.21±0.04 (6.17)	0.70±0.04	8.71±0.09 (1.95)	57.21*	7.54±0.02 (28.8)	8.44±0.05	8.05±0.96	6.63±0.02	81.4±6.52
$CHO_{INDhNOP}$ (10μM induced) 1μM N/OFQ	8.32±0.04 (4.79)	0.61±0.03	9.05±0.07 (0.89)	47.95*	7.70±0.02 (20)	8.66±0.04	6.43±0.75	6.87±0.09	79.2±6.9
CHO_{hNOP} (PTx-treated)	8.02±0.02 (9.55)	0.81±0.02	8.91±0.29 (1.23)	28*	7.78±0.11 (16.6)	8.23±0.03	13.10±0.60	6.53±0.05	71.5±3.20
Rat cerebral cortex	8.41±0.01 (3.90)	0.84±0.02	8.62±0.06 (2.40)	77*	7.46±0.14 (34.67)	8.84±0.01*	10.1±0.91	7.03±0.05	61.4±6.41

Table 7-1. Displacement of GTPγ[^{35}S] by increasing concentrations of GTPγS in membranes prepared from CHO_{hNOP} (treated and non-treated with 100ng/ml PTX, $CHO_{INDhNOP}$ non-induced, with and without PTx pre-treatment and induced with 10μM ponasterone A in the absence and presence of 1μM N/OFQ and rat cerebral cortex homogenate. Data are mean±SEM for n≥3. Scatchard data were analysed with a two-site Scatchard equation using Kell VI (Biosoft). * value significantly different ($p<0.05$)ANOVA to respective CHO_{hNOP} value.

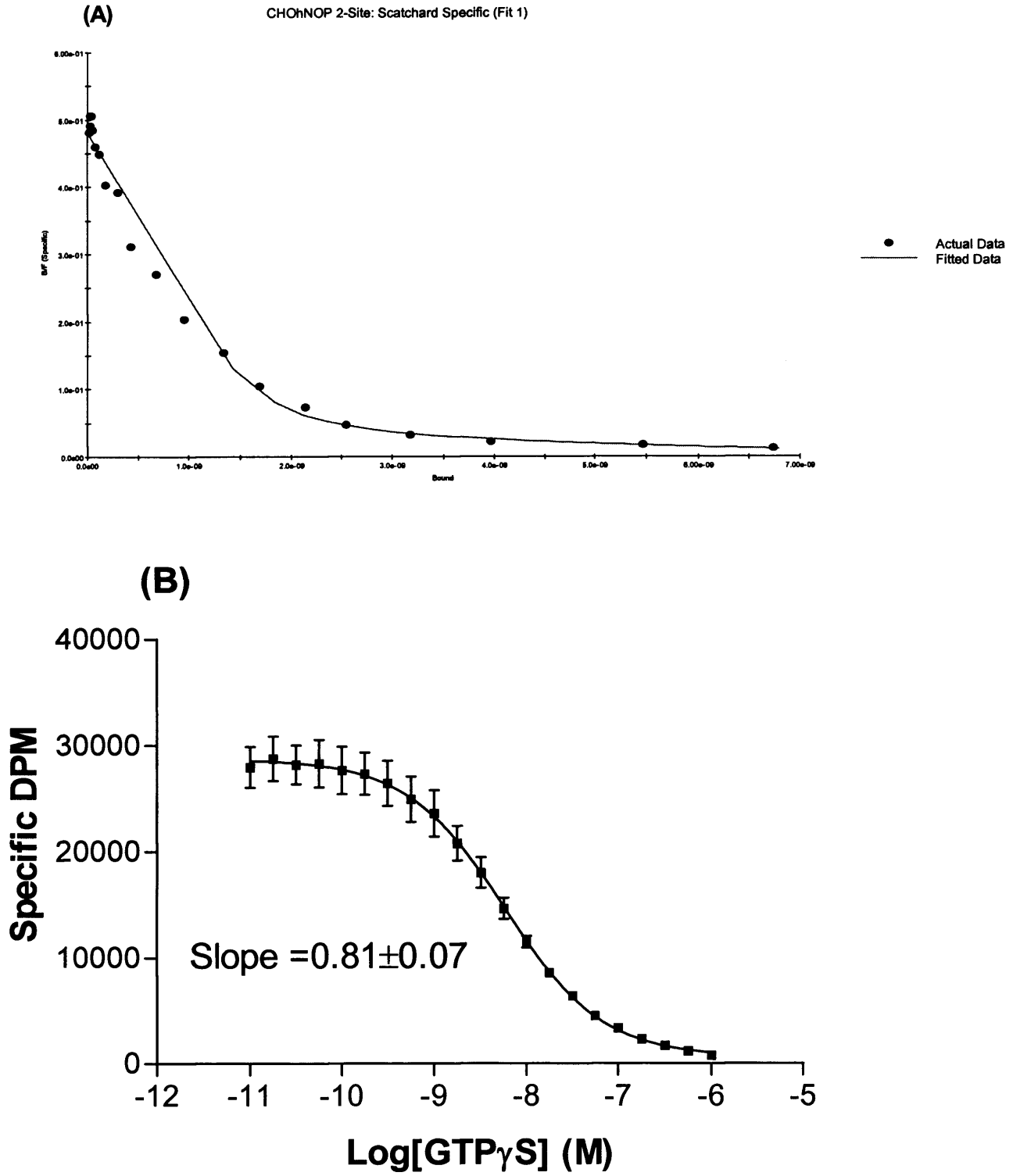

Figure 7-2. (A) 2-site Scatchard anaylsis for GTPγS isotope dilution of GTPγ[^{35}S] in CHO_{hNOP} membranes, (B) same data plotted as raw dpm using a semi-log plot, fit to a sigmoid curve of variable slope.

From the data analysis it was possible to determine the stoichiometry between receptor and G-protein i.e. how many G-proteins are stimulated per receptor. The stoichiometry was seen to increase as receptor density was reduced i.e. 19.8 fmol GTPγS / fmol [*leucyl*-^{3}H]N/OFQ (20:1) at an expression of 23.5fmol [*leucyl*-^{3}H]N/OFQ / mg protein compared to 1fmol GTPγS / fmol [*leucyl*-^{3}H]N/OFQ at 1101fmol [*leucyl*-^{3}H]N/OFQ / mg protein (1:1), see Table 7-2.

7.5 Agonist Stimulated GTPγ[^{35}S] binding

In membranes from CHO_{hNOP} cells stably expressing the human NOP receptor, the effect of a range of ligands that were peptide (N/OFQ, Ac-RYYRIK-NH_2, Ac-RYYRWK-NH_2), pseudo-peptide ([F/G]N/OFQ(1-13)NH_2) and synthetic (NalBzOH) were assayed for their ability to promote binding of GTPγS, see Table 7-3 and Figure 7-4. In order that the stimulated fraction of GTPγS could be measured a low concentration (5μM) of GDP was included.

In the absence of ligand the binding of GTPγS to CHO_{hNOP} membranes was to low and high affinity sites with pIC_{50} values of 7.82 and 6.95 respectively. All ligands used were at a fixed concentration of 1μM (except NalBzOH included at 10μM) and stimulated the binding of GTPγS to single sites, see Table 7-3. There is close agreement between IC_{50} values derived from sigmoid analysis of raw dpm and those from K_D (Scatchard) measures of GTPγS affinity.

E_{max} values (DPM) for N/OFQ, [F/G]N/OFQ(1-13)-NH_2, Ac-RYYRIK-NH_2, Ac-RYYRWK-NH_2 were not statistically different from one another, a finding that is attributed to the low (5μM) GDP concentration, known to reduce intrinsic activity between full and partial agonist with regards to guanine nucleotide exchange (Albrecht *et al.*, 1998; Bigoni *et al.*, 2002a). The E_{max} of NalBzOH was significantly ($p<0.05$) reduced relative to all other ligands further highlighting the very low relative intrinsic activity of this ligand. Scatchard transformation masked the difference in stimulated GTPγS binding, for DPM NalBzOH represented only 0.17 of that elicited by N/OFQ. However, for Scatchard analysis this fraction was as high as 0.70 – attributed to large dilution factors encountered with this form of analysis. There was however, good agreement between IC_{50} values and K_D values for the different ligands.

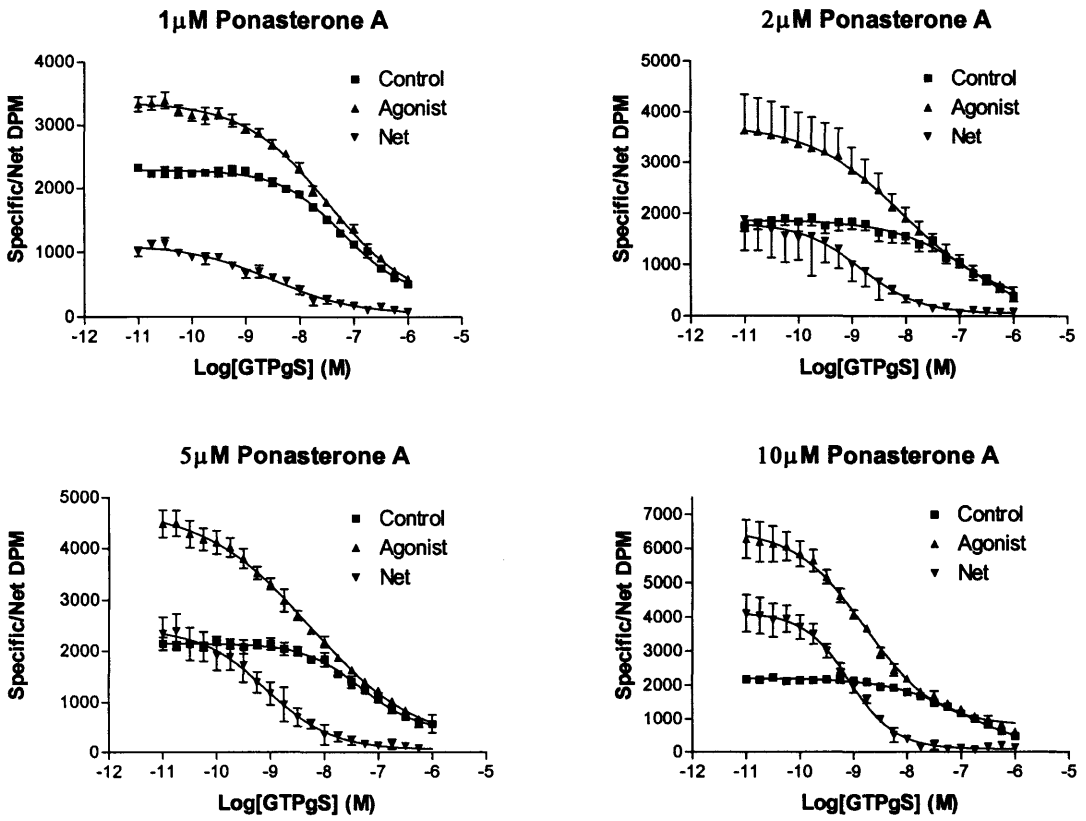

Figure 7-3. Binding of GTPγS to $CHO_{INDhNOP}$ cell membranes differently induced with ponasterone A. Control – represents GTPγS binding under basal conditions, Agonist represents the binding of GTPγS in the presence of 1μM N/OFQ and Net is agonist stimulated minus basal i.e. response attributable to agonist only.

[Induction] (Ponasterone A)	*Basal (pIC_{50})*	*Net (pIC_{50})*	*Slope*	*B_{max} (fmol GTPγS/mg protein)*	*pK_D (nM)*	*Stochiometry*
1μM	7.18±0.05	8.51±0.05	0.62±0.11	476.4±97	8.76 (1.75±0.39)	19.8
2μM	6.73±0.24	8.86±0.08*	0.79±0.08	611.7±134	8.83 (1.42±0.29)	9
5μM	7.27±0.11	9.07±0.06*	0.67±0.03	675.8±104*	8.79 (1.64±0.24)	3.5
10μM	6.87±0.17	9.07±0.07*	1.02±0.68	1090±100*	8.97 (1.06±0.11)	1

Table 7-2. GTPγS binding parameters for differently induced $CHO_{INDhNOP}$ cells. Data for basal GTPγS binding affinity and net stimulated GTPγS binding affinity are from analysis of raw dpm. B_{max} and K_D values for the net GTPγS binding are from Scatchard analysis. *significantly different to 1μM ponasterone A.

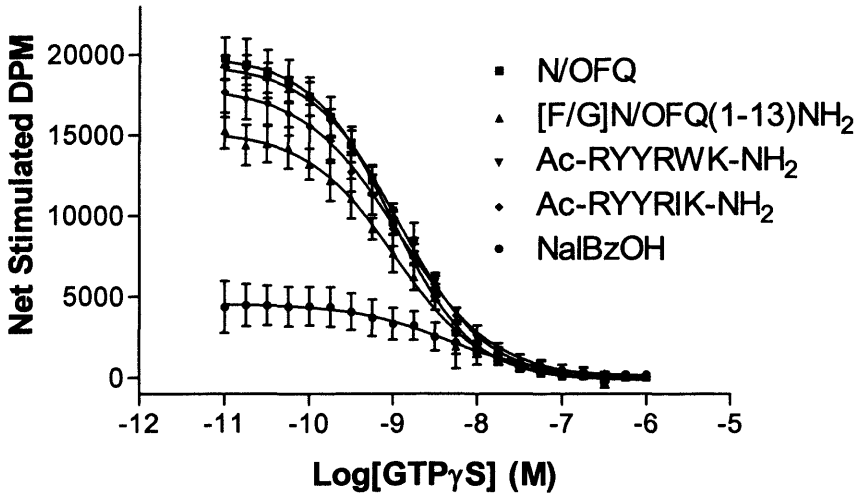

Figure 7-4. Net ligand (1 or 10μM) stimulated binding of GTPγ[^{35}S] to CHO_{hNOP} membranes in the presence of 5μM GDP.

Agonist	*pIC_{50} (nM)*	*K_D*	*E_{max} (DPM)*	*Slope*
N/OFQ	9.03±0.02 (0.93)	0.88±0.03	19,901±1450	0.91
[F/G]	8.99±0.05 (1.02)	1.46±0.03	15,244±1248	0.85
Ac-RYYRWK	8.94±0.01 (1.15)	1.15± 0.02	19,454±851	0.83
Ac-RYYRIK	8.92±0.03 (1.20)	1.30±0.13	18,498±1687	0.79
NalBzOH	8.44±0.06 (3.63)*	4.36±0.61	3358±577*	0.95

Table 7-3. Binding for GTPγ[^{35}S] in the absence (control) and presence of different agonists (1μM) to 20μg of CHO_{hNOP} homogenate in the presence of 5μM GDP. Data are mean±SEM for n≥3 experiments. * Significantly different to N/OFQ value.

7.5.1 GDP Binding Parameters

The ability of GDP to displace the binding of GTPγ[^{35}S] to CHO_{hNOP} membranes was measured in the absence and presence of 1μM N/OFQ. Data were fit to a two site sigmoid analysis. In the absence of agonist, GDP displaced the binding of GTPγ[^{35}S] with both high and low affinity, however the high affinity site represented the majority of GDP binding ~77%. In the presence of 1μM N/OFQ high affinity GDP binding was also apparent, but only represented 32% of the total binding. A number

of other full and partial agonists, [Arg^{14},Lys^{15}]N/OFQ, [F/G]N/OFQ(1-13)NH_2, Ac-RYYRIK-NH_2, Ac-RYYRWK-NH_2 and Naloxone Benzoylhydrazone (NalBzOH), were tested for their ability to affect the affinity of GDP, see Figure 7-5 and Table 7-4. All ligands reduced the fraction of high affinity binding for GDP (relative to basal) in a manner dependent on ligand efficacy i.e. high efficacy ligands causing a greater percentage reduction. While the pIC_{50} for high affinity GDP binding did not decrease in the presence of 1μM N/OFQ, 7.04 compared to 6.89 (basal), N/OFQ produced a statistically significant reduction in the pIC_{50} for the low affinity fraction, pIC_{50} from 5.57 to 5.03, see Table 7-4. The agonist evoked decrease in affinity for GDP binding appeared dependent upon the efficacy of the ligand. Hence GDP displayed three distinct binding affinities; i) a high affinity, conserved in the presence and absence of ligand, ii) an intermediate affinity, present as a low fraction under basal conditions and iii) a low affinity, present during receptor activation representing the majority of binding.

The optimal GDP concentration for maximal net ligand stimulated GTPγ[^{35}S] binding differed between ligands. These differences were most apparent with NalBzOH. While maximum stimulated binding of GTPγ[^{35}S] for N/OFQ was achieved with ~1μM GDP for NalBzOH this was ~10-fold less at ~100nM, see Figure 7-6. Despite there being differences in the optimal GDP concentration, agonists produced increases in the binding of GTPγ[^{35}S] at all GDP concentrations,
Figure 7-6.

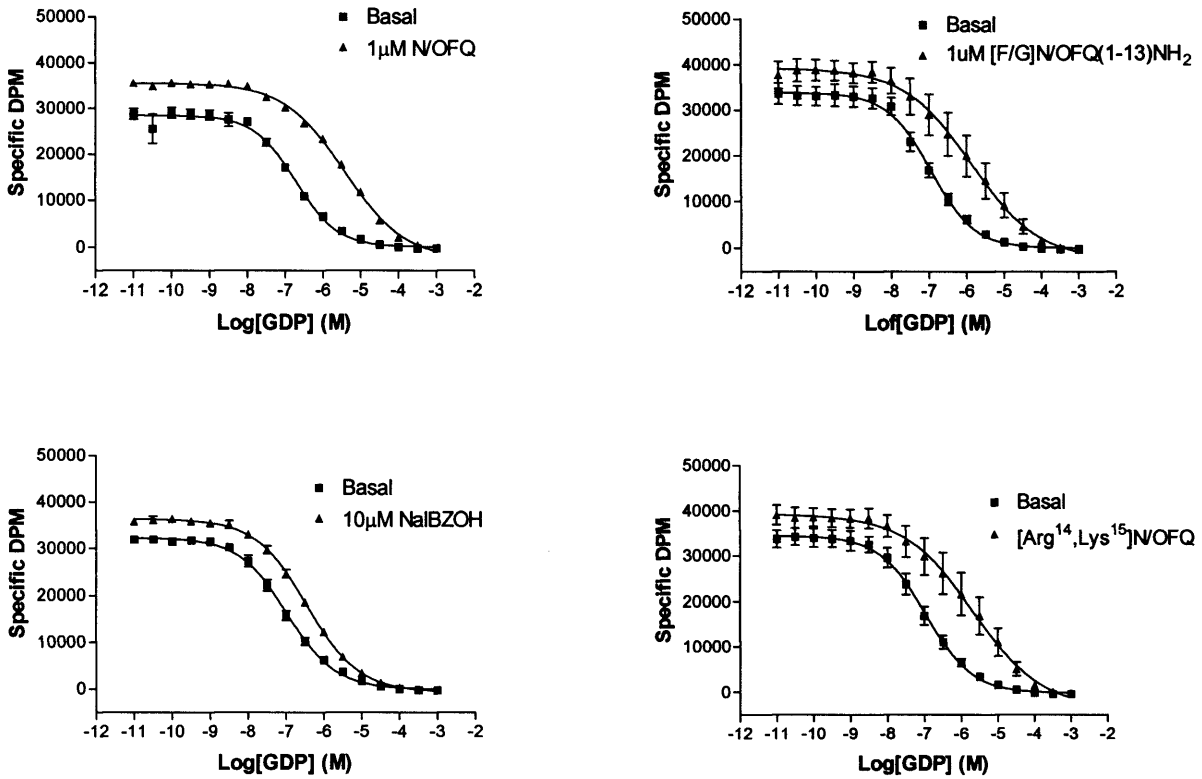

Figure 7-5. Binding of GDP to CHO_{hNOP} membranes in the presence and absence of different NOP receptor ligands, measured by the displacement of a fixed concentration of GTPγ[^{35}S].

Ligand	*Fraction (High)*	*High (pIC_{50})*	*Low(pIC_{50})*
Control	0.77±0.008	7.04±0.02	5.57±0.03
N/OFQ	0.32±0.01	6.89±0.08	5.03±0.001
Control	0.77±0.06	7.24±0.03	5.69±0.11
[F/G]	0.46±0.08	7.02±0.16	5.17±0.13
Control	0.74±0.03	7.31±0.06	5.74±0.03
[Arg^{14},Lys^{15}]	0.39±0.09	7.11±0.08	5.10±0.09
Control	0.74±0.01	7.32±0.08	5.68±0.13
NalBzOH (10μM)	0.50±0.02*	7.18±0.06	5.75±0.06
Control	0.78±0.03	7.42±0.13	5.78±0.16
Ac-RYYRIK-NH^2	0.51±0.08	7.23±0.20	5.42±0.23
Control	0.78±0.03	7.42±0.13	5.78±0.16
Ac-RYYRWK-NH^2	0.50±0.09	7.18±0.18	5.24±0.20

Table 7-4. GDP displacement of GTPγ[^{35}S] in the absence (control) and presence of different NOP receptor ligands. The fraction of high affinity binding sites for control samples were not different from one another ($p>0.05$), whilst the fraction of high affinity binding sites in the presence of agonist were all significantly different to their respective controls ($p<0.05$) . Data are mean±SEM for n=3 experiments. *$p<0.05$ relative to N/OFQ fraction (high).

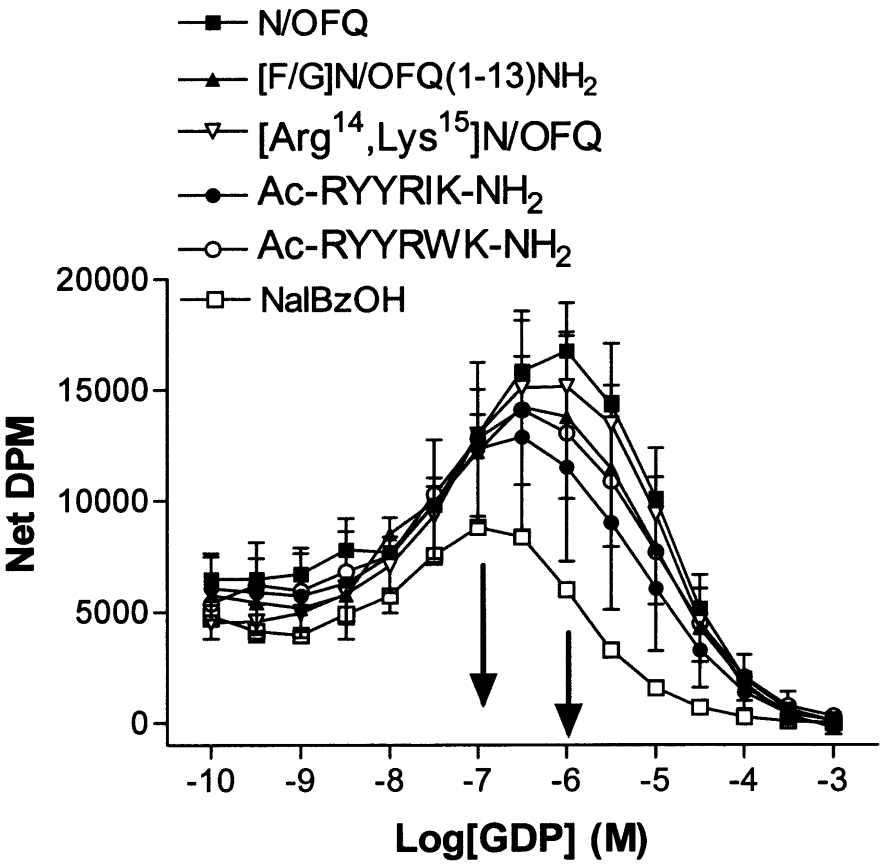

Figure 7-6. Net stimulated GTPγ[^{35}S] binding to CHO_{hNOP} membranes over a range of different GDP concentrations by ligands of varying efficacy. Arrows show the optimal GDP concentration for NalBzOH and N/OFQ.

7.5.2 GTPγ[^{35}S] Association Kinetics

The association kinetics of GTPγ[^{35}S] were studied in CHO_{hNOP} membranes in the presence and absence of 1μM N/OFQ, GDP was included at a concentration of 1μM. The association of GTPγ[^{35}S] is measured as the observed association rate and would need to be corrected for K_{-1} in order to equate to K_{+1}, the true association rate. Data are presented here as the observed association rate (K_{obs}), and if the published reports are to be believed (Bokoch *et al.*, 1984; Sternweis *et al.*, 1984), then the irreversibility of GTPγ[^{35}S] binding to Gα subunits will therefore liken to K_{+1}, since K_{-1} will essentially be zero. However, more recent whole membrane studies have shown that the binding of GTPγ[^{35}S] is indeed reversible and would mean association data here are K_{obs} (Breivogel *et al.*, 1998)

The association rate (K_{obs}) for GTPγ[^{35}S] increased from 0.017min^{-1} in the absence of ligand to 0.047 min^{-1} in the presence of 1μM N/OFQ. GTPγ[^{35}S] binding reached a plateau at ~120min and was stable up to 240min. In the presence of N/OFQ GTPγ[^{35}S] binding was seen to peak at ~90min after which there appeared to be a small decrease in bound GTPγ[^{35}S], however this did not reach statistical significance see Figure 7-7. Since the binding of GTPγ[^{35}S] was stable in the absence of ligand, it is believed that this decrease may be a receptor / ligand mediated phenomenon, see Figure 7-7. The low efficacy NOP receptor ligand, NalBzOH was studied for its ability to alter the association kinetics of GTPγ[^{35}S]. In the presence of 10μM NalBzOH the association kinetics of GTPγ[^{35}S] were the same as under basal conditions, 0.018min^{-1} compared with 0.017min^{-1} respectively. Despite this the binding of GTPγ[^{35}S] in the presence of NalBzOH showed a steady increase over a 4hr period and the maximal response was greater than under basal conditions, 10444±478.7 DPM (basal) relative to 17393±1494 DPM, see Figure 7-7, i.e. full agonists increase the rate of association.

Association binding kinetics were also measured at a lower 0.1μM GDP concentration. As the GDP concentration was reduced from 1 to 0.1μM the basal association rate increased from 0.017min^{-1} to 0.03min^{-1} (this was not statistically different), see Table 7-5. GTPγ[^{35}S] binding in the presence of N/OFQ peaked at ~90mins (K_{obs} 0.06) whilst in its absence GTPγ[^{35}S] association did not peak until ~120mins. As with the higher GDP concentration the binding of GTPγ[^{35}S] in the presence of N/OFQ appeared to decrease toward the end of the time course, but again this failed to reach statistical significance.

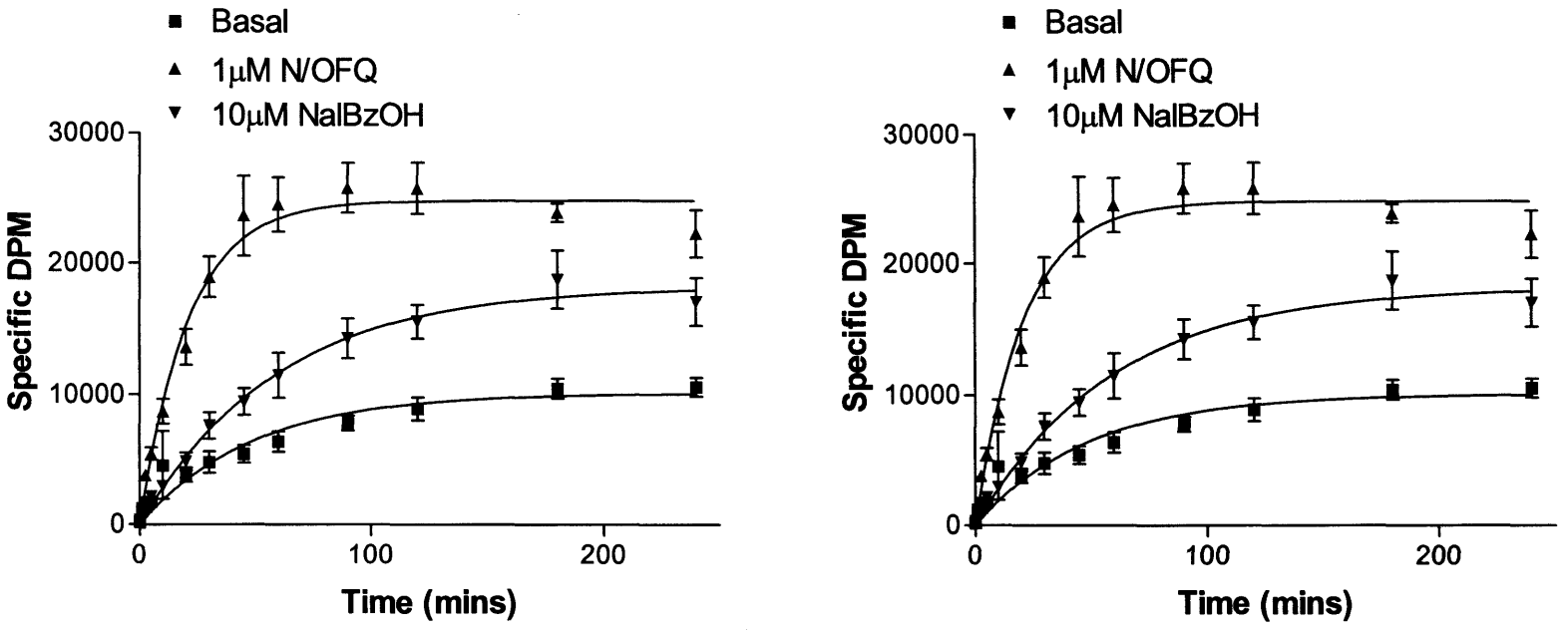

Figure 7-7. Association kinetics for basal and stimulated binding of GTPγ[^{35}S]. Association of GTPγ[^{35}S] at 1μM GDP in the presence of 1μM N/OFQ, 10μM NalBzOH and under basal conditions (left). Association of GTPγ[^{35}S] at 0.1μM GDP in the absence and presence of 1μM N/OFQ.

	1μM GDP		0.1μM GDP	
	Maximum (DPM)	K_{obs}	Maximum (DPM)	K_{obs}
Basal	10444±4797	0.017±0.001	25811±2775	0.034±0.01
1μM N/OFQ	24703±1187	0.045±0.002	34876±3245	0.060±0.02
10μM NalBzOH	17393±1494	0.018±0.001	----	----

Table 7-5. Association rates under basal conditions and in the presence of N/OFQ at GDP concentrations 1μM and 0.1μM and for NalBzOH at 1μM. Data mean±SEM for n≥4 experiments. K_{obs} = observed association rate constant, min^{-1}.

7.5.3 Influence of receptor density of GDP binding parameters

The effect of receptor density on GDP affinity was examined in $CHO_{INDhNOP}$ cells induced with 5μM, 2μM and 1μM ponasterone A. While the basal characteristics of GDP binding did not change from those determined in CHO_{hNOP} membranes, GDP binding parameters differed in the presence of ligand. The fraction of high affinity GDP binding in the presence of 1μM N/OFQ with CHO_{hNOP} membranes decreased from ~77% to ~32% (58% reduction) but at a lower receptor density (5μM ponasterone A) the decrease in the high GDP affinity fraction was small ~74% to ~63% (15% reduction). The decrease in the percentage of high affinity GDP binding sites was dependent upon receptor expression diminishing by only 12% at 2μM ponasterone A and 4% at 1μM ponasterone A, see Table 7-6 and Figure 7-8.

Induction [Ponasterone] (μM)	Basal			1μM N/OFQ			Reduction in high affinity fraction
	Fraction (high)	pIC_{50} (High)	pIC_{50} (Low)	Fraction (high)	pIC_{50} (High)	pIC_{50} (Low)	
1	0.80±0.02	6.87±0.07	5.20±0.15	0.77±0.01	6.83±0.06	5.01±0.11	4%
2	0.78±0.02	7.15±0.11	5.60±0.13	0.69±0.03*	7.06±0.12	5.07±0.08	12%
5	0.74±0.03	7.06±0.06	5.65±0.08	0.63±0.06	6.80±0.13	4.80±0.11	15%

Table 7-6. The effect of hNOP receptor expression on basal and stimulated (1μM N/OFQ) GDP binding parameters. High and low affinity values do not differ between basal and stimulated. *$p<0.05$ (ANOVA) statistically significant change in the fraction of high affinity binding relative to basal.

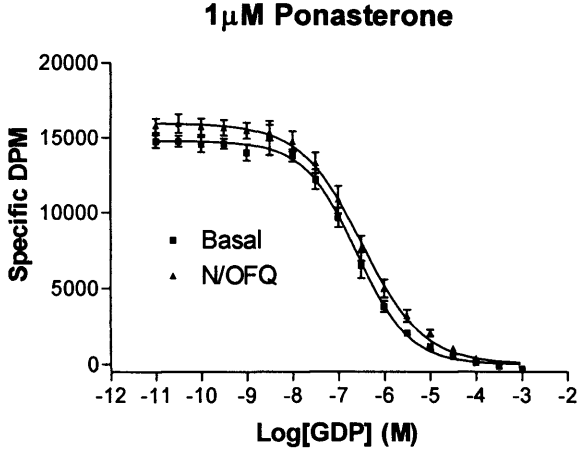

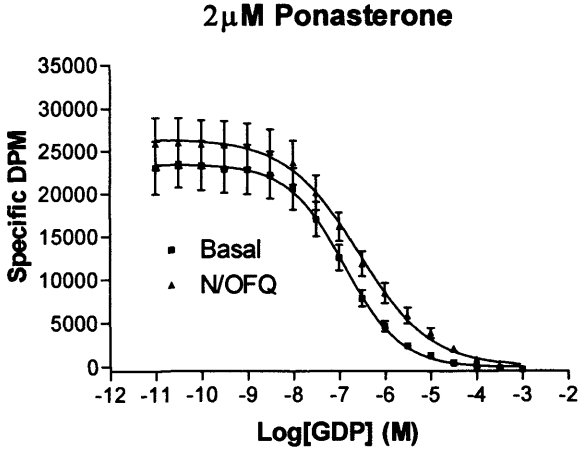

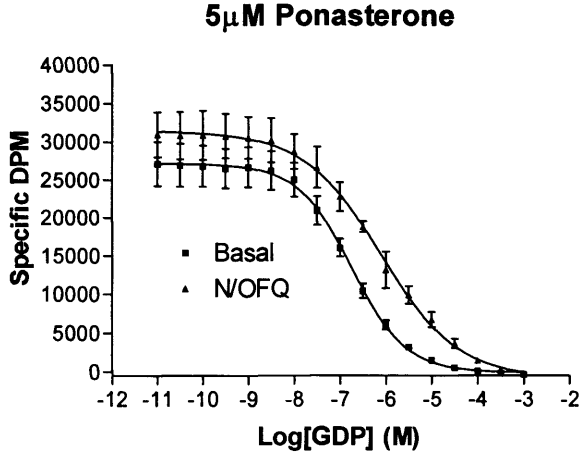

Figure 7-8. Binding of GTPγ[^{35}S] in the absence and presence of 1μM N/OFQ over a range of GDP concentrations in $CHO_{INDhNOP}$ membranes differently induced with ponasterone A.

7.6 Discussions

The binding affinity of GTPγS to membranes from rat cerebral cortex and CHO cells (differentially expressing the human recombinant NOP receptor) was shown to be unaffected by receptor presence, or receptor density, Table 7-1. Scatchard analysis was used to determine G-protein densities, high affinity (pK_D between 8.23-8.84) with capacity of between 6.4 and 13.1pmol/mg protein and low affinity (pK_D between 6.53-7.03) with capacity of between 61-81pmol/mg protein. The binding of GTPγS was also analysed as raw dpm and fit to sigmoid curves, revealing both high (pIC_{50} 8.58-9.05) and low (pIC_{50} 7.42-7.78) affinity fractions. The agonist-stimulated capacity for binding of GTPγS was also investigated in CHO_{hNOP} cell membranes. The maximum stimulated GTPγ[^{35}S] binding was consistent for those ligands investigated here except for NalBzOH, which displayed reduced efficacy regarding stimulation of GTPγ[^{35}S] binding. Scatchard analysis (data not shown) of net N/OFQ stimulated GTPγS binding in CHO_{hNOP} membranes suggests an E_{max} of ~5pmolGTPγ[^{35}S]/mg protein, i.e. stochiometry of one to 2.5 between receptor and G-protein, i.e. one receptor will activate ~2 G-proteins. The data for net N/OFQ stimulated binding reported here is similar to that of (Albrecht *et al.*, 1998), who reported a stimulatory guanine nucleotide capacity of 3.03 pmol/mg protein in rat cerebral cortex.

The binding of GTPγ[^{35}S] to CHO_{hNOP} membranes was displaced by GDP in a concentration dependent manner and was best modelled with a 2-site analysis. In the absence of ligand GDP displaced GTPγ[^{35}S] with a relatively high affinity, pIC_{50} of 7.04-7.32 and low affinity pIC_{50} 5.57-5.74, see Table 7-4. The former, high affinity GDP binding site represented 77% of the total binding. In the presence of ligand GDP was seen to bind to a similar high affinity site as that seen under basal conditions (pIC_{50} 6.89-7.18) but this represented a smaller fraction of the total binding (~33%). In the presence of the higher efficacy ligands (N/OFQ, [Arg^{14},Lys^{15}]N/OFQ, [F/G]N/OFQ(1-13)NH_2) the affinity of the low affinity GDP binding site was reduced, pIC_{50} between 5.03-5.17 (Table 7-4), compared to the basal pIC_{50} of between 5.57-5.74. The reduction in low affinity GDP binding was less for the hexapeptides Ac-RYYRIK-NH_2, Ac-RYYRWK-NH_2 and no change was apparent with the low efficacy ligand NalBzOH. Interestingly in the presence of ligand the fraction of high affinity GDP sites was reduced in a manner dependent upon ligand efficacy.

Therefore ligand efficacy, with respect to stimulation of GTPγS binding, can be viewed via its ability to reduce the number of high affinity GDP binding sites and also reducing GDP affinity.

The effect of receptor density on GDP binding parameters showed that basal binding was unaffected by NOP receptor density. This suggests that basal proportions of high affinity GDP binding sites are unaffected by receptor pre-coupling which would be expected to reduce this fraction. In the presence of 1μM N/OFQ there is a modest inverse relationship between receptor density and the fraction of high affinity GDP binding sites, decreasing from 77-63%. In the presence of N/OFQ, GDP affinity at the high affinity GDP binding site was the same as for basal conditions at all induction concentrations studied. At the low GDP affinity binding site the presence of 1μM N/OFQ caused a significant reduction in the pIC_{50} (relative to basal) at 2μM and 5μM ponasterone A induction concentrations, see Table 7-6.

Quantification of the association kinetics for the binding of GTPγ[^{35}S] was made in the presence and absence of 1μM N/OFQ at 1 and 0.1μM GDP concentrations.
The association rate (K_{obs}) of GTPγ[^{35}S] in the presence and absence of 1μM N/OFQ (1μM GDP), revealed that N/OFQ increased both the association kinetics and maximal binding of GTPγ[^{35}S]. Reducing the GDP concentration 10-fold to 0.1μM lead to a small increase (although not statistically different) in both the association rate and maximal binding of GTPγ[^{35}S] in the presence and absence of 1μM N/OFQ. At both 1μM and 0.1μM GDP concentrations 1μM N/OFQ increased the observed association rate of GTPγ[^{35}S], association rates were 0.047 and 0.060 min^{-1} respectively. It can therefore be hypothesised that N/OFQ through reduction of GDP affinity indirectly increases the association kinetics of GTPγ[^{35}S] or vice versa. The ability of a low efficacy ligand (10μM NalBzOH) to affect the association rate of GTPγ[^{35}S] was also studied with 1μM GDP. Whilst 10μM NalBzOH caused little or no change in the association rate of GTPγ[^{35}S], maximal binding was greater and increased over a 4hr period. Relative to the full agonist N/OFQ, both the maximal response and the association rate were lower.

While values from plots for raw dpm data cannot be considered absolute and hence comparable to other reports they are useful in relative internal comparisons. The use of low concentrations of GTPγ[^{35}S] (hence limited distortion of data from the mass of radiolabel) and good agreement between pK_D and pIC_{50} values, adds weight to use of raw dpm data as a measure of the binding parameters of guanine nucleotide exchange. Despite the potential of data to be distorted when deriving values from isotope dilution experiments, there is some agreement between K_D values measured here with those reported by other groups (Albrecht *et al.*, 1998). In rat cerebellar membranes basal binding of GTPγS in the absence of GDP was modelled to 2-sites with K_D values of 1.45nM (high affinity) and 93nM (low affinity), which are comparable to K_D values of 1.57nM (high affinity) and 46nM (low affinity) (Albrecht *et al.*, 1998).
To measure agonist stimulated GTPγS binding micro-molar concentrations of GDP are required, to reduce the basal binding of GTPγS (Traynor *et al.*, 1995). In the presence of 5μM GDP, under basal conditions, GTPγ[^{35}S] bound to CHO_{hNOP} membranes with high (pIC_{50} 7.82±0.17) and low affinity (pIC_{50} 6.95±0.15), the former representing ~42% of the total binding. In the presence of different NOP receptor ligands the binding of GTPγS was to a single high affinity site. The affinity of this site was greater than the high affinity GTPγS binding detected under basal conditions and was conserved amongst all ligands, except for NalBzOH. The increase in GTPγS affinity promoted by NalBzOH was less than for the other ligands, although greater than basal, suggesting that the ligand mediated increase in GTPγS affinity could be related to ligand efficacy. The lack of difference in GTPγS affinities promoted by different ligands investigated here suggests the agonist induced conformational change in G-protein structure is conserved amongst ligands. However this is in contrast to what is suggested in the cubic ternary complex model for GPCR – G-protein interactions. It may also be speculated that the guanine nucleotide binding site promoted by agonists differs from that promoted by the non-liganded receptor given the 3-fold change ($p<0.05$, unpaired t-test) in GTPγS high affinity seen between CHO_{hNOP} in the absence of N/OFQ (saturation binding) and that in the presence of N/OFQ (agonist binding). Therefore there are three different affinity states evident for the binding of GTPγ[^{35}S]; (i) a high affinity site seen in the presence of agonist

(affected by ligand efficacy), (ii) an intermediate affinity site seen under basal conditions and (iii) a low affinity site seen under basal conditions.

Using the ecdysone inducible expression system the effect of cell surface receptor density on binding characteristics of both GDP and GTPγS was studied. Net N/OFQ (1μM) stimulated GTPγS binding affinity remained consistent over all induction concentrations, the lower expression showed a slight difference in GTPγS affinity, most likely attributed to very low expression and hence a low signal to noise ratio.
If the maximal capacity for stimulated binding of GTPγS by 1μM N/OFQ is studied at different receptor densities it can be seen that the response does not increase as a linear function of receptor number. For a 40-fold difference in receptor number, ~23.5fmol/mg protein (1μM ponasterone A) compared to ~1101fmol/mg protein (10μM ponasterone A), there is only a 2.3-fold difference in the 1μM N/OFQ stimulated response, 476.4fmol GTPγS/mg protein (1μM ponasterone A) compared to 1090fmol GTPγS/mg protein (10μM ponasterone A).

The binding of GDP was modelled to two sites and under basal conditions GDP bound with high and low affinity, of which the high affinity binding represented a greater proportion of the total. Ligand receptor activation reduced the fraction of high affinity binding sites but had no effect on the affinity of this site. Interestingly, this decrease was dependent on ligand efficacy, i.e. high efficacy agonists causing a greater reduction. The affinity of GDP for the lower affinity binding site was reduced also in a manner dependent upon the efficacy of the ligand. N/OFQ, [Arg^{14},Lys^{15}]N/OFQ, [F/G]N/OFQ(1-13)NH_2, Ac-RYYRIK-NH_2, Ac-RYYRWK-NH_2 all reduced the affinity of the low affinity binding site by between 2-3-fold although no such reduction in affinity was apparent in the presence of naloxone benzylohydrazone. NalBzOH caused no change in the lower affinity GDP binding site however this is explained by the low efficacy of this partial agonist, which has been reported previously (Bigoni *et al.*, 2002a).

8 Final Discussions

SAR Studies

In the SAR study three ligands of particular importance were identified, [(pF)Phe^4,Arg^{14},Lys^{15}]N/OFQ-NH_2 a highly potent full agonist, [F/G,(pF)Phe^4,Arg^{14},Lys^{15}]N/OFQ-NH_2, a highly potent partial agonist and finally [Nphe^1,Arg^{14},Lys^{15}]N/OFQ-NH_2 a high potency competitive antagonist.

In the agonist template it can be seen that potency of the control N/OFQ(1-17)NH_2 ligand showed ~10-fold difference between cAMP and GTPγ[^{35}S] assays, the former displaying the higher value. Also the potency in cAMP assays of 9.94 is very close to its affinity pK_i of 10.31 measured with [*leucyl*-^{3}H]N/OFQ competition binding. Theoretically, assuming a receptor reserve the functional response curves of a full agonist would lie to the left of its occupancy curve, i.e. 100% occupancy is not required to elicit a maximal response. The greater the gap between response and occupancy curves the greater the receptor reserve of the system, see Figure 8-1 which depicts differences in the lateral displacement between occupancy and response curves for a variety of different tissue preparations.

For a partial agonist it is expected that response and occupancy curves would lie close together, i.e. 100% occupancy being required to elicit its maximal response, which is typically lower than that of a full agonist. It can be seen that for GTPγ[^{35}S], response curves lie to the right of the occupancy i.e. pEC_{50} of 8.98 and pK_i of 10.31±0.04 for N/OFQ at CHO_{hNOP}. For cAMP assays potency values are very close to ligand affinity. Therefore fractional occupancy and fractional response curves, using cAMP as a marker of agonist activity, will lie close to one another.

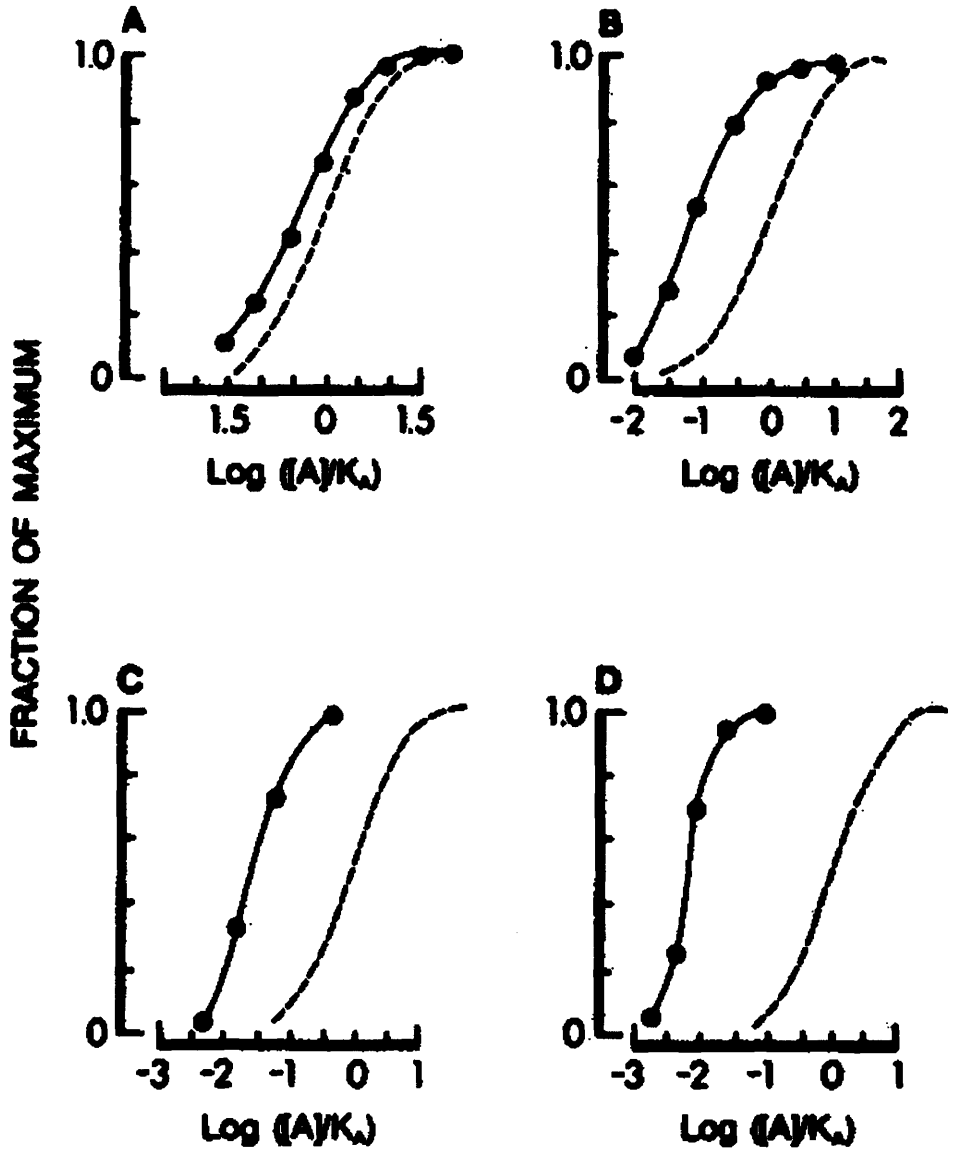

Figure 8-1. Effect of different stimulus response coupling on the relative lateral displacement of occupancy and response curves, (A) Phenylephrine in rabbit muscle, (B) norepinephrine in rabbit aorta, (C) carbachol in guinea pig ileum, (D) acetylcholine in guinea pig ileum. Y axis represents fraction of maximal response (solid line) or occupancy (dashed line), taken from (Kenakin, 1997)

Theory does not appear to match the data presented here i.e. functional assay potency values are either far lower or close to determinants of affinity. Theoretically this should be the other away round. It must be highlighted at this point that the different assays used here are carried out in different buffers, optimised for measuring different responses. [*leucyl*-^{3}H]N/OFQ competition binding assays are performed on membrane fragments in buffer devoid of guanine nucleotides, sodium and other metal ions, all of which are known to reduce binding to opioid receptors. However functional measures of potency are carried out not only on membrane fragments but also on whole cells and whole tissue preparations. Further, the buffers used for measuring functional receptor activation (as opposed to simply ligand binding) contain different concentrations of metal ions and guanine nucleotides. Consequently for a given concentration of ligand fractional receptor occupancy will vary in the different systems under investigation, although it should be assumed that occupancy would be lower in the functional systems due to buffer conditions.

Despite the assumed differences in occupancy between the assays employed values of potency for cAMP and pK_i values are very close to one another. The lack of difference is attributed to the position in the transduction cascade at which the effector (cAMP) is measured. For cAMP the initial response of receptor activation is highly amplified until the final effector point is reached i.e. one activated receptor may activate multiple G-proteins and each respective G-protein can then affect multiple enzymes etc. Hence the greater the number of steps in the transduction pathway along with the knowledge that these different intracellular effectors are often saturable means fractional occupancy response curves will often be non linear. The degree of non-linearity will depend on the number of steps there are in signal cascade between receptor and effector and the degree to which those steps are saturable, see Figure 8-2

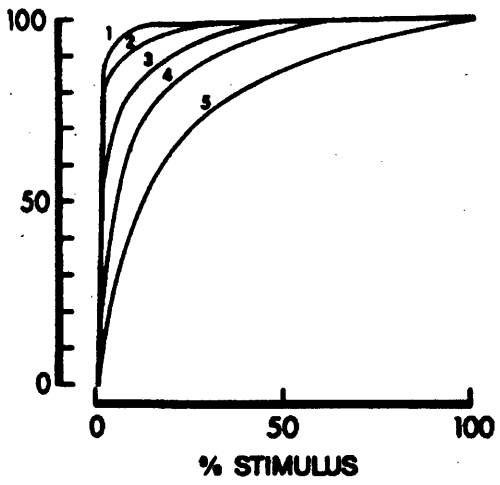

	Tissue	Drug
1	Rabbit Fundus	Carbachol
2	G.P. Ileum	Acetlycholine
3	G.P. Ileum	Carbachol
4	Rabbit Aorta	Carbachol
5	G.P. Ileum	Pilocarpine

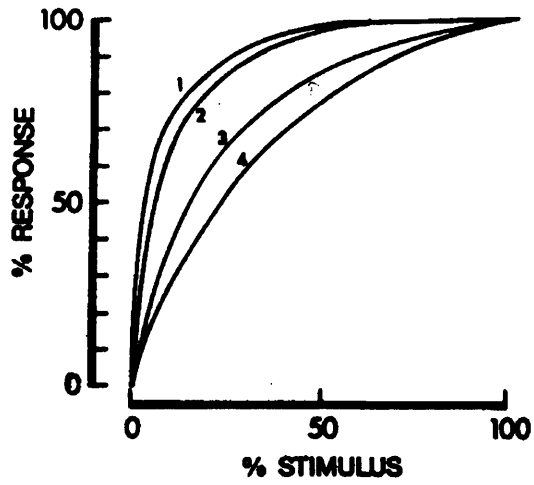

	Tissue	Drug
1	Rabbit Aorta	Norepinephrine
2	Rabbit Aorta	Epinephrine
3	Rabbit papillary	Metaraminol
4	Rabbit papillary	Phenyleprine

Figure 8-2. Stimulus response graphs for muscarinic receptor agonist (left) and α-adrenoceptor agonist (right) in a variety of tissue preparations (Kenakin, 1997). Increasing non-linearity demonstrates differences in coupling efficiency of tissues and efficacy of ligands.

Since there are a number of 'steps' between receptor activation and final effector for measures of cAMP i.e. receptor – G-protein – enzyme, a full agonist is likely to elicit a 100% inhibition of forskolin stimulated cAMP at a low fractional occupancy. Because of the low fractional occupancy required to elicit a maximal response, measures of agonist potency for inhibition if cAMP are high and in this way comparable to measures of affinity. The amplified stimulus response coupling in this system is further highlighted by the finding that the [F/G]N/OFQ(1-17)NH_2 (b-series) of ligands, which behaved as antagonists in the mouse *vas deferens* and partial agonists for GTPγ[^{35}S], were full agonists in cAMP assays.

The stimulus response coupling for the *vas deferens* bioassay appears to be less than for either GTPγ[^{35}S] or cAMP assays. This bioassay is performed on native tissues where receptor density will be far lower than in a recombinant system. Certainly in the *vas deferens* assay there was little or no robust agonist response to the [F/G]N/OFQ(1-17)NH_2 series (b-series) of ligands, whereas for GTPγ[^{35}S] and cAMP assays these ligands were partial and full agonists respectively. However, data in the mouse *vas deferens* (Chapter 3) does contradict the [F/G] data in the SAR study (Chapter 1). Differences in the stimulus response coupling are reiterated with the [Nphe^1] (c-series) series of analogs which in general showed (i) no agonist activity in the mVD, (ii) displayed no or low efficacy agonist activity for ability to stimulate GTPγ[^{35}S] and (iii) moderate to high efficacy with cAMP as an agonist screen.

Whilst agonist potency is higher when studying cAMP, antagonist potency is appreciably lower. For example the pEC_{50} value for N/OFQ in GTPγ[^{35}S] and cAMP is 8.98 and 9.94 respectively. However determinants of [Nphe^1,Arg^{14},Lys^{15}] antagonist potency give pA_2 values of 9.13 and 7.11 in GTPγ[^{35}S] and cAMP respectively. Because of the amplification steps from receptor activation to effector (cAMP) the presence of a receptor reserve or coupling reserve is evident. One explanation for the lower determinants of antagonist potency may be as follows; an antagonist would have to occupy a given fraction of the total receptor number (dependent on the receptor reserve) to have any noticeable effect. For an antagonist to be 'effective' its fractional occupancy would have to be greater in a system with an appreciable receptor reserve i.e. its effective concentration or pA_2/pK_B would be greater. Therefore the potency of an antagonist may be under-estimated in an amplified system, where receptor reserves are more prominent. Nevertheless using whole cells versus membranes and buffers of different composition along with assays being performed at different temperatures will also play a factor in the differences seen for antagonist potency here.

Between the *vas deferens* assay and GTPγ[^{35}S] assay relative differences in potency are greater for the antagonist series than for the agonist series. Between the two assays the difference in agonist (N/OFQ(1-17)NH_2) potency is normally <1.0 log unit, while for the antagonist series (Nphe^1) the difference is closer to 2 log units. It is clear that buffers are different for the two assays and concentrations of intracellular

elements such as GDP will also be different, all factors that affect ligand affinity/efficacy and hence potency. However would this not cause greater disparity between agonist potency values than antagonist, especially given the knowledge that antagonist affinity is unaffected by receptor/G-protein coupling or sodium ions (Ardati *et al.*, 1997)? The need for testing of drugs in multiple assay systems preferably that measure responses at different points along a signal cascade are highlighted in this study.

Inducible expression

In chapter 2 the effect of different receptor densities on ligand intrinsic activity was measured. Intrinsic activity is useful as a comparison of ligand efficacy, in a sense of rank order (i.e. it can be said that N/OFQ(1-13)-NH_2 is more efficacious than [F/G]N/OFQ(1-13)-NH_2) but it is not possible to infer molecular properties of agonism, such as intrinsic efficacy (i.e. the response per unit pharmacon receptor), from comparison of tissue maxima (Kenakin, 1997). However, in cases where fractional occupancy response curves are of a more linear nature, in the absence of a receptor reserve or when the maximal tissue response has not been reached, comparison of intrinsic activity (maximal tissue response) can represent a closer measure of intrinsic efficacy. Although this will need rigorous experimental validation (Kenakin, 2002). Since the relative intrinsic activity of [F/G]N/OFQ(1-13)-NH_2 largely did not change (0.37-0.55) for GTPγ[^{35}S] binding over different receptor densities an excess of receptor or saturation in response cannot be inferred. Given there is no or little change in the relative intrinsic activity between [F/G]N/OFQ(1-13)-NH_2 and N/OFQ(1-13)-NH_2, it may be suggested that the later ligand is not returning the systems maximum response regarding GTPγ[^{35}S] binding. Given a high density of available guanine nucleotide binding sites (Albrecht *et al.*, 1998) and promiscuity in receptor coupling (Yung *et al.*, 1999) it is not surprising that under the assay conditions (high GDP, moderate Mg^{2+}) GTPγ[^{35}S] binding is not saturating and therefore the static relative intrinsic activity between [F/G]N/OFQ(1-13)-NH_2 and N/OFQ(1-13)-NH_2. For cAMP measurements at a 2μM ponasterone A induction the maximal tissue response was not reached (<100%), even by the full agonist N/OFQ(1-13)NH_2, at which point the relative intrinsic activity of

[F/G]N/OFQ(1-13)-NH_2 is 0.48. Based on these findings it can be suggested that the intrinsic efficacy of [F/G]N/OFQ(1-13)NH_2 is ~0.4-0.5.

Ariens introduced the term intrinsic activity to describe the property of agonism (Ariens, 1954). The concept of intrinsic activity was a proportionality factor between tissue response and receptor occupancy to represent an effect per unit of pharmacon receptor complex. Since Areins' model assumed a linear relationship between occupancy and response the magnitude of intrinsic activity was equal to the magnitude of the maximal response. Ligands were denoted with values of α, a full agonist = 1 (100%), a partial agonist may for example = 0.4 (40%). However a measure of intrinsic activity or maximal tissue response cannot be used to characterise the action of a drug since the maximal response of a drug will be both tissue and drug related. Hence classification of efficiacy would then depend on the tissue in which the drug response is measured. For example it can be seen in this thesis that the maximal response of [F/G]N/OFQ(1-13)NH_2 not only varies for the intracellular response studied but also with varying receptor densities. This is highlighted where the maximal response of [F/G]N/OFQ(1-13)NH_2 varies between tissue preparations in the same species i.e. mouse *vas deferens* versus colon.

A system with no receptor reserve would offer the closest insight into the relative intrinsic activity for a partial agonist since both the partial and full agonist would occupy the same number of receptors (100% occupancy) to elicit their maximal response. Under these conditions differences in the maximal responses would then parallel the difference in their relative intrinsic efficacy. Occupancy response curves would need to be linear in nature for this to be true.

Intrinsic efficacy is a dimensionless proportionality factor and represents the response per receptor molecule produced by an agonist. For example a given ligand may require 10% occupancy to generate a given response whilst another would require 80% to elicit the same response. Comparison of occupancy / fraction of maximal response graphs can be used to gain measures of relative intrinsic efficacies. Although in practice these are hard to construct .

In this thesis intrinsic activity (maximal response) is presented and seen to vary with changing receptor number. However a measure of true efficacy for a ligand would not change. A plot of fractional occupancy against fractional response for a partial agonist would look the same over different receptor densities. Therefore the pEC_{50} would remain consistent (see Figure 8-3), although, I feel this relies on an increasing E_{max} (see full agonist below).

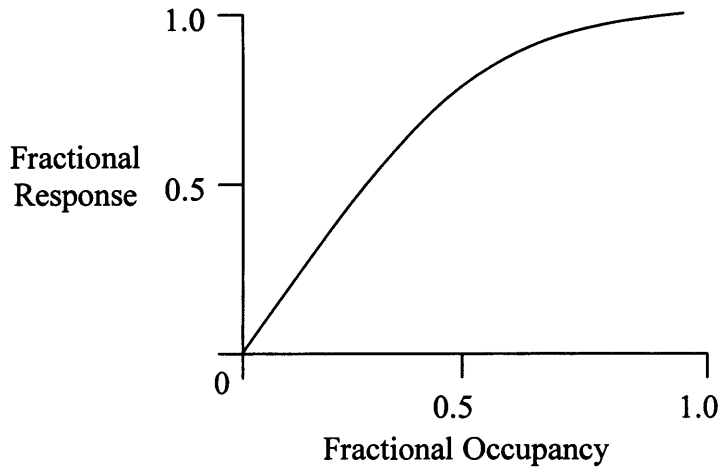

Figure 8-3. Example of a theoretical fractional occupancy response curve.

Whilst a partial agonist does not always produce a maximal tissue response a full agonist will. For a full agonist once the maximal response of the system is achieved increasing receptor number will introduce a greater and greater receptor reserve and the fractional occupancy-response curve is likely to become a steeper and steeper rectangular hyperbola. If it is assumed for a full agonist that its maximum response is generated when in occupancy of a given number of receptors. If the number of receptors in that same system are increased, occupancy of the same number of receptors will again elicit a maximum response. However because there are a greater number of total receptors the fraction occupied will have decreased. In this way a steepening of the fractional occupancy / response curve would be seen (see Figure 8-4). Since with an increase in receptor number there is a decrease in the fractional occupancy required to generate the 0.5 (50%) response, then a decrease in the pEC_{50} will occur.

Low receptor density

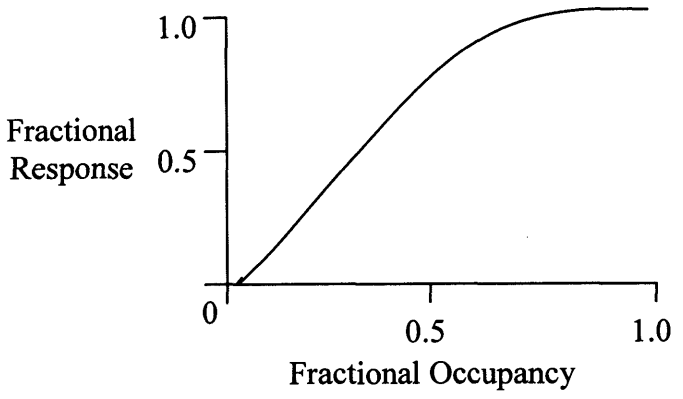

Moderate receptor density (small receptor reserve)

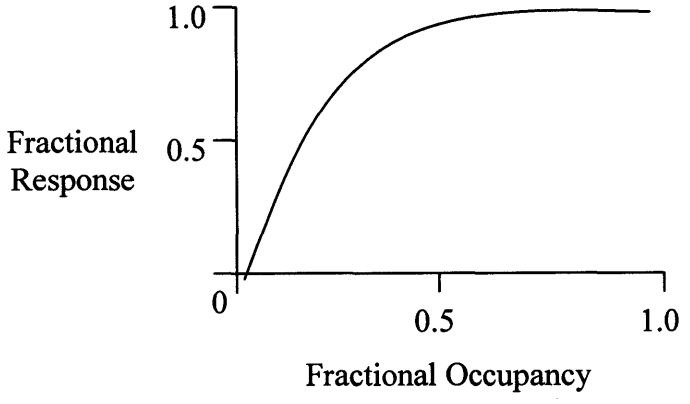

High receptor density (greater receptor reserve)

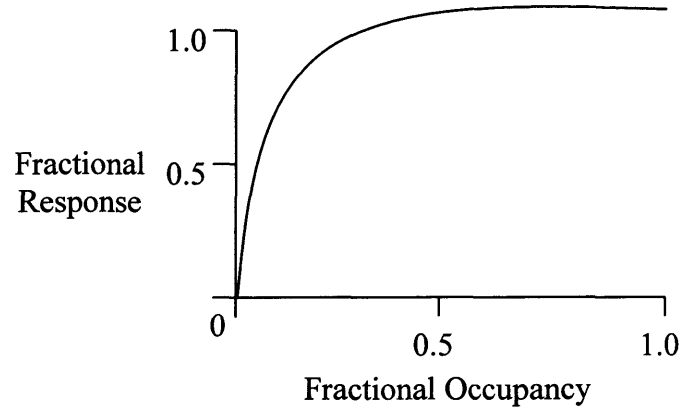

Figure 8-4. Theoretical fractional occupancy response curves for a full agonist in three systems ranging from no receptor reserve to high receptor reserve. Curves become progressively more non-linear as receptor reserve increases in capacity.

The fractional occupancy / response curves for a partial and full agonist would be shifted to the left as receptor density increased, i.e. less fractional occupancy required for a given response, see Figure 8-5.

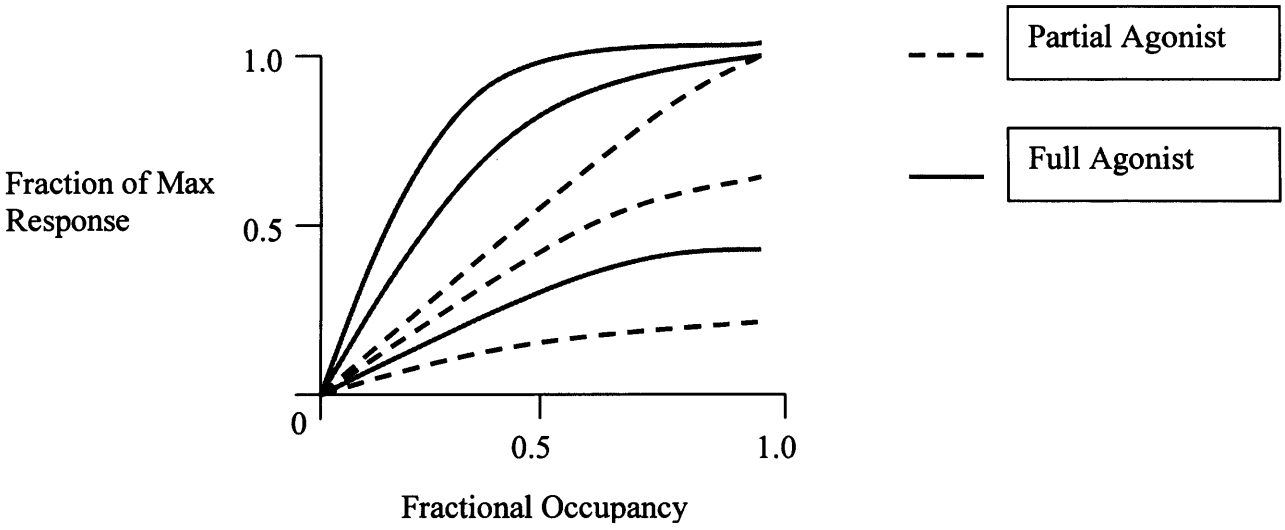

Figure 8-5. Theoretical occupancy response curves for full and partial agonists in a system with an increasing receptor reserve.

The definition of intrinsic efficacy is most accurate, or closer to Ariens' original ideas, for the lowest receptor densities i.e. when occupancy response curves are likely to be more linear in nature. It is at this receptor density that comparisons of intrinsic activity are valid as measures of intrinsic efficacy.

Regarding the data in section 4, if the E_{max} is plotted as a function of receptor density (B_{max}) for the full agonist N/OFQ(1-13)NH_2 and the partial agonist [F/G]N/OFQ(1-13)NH_2 there is a hyperbolic relationship between the two, see Figure 8-6.

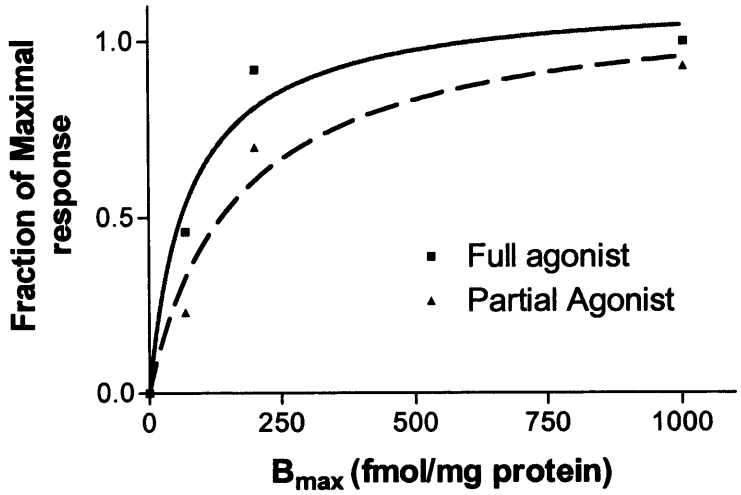

Figure 8-6. Relationship between fractional response (stimulation of $GTP\gamma^{35}S$ binding) and NOP receptor density, B_{max}, for $N/OFQ(1\text{-}13)NH_2$ (full agonist) and $[F/G]N/OFQ(1\text{-}13)NH_2$ (partial agonist).

As receptor density increases there is a change in relative intrinsic activity, as seen by the changing spatial difference between the two curves in Figure 8-6. Both ligand response curves follow hyperbolic functions with that of the full agonist being steeper and hence achieving a maximal response at low receptor densities. Further increases receptor number have no effect on the maximum response produced by the full agonist. For the partial agonist the hyperbola is less steep and does not produce a maximum response at low receptor densities, hence changes in B_{max} will affect E_{max} over a wider range.

In Virto *studies*

As with *in vitro* assays, bioassays on isolated tissues also require definition of optimal conditions in order that responses can be measured in a clear and repeatable manner. For isolated tissue preparations optimal conditions can be identified from length-tension curves, Figure 8-7. For the *vas deferens* the tissue responds to electrical field stimulation to produce an active tension and as stated by Kenakin (Kenakin, 1997); "the dependence of the magnitude of the active tension, the dependent variable of interest in pharmacological experiments, on the basal resting tension placed on the muscle is defined by the length-tension curve for the muscle". For the mouse colon bioassays contraction response is measured as isometric tension generated, while for

the *vas deferens* response is established as isotonic shortening with a given load, Figure 8-8.

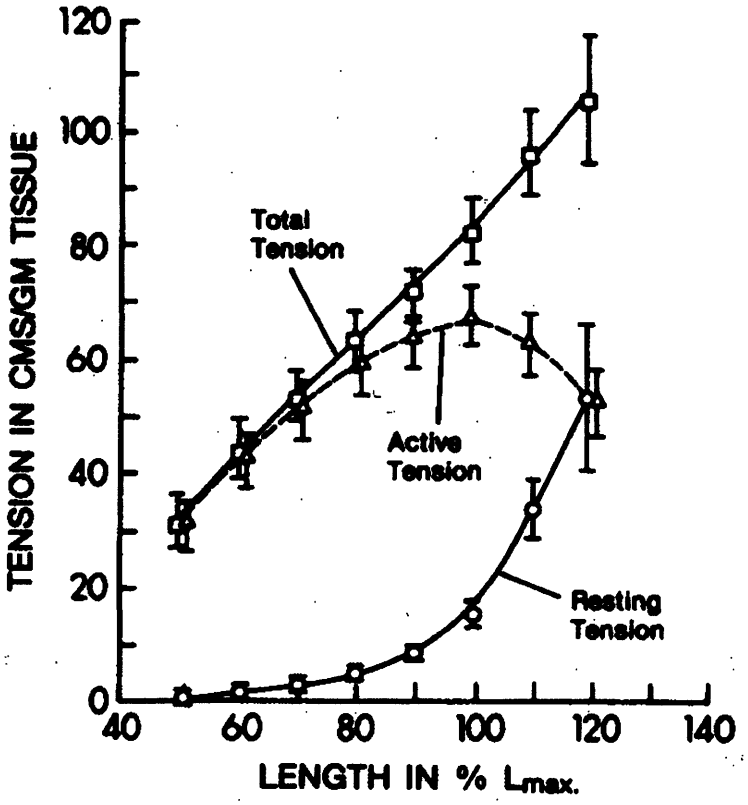

Figure 8-7. The effect of applied resting tension and isolated tissue length on tissue response i.e. active tension. There is an apparent bell shaped curve for active tension so that optimal response over basal is seen with a given tissue length at a specific resting tension.

In the *vas deferens* [F/G]N/OFQ(1-13)NH_2 showed a high degree (α=0.73) of agonist activity, in contrast to the initial study which showed the ligand as an antagonist. While it is still possible to determine antagonist potency, for a partial agonist, there may be some error, inferred by the degree of residual agonist activity and the coupling efficiency of the test system i.e. a high efficiency system will potentiate the relative intrinsic activity of a partial agonist. Based on this it is likely that there would be a degree of error in the derived pK_B for [F/G]N/OFQ(1-13)NH_2 given an α value of 0.73. (This effect can be overcome through testing of partial agonist-antagonist potency in systems where the degree of residual agonism is limited or absent). This error in antagonist potency is seemingly confirmed when data are compared to the pK_B value for [F/G]N/OFQ(1-13)NH_2 derived using GTPγ[^{35}S] in $CHO_{INDhNOP}$

membranes expressing 25fmol/mg protein of receptor. However, these differences may in part be attributable to disparity in the assay conditions.

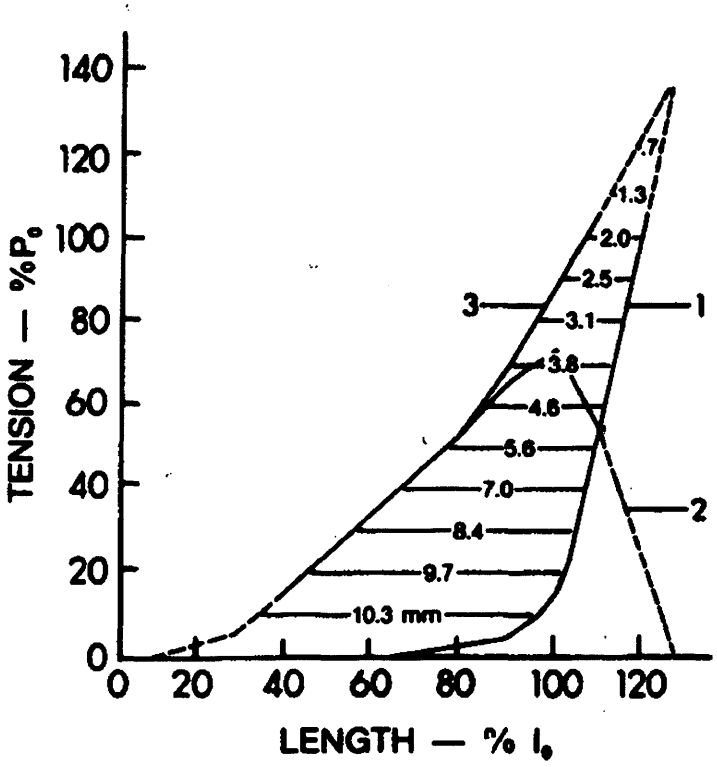

Figure 8-8. Isotonic tissue shortening in canine trachea. Muscle tension given as percentage of mean active tension. Muscle length as percentage of L_{max}. Numbers refer to resting tension (1), active tension (2) and total tension (3). Horizontal lines joining curves 1 and 3 refer to the shortening that the muscle is capable of at various afterloads.

A factor validating the *vas deferens* derived pK_B is the knowledge that the pEC_{50} and pK_B for [F/G]N/OFQ(1-13)NH_2 are in close agreement with one another. Since the pEC_{50} predicts the pK_B, for a partial agonist and *vice versa* this method of comparison limits ambiguity from comparison of inter-assay pK_B values. Therefore the difference in the pK_B derived for [F/G]N/OFQ(1-13)NH_2 between the *vas deferens* and GTPγ[^{35}S] assay is from the different assay conditions, species difference in NOP will also play a major factor.

Partial agonists Ac-RYYRIK-NH_2, Ac-RYYRWK-NH_2 and [F/G]N/OFQ(1-13)NH_2 were also characterised in the mouse colon, a peripheral tissue preparation known to be sensitive to NOP receptor ligands. The order of relative intrinsic activity for these ligands is the same as presented using the ecdysone inducible system in GTPγ[^{35}S]

assays. At a receptor density of 191±26fmol/mg protein relative intrinsic activities of Ac-RYYRWK-NH_2 and [F/G]N/OFQ(1-13)NH_2 are 0.58 and 0.30 respectively. Hence in the mouse colon the efficacy is higher for both Ac-RYYRWK-NH_2 and [F/G]N/OFQ(1-13)NH_2 compared with a recombinant system that expresses ~200fmol/mg of the human NOP receptor. These findings further suggest that the colon expresses a NOP receptor density greater than 200fmol/mg of tissue, although this tissue is often characterised by its low NOP receptor density.

Immunoprecipitation Studies

Previous studies suggest CHO cells express predominantly G_{i3} and G_{o2} (Law *et al.*, 1993; Rens-Domiano *et al.*, 1992). The use of antibodies directed at specific G-proteins subtypes allows subtyoes of G-protein recruited, through ligand receptor activation, to be determined. In this study the development of the immunoprecipitation technique highlighted the efficiency of the assay to be low. In a standard GTPγ[^{35}S] assay high GDP concentrations (100μM) are used to optimise the increase in GTPγ[^{35}S] binding over basal i.e. stimulation factor. However, this will be at the expense of absolute counts bound. For example reducing GDP from 100μM to 5μM (20μg CHO_{hNOP} homogenate) increased N/OFQ stimulated GTPγ[^{35}S] binding from 3929 DPM to 24255 DPM (Bigoni *et al.*, 2002a). While raw DPM is increased through GDP reduction, increase over basal is optimal at 100μM GDP, e.g. a stimulation factor of 10.2±0.79 (100μM) relative to 3.67±0.26 (5μM). Overall the immunoprecipitation assay appears less efficient given the 6-fold difference in net stimulated dpm compared to the 'classical' GTPγ[^{35}S] binding methodology. Although there was less disparity between the two techniques when stimulation factors are compared 3.67 (classical) relative to 2.63±0.16 (immunoprecipitation).

Guanine Nucleotide Binding Studies

In order that guanine nucleotide binding characteristics could be studied a series of GTPγ[^{35}S] competition assays were performed. The binding capacity/affinity of those nucleotides central in G-protein signalling were studied in depth. The binding of GTPγ[^{35}S] was to two sites, the capacity of the low affinity guanine nucleotide binding site was high. Although it must be borne in mind that experiments were performed over a 4hr period in the absence of GDP and hence GTPγS binding would

most likely be to all sub-types of heterotrimeric and monomeric guanine nucleotide binding proteins. Indeed Albrecht (Albrecht *et al.*, 1998) reported a basal binding capacity for GTPγS of ~47pmol/mg protein in rat cerebral cortex preparations.

It has been previously suggested that due to the non-hydrolysable nature of GTPγ[^{35}S] that its binding is irreversible, hence experiments are performed under non-equilibrium conditions and data can only be considered 'apparent'. The binding of GTPγ[^{35}S] has been shown to be dissociable from rat cerebellar membranes by addition of 30μM 'cold' GTPγS, consequently GTPγ[^{35}S] experiments can be performed under equilibrium conditions (Breivogel *et al.*, 1998). In agreement with this study, the association kinetics for GTPγ[^{35}S] binding here reached equilibrium after ~90mins. If GTPγ[^{35}S] binding were not dissociable then GTPγ[^{35}S] association would continue until all guanine binding sites were saturated. GTPγ[^{35}S] dissociation is suggested from the finding that the B_{max} at basal equilibrium is less than the B_{max} determined in the presence of agonist. Therefore under basal conditions not all guanine nucleotide binding sites had been occupied and basal equilibrium must represents an inter-play between association and dissociation. Whilst it is clear that the binding of GTPγ[^{35}S] may be performed under equilibrium conditions data should still be considered apparent when performed with GDP, which will affect GTPγ[^{35}S] binding parameters. Data from saturation experiments performed here may be considered absolute given the absence of GDP and assay duration (4hr).

If the maximal capacity for stimulated binding of GTPγS by 1μM N/OFQ is studied at different receptor densities it can be seen that the response does not increase as a linear function of receptor number. For a 40-fold difference in receptor number, ~23.5fmol/mg protein (1μM ponasterone A) compared to ~1101fmol/mg protein (10μM ponasterone A), there is only a 2.3-fold difference in the 1μM N/OFQ stimulated response, 476.4fmol GTPγS/mg protein (1μM ponasterone A) compared to 1090fmol GTPγS/mg protein (10μM ponasterone A). Hence the stoichiometry between receptor and G-protein was greater (1:20) at the lower expression of hNOP than at the higher expression (1:1). Similar findings have been reported for the MOP receptor whose response per unit receptor (dubbed amplification factor in the article) is 20-fold greater in rat thalamus which expresses 0.74pmol/mg protein compared with CHO cells expressing 6.78pmol/mg protein of the recombinant mouse MOP

receptor (Selley *et al.*, 1998). Similar findings were reported between opioid receptors DOP / KOP compared to cannabinoid receptors (Sim *et al.*, 1996). Despite a 10-fold greater cannabinoid receptor density in cerebral cortex preparations relative to either of the opioid receptors the maximal stimulation of GTPγ[^{35}S] between the three receptors were remarkably similar. In a situation where there is high receptor expression the available pool of G-proteins are more likely to adopt the α- GTPγ[^{35}S] bound form reducing the ability of the receptor to interact with multiple G-proteins. When receptor density is lower there will be less predominance of the α- GTPγ[^{35}S] hence increasing the chance of multiple receptor G-protein interaction. Therefore differences in maximal response may be more reliant on the ratio of receptor to G-protein as opposed simply to maximal receptor number.

Through analysis of the guanine diphosphate binding characteristics it was apparent that there may be three affinity sites for the binding of GDP, a conserved high affinity site, an intermediate affinity site (in the absence of agonist) and a low affinity site seen in the presence of high efficacy agonists. Through rearrangement of the Cheng and Prusoff equation (Breivogel *et al.*, 1998; Cheng *et al.*, 1973) the effect of GDP on the affinity of GTPγ[^{35}S] at the three hypothesised binding sites can be predicted based on the concentration of GDP present and its affinity for the different binding sites. The pIC_{50} values for GDP determined here were 0.1, 2.5 and 10μM for the high, intermediate and low (agonist induced) affinity sites which corresponds to a 51, 3 and 1.5 – fold shift in the affinity of GTPγ[^{35}S] for these respective sites by the addition of 5μM GDP used here. This predicts the affinity GTPγ[^{35}S] (assuming a K_D of 2.88nM) to be 150nM at the high affinity site, 8.64 at the intermediate affinity site and 4.32nM at the low affinity site, in the presence of 5μM GDP. Indeed these values are close to those measured here 252-135nM (low affinity basal), 5.89-2.19nM (intermediate affinity basal) and 4.0-0.93nM (high single affinity in presence of ligand). Additionally the low and high affinity sites for GDP and GTPγ[^{35}S] appear to be reciprocal to one another. Therefore those sites that have high affinity for GDP will have low affinity for GTPγ[^{35}S] and vice versa.

It can be seen that the affinity of GTPγ[^{35}S] is regulated by GDP and receptor activation causes increased binding of GTPγ[^{35}S] through a reduction in GDP affinity.

Plotting the GDP dependence of agonist specific stimulated GTPγ[^{35}S] reveals that agonists of different efficacy differ in their optimal requirement for GDP.

There is much controversy over the supraspinal effects of N/OFQ. Original studies reported intracerebroventricular (i.c.v.) administration caused hyperalgesia compared to vehicle-treated groups. It has since been shown that there is no difference in the pain threshold of i.c.v. N/OFQ administered-groups and vehicle administered groups. Therefore it is assumed that N/OFQ does not cause hyperalgesia but reverses the opioid mediated stress induced analgesia caused by the experimental procedure. NOP antagonists appear to possess analgesic activity via reduction in endogenous central nociceptinergic tone. The anti-opioid role of N/OFQ has subsequently been validated and N/OFQ is known to counteract analgesia elicited through the endogenous opioid system and analgesia from exogenously applied morphine. Chronic use of MOP receptor analgesics, such as morphine, results in tolerance and a reduction in analgesia from a fixed dose. The anti-analgesic action of the NOP – N/OFQ system may play a key role in development of this type of tolerance. Indeed it has been shown that NOP knockout mice show a partial loss of tolerance to morphine and that there is up regulation of N/OFQ production in chronic morphine tolerant mice (Kest *et al.*, 2001). Analgesic tolerance that develops from repeated exposure to morphine was markedly attenuated in NOP knock out mice. Acute morphine analgesia was unaffected in NOP KO species. This action has also been confirmed through the actions of potent selective NOP antagonists, which additionally attenuate morphine tolerance (Ueda *et al.*, 2000). These findings suggest the NOP / N/OFQ system contributes to the neuro-plasticity that accompanies tolerance from chronic morphine exposure (Ueda *et al.*, 2000). NOP blockade may prove useful in reducing tolerance to opioids and/or reducing the dose required to provide analgesia.

Acute pain is often treated satisfactorily with the use of currently available analgesics however chronic pain states, especially neuropathic pain respond poorly to opioid analgesics. Studies with NOP receptor antagonists have demonstrated an antinociceptive role (tail withdrawal test) and support a role of endogenous N/OFQ to the induction of or maintenance of supraspinal hyperalgsia or antianalgesia. A number of pharmaceutical companies have NOP molecules in development, some of these are in clinical trials, Table 8-1.

Company	Compound	Pharmacology	Indication	Dev stage
CoCensys	CO106284	Antagonist	Not specified	Pre-Clin*
Japan Tobacco	JTC801	Antagonist	Pain	I and II
SRI International	Various	Agonist & Antagonist	Pain	Pre-Clin
Roche	Ro646198	Agonist	Anxiety	Pre-Clin
Zealand Pharma	ZP120	Agonist	Heart Failure	II

Figure 8-1. NOP ligands and the development pipeline (* Withdrawn)

There is current interest in the development of drugs with "dual actions" for example drugs with activity at more than one opioid receptor and can act in a synergistic manner. Co-administration of MOP and DOP agonists have been shown to have a synergistic analgesic action, for example sub-antinociceptive doses of leu-enkephalin potentiate the analgesia elicited by morphine. Further there is evidence to show that administration of DOP receptor antagonists reduce tolerance, physical dependence and other side effects of MOP receptor agonists without detriment to their analgesic action. Development of tolerance and dependence to morphine following chronic dosing was blocked by antisense oligoneucleotides directed against the DOP receptor. In a similar vain the partial agonist activity of buprenorphine, an opioid analgesic used for the treatment of moderate to severe pain, is belived to be through an action at both MOP and NOP receptor. "In both animals and humans a hallmark of the antinociceptive action of buprenorphine is the production of a ceiling effect or a bell shaped curve" (Cowan, 2003). The ceiling effect, which is seen in man, may be caused simply through buprenorphine partial agonist activity. However subsequent activation of NOP receptor mediated anti-opioid activity may set the ceiling response of buprenorphine and is certainly responsible for the falling phase of buprenorphines bell shaped curve. It maybe also suggested that the supraspinal actions of NOP not only compromise the MOP mediated actions of buprenorphine but also override the possible spinal NOP mediated antinociception of buprenorphine.

It is therefore apparent that the N/OFQ-NOP system has an important role to play in a variety of acute and chronic pain states and both agonist and, more likely, antagonists have therapeutic role(s). The development of clinically relevant drugs requires that drugs are correctly characterised, ideally at the earliest possible stage in their

development i.e. *in vitro* characterisation. Not only does this study identify ligands that are proving invaluable tools in the delineation of the role(s) of the N/OFQ-NOP receptor system i.e. UFP-101, we also present a number of systems and methods wereby more precise measures of ligand efficacy can be determined. The importance of clearly defining the efficacy of a drug is of great importance none more so than with the NOP receptor. Indeed the efficacy of a NOP receptor ligand can determine whether or not a drug would have a hyperalgesic effect or anti-nocicepive effect. Further knowledge of partial agonist efficacy is also of great significance as this will affect the role a drug will take in tissues of different expression, for example the profile for a low to medium efficacy ligand could show antagonistic actions in the PNS, typically where receptor densities are lower and agonism at supraspinal sites where receptor densities are expected to be higher. Also the effects of different disease states on receptor expression may play highly influential roles on ligand responses and hence precise knowledge of a drugs efficacy should not be over looked.

Overall this thesis has discovered a great deal about the N/OFQ – NOP system. Through the systematic SAR studies novel ligands, such as UFP-101, have been identied which have proven invaluable in delineation of the physiology of the NOP system. Indeed UFP-101 has highlighted the use of NOP receptor antagonists not only as novel analgesics but have also been shown to have antidressant like activity. However, it must be borne in mine that some of the early characterisation of novel componds performed in this thesis are of paramount importance for the identification of potentially future therapteutics leads. The use inducible receptor expression, coupled to multiple assay examination is a powerful tool for assesing the true pharmacological nature of a ligand which, still today, is often wrongly characterised. The further investigations of guanine nucleotide binding and its relation to efficacy is highly relevant in modern pharmacology where there is great interest in defining the efficacy of drugs with hot topics such as ensemble theory being raised.
I hope that the work reported here will help in the development of a very interesting and important field in therapeutic medicine.

9 References

Akil, H, Owens, C, Gutstein, H, Taylor, L, Curran, E, Watson, S (1998) Endogenous opioids: overview and current issues. *Drug Alcohol Depend.* **51**(1-2): 127-140.

Albrecht, E, Samovilova, NN, Oswald, S, Baeger, I, Berger, H (1998) Nociceptin (orphanin FQ): high-affinity and high-capacity binding site coupled to low-potency stimulation of guanylyl-5'-O-(gamma-thio)-triphosphate binding in rat brain membranes. *J. Pharmacol. Exp. Ther.* **286**(2): 896-902.

Ames, RS, Sarau, HM, Chambers, JK, Willette, RN, Aiyar, NV, Romanic, AM, Louden, CS, Foley, JJ, Sauermelch, CF, Coatney, RW, Ao, Z, Disa, J, Holmes, SD, Stadel, JM, Martin, JD, Liu, WS, Glover, GI, Wilson, S, McNulty, DE, Ellis, CE, Elshourbagy, NA, Shabon, U, Trill, JJ, Hay, DW, Douglas, SA, et al. (1999) Human urotensin-II is a potent vasoconstrictor and agonist for the orphan receptor GPR14. *Nature* **401**(6750): 282-286.

Andressen, KW, Norum, JH, Levy, FO, Krobert, KA (2006) Activation of adenylyl cyclase by endogenous G(s)-coupled receptors in human embryonic kidney 293 cells is attenuated by 5-HT(7) receptor expression. *Mol. Pharmacol.* **69**(1): 207-215.

Anton, B, Fein, J, To, T, Li, X, Silberstein, L, Evans, CJ (1996) Immunohistochemical localization of ORL-1 in the central nervous system of the rat. *J. Comp. Neurol.* **368**(2): 229-251.

Ardati, A, Robert A. Henningsen, Jacqueline Higelin, Rainer K. Reinscheid, Olivier Civelli, Frederick J. Monsma, J (1997) Interaction of [3H]Orphanin FQ and 125I-Try14-Orphanin FQ with the Orphanin Receptor: Kinetics and Modulation by Cations and Guanine Nucleotides. *Molecular Pharmacology* **51**: 816-824.

Ariens, EJ (1954) Affinity and intrinsic activity in the theory of competitive inhibition. I. Problems and theory. *Arch. Int. Pharmacodyn. Ther.* **99**(1): 32-49.

Becker, JA, Wallace, A, Garzon, A, Ingallinella, P, Bianchi, E, Cortese, R, Simonin, F, Kieffer, BL, Pessi, A (1999) Ligands for kappa-opioid and ORL1 receptors identified from a conformationally constrained peptide combinatorial library. *J. Biol. Chem.* **274**(39): 27513-27522.

Berg, KA, Maayani, S, Goldfarb, J, Scaramellini, C, Leff, P, Clarke, WP (1998) Effector pathway-dependent relative efficacy at serotonin type 2A and 2C receptors: evidence for agonist-directed trafficking of receptor stimulus. *Mol. Pharmacol.* **54**(1): 94-104.

Berger, H, Bigoni, R, Albrecht, E, Richter, RM, Krause, E, Bienert, M, Calo, G (2000a) The nociceptin/orphanin FQ receptor ligand acetyl-RYYRIK-amide exhibits antagonistic and agonistic properties. *Peptides* **21**(7): 1131-1139.

Berger, H, Calo, G, Albrecht, E, Guerrini, R, Bienert, M (2000b) [Nphe(1)]NC(1-13)NH(2) selectively antagonizes nociceptin/orphanin FQ-stimulated G-protein activation in rat brain. *J. Pharmacol. Exp. Ther.* **294**(2): 428-433.

Berlot, CH, Bourne, HR (1992) Identification of effector-activating residues of Gs alpha. *Cell* **68**(5): 911-922.

Berzetei-Gurske, IP, Schwartz, RW, Toll, L (1996) Determination of activity for nociceptin in the mouse vas deferens. *Eur. J. Pharmacol.* **302**(1-3): R1-2.

Bigoni, R, Calo, G, Guerrini, R, Strupish, JW, Rowbotham, DJ, Lambert, DG (2001) Effects of nociceptin and endomorphin 1 on the electrically stimulated human vas deferens. *Br. J. Clin. Pharmacol.* **51**(4): 355-358.

Bigoni, R, Cao, G, Rizzi, A, Okawa, H, Regoli, D, Smart, D, Lambert, DG (2002a) Effects of naloxone benzoylhydrazone on native and recombinant nociceptin/orphanin FQ receptors. *Can. J. Physiol. Pharmacol.* **80**(5): 407-412.

Bigoni, R, Giuliani, S, Calo, G, Rizzi, A, Guerrini, R, Salvadori, S, Regoli, D, Maggi, CA (1999) Characterization of nociceptin receptors in the periphery: in vitro and in vivo studies. *Naunyn. Schmiedebergs Arch. Pharmacol.* **359**(3): 160-167.

Bigoni, R, Rizzi, D, Rizzi, A, Camarda, V, Guerrini, R, Lambert, DG, Hashiba, E, Berger, H, Salvadori, S, Regoli, D, Calo, G (2002b) Pharmacological characterization of [(pX)Phe4]nociceptin(1-13)amide analogs: I) in vitro studies. *Naunyn-Schmiedebergs Arch. Pharmacol.* **365**: 442-449.

Bokoch, GM, Katada, T, Northup, JK, Ui, M, Gilman, AG (1984) Purification and properties of the inhibitory guanine nucleotide-binding regulatory component of adenylate cyclase. *J. Biol. Chem.* **259**(6): 3560-3567.

Borgland, SL, Connor, M, Christie, MJ (2001) Nociceptin inhibits calcium channel currents in a subpopulation of small nociceptive trigeminal ganglion neurons in mouse. *J Physiol* **536**(Pt 1): 35-47.

Breivogel, CS, Selley, DE, Childers, SR (1998) Cannabinoid receptor agonist efficacy for stimulating [35S]GTPgammaS binding to rat cerebellar membranes correlates with agonist-induced decreases in GDP affinity. *J. Biol. Chem.* **273**(27): 16865-16873.

Brown, BL, Albano, JD, Ekins, RP, Sgherzi, AM (1971) A simple and sensitive saturation assay method for the measurement of adenosine 3':5'-cyclic monophosphate. *Biochem. J.* **121**(3): 561-562.

Butour, JL, Moisand, C, Mazarguil, H, Mollereau, C, Meunier, JC (1997) Recognition and activation of the opioid receptor-like ORL 1 receptor by nociceptin, nociceptin analogs and opioids. *Eur. J. Pharmacol.* **321**(1): 97-103.

Cabrera-Vera, TM, Vanhauwe, J, Thomas, TO, Medkova, M, Preininger, A, Mazzoni, MR, Hamm, HE (2003) Insights into G protein structure, function, and regulation. *Endocr. Rev.* **24**(6): 765-781.

Calo, G, Bigoni, R, Rizzi, A, Guerrini, R, Salvadori, S, Regoli, D (2000a) Nociceptin/orphanin FQ receptor ligands. *Peptides* **21**(7): 935-947.

Calo, G, Guerrini, R, Bigoni, R, Rizzi, A, Marzola, G, Okawa, H, Bianchi, C, Lambert, DG, Salvadori, S, Regoli, D (2000b) Characterization of [Nphe(1)]nociceptin(1-13)NH(2), a new selective nociceptin receptor antagonist. *Br. J. Pharmacol.* **129**(6): 1183-1193.

Calo, G, Guerrini, R, Rizzi, A, Salvadori, S, Burmeister, M, Kapusta, DR, Lambert, DG, Regoli, D (2005) UFP-101, a peptide antagonist selective for the nociceptin/orphanin FQ receptor. *CNS Drug Rev* **11**(2): 97-112.

Calo, G, Guerrini, R, Rizzi, A, Salvadri, S, Regoli, D (2000c) Pharmacology of nociceptin and its receptor: a novel threapeutic target. *Br. J. Pharmacol.* **129**(7): 1261-1283.

Calo, G, Rizzi, A, Bogoni, G, Neugebauer, V, Salvadori, S, Guerrini, R, Bianchi, C, Regoli, D (1996) The mouse vas deferens: a pharmacological preparation sensitive to nociceptin. *Eur. J. Pharmacol.* **311**(1): R3-5.

Calo, G, Rizzi, A, Marzola, G, Guerrini, R, Salvadori, S, Beani, L, Regoli, D, Bianchi, C (1998) Pharmacological characterization of the nociceptin receptor mediating hyperalgesia in the mouse tail withdrawal assay. *Br. J. Pharmacol.* **125**(2): 373-378.

Calo, G, Rizzi, A, Rizzi, D, Bigoni, R, Guerrini, R, Marzola, G, Marti, M, McDonald, J, Morari, M, Lambert, DG, Salvadori, S, Regoli, D (2002) [Nphe1,Arg14,Lys15]nociceptin-NH2, a novel potent and selective antagonist of the nociceptin/orphanin FQ receptor. *Br. J. Pharmacol.* **136**(2): 303-311.

Capra, V, Veltri, A, Foglia, C, Crimaldi, L, Habib, A, Parenti, M, Rovati, GE (2004) Mutational analysis of the highly conserved ERY motif of the thromboxane A2 receptor: alternative role in G protein-coupled receptor signaling. *Mol. Pharmacol.* **66**(4): 880-889.

Cheng, Y, Prusoff, WH (1973) Relationship between the inhibition constant (K1) and the concentration of inhibitor which causes 50 per cent inhibition (I50) of an enzymatic reaction. *Biochem. Pharmacol.* **22**(23): 3099-3108.

Civelli, O, Nothacker, H-P, Saito, Y, Wang, Z, Lin, SHS, Reinscheid, RK (2001) Novel neurotransmitters as natural ligands of orphan G-protein-coupled receptors. *Trends Neurosci.* **24**(4): 230-237.

Clarke, S, Czyzyk, T, Ansonoff, M, Nitsche, JF, Hsu, MS, Nilsson, L, Larsson, K, Borsodi, A, Toth, G, Hill, R, Kitchen, I, Pintar, JE (2002) Autoradiography of opioid and ORL1 ligands in opioid receptor triple knockout mice. *Eur. J. Neurosci.* **16**(9): 1705-1712.

Cole, SL, Schindler, M, Sellers, LA, Humphrey, PP (2001) Titrating the expression of a Gi protein-coupled receptor using an ecdysone-inducible system in CHO-K1 cells. *Receptors Channels* **7**(4): 289-302.

Connor, M, Christie, MD (1999a) Opioid receptor signalling mechanisms. *Clin. Exp. Pharmacol. Physiol.* **26**(7): 493-499.

Connor, M, Christie, MJ (1998) Modulation of Ca2+ channel currents of acutely dissociated rat periaqueductal grey neurons. *J Physiol* **509 (Pt 1):** 47-58.

Connor, M, Vaughan, CW, Chieng, B, Christie, MJ (1996) Nociceptin receptor coupling to a potassium conductance in rat locus coeruleus neurones in vitro. *Br. J. Pharmacol.* **119**(8): 1614-1618.

Connor, M, Vaughan, CW, Jennings, EA, Allen, RG, Christie, MJ (1999b) Nociceptin, Phe(1)psi-nociceptin(1 - 13), nocistatin and prepronociceptin(154 - 181) effects on calcium channel currents and a potassium current in rat locus coeruleus in vitro. *Br. J. Pharmacol.* **128**(8): 1779-1787.

Cordeaux, Y, Briddon, SJ, Megson, AE, McDonnell, J, Dickenson, JM, Hill, SJ, Ferguson, KM, Higashijima, T, Smigel, MD, Gilman, AG (2000) Influence of receptor number on functional responses elicited by agonists acting at the human adenosine A(1) receptor: evidence for signaling pathway-dependent changes in agonist potency and relative intrinsic activity. The influence of bound GDP on the kinetics of guanine nucleotide binding to G proteins. *Mol. Pharmacol.* **58**(5): 1075-1084.

Cowan, A (2003) Buprenorphine: new pharmacological aspects. *Int. J. Clin. Pract. Suppl.*(133): 3-8; discussion 23-24.

Cox, BM, Chavkin, C, Christie, MJ, Civelli, O, Evans, C, Hamon, MD, Hoellt, V, Kieffer, B, Kitchen, I, McKnight, AT, Meunier, JC, Portoghese, PS (2000) Opioid receptors. In The IUPHAR Compendium of Receptor Characterization and Classification. ed. Girdlestone, D. *London IUPHAR Media Ltd.*: 321-333.

Darlison, MG, Greten, FR, Harvey, RJ, Kreienkamp, HJ, Stuhmer, T, Zwiers, H, Lederis, K, Richter, D (1997) Opioid receptors from a lower vertebrate (Catostomus commersoni): sequence, pharmacology, coupling to a G-protein-gated inward-rectifying potassium channel (GIRK1), and evolution. *Proc. Natl. Acad. Sci. U. S. A.* **94**(15): 8214-8219.

Dascal, N (2001) Ion-channel regulation by G proteins. *Trends Endocrinol Metab* **12**(9): 391-398.

Dautzenberg, FM, Wichmann, J, Higelin, J, Py-Lang, G, Kratzeisen, C, Malherbe, P, Kilpatrick, GJ, Jenck, F (2001) Pharmacological characterization of the novel nonpeptide orphanin FQ/nociceptin receptor agonist Ro 64-6198: rapid and reversible desensitization of the ORL1 receptor in vitro and lack of tolerance in vivo. *J. Pharmacol. Exp. Ther.* **298**(2): 812-819.

Dhawan, BN, Cesselin, F, Raghubir, R, Reisine, T, Bradley, PB, Portoghese, PS, Hamon, M (1996) International Union of Pharmacology. XII. Classification of opioid receptors. *Pharmacol. Rev.* **48**(4): 567-592.

Dooley, CT, Houghten, RA (2000) Orphanin FQ/nociceptin receptor binding studies. *Peptides* **21**(7): 949-960.

Dooley, CT, Spaeth, CG, Berzetei-Gurske, IP, Craymer, K, Adapa, ID, Brandt, SR, Houghten, RA, Toll, L (1997) Binding and in vitro activities of peptides with high affinity for the nociceptin/orphanin FQ receptor, ORL1. *J. Pharmacol. Exp. Ther.* **283**(2): 735-741.

Faber, ES, Chambers, JP, Evans, RH, Henderson, G (1996) Depression of glutamatergic transmission by nociceptin in the neonatal rat hemisected spinal cord preparation in vitro. *Br. J. Pharmacol.* **119**(2): 189-190.

Feldman, RS (1997) *Principles of Neuropsychopharmacology*. Sinauer Associates Incorporated.

Ferguson, KM, Higashijima, T, Smigel, MD, Gilman, AG (1986) The influence of bound GDP on the kinetics of guanine nucleotide binding to G proteins. *J. Biol. Chem.* **261**(16): 7393-7399.

Fischer, A, Forssmann, WG, Undem, BJ (1998) Nociceptin-induced inhibition of tachykinergic neurotransmission in guinea pig bronchus. *J. Pharmacol. Exp. Ther.* **285**(2): 902-907.

Florin, S, Suaudeau, C, Meunier, JC, Costentin, J (1996) Nociceptin stimulates locomotion and exploratory behaviour in mice. *Eur. J. Pharmacol.* **317**(1): 9-13.

Foord, SM, Bonner, TI, Neubig, RR, Rosser, EM, Pin, JP, Davenport, AP, Spedding, M, Harmar, AJ (2005) International Union of Pharmacology. XLVI. G protein-coupled receptor list. *Pharmacol. Rev.* **57**(2): 279-288.

Gaveriaux-Ruff, C, Kieffer, BL (2002) Opioid receptor genes inactivated in mice: the highlights. *Neuropeptides* **36**(2-3): 62-71.

Gether, U (2000) Uncovering molecular mechanisms involved in activation of G protein-coupled receptors. *Endocr. Rev.* **21**(1): 90-113.

Gether, U, Johansen, TE, Snider, RM, Lowe, JA, 3rd, Emonds-Alt, X, Yokota, Y, Nakanishi, S, Schwartz, TW (1993) Binding epitopes for peptide and non-peptide ligands on the NK1 (substance P) receptor. *Regul. Pept.* **46**(1-2): 49-58.

Gether, U, Kobilka, BK (1998) G protein-coupled receptors. II. Mechanism of agonist activation. *J. Biol. Chem.* **273**(29): 17979-17982.

Gether, U, Lin, S, Kobilka, BK (1995) Fluorescent labeling of purified beta 2 adrenergic receptor. Evidence for ligand-specific conformational changes. *J. Biol. Chem.* **270**(47): 28268-28275.

Giuliani, S, Maggi, CA (1996) Inhibition of tachykinin release from peripheral endings of sensory nerves by nociceptin, a novel opioid peptide. *Br. J. Pharmacol.* **118**(7): 1567-1569.

Giuliani, S, Maggi, CA (1997) Prejunctional modulation by nociceptin of nerve-mediated inotropic responses in guinea-pig left atrium. Inhibition of tachykinin release from peripheral endings of sensory nerves by nociceptin, a novel opioid peptide. *Eur. J. Pharmacol.* **332**(3): 231-236.

Grisel, JE, Farrier, DE, Wilson, SG, Mogil, JS (1998) [Phe1psi(CH2-NH)Gly2]nociceptin-(1-13)-NH2 acts as an agonist of the orphanin FQ/nociceptin receptor in vivo. *Eur. J. Pharmacol.* **357**(1): R1-3.

Guerrini, R, Calo, G, Bigoni, R, Rizzi, A, Varani, K, Toth, G, Gessi, S, Hashiba, E, Hashimoto, Y, Lambert, DG, Borea, PA, Tomatis, R, Salvadori, S, Regoli, D (2000a) Further studies on nociceptin-related peptides: discovery of a new chemical template with antagonist activity on the nociceptin receptor. *J. Med. Chem.* **43**(15): 2805-2813.

Guerrini, R, Calo, G, Bigoni, R, Rizzi, D, Rizzi, A, Zucchini, M, Varani, K, Hashiba, E, Lambert, DG, Toth, G, Borea, PA, Salvadori, S, Regoli, D (2001) Structure-activity studies of the Phe(4) residue of nociceptin(1-13)-NH(2): identification of highly potent agonists of the nociceptin/orphanin FQ receptor. *J. Med. Chem.* **44**(23): 3956-3964.

Guerrini, R, Calo, G, Lambert, DG, Carra, G, Arduin, M, Barnes, TA, McDonald, J, Rizzi, D, Trapella, C, Marzola, E, Rowbotham, DJ, Regoli, D, Salvadori, S (2005) N- and C-terminal modifications of nociceptin/orphanin FQ generate highly potent NOP receptor ligands. *J. Med. Chem.* **48**(5): 1421-1427.

Guerrini, R, Calo, G, Rizzi, A, Bianchi, C, Lazarus, LH, Salvadori, S, Temussi, PA, Regoli, D (1997) Address and message sequences for the nociceptin receptor: a structure-activity study of nociceptin-(1-13)-peptide amide. *J. Med. Chem.* **40**(12): 1789-1793.

Guerrini, R, Calo, G, Rizzi, A, Bigoni, R, Bianchi, C, Salvadori, S, Regoli, D (1998) A new selective antagonist of the nociceptin receptor. *Br. J. Pharmacol.* **123**(2): 163-165.

Guerrini, R, Calo, G, Rizzi, A, Bigoni, R, Rizzi, D, Regoli, D, Salvadori, S (2000b) Structure-activity relationships of nociceptin and related peptides: comparison with dynorphin A. *Peptides* **21**(7): 923-933.

Hao, J-X, Xu, IS, Wiesenfeld-Hallin, Z, Xu, X-J (1998) Anti-hyperalgesic and anti-allodynic effects of intrathecal nociceptin/orphanin FQ in rats after spinal cord injury, peripheral nerve injury and inflammation. *Pain* **76**(3): 385-393.

Hashiba, E, Harrison, C, Galo, G, Guerrini, R, Rowbotham, DJ, Smith, G, Lambert, DG (2001) Characterisation and comparison of novel ligands for the nociceptin/orphanin FQ receptor. *Naunyn. Schmiedebergs Arch. Pharmacol.* **363**(1): 28-33.

Hashiba, E, Lambert, DG, Farkas, J, Toth, G, Smith, G (2002a) Comparison of the binding of [(3)H]nociceptin/orphaninFQ(1-13)NH(2), [(3)H]nociceptin/orphaninFQ(1-17)OH and [(125)I]Tyr(14)nociceptin/orphaninFQ(1-

17)OH to recombinant human and native rat cerebrocortical nociceptin/orphanin FQ receptors. *Neurosci. Lett.* **328**(1): 5-8.

Hashiba, E, Lambert, DG, Jenck, F, Wichmann, J, Smith, G (2002b) Characterisation of the non-peptide nociceptin receptor agonist, Ro64-6198 in Chinese hamster ovary cells expressing recombinant human nociceptin receptors. *Life Sci.* **70**(15): 1719-1725.

Hawes, BE, Graziano, MP, Lambert, DG (2000) Cellular actions of nociceptin: transduction mechanisms. *Peptides* **21**(7): 961-967.

Heinricher, MM, McGaraughty, S, Tortorici, V (2001) Circuitry underlying antiopioid actions of cholecystokinin within the rostral ventromedial medulla. *J. Neurophysiol.* **85**(1): 280-286.

Helyes, Z, Nemeth, J, Pinter, E, Szolcsanyi, J (1997) Inhibition by nociceptin of neurogenic inflammation and the release of SP and CGRP from sensory nerve terminals. *Br. J. Pharmacol.* **121**(4): 613-615.

Herzyk, P, Hubbard, RE (1995) Automated method for modeling seven-helix transmembrane receptors from experimental data. *Biophys. J.* **69**(6): 2419-2442.

Higashijima, T, Ferguson, KM, Sternweis, PC, Smigel, MD, Gilman, AG (1987) Effects of Mg2+ and the beta gamma-subunit complex on the interactions of guanine nucleotides with G proteins. *J. Biol. Chem.* **262**(2): 762-766.

Hille, B (2001) *Ionic Channels of Excitable Membranes*. Sinauer Associates.

Hogshire, J (1994) *Opium for the Masses: A Pratical Guide to Growing Opium Poppies and Making Opium*. Loom Panics Unlimited.

Hughes, J, Kosterlitz, HW, Leslie, FM (1975a) Effect of morphine on adrenergic transmission in the mouse vas deferens. Assessment of agonist and antogonist potencies of narcotic analgesics. *Br. J. Pharmacol.* **53**(3): 371-381.

Hughes, J, Smith, TW, Kosterlitz, HW, Fothergill, LA, Morgan, BA, Morris, HR (1975b) Identification of two related pentapeptides from the brain with potent opiate agonist activity. *Nature* **258**(5536): 577-580.

Ikeda, K, Kobayashi, K, Kobayashi, T, Ichikawa, T, Kumanishi, T, Kishida, H, Yano, R, Manabe, T (1997) Functional coupling of the nociceptin/orphanin FQ receptor with the G-protein-activated K+ (GIRK) channel. *Brain Res. Mol. Brain Res.* **45**(1): 117-126.

Ingram, SL, Williams, JT (1994) Opioid inhibition of Ih via adenylyl cyclase. *Neuron* **13**(1): 179-186.

Inoue, M, Kobayashi, M, Kozaki, S, Zimmer, A, Ueda, H (1998) Nociceptin/orphanin FQ-induced nociceptive responses through substance P release from peripheral nerve endings in mice. *Proc. Natl. Acad. Sci. U. S. A.* **95**(18): 10949-10953.

Inoue, M, Matsunaga, S, Rashid, MH, Yoshida, A, Mizuno, K, Sakurada, T, Takeshima, H, Ueda, H (2001) Pronociceptive effects of nociceptin/orphanin FQ (13-17) at peripheral and spinal level in mice. *J. Pharmacol. Exp. Ther.* **299**(1): 213-219.

Itoh, H, Gilman, AG (1991) Expression and analysis of Gs alpha mutants with decreased ability to activate adenylylcyclase. *J. Biol. Chem.* **266**(24): 16226-16231.

Jenck, F, Moreau, JL, Martin, JR, Kilpatrick, GJ, Reinscheid, RK, Monsma, FJ, Jr., Nothacker, HP, Civelli, O (1997) Orphanin FQ acts as an anxiolytic to attenuate behavioral responses to stress. *Proc. Natl. Acad. Sci. U. S. A.* **94**(26): 14854-14858.

Jenck, F, Wichmann, J, Dautzenberg, FM, Moreau, JL, Ouagazzal, AM, Martin, JR, Lundstrom, K, Cesura, AM, Poli, SM, Roever, S, Kolczewski, S, Adam, G, Kilpatrick, G (2000) A synthetic agonist at the orphanin FQ/nociceptin receptor ORL1: anxiolytic profile in the rat. *Proc. Natl. Acad. Sci. U. S. A.* **97**(9): 4938-4943.

Jennings, EA (2001) Postsynaptic K+ current induced by nociceptin in medullary dorsal horn neurons. *Neuroreport* **12**(3): 645-648.

Johnson, EE, Gibson, H, Nicol, B, Zanzinger, J, Widdowson, P, Hawthorn, M, Toth, G, Farkas, J, Guerrini, R, Lambert, DG (2003) Characterization of nociceptin/orphanin FQ binding sites in dog brain membranes. *Anesth. Analg.* **97**(3): 741-747.

Kapusta, DR, Chang, JK, Kenigs, VA (1999) Central administration of [Phe1psi(CH2-NH)Gly2]nociceptin(1-13)-NH2 and orphanin FQ/nociceptin (OFQ/N) produce similar cardiovascular and renal responses in conscious rats. *J. Pharmacol. Exp. Ther.* **289**(1): 173-180.

Kawamoto, H, Ozaki, S, Itoh, Y, Miyaji, M, Arai, S, Nakashima, H, Kato, T, Ohta, H, Iwasawa, Y (1999) Discovery of the first potent and selective small molecule opioid receptor-like (ORL1) antagonist: 1-[(3R,4R)-1-cyclooctylmethyl-3- hydroxymethyl-4-piperidyl]-3-ethyl-1, 3-dihydro-2H-benzimidazol-2-one (J-113397). *J. Med. Chem.* **42**(25): 5061-5063.

Kenakin, T (2002) Drug efficacy at G protein-coupled receptors. *Annu. Rev. Pharmacol. Toxicol.* **42**: 349-379.

Kenakin, T (1997) *Pharmacologic Analysis of Drug-Receptor Interaction*. Lippincott-Raven.

Kest, B, Hopkins, E, Palmese, CA, Chen, ZP, Mogil, JS, Pintar, JE (2001) Morphine tolerance and dependence in nociceptin/orphanin FQ transgenic knock-out mice. *Neuroscience* **104**(1): 217-222.

Kieffer, BL (1999) Opioids: first lessons from knockout mice. *Trends Pharmacol. Sci.* **20**(1): 19-26.

King, MA, Rossi, GC, Chang, AH, Williams, L, Pasternak, GW (1997) Spinal analgesic activity of orphanin FQ/nociceptin and its fragments. *Neurosci. Lett.* **223**(2): 113-116.

Kjelsberg, MA, Cotecchia, S, Ostrowski, J, Caron, MG, Lefkowitz, RJ (1992) Constitutive activation of the alpha 1B-adrenergic receptor by all amino acid substitutions at a single site. Evidence for a region which constrains receptor activation. *J. Biol. Chem.* **267**(3): 1430-1433.

Kong, H, Raynor, K, Yano, H, Takeda, J, Bell, GI, Reisine, T (1994) Agonists and antagonists bind to different domains of the cloned kappa opioid receptor. *Proc. Natl. Acad. Sci. U. S. A.* **91**(17): 8042-8046.

Law, PY, Kouhen, OM, Solberg, J, Wang, W, Erickson, LJ, Loh, HH (2000) Deltorphin II-induced rapid desensitization of delta-opioid receptor requires both phosphorylation and internalization of the receptor. *J. Biol. Chem.* **275**(41): 32057-32065.

Law, SF, Yasuda, K, Bell, GI, Reisine, T (1993) Gi alpha 3 and G(o) alpha selectively associate with the cloned somatostatin receptor subtype SSTR2. *J. Biol. Chem.* **268**(15): 10721-10727.

Lee, E, Taussig, R, Gilman, AG (1992) The G226A mutant of Gs alpha highlights the requirement for dissociation of G protein subunits. *J. Biol. Chem.* **267**(2): 1212-1218.

Lee, K, Nicholson, JR, McKnight, AT (1997) Nociceptin hyperpolarises neurones in the rat ventromedial hypothalamus. *Neurosci. Lett.* **239**(1): 37-40.

Lowry, OH, Nira, J, Rosenbrough, A, Farr, L, Randall, RJ (1951) Protein measurements with the Folin phenol reagent. *J. Biol. Chem.* **193**: 265-275.

Luo, C, Kumamoto, E, Furue, H, Chen, J, Yoshimura, M (2002) Nociceptin inhibits excitatory but not inhibitory transmission to substantia gelatinosa neurones of adult rat spinal cord. *Neuroscience* **109**(2): 349-358.

Luo, C, Kumamoto, E, Furue, H, Yoshimura, M (2001) Nociceptin-induced outward current in substantia gelatinosa neurones of the adult rat spinal cord. *Neuroscience* **108**(2): 323-330.

Lutfy, K, Eitan, S, Bryant, CD, Yang, YC, Saliminejad, N, Walwyn, W, Kieffer, BL, Takeshima, H, Carroll, FI, Maidment, NT, Evans, CJ (2003) Buprenorphine-induced antinociception is mediated by mu-opioid receptors and compromised by concomitant activation of opioid receptor-like receptors. *J. Neurosci.* **23**(32): 10331-10337.

Maloteaux, JM, Gossuin, A, Pauwels, PJ, Laduron, PM (1983) Short-term disappearance of muscarinic cell surface receptors in carbachol-induced desensitization. *FEBS Lett.* **156**(1): 103-107.

Martin, EL, Rens-Domiano, S, Schatz, PJ, Hamm, HE (1996) Potent peptide analogues of a G protein receptor-binding region obtained with a combinatorial library. *J. Biol. Chem.* **271**(1): 361-366.

Mason, SL, Ho, M, Nicholson, J, McKnight, AT (2001) In vitro characterization of Ac-RYYRWK-NH(2), Ac-RYYRIK-NH(2) and [Phe(1)CPsi(CH(2)-NH)Gly(2)] nociceptin(1-13)NH(2) at rat native and recombinant ORL(1) receptors. *Neuropeptides* **35**(5-6): 244-256.

Mathis, JP, Goldberg, IE, Rossi, GC, Leventhal, L, Pasternak, GW (1998) Antinociceptive analogs of orphanin FQ/nociceptin(1-11). *Life Sci.* **63**(11): PL 161-166.

McDonald, J, Barnes, TA, Okawa, H, Williams, J, Calo, G, Rowbotham, DJ, Lambert, DG (2003) Partial agonist behaviour depends upon the level of nociceptin/orphanin FQ receptor expression: studies using the ecdysone-inducible mammalian expression system. *Br. J. Pharmacol.* **140**(1): 61-70.

Meis, S, Pape, HC (1998) Postsynaptic mechanisms underlying responsiveness of amygdaloid neurons to nociceptin/orphanin FQ. *J. Neurosci.* **18**(20): 8133-8144.

Melzack, R, Wall, PD (1996) *The Challenge of Pain*. Penguin Books Ltd.

Menzies, JR, Glen, T, Davies, MR, Paterson, SJ, Corbett, AD (1999) In vitro agonist effects of nociceptin and [Phe(1)psi(CH(2)-NH)Gly(2)]nociceptin(1-13)NH(2) in the mouse and rat colon and the mouse vas deferens. *Eur. J. Pharmacol.* **385**(2-3): 217-223.

Meunier, J (2000) The potential therapeutic value of nociceptin receptor agonists and antagonists. *Exp. Opin. Ther. Patents* **10**(4): 371-388.

Meunier, JC, Mollereau, C, Toll, L, Suaudeau, C, Moisand, C, Alvinerie, P, Butour, JL, Guillemot, JC, Ferrara, P, Monsarrat, B, et al. (1995) Isolation and structure of the endogenous agonist of opioid receptor-like ORL1 receptor. *Nature* **377**(6549): 532-535.

Milligan, G (2003) Principles: Extending the utility of [^{35}S]GTPgammaS binding assays. *Trends Pharmacol. Sci.* **24**(2): 87-90.

Milligan, G (1988) Techniques used in the identification and analysis of function of pertussis toxin-sensitive guanine nucleotide binding proteins. *Biochem. J.* **255**: 1-13.

Minami, T, Okuda-Ashitaka, E, Nishizawa, M, Mori, H, Ito, S (1997) Inhibition of nociceptin-induced allodynia in conscious mice by prostaglandin D2. *Br. J. Pharmacol.* **122**(4): 605-610.

Mirzadegan, T, Benko, G, Filipek, S, Palczewski, K (2003) Sequence analyses of G-protein-coupled receptors: similarities to rhodopsin. *Biochemistry (Mosc).* **42**(10): 2759-2767.

Mogil, JS, Grisel, JE (1998) Transgenic studies of pain. *Pain* **77**(2): 107-128.

Mogil, JS, Nessim, LA, Wilson, SG (1999) Strain-dependent effects of supraspinal orphanin FQ/nociceptin on thermal nociceptive sensitivity in mice. *Neurosci. Lett.* **261**(3): 147-150.

Mogil, JS, Pasternak, GW (2001) The molecular and behavioral pharmacology of the orphanin FQ/nociceptin peptide and receptor family. *Pharmacol. Rev.* **53**(3): 381-415.

Mollereau, C, Mouledous, L (2000) Tissue distribution of the opioid receptor-like (ORL1) receptor. *Peptides* **21**(7): 907-917.

Mons, N, Cooper, DM (1995) Adenylate cyclases: critical foci in neuronal signaling. *Trends Neurosci.* **18**(12): 536-542.

Nicholson, JR, Paterson, SJ, Menzies, JR, Corbett, AD, McKnight, AT (1998) Pharmacological studies on the "orphan" opioid receptor in central and peripheral sites. *Can. J. Physiol. Pharmacol.* **76**(3): 304-313.

Nishi, M, Houtani, T, Noda, Y, Mamiya, T, Sato, K, Doi, T, Kuno, J, Takeshima, H, Nukada, T, Nabeshima et, a (1997a) Unrestrained nociceptive response and disregulation of hearing ability in mice lacking the nociceptin/orphaninFQ receptor. *The EMBO Journal* **16**(8): 1858-1864.

Nishi, M, Houtani, T, Noda, Y, Mamiya, T, Sato, K, Doi, T, Kuno, J, Takeshima, H, Nukada, T, Nabeshima, T, Yamashita, T, Noda, T, Sugimoto, T (1997b) Unrestrained nociceptive response and disregulation of hearing ability in mice lacking the nociceptin/orphaninFQ receptor. *EMBO J.* **16**(8): 1858-1864.

No, D, Yao, TP, Evans, RM (1996) Ecdysone-inducible gene expression in mammalian cells and transgenic mice. *Proc. Natl. Acad. Sci. U. S. A.* **93**(8): 3346-3351.

Noda, Y, Mamiya, T, Nabeshima, T, Nishi, M, Higashioka, M, Takeshima, H (1998) Loss of antinociception induced by naloxone benzoylhydrazone in nociceptin receptor-knockout mice. *J. Biol. Chem.* **273**(29): 18047-18051.

Oehme, I, Bosser, S, Zornig, M (2006) Agonists of an ecdysone-inducible mammalian expression system inhibit Fas Ligand- and TRAIL-induced apoptosis in the human colon carcinoma cell line RKO. *Cell Death Differ.* **13**(2): 189-201.

Okada, K, Sujaku, T, Chuman, Y, Nakashima, R, Nose, T, Costa, T, Yamada, Y, Yokoyama, M, Nagahisa, A, Shimohigashi, Y (2000) Highly potent nociceptin analog containing the Arg-Lys triple repeat. *Biochem. Biophys. Res. Commun.* **278**(2): 493-498.

Okawa, H, Hirst, RA, Smart, D, McKnight, AT, DG, L (1998a) Studies on the coupling of recombinant ORL-1 receptors to adenylyl cyclase. *British Journal of Pharmacology (Abstract)*: 123:218P.

Okawa, H, Hirst, RA, Smart, D, McKnight, AT, Lambert, DG (1998b) Rat central ORL-1 receptor uncouples from adenylyl cyclase during membrane preparation. *Neurosci. Lett.* **246**(1): 49-52.

Okawa, H, Nicol, B, Bigoni, R, Hirst, RA, Calo, G, Guerrini, R, Rowbotham, DJ, Smart, D, McKnight, AT, Lambert, DG (1999) Comparison of the effects of [Phe1psi(CH2-NH)Gly2]nociceptin(1-13)NH2 in rat brain, rat vas deferens and CHO cells expressing recombinant human nociceptin receptors. *Br. J. Pharmacol.* **127**(1): 123-130.

Olianas, MC, Maullu, C, Ingianni, A, Onali, P (1999) [Phe1phi(CH2-NH)Gly2]nociceptin-(1-13)-NH2 acts as a partial agonist at ORL1 receptor endogenously expressed in mouse N1E-115 neuroblastoma cells. *Neuroreport* **10**(5): 1127-1131.

Osinski, MA, Bass, P, Gaumnitz, EA (1999) Peripheral and central actions of orphanin FQ (nociceptin) on murine colon. *Am. J. Physiol.* **276**(1 Pt 1): G125-131.

Ozaki, S, Kawamoto, H, Itoh, Y, Miyaji, M, Iwasawa, Y, Ohta, H (2000) A potent and highly selective nonpeptidyl nociceptin/orphanin FQ receptor (ORL1) antagonist: J-113397. *Eur. J. Pharmacol.* **387**(3): R17-18.

Pan, Z, Hirakawa, N, Fields, HL (2000) A cellular mechanism for the bidirectional pain-modulating actions of orphanin FQ/nociceptin. *Neuron* **26**(2): 515-522.

Patel, HJ, Giembycz, MA, Spicuzza, L, Barnes, PJ, Belvisi, MG (1997) Naloxone-insensitive inhibition of acetylcholine release from parasympathetic nerves innervating guinea-pig trachea by the novel opioid, nociceptin. *Br. J. Pharmacol.* **120**(5): 735-736.

Paterlini, G, Portoghese, PS, Ferguson, DM (1997) Molecular simulation of dynorphin A-(1-10) binding to extracellular loop 2 of the kappa-opioid receptor. A model for receptor activation. *J. Med. Chem.* **40**(20): 3254-3262.

Paton, WD (1957) The action of morphine and related substances on contraction and on acetylcholine output of coaxially stimulated guinea-pig ileum. *Br J Pharmacol Chemother* **12**(1): 119-127.

Persani, L, Lania, A, Alberti, L, Romoli, R, Mantovani, G, Filetti, S, Spada, A, Conti, M (2000) Induction of specific phosphodiesterase isoforms by constitutive activation of the cAMP pathway in autonomous thyroid adenomas. *J. Clin. Endocrinol. Metab.* **85**(8): 2872-2878.

Phillips, HJ (1973). In: *In Dye Exclusion Tests for Cell Viability*, PF, K, MK, P (eds), p p 406. New York: Academic Press.

Pierce, KL, Premont, RT, Lefkowitz, RJ (2002) Seven-transmembrane receptors. *Nat Rev Mol Cell Biol* **3**(9): 639-650.

Pogozheva, ID, Lomize, AL, Mosberg, HI (1998) Opioid receptor three-dimensional structures from distance geometry calculations with hydrogen bonding constraints. *Biophys. J.* **75**(2): 612-634.

Rang, HP, Dale, MM, Ritter, JM (1995). In: *Pharmacology* Vol. Fourth Edition, pp 589-602: Churchill Livingstone.

Reinscheid, RK, Ardati, A, Monsma, FJ, Jr., Civelli, O (1996) Structure-activity relationship studies on the novel neuropeptide orphanin FQ. *J. Biol. Chem.* **271**(24): 14163-14168.

Reinscheid, RK, Nothacker, HP, Bourson, A, Ardati, A, Henningsen, RA, Bunzow, JR, Grandy, DK, Langen, H, Monsma, FJ, Jr., Civelli, O (1995) Orphanin FQ: a neuropeptide that activates an opioidlike G protein-coupled receptor. *Science* **270**(5237): 792-794.

Rens-Domiano, S, Law, SF, Yamada, Y, Seino, S, Bell, GI, Reisine, T (1992) Pharmacological properties of two cloned somatostatin receptors. *Mol. Pharmacol.* **42**(1): 28-34.

Rizzi, A, Bigoni, R, Calo, G, Guerrini, R, Salvadori, S, Regoli, D (1999) [Nphe(1)]nociceptin-(1-13)-NH(2) antagonizes nociceptin effects in the mouse colon. *Eur. J. Pharmacol.* **385**(2-3): R3-5.

Rizzi, A, Rizzi, D, Marzola, G, Regoli, D, Larsen, BD, Petersen, JS, Calo, G (2002a) Pharmacological characterization of the novel nociceptin/orphanin FQ receptor ligand, ZP120: in vitro and in vivo studies in mice. *Br. J. Pharmacol.* **137**(3): 369-374.

Rizzi, D, Rizzi, A, Bigoni, R, Camarda, V, Marzola, G, Guerrini, R, De Risi, C, Regoli, D, Calo, G (2002b) [Arg(14),Lys(15)]nociceptin, a highly potent agonist of the nociceptin/orphanin FQ receptor: in vitro and in vivo studies. *J. Pharmacol. Exp. Ther.* **300**(1): 57-63.

Rosenkilde, MM, Kledal, TN, Schwartz, TW (2005) High constitutive activity of a virus-encoded seven transmembrane receptor in the absence of the conserved DRY motif (Asp-Arg-Tyr) in transmembrane helix 3. *Mol. Pharmacol.* **68**(1): 11-19.

Rossi, GC, Perlmutter, M, Leventhal, L, Talatti, A, Pasternak, GW (1998) Orphanin FQ/nociceptin analgesia in the rat. *Brain Res.* **792**(2): 327-330.

Ruscheweyh, R, Sandkuhler, J (2001) Bidirectional actions of nociceptin/orphanin FQ on A delta-fibre-evoked responses in rat superficial spinal dorsal horn in vitro. *Neuroscience* **107**(2): 275-281.

Sakurada, T, Katsuyama, S, Sakurada, S, Inoue, M, Tan-No, K, Kisara, K, Sakurada, C, Ueda, H, Sasaki, J (1999) Nociceptin-induced scratching, biting and licking in mice: involvement of spinal NK1 receptors. *Br. J. Pharmacol.* **127**(7): 1712-1718.

Sandin, J, Georgieva, J, Silberring, J, Terenius, L (1999) In vivo metabolism of nociceptin/orphanin FQ in rat hippocampus. *Neuroreport* **10**(1): 71-76.

Scheer, A, Fanelli, F, Costa, T, De Benedetti, PG, Cotecchia, S (1997) The activation process of the alpha1B-adrenergic receptor: potential role of protonation and hydrophobicity of a highly conserved aspartate. *Proc. Natl. Acad. Sci. U. S. A.* **94**(3): 808-813.

Schertler, GF, Villa, C, Henderson, R (1993) Projection structure of rhodopsin. *Nature* **362**(6422): 770-772.

Schwartz, TW, Gether, U, Schambye, HT, Hjorth, SA (1995) Molecular mechanism of action of non-peptide ligands for peptide receptors. *Curr Pharm Design* **1**: 325–342.

Selley, DE, Liu, Q, Childers, SR (1998) Signal transduction correlates of mu opioid agonist intrinsic efficacy: receptor-stimulated [35S]GTP gamma S binding in mMOR-CHO cells and rat thalamus. *J. Pharmacol. Exp. Ther.* **285**(2): 496-505.

Sim, LJ, Selley, DE, Xiao, R, Childers, SR (1996) Differences in G-protein activation by mu- and delta-opioid, and cannabinoid, receptors in rat striatum. *Eur. J. Pharmacol.* **307**(1): 97-105.

Smart, D, Hirst, RA, Hirota, K, Grandy, DK, Lambert, DG (1997) The effects of recombinant rat mu-opioid receptor activation in CHO cells on phospholipase C, [Ca2+]i and adenylyl cyclase. *Br. J. Pharmacol.* **120**(6): 1165-1171.

Smith, TF, Gaitatzes, C, Saxena, K, Neer, EJ (1999) The WD repeat: a common architecture for diverse functions. *Trends Biochem. Sci.* **24**(5): 181-185.

Sprang, SR (1997) G protein mechanisms: insights from structural analysis. *Annu. Rev. Biochem.* **66**: 639-678.

Sternweis, PC, Robishaw, JD (1984) Isolation of two proteins with high affinity for guanine nucleotides from membranes of bovine brain. *J. Biol. Chem.* **259**(22): 13806-13813.

Suder, P, Kotlinska, J, Legowska, A, Smoluch, M, Hohne, G, Chervet, J-P, Rolka, K, Silberring, J (2000) Determination of nociceptin-orphanin FQ metabolites by capillary LC-MS. *Brain Research Protocols* **6**(1-2): 40-46.

Taylor, CW (1990) The role of G proteins in transmembrane signalling. *Biochem. J.* **272**(1): 1-13.

Tennant, JR (1964) Evaluation of the Trypan Blue Technique for Determination of Cell Viability. *Transplantation* **12**: 685-694.

Terenius, L, Sandin, J, Sakurada, T (2000) Nociceptin/orphanin FQ metabolism and bioactive metabolites. *Peptides* **21**(7): 919-922.

Topham, CM, Mouledous, L, Poda, G, Maigret, B, Meunier, JC (1998) Molecular modelling of the ORL1 receptor and its complex with nociceptin. *Protein Eng.* **11**(12): 1163-1179.

Tortora, GJ, Anagnostakos, NP (1990) *Principles of Anatomy and Physiology*. Harper Collins.

Traynor, JR, Nahorski, SR (1995) Modulation by mu-opioid agonists of guanosine-5'-O-(3-[35S]thio)triphosphate binding to membranes from human neuroblastoma SH-SY5Y cells. *Mol. Pharmacol.* **47**(4): 848-854.

Ueda, H, Inoue, M, Takeshima, H, Iwasawa, Y (2000) Enhanced spinal nociceptin receptor expression develops morphine tolerance and dependence. *J. Neurosci.* **20**(20): 7640-7647.

Unger, VM, Hargrave, PA, Baldwin, JM, Schertler, GF (1997) Arrangement of rhodopsin transmembrane alpha-helices. *Nature* **389**(6647): 203-206.

Unger, VM, Schertler, GF (1995) Low resolution structure of bovine rhodopsin determined by electron cryo-microscopy. *Biophys. J.* **68**(5): 1776-1786.

Van Craenenbroeck, K, Vanhoenacker, P, Leysen, JE, Haegeman, G (2001) Evaluation of the tetracycline- and ecdysone-inducible systems for expression of neurotransmitter receptors in mammalian cells. *Eur. J. Neurosci.* **14**(6): 968-976.

Vaughan, CW, Ingram, SL, Christie, MJ (1997a) Actions of the ORL1 receptor ligand nociceptin on membrane properties of rat periaqueductal gray neurons in vitro. *J. Neurosci.* **17**(3): 996-1003.

Vaughan, CW, Ingram, SL, Connor, MA, Christie, MJ (1997b) How opioids inhibit GABA-mediated neurotransmission. *Nature* **390**(6660): 611-614.

Wadenberg, ML (2003) A review of the properties of spiradoline: a potent and selective kappa-opioid receptor agonist. *CNS Drug Rev* **9**(2): 187-198.

Walsh, SL, Strain, EC, Abreu, ME, Bigelow, GE, Wadenberg, ML (2001) Enadoline, a selective kappa opioid agonist: comparison with butorphanol and hydromorphone in humans. A review of the properties of spiradoline: a potent and selective kappa-opioid receptor agonist. *Psychopharmacology (Berl).* **157**(2): 151-162.

Wang, J-L, Zhu, C-B, Cao, X-D, Wu, G-C (1999) Distinct effect of intracerebroventricular and intrathecal injections of nociceptin/orphanin FQ in the rat formalin test. *Regul. Pept.* **79**(2-3): 159-163.

Wang, JB, Johnson, PS, Imai, Y, Persico, AM, Ozenberger, BA, Eppler, CM, Uhl, GR (1994) cDNA cloning of an orphan opiate receptor gene family member and its splice variant. *FEBS Lett.* **348**(1): 75-79.

Wess, J (1998) Molecular basis of receptor/G-protein-coupling selectivity. *Pharmacol. Ther.* **80**(3): 231-264.

Yamada, H, Nakamoto, H, Suzuki, Y, Ito, T, Aisaka, K (2002) Pharmacological profiles of a novel opioid receptor-like1 (ORL(1)) receptor antagonist, JTC-801. *Br. J. Pharmacol.* **135**(2): 323-332.

Yazdani, A, Takahashi, T, Bagnol, D, Watson, SJ, Owyang, C (1999) Functional significance of a newly discovered neuropeptide, orphanin FQ, in rat gastrointestinal motility. *Gastroenterology* **116**(1): 108-117.

Yuan, CS, Israel, RJ (2006) Methylnaltrexone, a novel peripheral opioid receptor antagonist for the treatment of opioid side effects. *Expert Opin Investig Drugs* **15**(5): 541-552.

Yung, LY, Joshi, SA, Chan, RY, Chan, JS, Pei, G, Wong, YH (1999) GalphaL1 (Galpha14) couples the opioid receptor-like1 receptor to stimulation of phospholipase C. *J. Pharmacol. Exp. Ther.* **288**(1): 232-238.

During the course of my PhD I have published the following papers on opioid receptors. Not all of this work has been included in this thesis.

Reviews and articles

[1] **Full peer reviewed papers**

[1] Calo, G., Rizzi, A., Rizzi, D., Bigoni, R., Guerrini, R., Marzola, G., Marti, M., **McDonald, J.**, Morari, M., Lambert, D.G., Salvadori, S. and Regoli, D. (2002). [Nphe(1),Arg(14),Lys(15)]Nociceptin-NH(2), a novel potent and selective antagonist of the nociceptin/orphanin FQ receptor. *Br J Pharmacol*, **136**, 303-311.

[2] **McDonald, J.**, Barnes, T.A., Calo, G., Guerrini, R., Rowbotham, D.J. and Lambert, D.G. (2002) Effects of [(pF)Phe(4)]nociceptin/orphanin FQ-(1-13)NH(2) on GTPg[^{35}S] binding and cAMP formation in Chinese hamster ovary cells expressing the human nociceptin/orphanin FQ receptor. *Eur J Pharmacol*, **443** 7-12.

[3] **McDonald, J.**, Barnes, T.A., Okawa, H., Williams, J., Calo, G., Rowbotham, D.J. and Lambert, D.G. (2003). Partial agonist behaviour depends upon the level of nociceptin/orphanin FQ receptor expression: studies using the ecdysone-inducible mammalian expression system, *Br J Pharmacol*, **140**, 61-70.

[4] Wright, K.E., **McDonald, J.**, Barnes, T.A., Rowbotham, D.J., Guerrini, R., Calo, G. and Lambert, D.G., Assessment of the activity of a novel nociceptin/orphanin FQ analogue at recombinant human nociceptin/orphanin FQ receptors expressed in Chinese hamster ovary cells, *Neurosci Lett*, **346** (2003) 145-8.

[5] **McDonald, J.**, Calo, G., Guerrini, R. and Lambert, D.G. (2003). UFP-101, a high affinity antagonist for the nociceptin/orphanin FQ receptor: radioligand and GTPg[^{35}S] binding studies, *Naunyn Schmiedebergs Arch Pharmacol*, **367** 183-7.

[6] Kitayama, M, Barnes, TA, Carra, G, **McDonald, J**, Calo, G, Guerrini, R, Rowbotham, DJ, Smith, G, Lambert, DG (2003) Pharmacological profile of the cyclic nociceptin/orphanin FQ analogues c[Cys(10,14)]N/OFQ(1-14)NH(2) and c[Nphe(1),Cys(10,14)]N/OFQ(1-14)NH(2). *Naunyn. Schmiedebergs Arch. Pharmacol.* **368**(6): 528-537.

[7] Johnson, EE, **McDonald, J**, Nicol, B, Guerrini, R, Lambert, DG (2004) Functional coupling of the nociceptin/orphanin FQ receptor in dog brain membranes. *Brain Res.* **1003**(1-2): 18-25.

[8] Carra, G., Rizzi, A., Guerrini, R., Barnes, T.A., **McDonald, J.**, Hebbes, C.P., Mela, F., Kenigs, V.A., Marzola, G., Rizzi, D., Gavioli, E., Zucchini, S., Regoli, D., Morari, M., Salvadori, S., Rowbotham, D.J., Lambert, D.G., Kapusta, D.R. & Calo, G. (2005). [(pF)Phe4,Arg14,Lys15]N/OFQ-NH2 (UFP-102), a highly potent and selective agonist of the nociceptin/orphanin FQ receptor. *J Pharmacol Exp Ther*, **312**, 1114-23.

[9] Guerrini, R., Calo, G., Lambert, D.G., Carra, G., Arduin, M., Barnes, T.A., **McDonald, J.**, Rizzi, D., Trapella, C., Marzola, E., Rowbotham, D.J., Regoli, D. &

Salvadori, S. (2005), N- and C-terminal modifications of nociceptin/orphanin FQ generate highly potent NOP receptor ligands. *J Med Chem*, **48**, 1421-7.

[10] Trapella, C, Guerrini, R, Piccagli, L, Calo, G, Carra, G, Spagnolo, B, Rubini, S, Fanton, G, Hebbes, C, **McDonald, J**, Lambert, DG, Regoli, D, Salvadori, S (2006) Identification of an achiral analogue of J-113397 as potent nociceptin/orphanin FQ receptor antagonist. *Bioorg. Med. Chem.* **14**(3): 692-704.

[11] Arduin, M, Spagnolo, B, Calo, G, Guerrini, R, Carra, G, Fischetti, C, Trapella, C, Marzola, E, **McDonald, J**, Lambert, DG, Regoli, D, Salvadori, S (2007) Synthesis and biological activity of nociceptin/orphanin FQ analogues substituted in position 7 or 11 with Calpha,alpha-dialkylated amino acids. *Bioorg. Med. Chem.*

[12] Spagnolo, B, Carra, G, Fantin, M, Fischetti, C, Hebbes, C, **McDonald, J**, Barnes, TA, Rizzi, A, Trapella, C, Fanton, G, Morari, M, Lambert, DG, Regoli, D, Calo, G (2007) Pharmacological Characterization of the Nociceptin/Orphanin FQ Receptor Antagonist SB-612111 [(-)-cis-1-Methyl-7-[[4-(2,6-dichlorophenyl)piperidin-1-yl]methyl]-6,7,8,9 -tetrahydro-5H-benzocyclohepten-5-ol]: In Vitro Studies. *J. Pharmacol. Exp. Ther.* **321**(3): 961-967.

[13] Kitayama, M, **McDonald, J**, Barnes, TA, Calo, G, Guerrini, R, Rowbotham, DJ, Lambert, DG. In vitro Pharmacological Characterization of a novel cyclic Nociceptin/Orphanin FQ Analogue c[Cys7,10]N/OFQ(1-13)NH2. *Naunyn. Schmiedebergs Arch. Pharmacol.* (in press Naunyn-00042-2007).

[14] Williams, JP, Thompson, JP, McDonald, J, Barnes, TA, Cote, T, Rowbotham, DJ, Lambert, DG Human Peripheral Blood Mononuclear Cells Express Nociceptin/Orphanin FQ but not μ, δ or κ Opioid Receptors. *Anesth. Analg.* (in press, 2007).

[15] Ibba, M, Kitayama, M, McDonald, J, Calo', G, Guerrini, R, Farkas, J, Toth, G, Lambert, DG Binding of the Novel Radioligand [^{3}H]UFP-101 to Recombinant Human and Native Rat Nociceptin/Orphanin FQ receptors. *Br J Pharmacol.* (submitted 2007).

Abstracts

British Pharmacological Society

Imperial College, University of London, London, Dec 2001:

[1] **McDonald J**, Barnes TA, Guerrini R, Calo G, Rowbotham DJ and Lambert DG. (2002). In vitro characterisation of [(pF)Phe^4]nociceptin(1-13)NH_2 a novel agonist for the NOP receptor. Brit. J. Pharmacol. 135:258P. (Poster Presentation).

Brighton, Hosted by William Harvey Research Institute, Jan 2003:

[2] **McDonald J**, Barnes TA, Williams J, Calo G, Rowbotham DJ and Lambert DG (2003) Studies of [Phe$^1\Psi$(CH_2-NH)Gly^2]N/OFQ(1-13)NH_2 at the recombinant human nociceptin receptor using the ecdysone inducible expression system. Brit. J. Pharmacol. 138:26P. (Oral Presentation).

[3] Kitayama M, Barnes TA, **McDonald J**, Calo G, Guerrini R, Smith G, Rowbotham DJ and Lambert DG (2003) Pharmacological profile of the cyclic nociceptin/orphanin FQ analogues c[$Cys^{10,14}$]N/OFQ(1-14)NH_2 and c[$Nphe^{1}$,$Cys^{10,14}$]N/OFQ(1-14)NH_2. Brit. J. Pharmacol. 138:223P. (Poster Presentation)

Guy's Hospital, Hosted by Kings College, University of London, London, Dec 2003:

[4] Carra G, **McDonald J**, Rizzi D, Barnes TA, Zucchini S, Guerrini R, Lambert DG and Calo G (2004) *In vitro* characterisation of a novel, highly potent nociceptin/orphanin FQ receptor agonist Brit. J. Pharmacol. 141:117P. (Poster Presentation).

Oral Presentations (non published)

[1] Neuropeptides 2004: XIV European Neuropeptides Club Meeting, San Juan de Alicante, Spain May 9-12, 2004 –"Novel potent peptide ligands for the nociceptin/orphanin FQ receptor ".

[2] September 2003 presented oral and poster communications at an international meeting in Camerino, Italy - Nociceptin/Orphanin FQ and its Receptor: Recent Physiopharmacological Achievements and Pharmacotherapeutic Perspectives.

[3] Presented at the House of Commons, SET for Britain 2004 - Young people in Science, Engineering and Medicine Technology. Nociceptin/Orphanin FQ Receptor (NOP) Antagonists - Development Of Novel Analgesics For The Treatment Of Pain.